

**SYNTHESIS, STRUCTURES, AND CHARACTERIZATION OF
METAL-ORGANOCARBOXYLATE COMPOUNDS**

A Dissertation
Presented to
the Faculty of the Department of Chemistry
University of Houston

In Partial Fulfillment
of the Requirements for the Degree
Doctor of Philosophy

By
Marlon T. Conato
May 2012

**SYNTHESIS, STRUCTURES, AND CHARACTERIZATION OF
METAL-ORGANOCARBOXYLATE COMPOUNDS**

Marlon T. Conato

APPROVED:

Dr. Allan J. Jacobson, Chairman

Dr. Angela Möller

Dr. Arnold M. Guloy

Dr. T. Randall Lee

Dr. Jack Y. Lu

Dr. Mark A. Smith, Dean
College of Natural Sciences and Mathematics

Acknowledgements

I am indebted to many people for sharing their ideas and wisdom. I would like express my gratitude to them and apologize to anyone that I have inadvertently forgotten. First and foremost, I would like to thank my advisor, Dr. J for imparting his knowledge and showing me the beauty of solids. His patience and enthusiasm have always been admirable, and he has taught me not to become a slave of my work but a slave of my passion. I also want to express my appreciation to the committee members, Dr. Möller, Dr. Guloy, Dr. Lee, and Dr. Lu for their time and effort to review my work. Their compassion and dedication to science continue to inspire me.

I would like to express my sincere gratitude to the past and present members of the AJJ group. Much of what I know in research, I learned from them. I would like thank my mentor in crystallography, Xiqu and my boss in the wet-lab work, Lumei. I thank former students, Kasia, Paola, and Manoj and senior researchers, Do, Susan, and Dr. Kim for the help and guidance at the early stages of my work. I acknowledge the present members of the group, Bee, Sam, Qiang, Dmitry, Julie, Tanya, Wenquan, Chengfei, and buddy Sang Ho for the camaraderie and fun experiences we had in and out of the lab. I am very grateful especially to Ellen, our overseer and who has always been there to provide us with whatever assistance that we need. A great big thanks to all.

My experiments would never have been completed without the help of several individuals who shared their valuable time and expertise. I gratefully acknowledge Dr. Cai and Dr. May for the consultation on organic synthesis, and the experts who trained and helped me with the use of instruments, Dr. Meen (SEM), Dr. Korp (XRD), Dr.

Anderson (NMR), Dr. Tang (PXRD), Boris (XPS), Pawilai (Au film deposition), and Yan (PPMS). I also thank Dr. Chen for adopting me in his lab in San Antonio (UTSA) several times, and his students Ming and Chunrui for helping me conduct the initial magnetic property studies.

I acknowledge several faculty members of the Department of Chemistry, in particular, my course work professors, Dr. Albright, Dr. Hoffman, Dr. Baldelli, Dr. Czernuscewicz, and Dr. Shiv. I also thank my *kababayans* professors, Doc Guloy and Doc Gobet for their availability whenever we need personal consults. I thank the staff who has helped me with other problems concerning other technical stuff, Roger (glass works), Mark (machine works), Jerry (computer works), Davy (electrical works), Hans (electronics), the department office personnel (paper works), and the graduate advisors during my stay, Gwen, Monique, and Chu.

My graduate school experience would never have been enjoyable without the company of my Filipino and honorary Filipino friends in Houston. Their companionship in several activities outside of the laboratory makes me feel a lot closer to home. I could never list down all of them but special thanks to Jane, Imee, Rads, Jack, Noemi, Gregggy, Arthur, Marj, Joon Hee, Mike, John Glenn, Ellie, Lette, Gino, Rio, Edta, Allan, Uriel and my good friend Natt. I also gratefully acknowledge the help and support of my friends outside of H-town, Tren, Dru, Yas, and Ena. I always feel blessed with having friends like them.

Last but not the least, my deepest gratitude goes to my family especially to my parents who always supported me in all my pursuits. This dissertation is dedicated to them.

**SYNTHESIS, STRUCTURES, AND CHARACTERIZATION OF
METAL-ORGANOCARBOXYLATE COMPOUNDS**

An Abstract of a Dissertation
Presented to
the Faculty of the Department of Chemistry
University of Houston

In Partial Fulfillment
of the Requirements for the Degree
Doctor of Philosophy

By
Marlon T. Conato
May 2012

Abstract

Reticular synthesis of metal-organic hybrid compounds deals with the interaction of two primary building components, namely metal connectors and organic linkers, to build structures for specific applications. This work focuses on studying the role of linear aromatic dicarboxylates as bridging linkers for the formation of magnetic and chiral framework materials.

A series of dicarboxylate-bridged nickel (II) cluster compounds were synthesized and their magnetic properties investigated. The compounds $\text{Ni}_3(1,4\text{-BDC})_3(\text{DMF})_2(\text{DMA})_2$ (**3-1**) and $\text{Ni}_3(1,4\text{-BDC})_3(\text{DMF})_4$ (**3-2**) [1,4-BDC = terephthalate, DMF = *N,N'*-dimethylformamide, and DMA = dimethylamine] have layered structures whereas $\text{Ni}_3(2,6\text{-NDC})_3(\text{DMF})_2(\text{DMA})_2$ (**3-3**) [2,6-NDC = naphthalate], $\text{Ni}_3(\mu_3\text{-O})(4,4'\text{-BPDC})_3(\text{DMA})_3$ (**3-4**) [4,4'-BPDC = 4,4'-biphenyldicarboxylate], and $\text{Ni}_4(\mu_3\text{-O})(1,4\text{-NDC})_4(\text{DMF})_2(\text{DMA})_2$ (**3-5**) [1,4-NDC = 1,4-naphthalenedicarboxylate] have three-dimensional frameworks.

An isoreticular series of chiral frameworks, $\text{Ni}_2\text{O}(\text{Asp})(1,4\text{-BDC})_{0.5}$ (**4-1**) [Asp= aspartate, $\text{Ni}_2\text{O}(\text{Asp})(1,4\text{-NDC})_{0.5}$ (**4-2**), $\text{Ni}_2\text{O}(\text{Asp})(2,6\text{-NDC})_{0.5}$ (**4-3**) and $\text{Ni}_2\text{O}(\text{Asp})(4,4'\text{-BPDC})_{0.5}$ (**4-4**)] were also prepared. These compounds are built from homochiral chains of $[\text{Ni}_2\text{O}(\text{L-Asp})(\text{H}_2\text{O})_2]$ connected by the aromatic dicarboxylate ligands. The compounds contain channels parallel to the chains with dimensions that depend on the lengths of the rigid dicarboxylate linkers. The sensitivity of the synthesis

of compound **4-1** toward several parameters such as pH, reaction time, and solvent system was studied.

Coordination compounds were also synthesized by the reaction of metal cations with a new ligand *meso*-1,4-phenylenebis(hydroxyacetic acid) (**H₂L**). Four new compounds, Ni₂L₂·(H₂O)₄ (**5-1**), CoL·H₂O (**5-2**), ZnL·H₂O (**5-3**), and PbL (**5-4**) were prepared in single crystal form and characterized by X-ray crystallography and IR spectroscopy.

In the final section, films of metal-organic compounds were grown on carboxylate-functionalized gold (Au) surfaces as an initial attempt towards developing functional metal-organic materials for device applications. Zinc terephthalate (MOF-5) crystals were deposited on top of Au substrates that were functionalized with self-assembled monolayers (SAMs) with COOH- terminal groups. Nucleation of MOF-5 crystals was induced by pretreatments with Zn²⁺ solutions. The kinetics of crystal growth was investigated by analysis of optical images of the films at different periods of crystallization to determine the particle size distribution. The procedure used to grow MOF-5 films on Au surfaces functionalized with SAMs was also used in the preparation of manganese formate and lanthanum formate films.

Table of Contents

	<u>Page</u>
Acknowledgments.....	iii
Abstract.....	vi
List of Figures.....	xi
List of Tables.....	xvi
 Chapter 1 Introduction	
1.1 Objectives of the Study.....	1
1.2 Background of the Study.....	1
1.3 Outline of the Dissertation.....	10
1.4 References.....	12
 Chapter 2 Experimental	
2.1 Synthesis.....	18
2.2 Characterization.....	20
2.3 References.....	24
 Chapter 3 Getting Connected: Trimeric and Tetrameric Clusters of Nickel(II) Octahedra in Metal-Organic Frameworks Based on Aromatic Dicarboxylates	
3.1 Introduction.....	26
3.2 Experimental Section.....	27
3.3 Results and Discussion.....	30
3.4 Conclusion.....	52

3.5	References.....	53
Chapter 4 Channeling Chirality: Isoreticular Synthesis of Dicarboxylate-Bridged Frameworks Based on a Homochiral Chain Compound [Ni₂O(L-Aspartate)(H₂O)₂]		
4.1	Introduction.....	57
4.2	Experimental Section.....	58
4.3	Results and Discussion.....	60
4.4	Conclusion.....	76
4.5	References.....	76
Chapter 5 A Tailored Linker: Synthesis and Structures of Metal Dicarboxylates Based on a New Ligand, <i>meso</i>-1,4-Phenylenebis(hydroxyacetic acid)		
5.1	Introduction.....	79
5.2	Experimental Section.....	81
5.3	Results and Discussion.....	85
5.4	Conclusion.....	101
5.5	References.....	103
Chapter 6 Assembly at the Surface: Preparation of Metal-Organic Framework Films on Functionalized Gold Surfaces		
6.1	Introduction.....	105
6.2	Experimental Section.....	106
6.3	Results and Discussion.....	108
6.4	Conclusion.....	126

6.5	References.....	126
Chapter 7	Conclusion.....	130
	References.....	134
Appendix.....		137

List of Figures

	<u>Page</u>
Figure 1.1. Schematic representation of the node-and-linker assembly in the generation of one- (1D), two- (2D), or three-dimensional (3D) MOF architectures.....	2
Figure 1.2 Influence of reaction temperature and pH in the variations of nickel(II)-terephthalate-2,2'-bipyridine structures. (Ref. 43).....	5
Figure 1.3 Representative structures of chiral MOFs prepared using the three general strategies; a) from achiral building blocks, b) by using chiral templating molecule (e.g. 1,2-propanediol), c) by using an enantiopure bridging linker (L).....	7
Figure 1.4 Examples of trimeric metal-clusters studied for their magnetic properties. (Ref. 52).....	8
Figure 1.5 Structures of MOFs based on iron-oxo cluster with a chiral antimony tartrate scaffold. (Ref. 55).....	9
Figure 3.1 Optical Microscope Images of the Crystals 3-1 to 3-5	32
Figure 3.2 a) The trimer in 3-1 ; b) the trimer in 3-2 ; c) view looking parallel and perpendicular to the layer in 3-1 ; d) the stacking of the layers in 3-1 and 3-2	34
Figure 3.3 a) The square arrangement of trimers in 3-3 formed by the bridging 2,6-NDC ligands into a three-dimensional framework; b) a view down c showing the coordinated DMF molecules occupying channels in the structure.....	36
Figure 3.4 a) The μ_3 -oxo-centered trimeric nickel cluster in 3-4 ; b&c) projection of the structure along the b and c axis showing the connections between the trimers.....	38
Figure 3.5 a) A view of the structure of 3-4 along b showing the cluster connectivity; b) the two interpenetrated frameworks.....	39
Figure 3.6 a) The tetrameric building unit in 3-5 ; b) a projection of the structure down c showing the channel arrangement.....	40

Figure 3.7	The coordination modes of the dicarboxylate bridges within the building units of compounds 3-1 to 3-5	42
Figure 3.8	Thermogravimetric data for compounds 3-1 to 3-5 (a to e).....	45
Figure 3.9	FT-IR spectra of compounds 3-1 to 3-5 (a to e).....	46
Figure 3.10	PXRD data of compounds 3-1 to 3-5 (a to e). The top plots are experimental patterns while the bottom plots are simulated patterns from the single crystal data.....	47
Figure 3.11	The magnetic molar susceptibility (χ_M) and inverse susceptibility ($1/\chi_M$) vs. temperature (T) for the compounds 3-1 , 3-2 , 3-4 , and 3-5 . The solid lines are least-squares fit to the Curie-Weiss law at high temperature range.....	49
Figure 3.12	The $\chi_M T$ vs. T curves for compounds 3-1 to 3-5 showing their different magnetic behaviors at temperatures below 50 K.....	51
Figure 4.1	Structures of the aromatic dicarboxylate linkers used in the study.....	59
Figure 4.2	a) Helical chain in 1D Ni-Asp ; b) Trimer building unit; c) Unit cell of 1D Ni-Asp viewed along <i>c</i> axis. (Ref. 13).....	62
Figure 4.3	Transformation of 1D Ni-Asp to 3D Ni-Asp connected by the $(\text{NiAsp}_2)^{2-}$ bridges. (Ref. 15).....	62
Figure 4.4	Crystal structures of 3D Ni-Asp a) showing the carboxylate bridging points in the linkages of the 1D Ni-Asp chains and b) the chiral channels perpendicular to the <i>c</i> axis i.e. the direction of the chiral chain. (Ref. 15).....	63
Figure 4.5	Powder diffraction pattern of compound 4-1 and the Le Bail fit to the PXRD pattern of 4-1 using the GSAS.....	64
Figure 4.6	Powder diffraction patterns and Le Bail fits (superimposed) of a) compound 4-2 , b) compound 4-3 , and c) compound 4-4	65
Figure 4.7	Powder diffraction patterns of the products from a 2:1:1 ratio of $\text{Ni}^{2+}:\text{L-H}_2\text{Asp}:1,4-\text{H}_2\text{BDC}$ set-ups prepared at a reaction time of a) 4 h, b) 12 h, c) 24 h, d) 48 h, e) 72 h, and f) 144 h.....	68
Figure 4.8	Powder diffraction patterns of the products based on compound 4-1	

with varying amounts of base at a ligand : TEA ratio of a) 1 : 0.67 (pH 3-4), b) 1 : 1.1 (pH 5-6), c) 1 : 1.4 (pH 6-7), and d) 1 : 5.3 (pH 9-10).....	70
Figure 4.9 PXRD patterns of compound 4-1 measured using the PANalytical X’Pert Pro high temperature measurement system at temperatures of a) 25 °C, b) 60 °C, c) 90 °C, d) 120 °C, e) 160 °C, and f) 180 °C. Sharp peaks at 39.7° and 46.2° are characteristic peaks of the Pt sample holder.....	72
Figure 4.10 Thermogravimetric plot for compound 4-1	73
Figure 4.11 a) Powder diffraction pattern of compound 4-1 for base comparison; b) PXRD pattern after heat treatment at 180 °C for 30 min; c) PXRD pattern after soaking back to DMF-H ₂ O solvent system.....	74
Figure 4.12 PXRD pattern of 4-1 heated at 180 °C (left) then reconditioned in 3 : 1 DMF : H ₂ O (right) for a) 30 min, b) 60 min, and c) 210 min.....	75
Figure 5.1 Structure of the new linker 1,4-phenylenebis(hydroxyacetic acid) (H₂L).....	80
Figure 5.2 ¹ H-NMR spectra of H₂L	86
Figure 5.3 FT-IR spectra of H₂L	86
Figure 5.4 Optical microscope images of the crystals 5-1 to 5-4	87
Figure 5.5 The metal coordination environments in compounds 5-1 to 5-4 (a to d, respectively).....	89
Figure 5.6 Coordination of the linker, L²⁻	90
Figure 5.7 Hydrogen bonding layers (top view) in compounds a) 5-1 , b) 5-2 , and c) 5-3 . Hydrogen bonds are represented by dashed lines (---).....	91
Figure 5.8 Crystal structure of the dimer unit in 5-1	92
Figure 5.9 Structures of compound 5-1 along <i>b</i> showing the perpendicular layers of dimeric units. Hydrogen bonds are represented by dashed lines (---).....	93
Figure 5.10 Distances and dihedral angle between planes of aromatic rings of adjacent dimers in 5-1	94

Figure 5.11	Chain structures of a) compound 5-2 and b) compound 5-3 and the guest water molecules surrounding the chains.....	95
Figure 5.12	Crystal structure of a) compound 5-2 along <i>b</i> axis and b) compound 5-3 along <i>c</i> axis. H-bonding interaction is represented as dashed lines (- - -).....	96
Figure 5.13	Crystal structure of 5-4 : a) 1-D chain unit and b) stacking of chains along <i>a</i> showing the weak Pb-O interaction represented as dashed lines (- - -).....	98
Figure 5.14	FT-IR spectra of compounds 5-1 to 5-4	99
Figure 5.15	PXRD data of compounds 5-1 and 5-4 . The top plots are experimental patterns while the bottom plots are simulated patterns from the single crystal data.....	100
Figure 5.16	TGA plot of compounds a) 5-1 and b) 5-4	102
Figure 6.1	Schematic representation of MOF-5 film deposited on Au-SAM substrate.....	109
Figure 6.2	Optical images of the Au-SAM-MOF-5 film products obtained by crystallization of pre-heated MOF-5 solution (literature method; Ref. 21) at a) lower magnification and b) higher magnification.....	110
Figure 6.3	Optical images of the Au-SAM-MOF-5 film products obtained by room-temperature synthesis using dilute crystallization solution at a) lower magnification and b) higher magnification.....	111
Figure 6.4	Schematic diagram of the pretreatment methods applied to Au-SAM substrate; a) high-temperature pretreatment and b) room-temperature pretreatment.....	112
Figure 6.5	Optical images of the Au-SAM-MOF-5 film products obtained by synthesis with substrate pretreatment at high temperature at a) lower magnification and b) higher magnification.....	113
Figure 6.6	Optical images of the Au-SAM-MOF-5 film products obtained by synthesis after substrate pretreatment with pH adjustment (pH = 8-9) at a) lower magnification and b) higher magnification; without pH	

adjustment (pH = 5) at c) lower magnification and d) higher magnification.....	114
Figure 6.7 Schematic view and optical images of the Au-SAM-MOF-5 films prepared using SAMs of different carbon chain lengths; a) using SAM16 and b) using SAM11.....	115
Figure 6.8 Optical images of the Au-SAM-MOF-5 films after a crystal growth period of 1 week at a) lower magnification and b) higher magnification.....	116
Figure 6.9 PXRD patterns and optical images (inset) of the same Au-SAM-MOF-5 film; a) freshly-prepared and b) after 24 h exposure to air. (*) denotes peaks from Au film).....	117
Figure 6.10 Images of the Au-SAM-MOF-5 films at crystal-growth period of: a) 2 days, b) 3 days, c) 4 days, d) 6 days, e) 8 days, f) 12 days, g) 16 days, and h) 20 days.....	119
Figure 6.11 PXRD patterns of the Au-SAM-MOF-5 film samples at crystal-growth period of: a) 1 day, b) 2 days, c) 3 days, d) 4 days, e) 8 days, f) 12 days, g) 16 days, and h) 20 days. (*) denotes peaks from Au film).....	120
Figure 6.12 Histograms of particle size distribution of Au-SAM-MOF-5 samples at different crystallization times (t) derived from image analysis by automatic binning.....	121
Figure 6.13 Histograms of particle size distribution of Au-SAM-MOF-5 samples at different crystallization times (t) derived from image analysis by manual binning.....	122
Figure 6.14 PXRD patterns and an optical image (inset) of a) Au-SAM-Mn(HCOO) ₂ and b) Au-SAM-La(HCOO) ₃ . (*) denotes peaks coming from Au film).....	125

List of Tables

	<u>Page</u>
Table 3.1 Crystallographic Data and Structure Refinement for Compounds 3-1 to 3-5	31
Table 3.2 Curie-Weiss Fit Parameters of the Compounds.....	49
Table 4.1 Lattice parameters from the Le Bail fits for compounds 4-1 to 4-4	66
Table 5.1 Crystallographic data and structure refinement for compounds 5-1 to 5-4	84
Table 5.2 Hydrogen bonding parameter in compounds 5-1 to 5-3	90
Table A3.1 Selected interatomic distances and angles for $\text{Ni}_3(1,4\text{-BDC})_3(\text{DMF})_2(\text{DMA})_2$ (3-1).....	145
Table A3.2 Selected interatomic distances and angles for $\text{Ni}_3(1,4\text{-BDC})_3(\text{DMF})_4$ (3-2).....	147
Table A3.3 Selected interatomic distances and angles for $\text{Ni}_3(2,6\text{-NDC})_3(\text{DMF})_2(\text{DMA})_2$ (3-3).....	169
Table A3.4 Selected interatomic distances and angles for $\text{Ni}_3(\mu_3\text{-O})(4,4'\text{-BPDC})_3(\text{DMA})_3$ (3-4).....	180
Table A3.5 Selected interatomic distances and angles for $\text{Ni}_4(\mu_3\text{-O})(1,4\text{-NDC})_4(\text{DMF})_2(\text{DMA})_2$ (3-5).....	200
Table A5.1 Selected interatomic distances and angles for $\text{Ni}_2(\text{C}_{10}\text{H}_8\text{O}_6)_2(\text{H}_2\text{O})_4$ (5-1).....	213
Table A5.2 Selected interatomic distances and angles for $\text{Co}(\text{C}_{10}\text{H}_8\text{O}_6)(\text{H}_2\text{O})_2\cdot\text{H}_2\text{O}$ (5-2).....	223
Table A5.3 Selected interatomic distances and angles for $\text{Zn}(\text{C}_{10}\text{H}_8\text{O}_6)(\text{H}_2\text{O})_2\cdot\text{H}_2\text{O}$ (5-3).....	232
Table A5.4 Selected interatomic distances and angles for $\text{Pb}(\text{C}_{10}\text{H}_8\text{O}_6)$ (5-4).....	239

Chapter 1

Introduction

1.1. Objectives of the Study

The general objective of this research is to investigate the reticular synthesis of metal-organic hybrid compounds, in particular, complexes with linear dicarboxylate linkers based on the node-and-linker methodology as a route towards the fabrication of materials for specific applications. This study focuses on the preparation of new compounds and the influence on their formation of systematic variations of the synthesis conditions such as reaction time, temperature, pH, and solvent system. The main characterization technique used is structure identification by X-ray crystallography; other physical properties were determined as suggested by the crystal structure of a specific compound.

1.2. Background of the Study

Research on the synthesis of a fascinating group of solids referred to as coordination polymers or metal organic frameworks (MOF) has increased significantly over the past decade due to their structural novelty and promising applications in catalysis, gas storage and separation.¹⁻²⁰ This is evident from the several excellent review articles on MOFs over the last five years.¹⁻⁸ The remarkable interest in MOFs is due in part to the reported high surface areas and the porous framework structures of these compounds. While their architectures are generally comparable to that of zeolites, MOF compounds are not as robust thus limiting their applications to a maximum temperature

limit of ~500 °C. In terms of synthesis, however, MOFs possess a large advantage over purely inorganic frameworks due to the variety of building blocks that can be used. MOFs typically are prepared under relatively mild conditions.²¹⁻²⁵

MOFs represent a new class of crystalline coordination compounds that have extended connectivity with backbones consisting of metal ions or metal clusters as ‘nodes’ and organic polydentate ligands as ‘linkers’. The various combinations of the two primary building components allow the formation of structures with different dimensionalities such as 1D chains, 2D layers, or 3D frameworks (Figure 1.1).¹⁻¹²

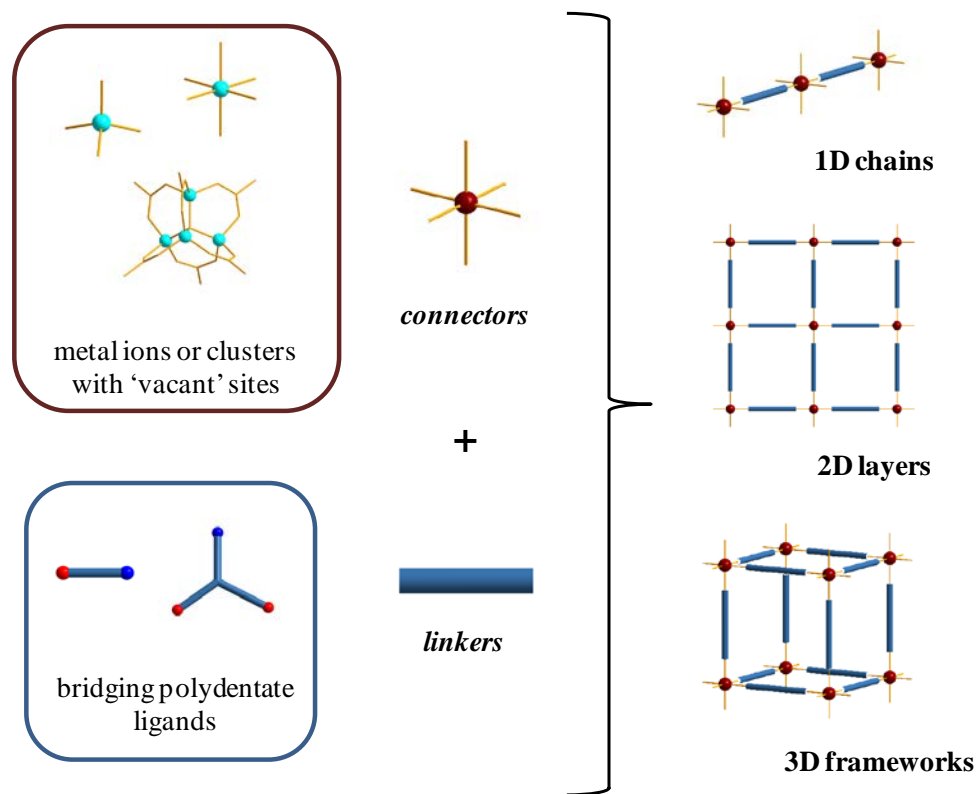


Figure 1.1. Schematic representation of the node-and-linker assembly in the generation of one- (1D), two- (2D), or three-dimensional (3D) MOF architectures.

Reticular Chemistry. The rational design of solids that have extended connectivity has been an active area in the continuing effort to develop new solid-state materials with superior properties. The node-and-linker approach in coordination compounds to create framework architectures was established more than two decades ago.²⁶⁻²⁷ Reticular chemistry is a term that refers to the assembly of the molecular building blocks, namely the connectors and the linkers, into predetermined structures.^{12,22-24,28-39} The term isoreticular refers to compounds with the same framework topology but different dimensions.^{12,29} The most widely used metal connectors are transition metal ions; the coordination environment depends on the specific metal and its oxidation state. As a consequence, various geometries such as linear, trigonal, tetrahedral, square pyramidal, square planar, and octahedral are possible. A convenient notation to describe connectors based on metal clusters is the term secondary building unit (SBU). SBUs are geometrical shapes that represent the metal-cluster units as a single ‘node’ entity and explicitly define points for linker extension in MOF assembly.^{8-10,14,24,33-41}

The linkers are usually organic ligands that bridge the metal connectors. They contain at least two donor atoms, mostly O-, N-, or S-donors and can be neutral or anionic. Their rigidity or flexibility, the distances between the two bridging groups, and extra functionality in the linker structure influence how the connectors arrange in the extended framework.^{8-10,25,38-42} One advantage of using organic ligands as linkers is the ability of organic chemists to synthesize organic molecules with complex structures, which further expands the diversity of MOF designs.⁴²

Besides the two primary building components, other auxiliary components include terminating ligands, counteranions, nonbonding guests, and/or template molecules. Terminating or blocking ligands set limits on the SBU assembly, while the counterions influence the metal environment and may be involved in other weak interactions acting as guest molecules. Nonbonding guests like solvent molecules can also form weak interactions with the other components or can serve as the space fillers in the structure. Another feature often encountered in MOFs is the interpenetration of two or more nets in the structure. Interpenetrating structures occasionally form from MOFs with large grids to compensate the void spaces usually occupied by solvent molecules or counterions.^{8-10,13,21,40-43}

MOF Synthesis. Several synthetic strategies for the preparation of crystalline MOF materials have been published in literature.^{8-12,14-15,40-44} The critical parameters during the synthesis include the specific solvent, reaction temperature, pH, and reactant concentrations. The synthesis can either be solvothermal or nonsolvothermal; the former means reactions carried out in closed vessels under autogenous pressure at above the boiling point of the solvent while the latter occur below the solvent's boiling point at ambient pressure. Temperature variation influences not only the final MOF structure, as condensed phases are often formed at higher temperatures, but also the morphology of the crystals since it directly affects the crystallization kinetics of the reaction. Reaction pH influences MOF synthesis by changing the degree of protonation of the organic ligands and consequently the coordination environment in the final product. For instance, in our laboratory, systematic variations on temperature and pH have been studied for the nickel(II)-terephthalate-2,2'-bipyridine system (Figure 1.2) and nickel(II)/cobalt(II)-2,4-

pyridinecarboxylate system.⁴⁵⁻⁴⁶ The generation of several structures with different compositions shows the effect of the various parameters on the final MOF structure, in particular, on the coordination modes of the bridging linkers.

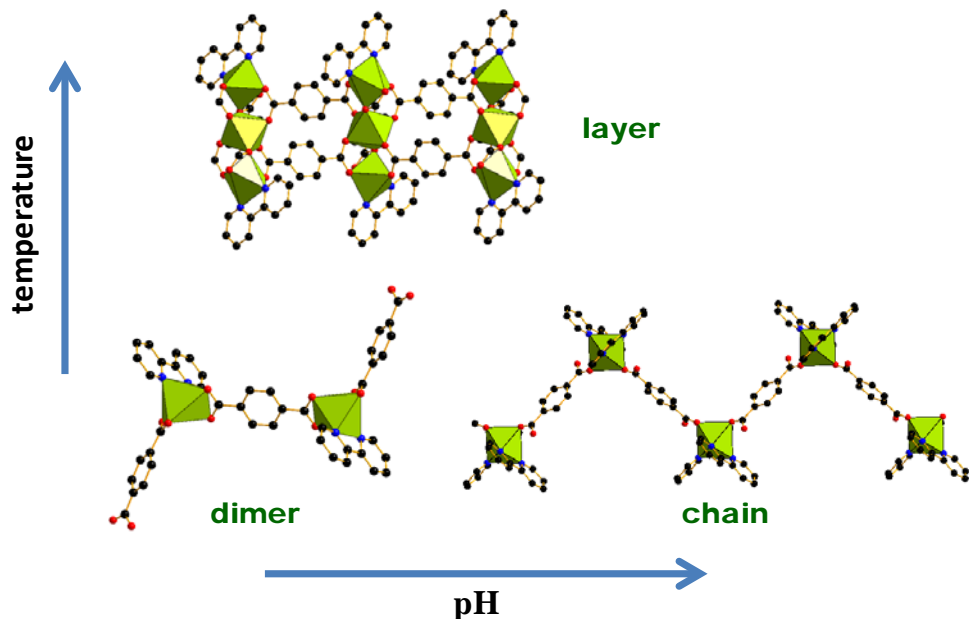


Figure 1.2. Influence of reaction temperature and pH in the variations of nickel(II)-terephthalate-2,2'-bipyridine structures. (Ref. 43)

Even the nature of the starting metal salt can affect the structure and morphology of the crystal products as was demonstrated for the well-known MOFs, MOF-5 ($\text{Zn}_4\text{O}[\text{C}_6\text{H}_4(\text{COO})_2]_3$) and HKUST-1 ($\text{Cu}_3[\text{C}_6\text{H}_3(\text{COO})_3]_2(\text{H}_2\text{O})_3 \cdot x\text{H}_2\text{O}$). Metal acetates are shown to yield smaller crystals than metal nitrates for both MOFs while metal chlorides did not produce any of the MOF phases under the conditions investigated.⁴⁷ Further changes in the pH and solvent system for both MOF-5 and HKUST-1 led to the formation of several other known and unknown phases.^{21,40,47}

Apart from the solvothermal and diffusion based crystallization methods in MOF synthesis, several other alternative routes have been reported. These include microwave-assisted, electrochemical, mechanochemical, and sonochemical syntheses methods. The use of the less conventional methods has been useful in the preparation of new compounds that cannot be obtained otherwise, as well as to generate particles of desired size and morphology to optimize the physical properties for a specific application. In general, both ultrasonic- and microwave-assisted synthesis produces MOF particles that are homogenously small. Variations in the compositional and process parameters, temperature program during crystal growth, and use of additives or microemulsions also influence the size and shape of the crystals.^{21,48}

While most studies on MOFs revolve around the high surface area, porosity and robustness of the framework structures, the manifestation of other interesting properties such as chirality and magnetism, dependent on the arrangement of the metal connectors and organic linkers, provides an added dimension to the solid state chemistry of these materials.

Chiral MOFs. The major driving force to prepare MOFs that have chiral structures is their potential use in enantioselective separation and asymmetric catalysis.⁴⁹⁻⁵¹ Three general approaches have been reported in making homochiral MOFs; (1) from asymmetric crystallization of achiral components without the use of any templating molecule, (2) using chiral templates to direct homochiral crystallization of achiral nodes and linkers, and (3) using metal ions or metal clusters as nodes and enantiopure ligands as linkers. Examples of some chiral MOF structures made using the three strategies are shown in Figure 1.3. A recent advancement in this area is the strategy of post-

modification where the chirality is introduced in the framework channels by synthetic modification of the bridging linkers after the target framework has been synthesized.⁵²

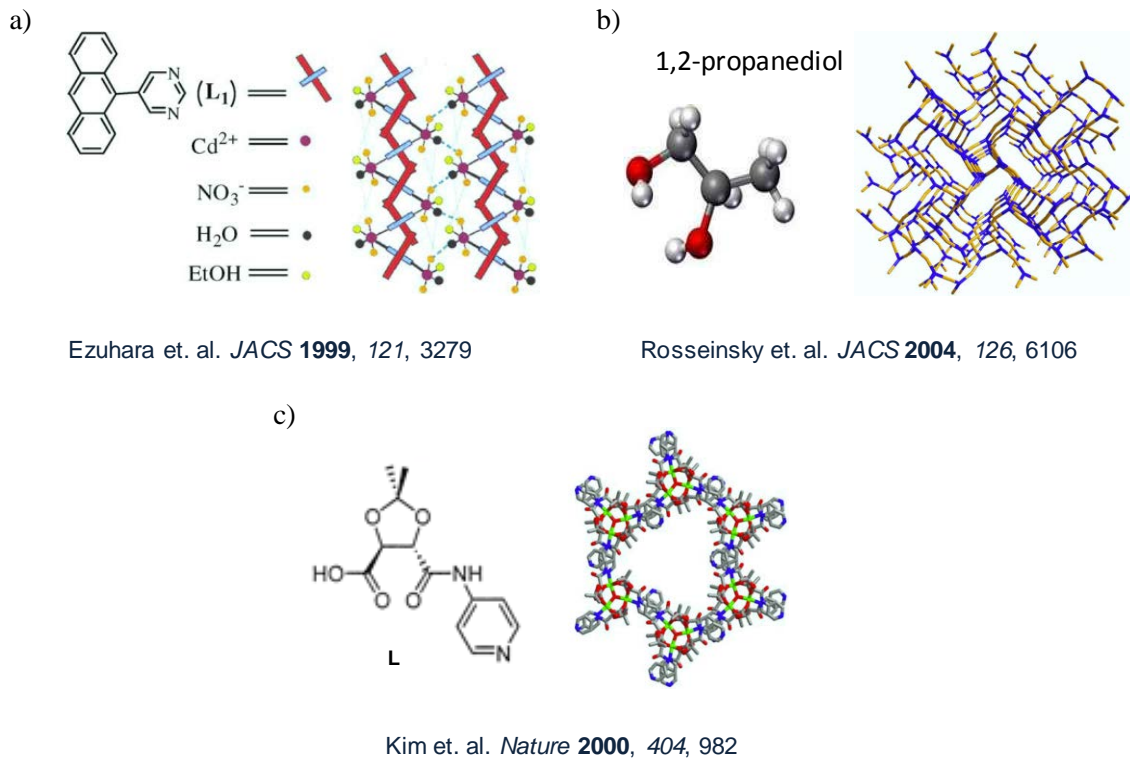


Figure 1.3. Representative structures of chiral MOFs prepared using the three general strategies; a) from achiral building blocks, b) by using chiral templating molecule (e.g. 1,2-propanediol), c) by using an enantiopure bridging linker (*L*).

Magnetic MOFs. Among the several subclasses of MOFs, such as IRMOF (isoreticular MOFs), PMOF (porous MOFs), ZIFs (zeolitic imidazole frameworks), and CMOF (chiral MOFs), the term magnetic MOFs is rather uncommon perhaps due to the fact that they may be classified under a general class of molecular magnets.⁵³ The magnetic properties of MOFs are a consequence of the magnetic interaction between

neighboring ions with magnetic moments which varies according to the structure and configuration. Small bridging linkers that may have two or three intervening atoms between the metal magnetic moment carriers can facilitate the interactions for low dimensional magnetic system studies. A report from our group has investigated the magnetic property of trimeric clusters of Mn(II) and Co(II) bridged by a fluorinated dicarboxylate linker and observed weak ferromagnetic interactions in the Mn-cluster (Figure 1.4).⁵⁴

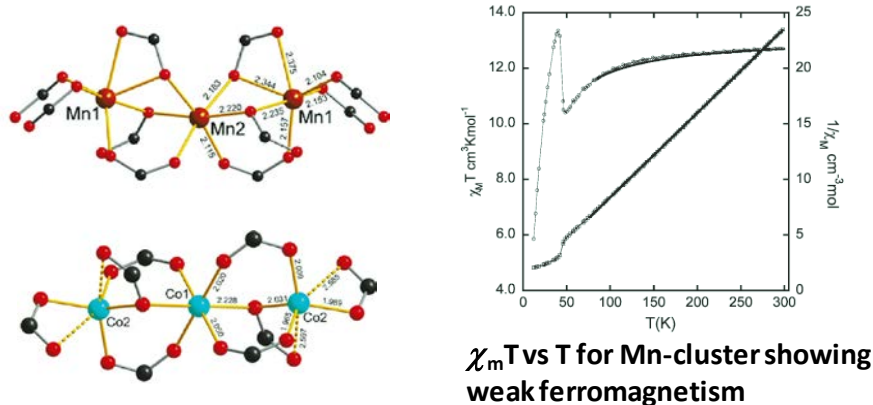


Figure 1.4. Examples of trimeric metal-clusters studied for their magnetic properties. (Ref. 52)

A more interesting MOF that has a complex structure, unusual magnetic properties, and simultaneously exhibits chirality is the group of complexes that has been prepared in our lab based on iron-oxo clusters sandwiched between two antimony tartrate fragments (Figure 1.5).⁵⁵ They preview a set of compounds that has the potential of combining chirality and magnetism and may give rise to highly desirable original

properties like magnetochiral dichroism or magnetization-induced second harmonic generation.⁵⁶⁻⁵⁷

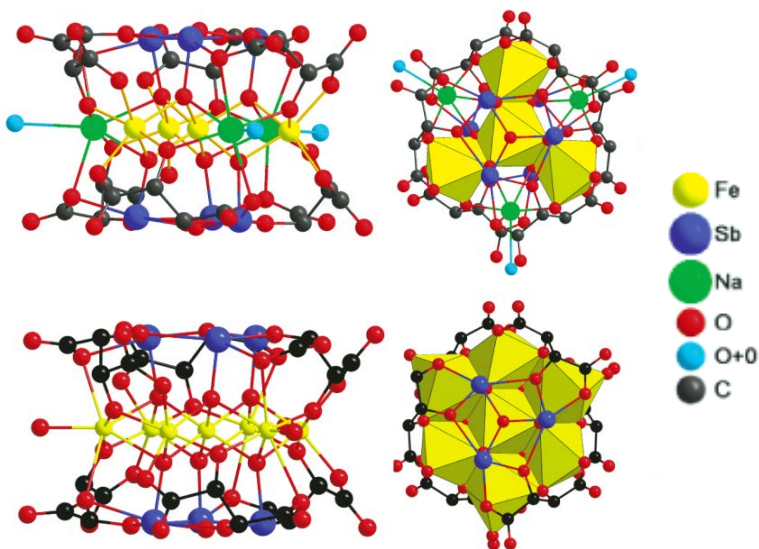


Figure 1.5. Structures of MOFs based on iron-oxo cluster with a chiral antimony tartrate scaffold. (Ref. 55)

MOF Thin Films. Interest in the fabrication of porous coatings has provided the motivation for studies of the deposition of MOFs as thin films. A recent review enumerates the different methods of MOF film preparation, the characteristic features of the products, and the test applications.⁵⁸⁻⁶³ The most studied thin film MOF is HKUST-1 prepared using a range of chemical and electrochemical methods on various substrates from metal or metal oxide films to polymer-oxide beads and textiles. Application-oriented studies such as the stepwise deposition of HKUST-1 on microcantilever or copper electrodes for sensing applications have been reported in literature.⁶³⁻⁶⁷ Moreover, mechanistic studies on the growth of HKUST-1 MOF films have also been the subject of

previous studies such as the effects on the deposition rate with changes on the copper(II) source and the orientation preference on COOH- vs. OH- terminated gold substrates.⁶⁸⁻⁷⁰ Studies with MOF-5 are less common but have been demonstrated for a number of substrates such as graphite, α -alumina, and functionalized gold substrates.⁷¹⁻⁷⁴

1.3. Outline of the Dissertation

This dissertation covers several aspects of MOF synthesis with the ultimate goal of generating crystalline products for structure determination. It includes work that provides support to the viability as well as complexity of reticular chemistry in the field of MOF crystal engineering. It also deals with the investigation of the consequent molecular and bulk-solid properties depending on the structures of the products generated. The linker is limited only to aromatic dicarboxylate compounds that have a linear orientation and function primarily as rigid spacers in the porous framework assembly. Presumably, variation of the length of the linker influences the size of the pores while maintaining the integrity of the SBUs. An added functionality such as chiral centers to the linker design further promotes the MOF assembly to form chiral architectures. The metal cations were mostly the commonly used transition metals such as divalent nickel, zinc, and cobalt, but other metals such as lead and lanthanide metal cations were used in some experiments.

Chapter 2 contains a brief description of the techniques that were employed covering the synthesis, crystal growth, and characterization methods. The basic concepts of the experimental procedure are discussed with explanation on the details that are critical in this investigation.

Synthesis of MOFs using the divalent nickel cation as the metal connector and linear aromatic dicarboxylates as linkers is described in Chapter 3. Crystal structures and their evolution in relation to the length of the dicarboxylate linker used are described in detail. Several different SBUs were generated from slight variations in the synthesis conditions mainly due to the several possible modes of coordination of the dicarboxylate ligands. The result highlights interesting structures for molecular magnetism studies yet shows that MOF assembly is not always predictable and that compounds formed by changing the linker dimension are not always isoreticular.

On the other hand, in Chapter 4 we show that given the right building unit such as a rigid chain SBU, an isoreticular type of synthesis in MOFs is possible. The same set of aromatic dicarboxylate linkers as in Chapter 3 was used as chain linkers to generate an isoreticular series of MOFs based on a homochiral $[\text{Ni}_2\text{O}(\text{Asp})]$ chains. Experiments on the variations in the synthesis conditions and the critical factors such as solvent and pH to obtain the correct product phase were monitored by powder X-ray diffraction.

Chapter 5 focuses on the preparation of new compounds based on a new linker 1,4-phenylenebis(hydroxyacetic acid) primarily designed to exhibit interesting chiral and magnetic properties. The new linker is a benzene analog of tartaric acid; the tartrate ligand has been widely used in MOF synthesis and studied for potential magnetochiral materials. The first examples of crystal data based on the designed linker and divalent metal cations are reported; however, the products obtained all have structures with low dimensionality and are achiral. A comprehensive description of the structures based on the single crystal diffraction data is provided.

New insights on growing thin films of MOF crystals are presented in Chapter 6. The synthesis is based on the zinc-terephthalate (MOF-5) cubic structure grown on top of gold films supported by thiocarboxylate self-assembled monolayers (SAMs). A method of generating dense films of highly-oriented MOF-5 crystals was discovered by treatment of the SAMs with a zinc solution to initiate nucleation at room temperature. Observations regarding the stability of MOF-5 films as well as crystal growth studies are included in the discussion as well as experiments on films of manganese- and lanthanum-formate MOFs.

Last, Chapter 7 is a summary of the results, a discussion of what was learned, some outstanding problems, and suggestions for future work.

1.4. References

1. Eds: Zhou, H.C.; Long, J.R.; Yaghi, O.M. Special Issue on Metal-Organic Frameworks. *Chem. Rev.* **2012**, *112*, 673–1268.
2. Eds: Long, J.R.; Yaghi, O.M. Themed Issue on Metal-Organic Frameworks. *Chem. Soc. Rev.* **2009**, *38*, 1201–1508.
3. Carne, A.; Carbonell, C.; Imaz, I.; Maspoch, D. *Chem. Soc. Rev.* **2011**, *40*, 291–305.
4. Kuppler, R.J.; Timmons, D.J.; Fang, Q.R.; Li, J.R.; Makal, T.A.; Young, M.D.; Yuan, D.; Zhao, D.; Zhuang, W.; Zhoun, H.C. *Coord. Chem. Rev.* **2009**, *253*, 3042–3066.
5. Yaghi, O.M.; Li, Q. *MRS Bulletin* **2009**, *34*, 682–690.
6. Robson, R. *Dalton Trans.* **2008**, 5113–5131.
7. Bureekaew, S.; Shimomura, S.; Kitagawa, S. *Sci. Technol. Adv. Mater.* **2008**, *9*, 014108.

8. Ferey, G. *Chem. Soc. Rev.* **2008**, *37*, 191–214.
9. James, S.L. *Chem. Soc. Rev.* **2003**, *32*, 276–288.
10. Rao, C.N.R.; Cheetham, A.K.; Thirumurugan, A. *J. Phys. Condens. Matter* **2008**, *20*, 083202.
11. Farha, O.K.; Hupp, J.T. *Acc. Chem. Res.* **2010**, *43*, 1166–1175.
12. Yaghi, O.M.; O’Keeffe, M.; Ockwig, N.W.; Chae, H.K.; Eddaoudi, M.; Kim, J. *Nature* **2003**, *423*, 705–714.
13. Kitagawa, S.; Kitaura, R.; Noro, S. *Angew. Chem. Int. Ed.* **2004**, *43*, 2334–2375.
14. Cheetham, A.K.; Ferey, G.; Loiseau, T. *Angew. Chem. Int. Ed.* **1999**, *38*, 3268–3292.
15. Yaghi, O.M.; Li, H.; Davis, C.; Richardson, D.; Groy, T.L. *Acc. Chem. Res.* **1998**, *31*, 474–484.
16. Rosi, N.L.; Eddaoudi, M.; Kim, J.; O’Keeffe, M.; Yaghi, O.M. *Cryst. Eng. Comm.* **2002**, *4*, 401–404.
17. Janiak, C. *Dalton Trans.* **2001**, 2781–2804.
18. Gu, Z.Y.; Yang, C.X.; Chang, N.; Yan, X.P. *Acc. Chem. Res.* **1998**, *31*, 474–484.
19. Dinca, M.; Long, J.R. *Angew. Chem. Int. Ed.* **2008**, *47*, 6766–6779.
20. Farrusseng, D.; Aguado, S.; Pinel, C. *Angew. Chem. Int. Ed.* **2009**, *48*, 7502–7513.
21. Stock, N.; Biswas, S. *Chem. Rev.* **2012**, *112*, 933–969.
22. Natarajan, S.; Mahata, P. *Chem. Soc. Rev.* **2009**, *38*, 2304–2318.
23. Rao, C.N.R.; Natarajan, S.; Vaidhyanathan, R. *Angew. Chem. Int. Ed.* **2004**, *43*, 1466–1496.
24. Furukawa, H.; Kim, J.; Ockwig, N.W.; O’Keeffe, M.; Yaghi, O.M. *J. Am. Chem. Soc.* **2008**, *130*, 11650–11661.

25. Robin, A.Y.; Fromm, K.M. *Coord. Chem. Rev.* **2006**, *250*, 2127–2157.
26. Johnson, J.W.; Jacobson, A.J.; Rich, S.M.; Brody, J.F. *J. Am. Chem. Soc.* **1981**, *103*, 5246–5247.
27. Hoskins, B.F.; Robson, R. *J. Am. Chem. Soc.* **1990**, *112*, 1546–1554.
28. Moulton, B.; Zawarotko, M.J. *Chem. Rev.* **2001**, *101*, 1629–1658.
29. Ockwig, N.W.; Delgado-Friedrichs, O.; O’Keeffe, M.; Yaghi, O.M. *Acc. Chem. Res.* **2005**, *38*, 176–182.
30. Sudik, A.C.; Cote, A.P.; Wong-Foy, A.G.; O’Keeffe, M.; Yaghi, O.M. *Angew. Chem. Int. Ed.* **2006**, *45*, 2528–2533.
31. Zawarotko, M.J. *Nature* **1999**, *402*, 242–243.
32. Zhang, J.; Huang, X.; Chen, X. *Chem. Soc. Rev.* **2009**, *38*, 2385–2396.
33. Eddaoudi, M.; Moler, D.B.; Li, H.; Chen, B.; Reineke, T.M.; O’Keeffe, M.; Yaghi, O.M. *Acc. Chem. Res.* **2001**, *34*, 319–330.
34. Parkash, M.J.; Soo Lah, M.S. *Chem. Commun.* **2009**, 3326–3341.
35. Rosi, N.L.; Eddaoudi, M.; Kim, J.; O’Keeffe, M.; Yaghi, O.M. *Angew. Chem. Int. Ed.* **2002**, *41*, 284–287.
36. Tranchamontagne, D.J.; Mendoza-Cortes, J.L.; O’Keeffe, M.; Yaghi, O.M. *Chem. Soc. Rev.* **2009**, *38*, 1257–1283.
37. Tranchemontagne, D.J.; Ni, Z.; O’Keeffe, M.; Yaghi, O.M. *Angew. Chem. Int. Ed.* **2008**, *47*, 5136–5147.
38. Natarajan, S.; Mandal, S. *Angew. Chem. Int. Ed.* **2008**, *47*, 4798–4828.
39. Perry IV, J.J.; Perman, J.A.; Zawarotko, M.J. *Chem. Soc. Rev.* **2009**, *38*, 1400–1417.
40. Cheetham, A.K.; Rao, C.N.; Feller, R.K. *Chem. Commun.* **2006**, *38*, 4780–4795.

41. Lin, W.; Rieter, W.J.; Taylor, K.M.L. *Angew. Chem. Int. Ed.* **2009**, *48*, 650–658.
42. Almeida Paz, F.A.; Klinowski, J.; Vilela, S.M.F.; Tome, J.P.C.; Cavaleiro, J.A.S.; Rocha, J. *Chem. Soc. Rev.* **2012**, *41*, 1088–1110.
43. Lu, J.Y. *Coord. Chem. Rev.* **2003**, *246*, 327–347.
44. Li, J.R.; Sculley, J.; Zhou, H.C. *Chem. Rev.* **2012**, *112*, 869–932.
45. Go, Y.B.; Wang, X.; Anokhina, E.V.; Jacobson, A.J. *Inorg. Chem.* **2005**, *44*, 8265–8271.
46. Derrickson, K.J. M.S. Thesis, University of Houston, **2008**.
47. Biemmi, E.; Christian, S.; Stock, N.; Bein, T. *Microporous Mesoporous Mater.* **2009**, *117*, 111–117.
48. Lin, Z.; Wragg, D.S.; Morris, R.E. *Chem. Commun.* **2006**, 2021–2023.
49. Kim, K.; Banerjee, M.; Yoon, M.; Das, S. *Top Curr. Chem.* **2010**, *293*, 115–153.
50. Yoon, M.; Srirambalaji, R.; Kim, K. *Chem. Rev.* **2012**, *112*, 1196–1231.
51. Ma, L.; Abney, C.; Lin, W. *Chem. Soc. Rev.* **2009**, *38*, 1248–1256.
52. Cohen, S.M. *Chem. Rev.* **2012**, *112*, 970–1000.
53. Kurmoo, M. *Chem. Soc. Rev.* **2009**, *38*, 1353–1379.
54. Wang, X.; Liu, L.; Conato, M.; Jacobson, A.J. *Cryst. Growth Des.* **2011**, *11*, 2257–2263.
55. Gao, Q.; Wang, X.; Conato, M.T.; Makarenko, T.; Jacobson, A.J. *Cryst. Growth Des.* **2011**, *11*, 4632–4638.
56. Train, C.; Gruselle, M.; Verdaguer, M. *Chem. Soc. Rev.* **2011**, *40*, 3297–3312.
57. Train, C.; Gheorghe, R.; Krstic, V.; Chamoreau, L.M.; Ovanesyan, N.S.; Rikken, G.L.J.A.; Gruselle, M.; Verdaguer, M. *Nat. Mater.* **2008**, *7*, 729–734.

58. Fischer, R.A.; Woll, C. *Angew. Chem. Int. Ed.* **2009**, *48*, 6205–6208.
59. Makiura, R.; Motoyama, S.; Umemura, Y.; Yamanaka, H.; Sakata, O.; Kitagawa, H. *Nat. Mater.* **2010**, *9*, 565–571.
60. Shekhah, O.; Liu, J.; Fischer, R.A.; Woll, C. *Chem. Soc. Rev.* **2011**, *40*, 1081–1106.
61. Zacher, D.; Schmid, R.; Woll, C.; Fischer, R.A. *Angew. Chem. Int. Ed.* **2011**, *50*, 176–199.
62. Zacher, D.; Shekhah, O.; Woll, C.; Fischer, R.A. *Chem. Soc. Rev.* **2009**, *38*, 1418–1429.
63. Betard, A.; Fischer, R.A. *Chem. Rev.* **2012**, *112*, 1055–1083.
64. Biemmi, E.; Darga, A.; Stock, N.; Bein, T. *Microporous Mesoporous Mater.* **2008**, *114*, 380–386.
65. Biemmi, E.; Scherb, C.; Bein, T. *J. Am. Chem. Soc.* **2007**, *129*, 8054–8055.
66. Zacher, D.; Baunemann, A.; Hermes, S.; Fischer, R.A. *J. Mater. Chem.* **2007**, *17*, 2785–2792.
67. Ameloot, R.; Stappers, L.; Fransaer, J.; Alaerts, L.; Sels, B.F.; De Vos, D.E. *Chem. Mater.* **2009**, *21*, 2580–2582.
68. Guo, H.; Zhu, G.; Hewitt, I.J.; Qiu, S. *J. Am. Chem. Soc.* **2009**, *131*, 1646–1647.
69. Hermes, S.; Schroder, F.; Chelmowski, R.; Woll, C.; Fischer, R.A. *J. Am. Chem. Soc.* **2005**, *127*, 13744–13745.
70. Shekhah, O.; Wang, H.; Zacher, D.; Fischer, R.A.; Woll, C. *Angew. Chem. Int. Ed.* **2009**, *48*, 5038–5041.
71. Hermes, S.; Zacher, D.; Baunemann, A.; Woll, C.; Fischer, R.A. *Chem. Mater.* **2007**, *19*, 2168–2173.

72. Scherb, C.; Schodel, A.; Bein, T. *Angew. Chem. Int. Ed.* **2008**, *47*, 5777–5779.
73. Yoo, Y.; Jeong, H.K. *Chem. Commun.* **2008**, 2441–2443.
74. Liu, Y.; Ng, Z.; Khan, E.A.; Jeong, H.K.; Ching, C.B.; Lai, Z. *Microporous Mesoporous Mater.* **2009**, *118*, 296–301.

Chapter 2

Experimental

2.1. Synthesis

Solvothermal Synthesis. The synthesis method used in this work for the preparation of metal-organic compounds is the solvothermal process. The synthesis involves chemical reactions of substances using a particular solvent heated in a sealed container at above ambient temperature and pressure.¹⁻² In particular, hydrothermal methods (water as the solvent) have proven effective in the synthesis of zeolites, metal oxides, chalcogenides, and other microporous materials.³⁻⁶ The use of non-aqueous solvents, i.e., solvothermal synthesis is an extension of the method to generate new crystalline phases and more structurally interesting materials including multifunctional coordination polymers.⁷⁻⁹

Typical reactions were carried out in 23-mL Teflon-lined stainless steel Parr autoclaves for 2-7 days at a temperature range of 150-180 °C under autogenous pressure. The autoclaves were placed in a Thermolyne Oven, Series 9000, preheated to a desired temperature and the cooling rate adjusted by a Eurotherm 91e controller. Parameters such as reactant concentration, oven temperature, cooling rate, reaction time, solvent system, and the amount of base were systematically varied to obtain pure phases of the product.

Preparation of Single Crystals. The synthetic methods used over the course of the study are solution crystallization techniques with the intent of growing crystals large enough for single crystal X-ray diffraction study.¹⁰ Several methods proved successful in

generating single crystals such as the classic ‘test tube layer-diffusion’ and the ‘Teflon bag’ solvothermal techniques.

The ‘Teflon-bag’ solvothermal technique is a variation of a regular solvothermal experiment with the reacting solids encased in a Teflon-bag membrane and placed in the Teflon liner with the solvent situated outside of the bag for slow diffusion. Single crystals of new nickel-dicarboxylate phases (**3-1**, **3-2**, **3-3**, **3-4** and **3-5**) were obtained using this technique (see Chapter 3). Single crystals of Ni^{2+} (**5-1**) and Pb^{2+} (**5-4**) with the *meso*-1,4-phenylenebis(hydroxyacetic acid) (**H₂L**) ligand, on the other hand, were generated by conventional hydrothermal synthesis without the need of a Teflon-bag membrane (see Chapter 5).

In the ‘test tube layer-diffusion’ technique, an organic ligand dissolved in a solvent is layered on top of a metal salt solution. Slow inter-diffusion of the reacting components afforded single crystals of Co^{2+} (**5-2**) and Zn^{2+} (**5-3**) with the **H₂L** ligand (see Chapter 5). A method of preparing highly oriented single crystals of zinc terephthalate (MOF-5) on top of functionalized gold films was also developed and this approach involves the introduction of nucleation sites before placing the material in the crystallization solution (see Chapter 6).

The production of single crystals on the nickel-aspartate-dicarboxylate systems, however, proved very elusive. Most of the single crystals obtained from many attempts were unwanted phases of nickel aspartate or nickel dicarboxylate with structures that have already been reported in the published literature (see Chapter 4).

For documentation purposes, optical images of the crystals were obtained using the Olympus BX41 microscope equipped with an Olympus DP12 digital camera. The

optical micrographs were also used for particle size-distribution analysis with the aid of the ImageJ¹¹ software (see Chapter 6).

2.2 Characterization

X-ray Crystallography. Crystal structures of the products were determined by single crystal X-ray diffraction whenever possible. In general, a single crystal of suitable dimension (ca. 0.1 mm × 0.1 mm × 0.1 mm) was carefully selected, picked up with a glass fiber-pin, and mounted on a goniometer. An N₂ cold stream was used to lower the temperature to 213 K. Low temperature measurement ensures that volatile components such as solvent molecules remain in the crystal throughout the experiment. The strategy is also helpful during the refinement of the data for compounds containing disordered molecules by locking them in fixed positions. X-ray measurements were performed using monochromated Mo K α radiation ($\lambda = 0.71073 \text{ \AA}$) on a Siemens SMART platform diffractometer equipped with a CCD area detector. Data collection, cell refinement and data reduction were performed using the APEX2 system.¹² Full data collection on a hemisphere of 1271 frames at 5 cm detector distance was performed using a narrow-frame method with scan widths of 0.30° in ω at an exposure time of 30 – 40 s per frame. Data were corrected for Lorentz factor, polarization, and X-ray absorption due to the variation in the path length through the detector faceplate. The maximum correction applied to the intensities was <1%. All structures were solved by direct methods using SHELXS97 and refined by difference Fourier techniques using SHELXL97, programs in the WinGX package.¹³ All non-hydrogen atoms were refined anisotropically. Hydrogen atoms were either located from difference maps or placed according to calculated

geometries in riding mode on the position of the parent atom. Molecular graphics and structure representations were made using the DIAMOND visualization software.¹⁴

Initial characterization of the products was performed by powder X-ray diffraction (PXRD) using the PANalytical X’Pert PRO diffractometer. The machine operates using a Cu target radiation ($\lambda = 1.54187 \text{ \AA}$) and an X’Celerator detector. Carefully-dried products were ground to fine powder and mounted flat on the sample holder before being placed on the powder diffractometer. In most cases, data were collected over the range 5-50° in 2θ with a step width of 0.008° and step time 0.067 s per step. The intensity and peak positions in the diffraction pattern are characteristic features of a substance and can be used for identification and/or determination of the purity of the phases present in the sample.¹⁵ For compounds **4-1** to **4-4**, high resolution PXRD data with 2θ range of 5-70° and a step width of 0.004° were used in the refinement of the lattice parameters using the GSAS software.¹⁶ The profile fits were then used to deduce the structures of the compounds by comparison with the known structure of [Ni_{2.5}(OH)(L-Asp)₂]·6.55H₂O.¹⁷ The abovementioned PXRD machine also used to perform high-temperature measurements to monitor temperature-dependent phase transformations of compound **4-1** (see Chapter 4). For MOF-5 film samples, X-ray diffraction was performed by placing the coated gold films directly on the machine with the zero point error accounted for by the characteristic Au peaks in the powder pattern (see Chapter 6).

Spectroscopic Analyses. Infrared (IR) analysis is a spectroscopic technique based on the resonant frequencies of the vibrational modes at which bonds in a molecule absorb.¹⁸ The IR spectra generated from the samples provide useful information regarding the types of bonds present in the structure especially the state of the organic

ligand component. For example, the technique can distinguish different modes of carboxylate binding to a metal through the magnitude of separation between the carboxylate stretches $\Delta = \nu_{as}(\text{COO}^-) - \nu_s(\text{COO}^-)$; values of $\Delta < 120 \text{ cm}^{-1}$ indicate chelating carboxylate group or a *syn-anti* bridging mode, $\Delta = 170 \pm 10 \text{ cm}^{-1}$ for ionic COO^- or *syn-syn* bridging coordination and $\Delta > 180 \text{ cm}^{-1}$ typical for monodentate coordination.¹⁹ It can also be used to establish the presence of water and solvent molecules with distinct group functionalities. Infrared (IR) measurements were performed on the Galaxy Series FTIR 5000 spectrometer in the range 400 to 4000 cm^{-1} at ambient conditions. Small amount of the sample was finely ground and thoroughly mixed with spectroscopic grade potassium bromide (KBr) and the mixture pressed on a hydraulic press forming a translucent pellet. The KBr pellet was then mounted on the spectrometer for data collection. The spectrum obtained establishes a database for new compounds or serves as a quick verification of the identity of previously reported compounds.

Another standard spectroscopic technique used in this work is the proton nuclear magnetic resonance (¹H-NMR) spectroscopy. This technique has been a routine tool in organic synthesis to elucidate structures of compounds based on the chemical shifts of a proton in accordance to the magnetic field surrounding it.²⁰ ¹H-NMR and IR spectroscopic analyses were applied to the ligand **H₂L** to determine the structure and purity of the synthesized product (see Chapter 5). A few milligrams of the compound was dissolved in deuterated chloroform solvent and transferred to a 5 mm NMR glass tubes then mounted to the NMR machine. The experiment was performed on the QE-300 (300 MHz) NMR system and the data was processed using NUTS²¹ software.

Thermogravimetric Analysis. The compounds were evaluated by thermogravimetric analysis which monitors the weight changes of the sample as a function of temperature.²² This analytical technique is a good confirmatory tool regarding the structural composition of the compounds previously determined by single crystal X-ray diffraction. Loss of solvent or guest molecules and coordinated ligands as well as the stepwise decomposition of the products can be quantitatively determined using TGA. The analysis was performed using Hi-Res TGA 2950 thermogravimetric system, usually starting from room temperature to 800 °C at a heating rate of 1 °C min⁻¹. Approximately 15 mg of the pure phase sample was placed on a platinum pan and mounted on a microbalance situated in the middle of the instrument's furnace before the start of an experiment. Compressed air was the gas of choice for the experiment to allow complete oxidation of the final residue into a known metal oxide form. The residue at the end of the analysis was monitored by powder X-ray diffraction for phase identification.

Magnetic Property Analysis. A fundamental characterization tool in transition metal chemistry is the determination of magnetic properties. Compounds **3-1** to **3-5**, for example, are interesting materials for magnetochemical studies because of the divalent nickel ions arranged as trimers and tetramers (see Chapter 3). Magnetic properties of these compounds were investigated using vibrating-sample magnetometry (VSM) which measures the magnetic moment of a sample as it is vibrated perpendicular to a magnetic field.²³ Around 15 mg of sample were placed on a polypropylene powder sample holder, fixed on the center of a brass trough, and positioned at the magnetometer. The experiment was conducted using the Quantum Design Physical Property Measurement System (QD-PPMS) equipped with a VSM accessory in the temperature range 2 to 300 K

at an applied field of 1000 Oe. Measurements were made in both zero-field cooled (ZFC) and field cooled (FC) conditions; the difference between the two modes is the application of magnetic field on the sample while cooling on the FC mode but not on the ZFC mode. Magnetization and hysteresis loop experiments were performed using a maximum field of 50000 Oe.

2.3. References

1. Stein, A.; Keller, S.W.; Mallouk, T.E. *Science* **1993**, *259*, 1558–1564.
2. Rabenau, A. *Angew. Chem Int. Ed. Engl.* **1985**, *24*, 1026–1040.
3. Cundy, C.S.; Cox, P.A. *Chem. Rev.* **2003**, *103*, 663–701.
4. Whittingham, M.S.; Guo, J.D.; Chen, R.; Chirayil, T.; Janauer, G.; Zavalij, P. *Solid State Ionics* **1995**, *75*, 257–268.
5. Yang, Y.T; Ibers, J.A. *J. Solid State Chem.* **1999**, *147*, 366–371.
6. Feng, S.; Xu, R. *Acc. Chem. Res.* **2001**, *34*, 239–247.
7. Demazeau, G. *J. Physics:Conf. Ser.* **2008**, *121*, 082003.
8. Walton, R.I. *Chem. Soc. Rev.* **2002**, *31*, 230–238.
9. Zhao, Y.; Li, K.; Li, J. *Z. Naturforsch.* **2010**, *65b*, 976–998.
10. Hullinger, J. *Angew. Chem. Int. Ed. Engl.* **1994**, *33*, 143–162.
11. Rasband, W.S. ImageJ; U. S. National Institutes of Health, Bethesda, Maryland, USA, <http://imagej.nih.gov/ij/>, **2011**.
12. *APEX2 User Manual*, Version 1.27; Bruker AXS Inc.: Madison, WI, **2005**.
13. Farrugia, L.J. *J. Appl. Cryst.* **1999**, *32*, 837–838.
14. Brandenburg, K. *DIAMOND*; Crystal Impact GbR, Bonn, Germany, **2006**.

15. Jenkins, R.; Snyder, R. *Introduction to X-ray Powder Diffractometry*, John Wiley and Sons: New York, **1996**.
16. Larson, A.C.; Von Dreele, R.B. *General Structure Analysis System (GSAS)*; Report LAUR 86-748, Los Alamos National Laboratory, **1994**.
17. Anokhina, E.V.; Go, Y.B.; Lee, Y.; Vogt, T.; Jacobson, A.J. *J. Am. Chem. Soc.* **2006**, 128, 9957–9962.
18. Nakamoto, K. *Infrared and Raman Spectra of Inorganic and Coordination Compounds*, John Wiley and Sons: New York, **1997**.
19. Zelenak, V.; Vargova, Z.; Gyoryova, K. *Spectrochim. Acta, Part A* **2007**, 66, 262–272.
20. Silverstein, R.M.; Webster, F.X. *Spectrometric Identification of Organic Compounds*, John Wiley and Sons: New York, **1997**.
21. *NUTS NMR Data Processing Software*, Demo version; Acorn NMR Inc., Livermore, CA, **2011**.
22. Wendlandt, W. W. *Thermal Analysis*, John Wiley and Sons, New York, **1986**.
23. Foner, S. *Rev. Sci. Instr.* **1959**, 30, 548–557.

Chapter 3

Getting Connected: Trimeric and Tetrameric Clusters of Nickel(II) Octahedra in Metal-Organic Frameworks Based on Aromatic Dicarboxylates

3.1. Introduction

The use of linked metal-organic polyhedra has been one of the cornerstones for the design of metal-organic frameworks (MOFs).¹⁻³ The many choices available for secondary building units and organic linkers has provided opportunities for the construction of novel architectures many with interesting physical properties.⁴⁻¹⁰ In particular, MOFs based on transition metals can show extended magnetic properties via coupling of the paramagnetic metal centers through the bridging organic linkers.¹⁰⁻¹¹ Magnetic coupling can be influenced by several factors such as the nature of metal connectivity, length of the linkers, and inclusion of guest molecules.¹²⁻¹⁴ Hence, an investigation of different configurations of similar metal cluster building units can provide support for the continuing development of magneto-structure relationships and the design of functional magnetic materials.

In MOFs, secondary building units comprised of metal oxoclusters, chains, or layers are linked by rigid and robust aromatic carboxylates to produce frameworks with high thermal stability.¹⁵⁻¹⁶ A drawback of the use of these ligands is that the different modes of coordination for the two oxygen atoms on every carboxylate group may give rise to different structures.¹⁷⁻¹⁹ This study involved linkers with coordinating carboxylate groups that are in a linear conformation with varying distances between them. The

transition metal connector was confined to divalent nickel to limit the possibilities due to variations of the central-atom coordination geometry.

The solvothermal syntheses, crystal structures, and characterization of a series of metal organic frameworks (MOFs), showing a variety of 2D and 3D architectures, based on dicarboxylate-bridged nickel(II) octahedra are reported in this chapter. Two layered compounds $\text{Ni}_3(1,4\text{-BDC})_3(\text{DMF})_2(\text{DMA})_2$ (**3-1**) and $\text{Ni}_3(1,4\text{-BDC})_3(\text{DMF})_4$ (**3-2**) [1,4-BDC = terephthalate, DMF = *N,N'*-dimethylformamide, and DMA = dimethylamine], and a framework compound $\text{Ni}_3(2,6\text{-NDC})_3(\text{DMF})_2(\text{DMA})_2$ (**3-3**) [2,6-NDC = naphthalate] were shown to have similar linear trinuclear nickel building units while the interpenetrated framework compound $\text{Ni}_3(\mu_3\text{-O})(4,4'\text{-BPDC})_3(\text{DMA})_3$ (**3-4**) [4,4'-BPDC = 4,4'-biphenyldicarboxylate] is based on a triangular trimeric nickel oxo-building unit. An unprecedented type of a tetrameric nickel building unit is found in the framework compound $\text{Ni}_4(\mu_3\text{-O})(1,4\text{-NDC})_4(\text{DMF})_2(\text{DMA})_2$ (**3-5**) [1,4-NDC = 1,4-naphthalenedicarboxylate]. Magnetic susceptibility data were collected for an initial assessment of their magnetic behavior based on the different configurations of the cluster building units.

3.2. Experimental Section

Materials and Measurements. All chemicals used in the synthesis were obtained commercially and used without further purification. Solvothermal reactions were carried out in 23-mL Teflon-lined Parr autoclaves at 150 to 180 °C for 48 to 96 h using *N,N*-dimethylformamide (DMF) as the solvent. Elemental analyses were performed by Galbraith Laboratories (Knoxville, TN). Infrared (IR) spectra were

recorded from KBr pellets using the Galaxy Series FTIR 5000 spectrometer in the range 400 to 4000 cm⁻¹. Thermal analyses were conducted on a Hi-Res TGA 2950 thermogravimetric (TG) analyzer from room temperature to 800 °C at a heating rate 1 °C min⁻¹ in air. Powder X-ray diffraction (PXRD) patterns were measured using the PANalytical X’Pert Pro powder diffractometer with a Cu target ($\lambda = 1.54187 \text{ \AA}$). Magnetic susceptibility data were collected on ground single crystalline samples using a Quantum Design Physical Property Measurement System (QD-PPMS) in the temperature range 2 to 300 K with an applied field of 1000 Oe. Hysteresis loops were monitored at temperatures below the observed transition temperatures using a maximum field of 50000 Oe.

Synthesis of Ni₃(1,4-BDC)₃(DMF)₂(DMA)₂ (3-1). A mixture of 95 mg (0.4 mmol) NiCl₂·6H₂O, 67 mg (0.4 mmol) 1,4-H₂BDC, 0.02 mL and 5 mL DMF was heated in a 23-mL Teflon-lined Parr autoclave at 170 °C for 96 h. Pale green plates were recovered by filtration, washed with DMF, and dried in air. Yield: 91% based on Ni. Anal. Calc. for Ni₃C₃₂O₁₄N₃H₃₂: C, 44.8%; H, 3.8%; N, 4.9%; Ni, 20.5%. Found: C, 44.2%; H, 4.5%; N, 5.6%; Ni, 19.9%.

Synthesis of Ni₃(1,4-BDC)₃(DMF)₄ (3-2). The same preparation described for the synthesis of **3-1** was used only at a lower temperature of 150 °C. Pale yellow-green plates were recovered by filtration, washed with DMF, and dried in air. Yield: 80% based on Ni. Anal. Calc. for Ni₃C₃₆O₁₆N₄H₄₀: C, 45.0%; H, 4.2%; N, 5.3%; Ni, 18.3%. Found: C, 44.6%; H, 4.4%; N, 5.7%; Ni, 18.5%.

Synthesis of Ni₃(2,6-NDC)₃(DMF)₂(DMA)₂ (3-3). A mixture of 95 mg (0.4 mmol) NiCl₂·6H₂O, 86 mg (0.4 mmol) 2,6-H₂NDC, 0.02 mL and 5 mL DMF was heated

in a 23-mL Teflon-lined Parr autoclave at 180 °C for 72 h. Green crystals were recovered by filtration, washed with DMF, and dried in air. Yield: 90% based on Ni. Anal. Calc. for $\text{Ni}_3\text{C}_{46}\text{O}_{14}\text{N}_4\text{H}_{44}$: C, 52.4%; H, 4.4%; N, 5.3%; Ni, 16.7%. Found: C, 51.6%; H, 4.2%; N, 5.3%; Ni, 16.9%.

Synthesis of $\text{Ni}_3(\mu_3\text{-O})(4,4'\text{-BPDC})_3(\text{DMA})_3$ (3-4). A mixture of 95 mg (0.4 mmol) $\text{NiCl}_2\cdot 6\text{H}_2\text{O}$, 97 mg (0.4 mmol) 4,4'- H_2BPDC , 0.02 mL TEA and 5 mL DMF was heated in a 23-mL Teflon-lined Parr autoclave at 180 °C for 96 h. Green crystals were isolated from a light green powder matrix by sonication and filtration techniques, then washed with DMF, and dried in air. Yield: 45% based on Ni. Anal. Calc. for $\text{Ni}_3\text{C}_{50}\text{O}_{16.5}\text{N}_4\text{H}_{59}$: C, 52.3%; H, 5.2%; N, 4.9%; Ni, 15.3%. Found: C, 53.2%; H, 4.6%; N, 4.3%; Ni 16.0%.

Synthesis of $\text{Ni}_4(\mu_3\text{-O})(1,4\text{-NDC})_4(\text{DMF})_2(\text{DMA})_2$ (3-5). A mixture of 95 mg (0.4 mmol) $\text{NiCl}_2\cdot 6\text{H}_2\text{O}$, 86 mg (0.4 mmol) 1,4- H_2NDC , 0.02 mL TEA and 5 mL DMF was heated in a 23-mL Teflon-lined Parr autoclave at 170 °C for 96 h. Green polyhedral crystals were isolated by filtration, washed with DMF, and dried in air. Yield: 87% based on Ni. Anal. Calc. for $\text{Ni}_4\text{C}_{56}\text{O}_{23}\text{N}_3\text{H}_{53}$: C, 49.1%; H, 3.9%; N, 3.1%; Ni, 17.1%. Found: C, 48.0%; H, 3.8%; N, 3.3%; Ni, 18.0%.

X-ray Crystallography. Single crystals of each compound with suitable dimensions were carefully selected, picked up with a glass fiber-pin, coated with paraffin oil, and mounted on a goniometer on an X-ray machine with a N_2 cold stream operating at 213 K. Measurements were made using monochromated Mo $\text{K}\alpha$ radiation ($\lambda = 0.71073 \text{ \AA}$) on a Siemens SMART platform diffractometer equipped with a CCD area detector. Data collection, cell refinement, and data reduction were performed using the

APEX2 system.²⁰ All structures were solved by direct methods using SHELXS97 and refined by difference Fourier techniques using SHELXL97 programs on the WinGX package.²¹ Molecular graphics and structure representations were done using the DIAMOND visualization software.²² Crystallographic data for the compounds are summarized in Table 3.1.

3.3. Results and Discussion

Syntheses. All nickel compounds were prepared under solvothermal conditions from the reaction of $\text{NiCl}_2 \cdot 6\text{H}_2\text{O}$ and the dicarboxylic acid ligands in DMF with few drops of TEA added. Compounds **3-1**, **3-2**, and **3-3** were prepared in high-yield as single-crystal products. The synthesis of compound **3-4**, especially at lower temperatures, produced a light green microcrystalline phase with significant amount of single crystals of **3-4** that were easily isolated by successive sonication and filtration. The same technique was employed to separate single crystals of **3-5** from a minor phase of light green powder. The different reaction temperatures used in the preparation of **3-1** (170 °C) and **3-2** (150 °C) influenced the structure of the final products evident from their different powder diffraction profiles. The least temperature sensitive product among the compounds is **3-3**, which is the only phase formed in the 150-180 °C range. The optical microscope images of the crystals are shown in Figure 3.1.

Table 3.1. Crystallographic Data and Structure Refinement for Compounds **3-1** to **3-5**.

Compounds	3-1	3-2	3-3	3-4	3-5
Formula	$\text{Ni}_3\text{C}_{34}\text{O}_{14}\text{N}_4\text{H}_{40}$	$\text{Ni}_3\text{C}_{36}\text{O}_{16}\text{N}_4\text{H}_{40}$	$\text{Ni}_3\text{C}_{46}\text{O}_{14}\text{N}_4\text{H}_{46}$	$\text{Ni}_3\text{C}_{50}\text{H}_{59}\text{O}_{16.5}\text{N}_4$	$\text{Ni}_4\text{C}_{62.5}\text{H}_{64}\text{O}_{21.3}\text{N}_{5.5}$
Formula weight	904.83	960.85	1055.00	1156.14	1467.48
Crystal system	Orthorhombic	Monoclinic	Monoclinic	Hexagonal	Trigonal
Space group	<i>Pbca</i>	<i>P2₁/n</i>	<i>P2₁/n</i>	<i>P6₃/mcm</i>	<i>R-3</i>
<i>a</i> , Å	9.6036(5)	13.9262(8)	11.3876(8)	14.2577(9)	48.857(7)
<i>b</i> , Å	18.2457(9)	9.6614(6)	19.0717(14)	14.2577 (9)	48.857(7)
<i>c</i> , Å	21.0411(10)	16.5066(10)	11.6655(8)	17.3594(11)	14.858(2)
α , degrees	90.00	90.00	90.00	90.00	90.00
β , degrees	90.00	108.989(1)	115.484(1)	90.00	90.00
γ , degrees	90.00	90.00	90.00	120.00	120.00
V , Å ³	3686.9(3)	2100.0(2)	2287.0(3)	3056.1(3)	30713(7)
Z	4	2	2	2	24
Temperature, K	223	223	223	223	223
ρ_c , g cm ⁻³	1.630	1.520	1.532	1.256	1.428
μ (MoK α), mm ⁻¹	1.590	1.404	1.294	0.977	1.163
R1, wR2 [$I > 2\sigma(I)$] ^a	0.0270, 0.0687	0.0273, 0.0736	0.0246, 0.0696	0.0530, 0.1579	0.0444, 0.1150
R1, wR2 (all data) ^a	0.0416, 0.0735	0.0345, 0.0772	0.0322, 0.0721	0.0574, 0.1626	0.0856, 0.1292

^a $R1 = \sum ||F_o| - |F_c|| / \sum |F_o|$; $wR2 = [\sum w(F_o^2 - F_c^2)^2 / \sum w(F_o^2)^2]^{1/2}$

Crystallographic studies have shown that all compounds except **3-2** contain dimethylamine (DMA) which is a product of the thermal decarbonylation of the solvent DMF.²³⁻²⁴ This process is critical for single crystal growth, known to be difficult for nickel terephthalates,²⁵ and also eliminates the necessity of adding chelating amine groups to provide terminating links to limit the number of connected NiO_n polyhedra.²⁵⁻²⁷ Syntheses took advantage of the slow hydrolysis of the solvent at an elevated temperature to form single crystal products.

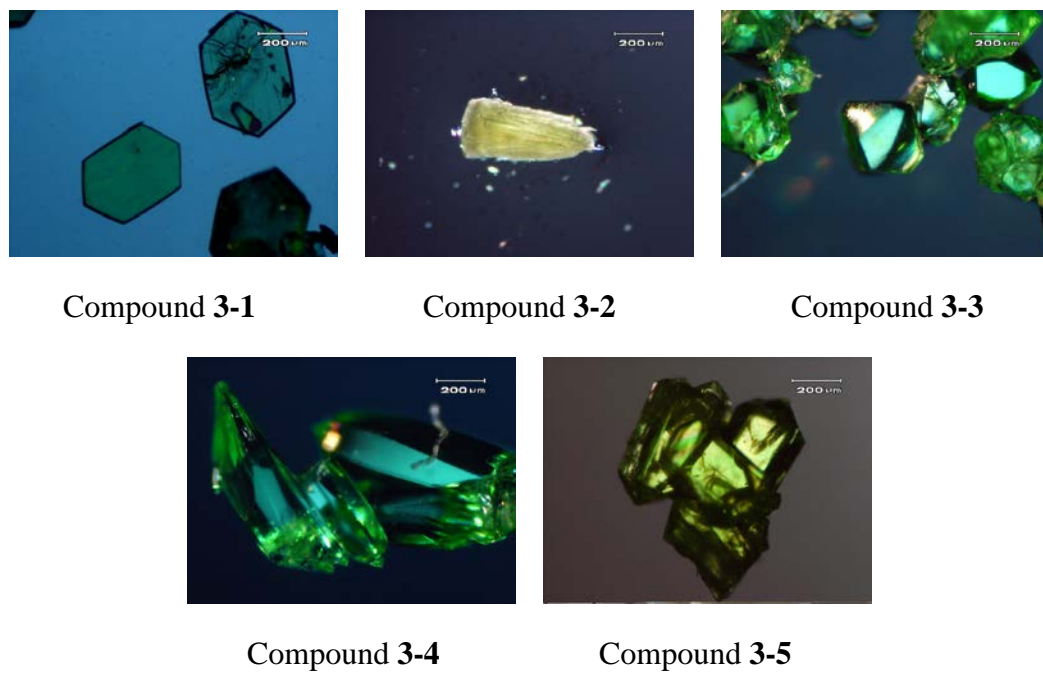


Figure 3.1. Optical microscope images of the crystals **3-1** to **3-5**.

Crystal Structures of $\text{Ni}_3(1,4\text{-BDC})_3(\text{DMF})_2(\text{DMA})_2$ (3-1) and $\text{Ni}_3(1,4\text{-BDC})_3(\text{DMF})_4$, (3-2). Compounds **3-1** and **3-2** are layered structures containing linear trimers of Ni-octahedra bridged by 1,4-BDC ligands in two different coordination modes. (Figure 3.2) Each trimer contains two inequivalent Ni ions; Ni1 at the ends and Ni2 in the center. In both **3-1** and **3-2**, Ni2 at the center of the trimer lies on an inversion center. The coordination environments of the Ni1-O octahedra are completed by DMA and DMF molecules in **3-1** (Figure 3.2a) and DMF molecules in **3-2** (Figure 3.2b) [Ni-O (DMF) distances; 2.1377(1) Å for **3-1** and 2.1022(1) Å for **3-2**]. In **3-2**, the DMF molecules in one coordination site are disordered over two positions. The first type of 1,4-BDC coordination is found in the linking of Ni1 and Ni2 in which the O atoms of the carboxylate bridge the two nickel atoms [Ni-O distances range from 2.0202(1) to 2.0347(1) Å]. In the second type, Ni1 is chelated by two O atoms from one carboxylate group leading to a distorted octahedral environment for Ni1 [Ni-O distance, 2.0746(1) Å and 2.2367(1) Å]. In compound **3-2**, the same coordination is observed except that the two DMA molecules in **3-1** are substituted by two DMF molecules in **3-2** [Ni-O distances range from 2.0098(1) to 2.1746(1) Å]. Each distorted Ni1 octahedra shares a corner with the regular Ni2-O octahedron to form the trimer which is bridged by 1,4-BDC ligands to six other trinuclear units of the same configuration. The resulting structure (Figure 3.2c) contains layers of thickness equal to the length of the trimeric cluster. The layers are stacked by weak van der Waals interactions of the DMA/DMF (**3-1**) or DMF molecules (**3-2**) oriented as spacers between two adjacent layers (Figure 3.2d).

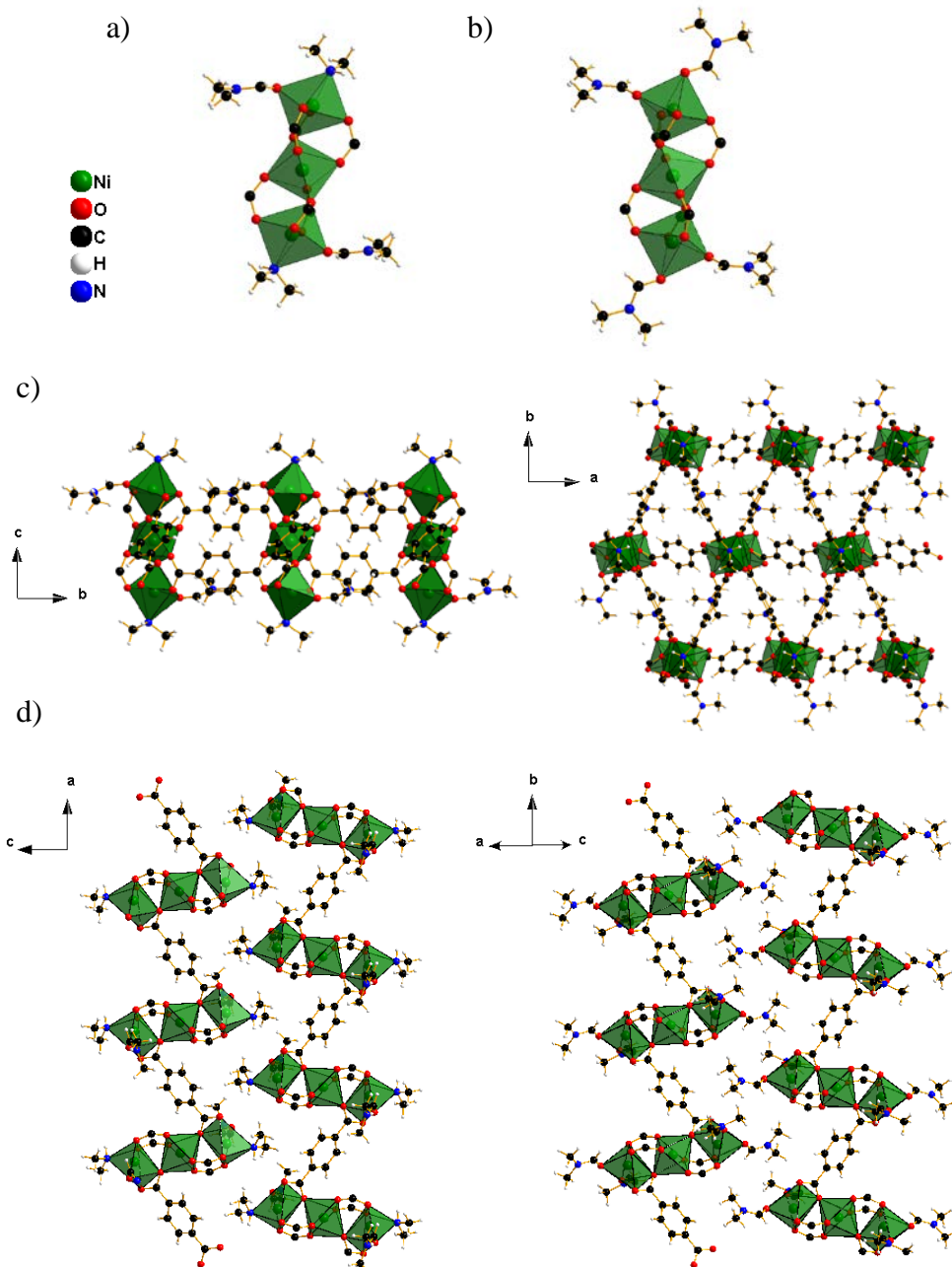


Figure 3.2. a) The trimer in **3-1**; b) the trimer in **3-2**; c) view looking parallel and perpendicular to the layer in **3-1**; d) the stacking of the layers in **3-1** and **3-2**.

Crystal Structure of Ni₃(2,6-NDC)₃(DMF)₂(DMA)₂ (3-3). Compound **3-3** is a three dimensional framework containing a trinuclear nickel building unit similar to the one found in **3-1** and **3-2** but with 2,6-NDC as the bridging ligand. Similar to the arrangement in **3-1** and **3-2**, six 2,6-NDC ligands including two chelating carboxylates connect each trimeric unit to six other similar building units [Ni-O distances range from 2.0176(1) to 2.1660(1) Å]. However, the bulkiness of the naphthalene rings and the offset of the bridging carboxylate groups favor the formation of a 3D network rather than the layers found in **3-1** and **3-2**. The framework structure comprises stepped layers of trimers. The bridging carboxylate units connect the trimers into a four-corner net (Figure 3.3a). Adjacent layers that are offset are connected by the 2,6-NDC groups that chelate the Ni ions. The trimer connectors are oriented such that the DMF and DMA molecules partially occupy the one dimensional channels formed along the *c*-axis [Ni-O distance, 2.0935(1) Å and Ni-N distance, 2.0679(2) Å] (Figure 3.3b). No other guest molecules are located inside these channels. A similar structure based on the same trimeric building unit of nickel(II) and the 2,6-NDC linker but with the use of a terminating amine ligand, has been reported previously.²⁸

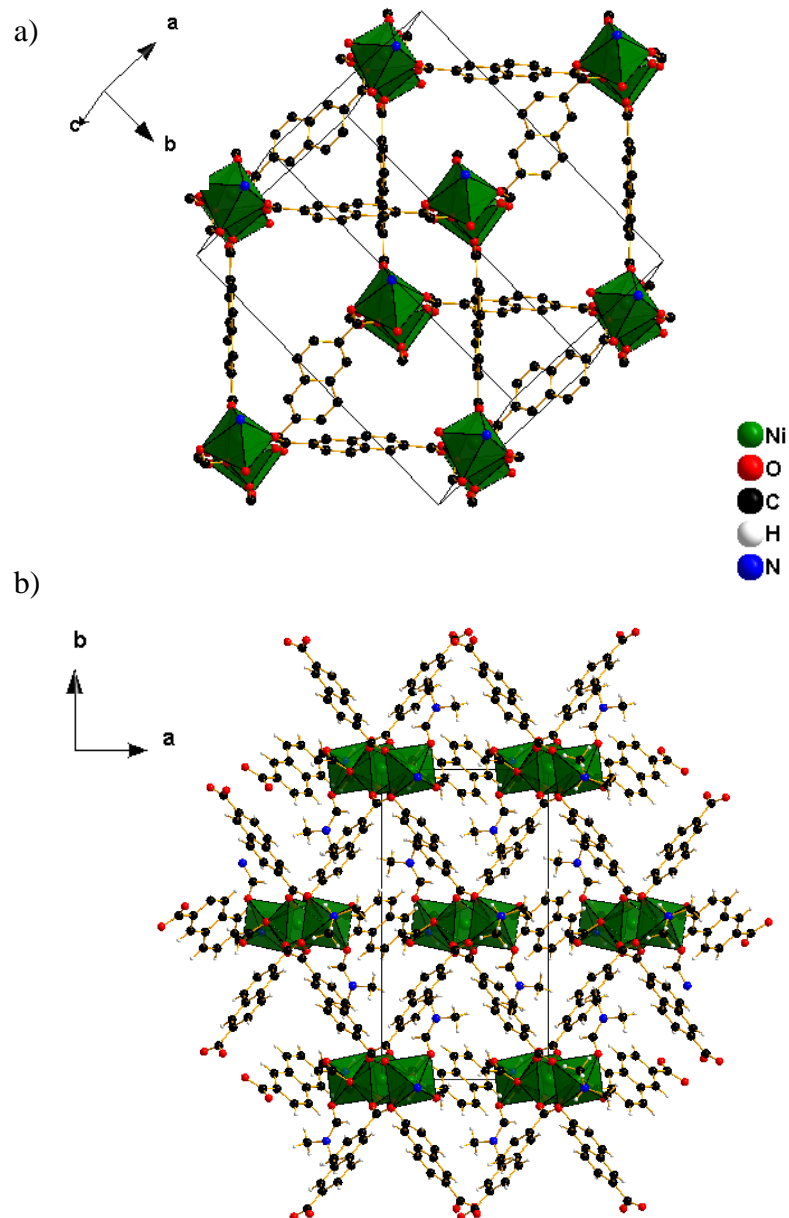


Figure 3.3. a) The arrangement of trimers in **3-3** formed by the bridging 2,6-NDC ligands into a three-dimensional framework; b) a view down *c* showing the coordinated DMF molecules occupying channels in the structure.

Crystal Structure of Ni₃(μ₃-O)(4,4'-BPDC)₃(DMA)₃ (3-4). Compound **3-4** is an interpenetrated framework consisting of a μ₃-oxo-centered trimeric nickel oxo-cluster bridged by 4,4'-BPDC ligands (Figure 3.4). The nickel atoms are octahedrally coordinated by five oxygen atoms and one nitrogen atom. Four of the oxygen atoms are from four different dicarboxylate ions [Ni-O distance, 2.0090(1) Å], one μ₃-O atom is shared by three Ni1 atoms [Ni-O distance, 2.0498(1) Å]. The N atom from the coordinated DMA molecule occupies the sixth coordination site [Ni-N distance, 2.1289(1) Å] (Figure 3.4a). Each 4,4'-BPDC ligand bridges in a *bis*-bidentate fashion with each carboxylate oxygen atom a member of a distinct Ni-octahedron. The building unit of three μ₃-oxo corner-shared nickel octahedra is connected to six other identical trimeric units via 4,4'-BPDC linkers forming a 3D networked structure (Figure 3.4b). This triangular trimeric nickel building unit has been observed previously with other ligands in framework structures which show gas absorption properties.²⁹⁻³⁰ Two-fold interpenetration is observed in the structure of **3-4** because of the long 4,4'-BPDC linkers, though the interpenetrated structure still leaves enough space to accommodate disordered dimethylamine guest molecules (Figure 3.5).

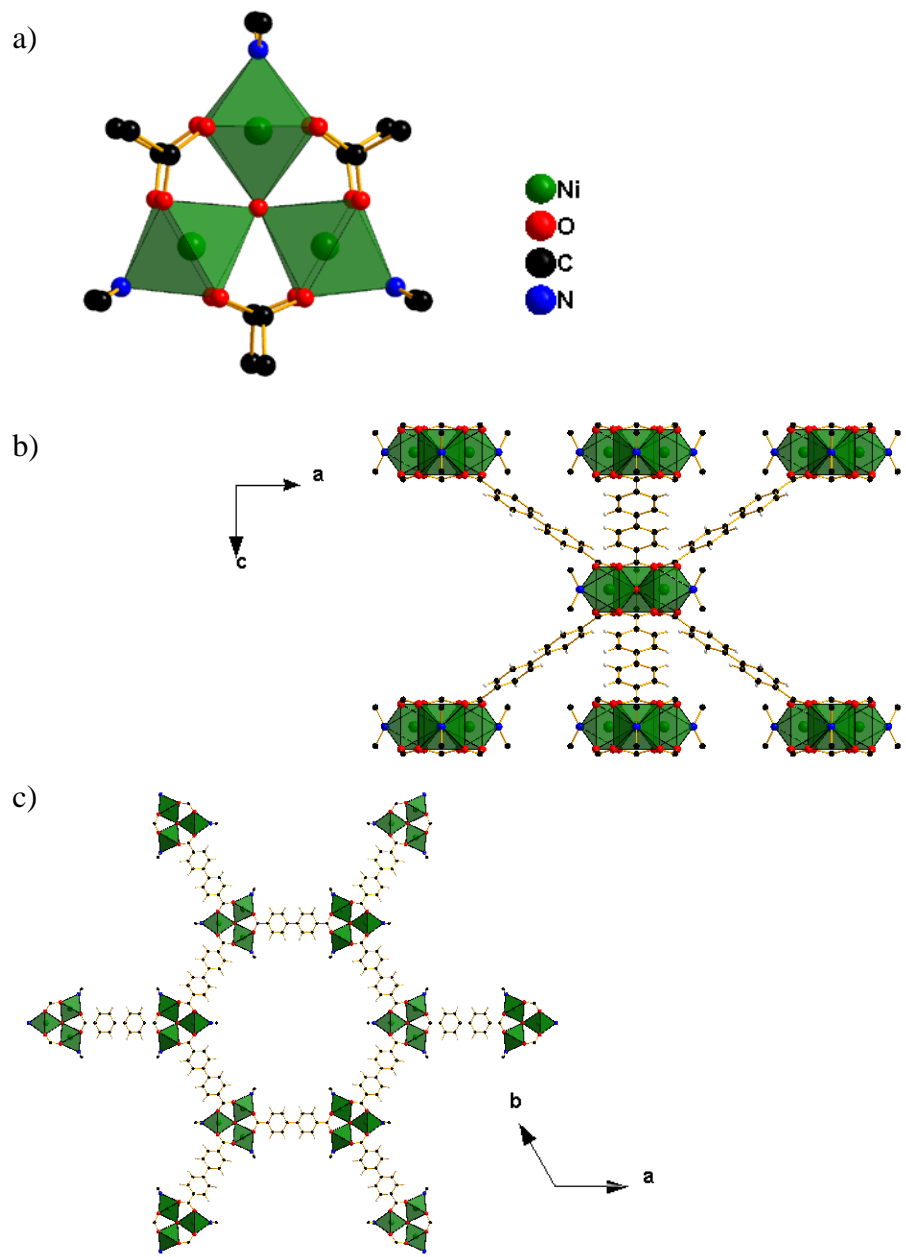


Figure 3.4. a) The μ_3 -oxo-centered trimeric nickel oxo-cluster in **3-4**; b&c) projection of the structure along the *b* and *c* axis showing the connections between the trimers.

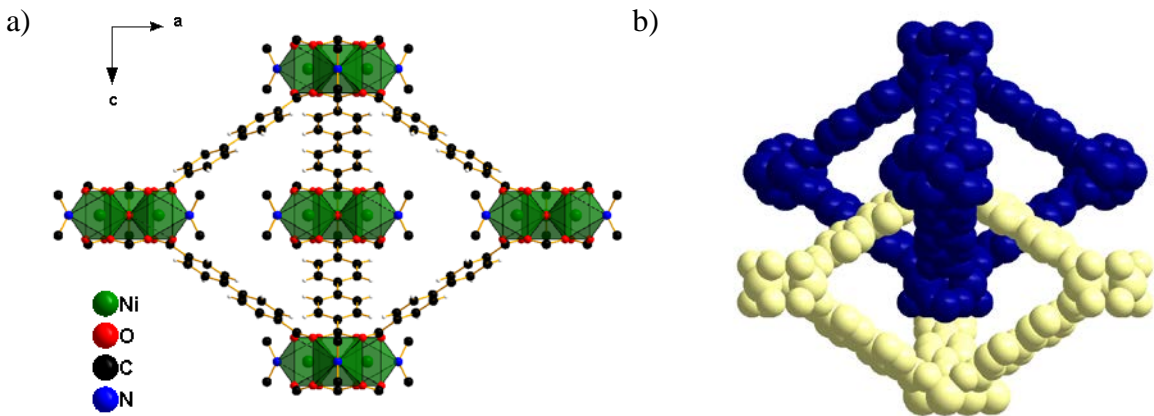


Figure 3.5. a) A view of the structure of **3-4** along *b* showing the cluster connectivity; b) the two interpenetrated frameworks.

Crystal Structure of $\text{Ni}_4(\mu_3\text{-O})(1,4\text{-NDC})_4(\text{DMF})_2(\text{DMA})_2$ (3-5**).** Compound **3-5** is a complex 3D framework that was obtained by using 1,4-naphthalenedicarboxylic acid (1,4-H₂NDC) as the linker. The dicarboxylate groups in this ligand are also arranged in a linear conformation, but the added phenyl ring resulted in the formation of an unprecedented type of tetranuclear nickel oxo building unit. (Figure 3.6) The building unit is made up of a $\mu_3\text{-O}$ trinuclear nickel bridged by dicarboxylates with an added edge-shared nickel octahedra attached to one of the trimer units [Ni-O distances range from 1.9704(41) to 2.1392(28) Å]. The tetranuclear units are connected to eight other connectors by the dicarboxylate linker exhibiting almost every possible coordination modes. This resulted to an intricate framework that generated three types of pores with unique characteristics; (1) a large channel surrounded by six tetranuclear units, (2) a smaller triangular cavity surrounded by three tetranuclear units, and (3) some elongated

holes oriented in different directions surrounded by four tetranuclear units. Disordered guest molecules were located inside the channels corresponding to DMA, DMF, and water.

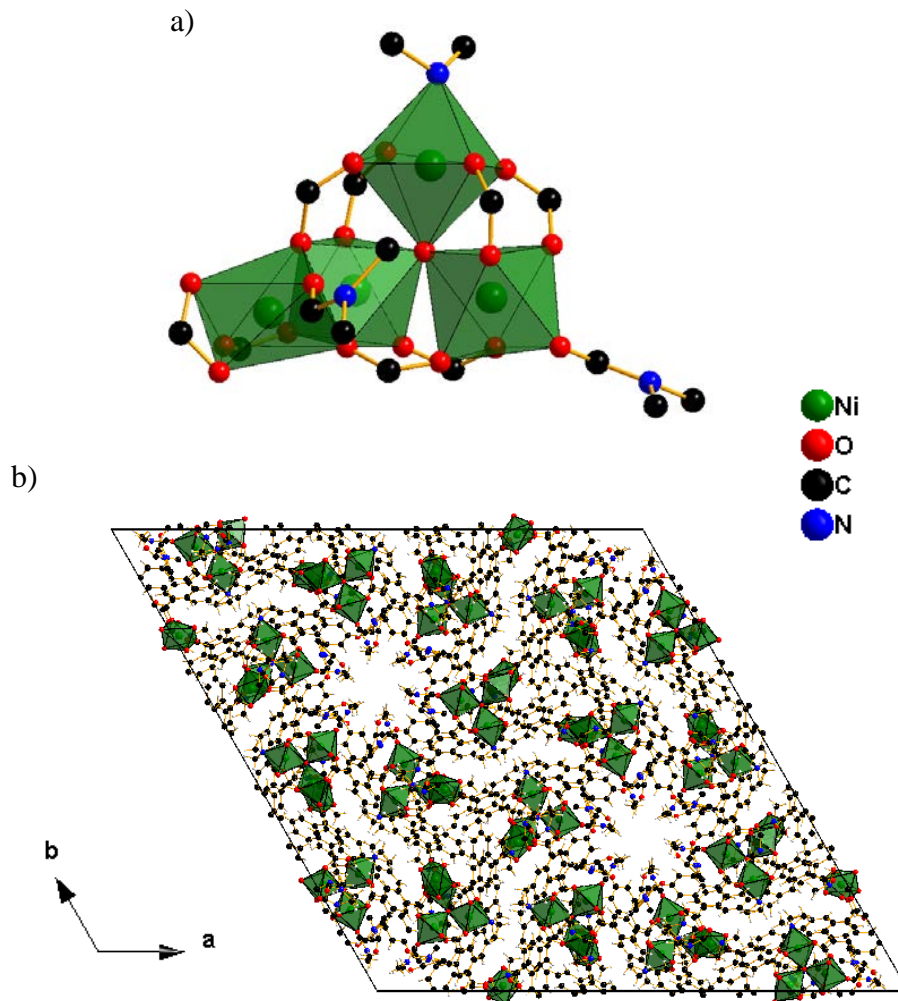


Figure 3.6. a) The tetrameric building unit in **3-5**; b) a projection of the structure down *c* showing the channel arrangement.

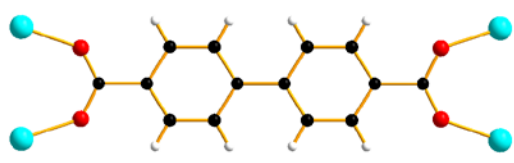
Coordination Modes of the Dicarboxylate Bridges. The apparent diversity of nickel-dicarboxylate structures observed is rationalized by the variety of coordination

modes exhibited by different dicarboxylate linkers. Shown in Figure 3.7 are the coordination and bridging modes of the four dicarboxylate linkers. Different dimensionality was observed in compounds **3-1** and **3-2** (2D) compared to **3-3** (3D) with the same structural building unit and coordination modes of 1,4-BDC and 2,6-NDC ligands, respectively. Each linker bridges two nickel cations of a building unit to two nickel cations of the other building unit in two different modes. A typical bidentate mode, with one oxygen atom connected to a discrete nickel atom and a chelated-bidentate coordination, wherein one of the carboxylate oxygen is connected to two nickel atoms, permits the linear trimeric-nickel configuration of the building units. The differing dimensionality, apparently, is a not consequence of the coordination modes but rather of the geometry on how the distorted octahedral SBUs of **3-1**, **3-2** and **3-3** are bridged to each other in three dimensional space. The 4,4'-BPDC linker in compound **3-4** displayed a uniform *bis*-bidentate coordination and coupled with a relatively long bridging linker leads to the interpenetrated structure with a triangular trimeric-nickel building unit. Three types of coordination modes for 1,4-NDC and three sets of different combinations of the modes lead to a complex tetrameric-nickel building unit of **3-5**. Typical bidentate, chelated bidentate, and tridentate coordination modes are present in the structure. Each building unit is bridged to eight other building units in a complex configuration with an unprecedented type of an eight-point extension SBU.

3-1 and 3-2



3-4



3-5

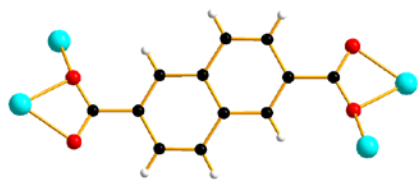
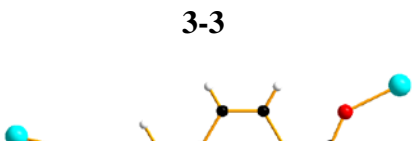


Figure 3.7. The coordination modes of the dicarboxylate bridges within the building units of compounds **3-1** to **3-5**.

Solvent Affinity and Thermogravimetry. Composition data obtained from the elemental analysis of all the compounds except **3-3** did not agree with the crystallographic formula due to the presence of very weakly bound solvent molecules. This is also evident from the thermogravimetric curves (Figures 3.8) of the compounds in air as shown by the sudden decrease in weight at the onset of the experiment up until the end of the isothermal region. The TG data for compound **3-1** suggests loss of one DMA molecule from the structure if the compound is kept at room temperature, in agreement with the result from the elemental analysis. The data for compounds **3-2** and **3-3**, on the other hand, showed a plateau in this region indicating no molecule loss below 100 °C. For the framework compounds **3-4** and **3-5** that contains guest molecules, substantial weight loss was observed (*ca* 13% for **3-4** and 10% for **3-5**) before and during the isothermal step. This illustrates the complexity of the framework structures and the capability of the compounds to adsorb solvent molecules inside the cavities. Multiple steps in the TG curve of **3-5** further shows the complexity of solvent loss. The elemental analysis for this compound was obtained after exchanging the weakly bound solvent molecules with water.

The initial weight loss is followed on heating by the loss of coordinated DMA and DMF molecules in the structural SBU. The total weight loss to this point showed loss of one DMA and two DMF molecules for **3-1** (26.12% calc., 26.22% expt.), loss of four DMF molecules for **3-2** (40.43% calc., 40.8% expt.), and the coordinated two DMA and two DMF molecules for **3-3** (22.41% calc., 22.39% expt.). The distinct step at around 300 °C in the TG curve of **3-4** corresponds to the loss of three coordinated DMA molecules (12.94% calc., 13.52% expt.), and similarly, the step at around 240 °C in the

TG curve of **3-5** can be assigned to the loss of two DMF and one DMA molecules (12.03% calc., *ca* 11.75% expt.) coordinated in the SBU.

The last decomposition step at around 350 °C indicates the loss of the dicarboxylate linkers and the complete decomposition of the compounds in air. Residual solids after the analyses were monitored by powder X-ray diffraction and identified as nickel oxide. The percent weight loss obtained matches closely with the calculated values considering complete decomposition to nickel oxide; compound **3-1** (50.25% calc., 48.39% expt.), compound **3-2** (46.26% calc., 45.36% expt.), compound **3-3** (60.91% calc., 59.59% expt.), compound **3-4** (65.72% calc., 64.27% expt.), and compound **3-5** (69.63% calc., 71.93% expt.).

FT-IR and PXRD Characterization. The infrared spectra of compounds **3-1** to **3-5** in the range 400 to 4000 cm⁻¹ are shown in Figure 3.9. Broad peaks at around 3600-3200 cm⁻¹ are mainly due to O-H stretches from surface water molecules. Peaks at 3100-2900 cm⁻¹ indicate the presence of C-H stretches from the organic linkers. Strong bands at 1700-1300 cm⁻¹ correspond to the various carboxyl symmetric and asymmetric vibrations resulting from several coordination modes of the carboxylate groups. Strong peaks below 900 cm⁻¹ are attributed to Ni-O vibrations.

Powder XRD patterns of the compounds are displayed in Figure 3.10. In general, the peak positions on the experimental PXRD patterns are in very good agreement with the simulated patterns. No significant extraneous peaks are present, indicative of the purity of the bulk products. Differences in intensities are most likely due to the preferred orientation of the powdered samples.

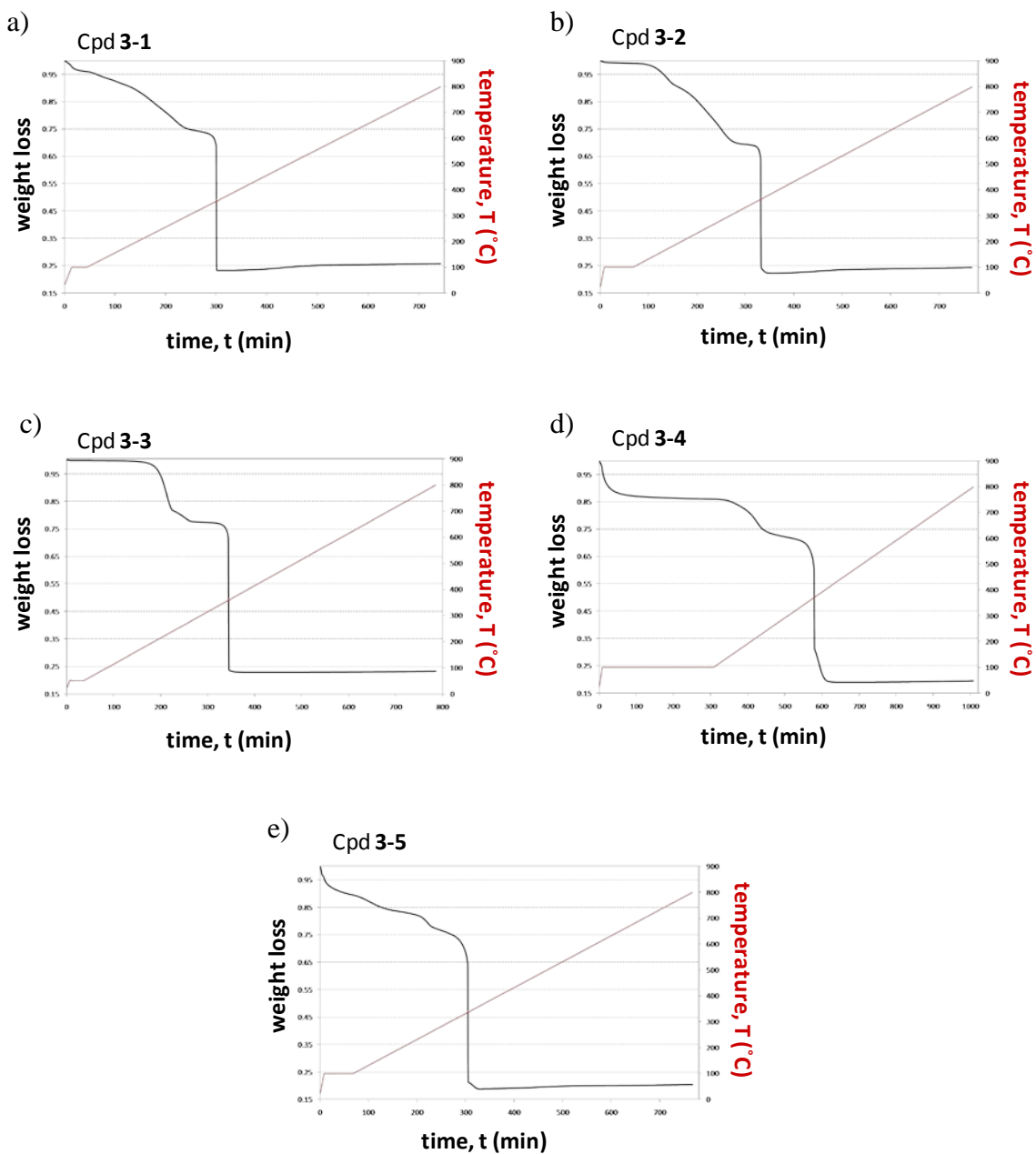


Figure 3.8. Thermogravimetric data for compounds **3-1** to **3-5** (a to e).

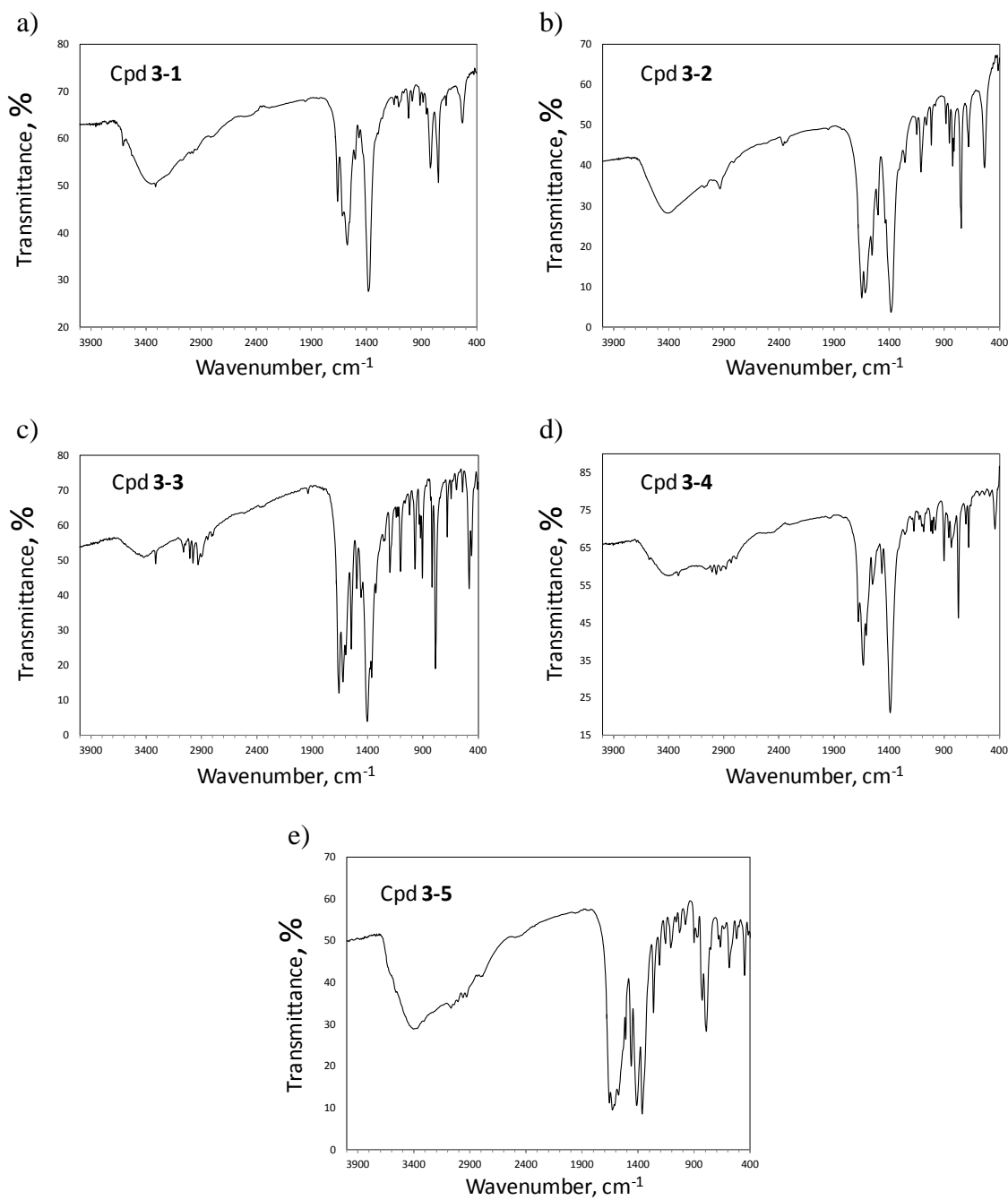


Figure 3.9. FT-IR spectra of compounds **3-1** to **3-5** (a to e).

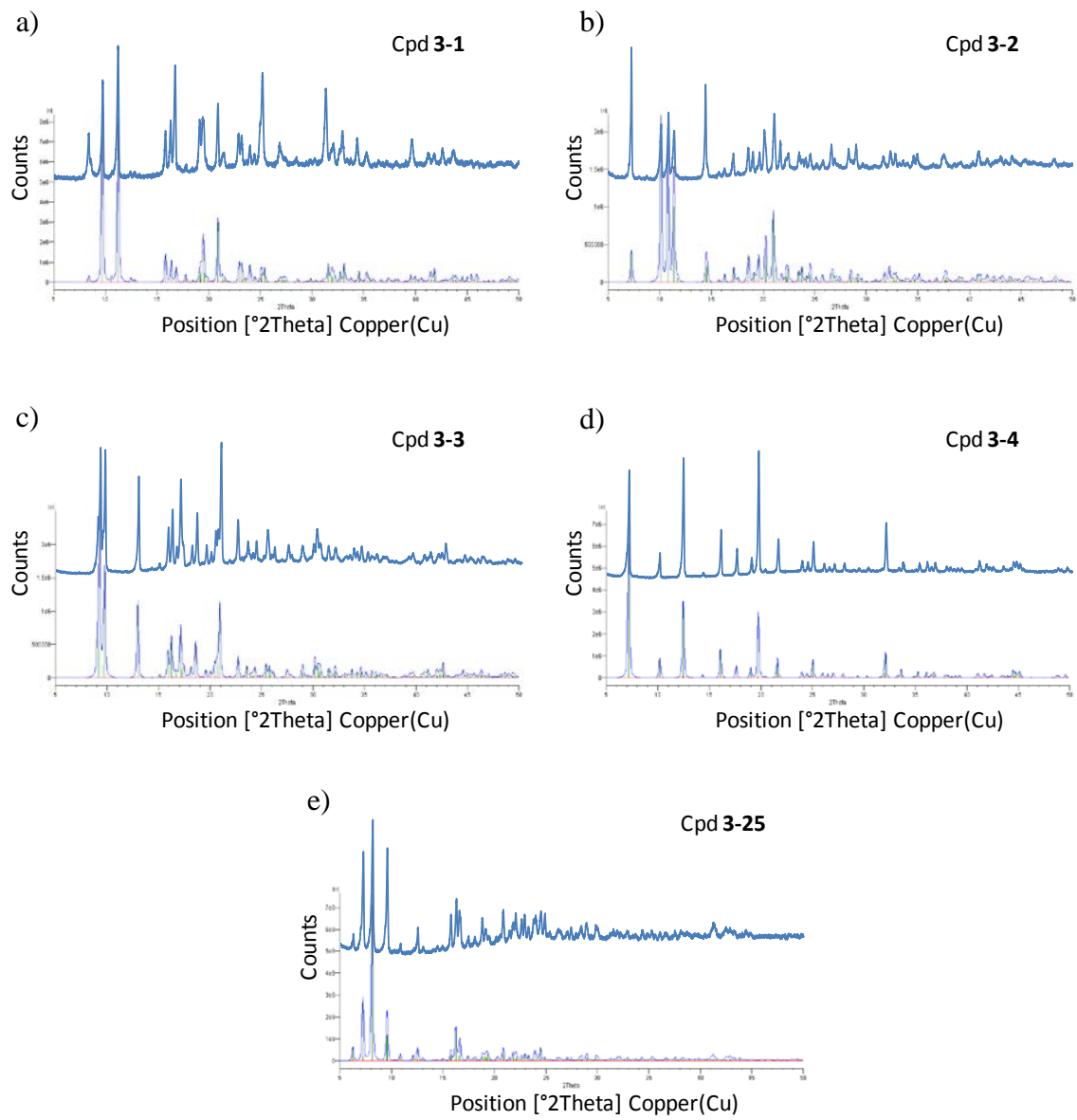


Figure 3.10. PXRD data of compounds **3-1** to **3-5** (a to e). The top plots are experimental patterns while the bottom plots are simulated patterns from the single crystal data.

Magnetic Properties. The temperature-dependent magnetic susceptibility of compounds **3-1** to **3-5** was measured at an applied magnetic field of 1000 Oe in the temperature range 2 to 300 K. The susceptibility data were corrected for diamagnetic contributions from the sample holder and the Pascal's correction estimated from half the molecular weight.³¹⁻³² The molecular weights were calculated from the TGA data of the samples collected at about the same time as the magnetic susceptibility measurements. This gives the best estimate for the molecular weight of the samples considering the problem with the loss of weakly bound solvent molecules at ambient conditions. The magnetic susceptibility and the reciprocal susceptibility data for **3-1**, **3-2**, **3-4**, and **3-5** are shown in Figure 3.11. The molar magnetic susceptibility data above 100 K for the trimers **3-1**, **3-2**, and **3-4** or above 50 K for **3-5** follows the Curie-Weiss law (CW), $\chi = C/(T-\theta)$ where C is the Curie constant and θ is the Weiss constant. The parameters obtained by fitting the data are shown in Table 3.2.

For compound **3-3**, the magnetic data showed significant anomalies due to ferromagnetic impurities that dominate the interactions in a system that is fairly dilute in terms of magnetic spins. The impurity was observed as black particles (possibly ferromagnetic nickel metal) on the surface of the **3-3** crystals. The impurity appears to increase when the sample is left in the supernatant solution for several weeks at ambient conditions. Several attempts to improve the purity of the sample before the magnetic susceptibility data collection were unsuccessful. A sensible CW fit over a temperature range was only possible after addition of a temperature independent parameter which gives a value that is difficult to rationalize.

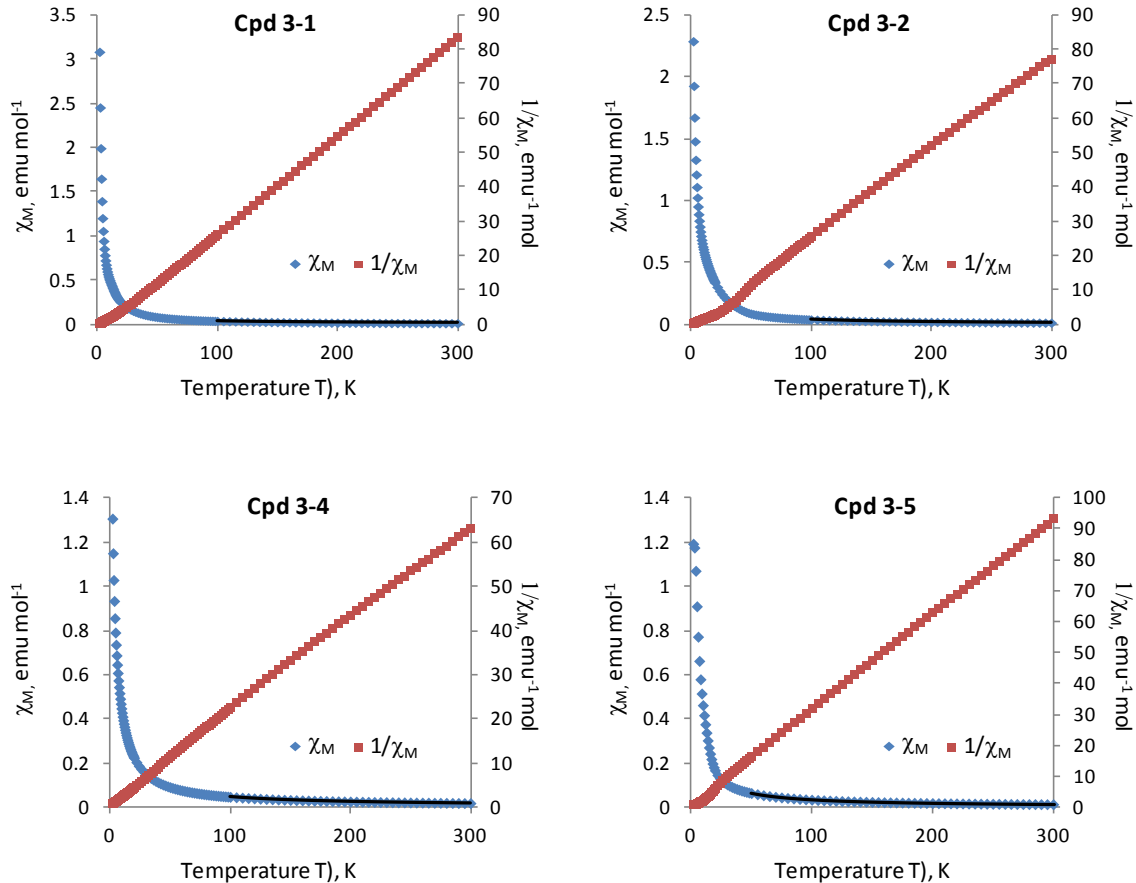


Figure 3.11. The magnetic molar susceptibility (χ_M) and inverse susceptibility ($1/\chi_M$) vs. temperature (T) for compounds **3-1**, **3-2**, **3-4**, and **3-5**. The solid lines are least-squares fit to the Curie-Weiss law in the high temperature region.

Table 3.2. Curie-Weiss Fit Parameters of the Compounds

Compounds	C (emu mol $^{-1}$ K)	θ (K)
3-1	3.630 (3)	5.90 (1)
3-2	3.648 (5)	4.82 (2)
3-4	3.298 (4)	-5.20 (2)
3-5	4.649 (2)	-3.27 (3)

A positive Weiss temperature (θ) value of 5.90 K and 4.82 K for **3-1** and **3-2** respectively suggests overall ferromagnetic interactions within the Ni₃ building units. The Curie constants (C) are 3.63 emu mol⁻¹ K for **3-1** and 3.65 emu mol⁻¹ K for **3-2** both higher than the expected spin-only value of 3.0 emu mol⁻¹ K with $g = 2.0$. The $\chi_M T$ versus T plots are shown in Figure 3.12. The room temperature $\chi_M T$ values at 3.69 emu mol⁻¹ K for **3-1** and 3.72 emu mol⁻¹ K for **3-2** agree well with the reported literature values for three noninteracting Ni(II) ions.³³⁻⁴³ The $\chi_M T$ versus T curves showed an increase in $\chi_m T$ values upon cooling with observed T_{max} at 12 K for **3-1** and 16.5 K for **3-2**. For compound **3-1**, on further cooling, the $\chi_M T$ product drops until 6.5 K then rises up again at lower temperatures. This behavior is different from that of **3-2** as the $\chi_M T$ curve continues to decrease with temperature at $T < T_{max}$.

The CW fit of the magnetic susceptibility data of the triangular trimer **3-4** gives a negative Weiss temperature of -5.20 K suggesting antiferromagnetic interactions within the cluster unit. The Curie constant of 3.30 emu mol⁻¹ K which is still higher than the spin-only value for a trimeric nickel unit, is within the range for reported values of Ni₃ clusters that have the same triangular configuration.⁴⁴⁻⁴⁵ The $\chi_M T$ versus T curve shows a slight decrease on cooling from 100 K to 28 K indicative of an antiferromagnetic behavior. As the temperature is decreased below 28 K, the $\chi_M T$ curve starts to increase and reaches a maximum value at 6 K. A sudden drop of the $\chi_M T$ values is observed upon further cooling.

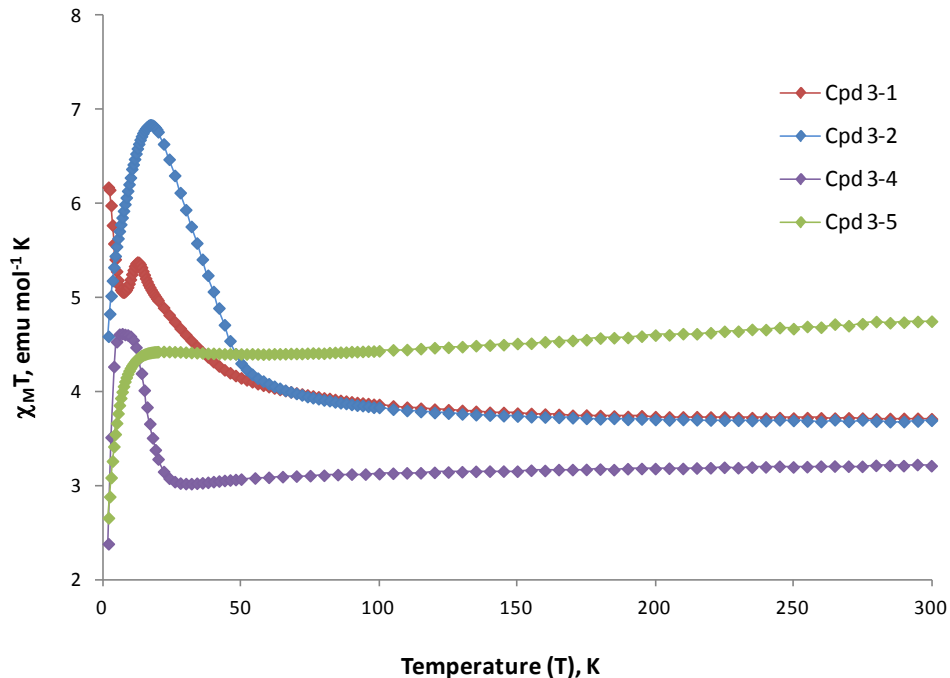


Figure 3.12. The $\chi_M T$ vs. T curves for compounds **3-1** to **3-5** showing their different magnetic behaviors at temperatures below 50 K.

The tetrameric nickel compound **3-5** has a C value of 4.65 emu mol⁻¹ K, higher than the expected spin-only value of 4.0 emu mol⁻¹ K ($g = 2.0$) for a non-interacting Ni₄ unit, and a θ value of -3.27 K suggesting antiferromagnetic interactions. The $\chi_M T$ value at 300 K is 4.75 emu mol⁻¹ K in agreement with a reported tetrameric nickel compound³⁷ but lower than the literature values reported for Ni₄ clusters that have cubane structures.^{38,46-47} The $\chi_M T$ curve for **3-5** generally behaves in a fashion typical to systems that exhibit antiferromagnetic interactions.

The changes in the effective moment evident at the low temperature ($T < 50$ K) region signify long range correlations between the magnetic moments and require further

detailed investigation. For the linear trimeric compounds **3-1** and **3-2**, the susceptibility data over the temperature range 2 to 300 K and 50 to 300 K were analyzed using an expression for a linear trimer model based on the spin Hamiltonian, $H = -2J_1(S_1S_2 + S_2S_3) - 2J_2(S_1S_3)$ ($S_1 = S_2 = S_3 = 1$) with S_1 and S_3 assigned for the terminal nickel ions and S_2 for the central nickel ion. Similarly, the data for the triangular trimeric-Ni compound **3-4** was evaluated using an equilateral triangle model with a spin Hamiltonian, $H = -2J(S_1S_2 + S_2S_3 + S_1S_3)$ and an isosceles triangle that has a Hamiltonian similar to the linear trimer model with J_1 and J_2 not equal to zero. The J values are small and fitting using MAGMUN4.1 software⁴⁸ generated values that are sensitive to the starting parameters and not well determined by the present data. The lower temperature transitions are not understood. An in-depth magneto-structural study and the determination of the strength of long range interactions will be necessary to completely understand the magnetic properties of these materials. The sample preparation also needs improvement for more accurate determinations.

3.4. Conclusion

Five new MOF compounds showing structural diversity based on nickel octahedra and aromatic dicarboxylate linkers were prepared as single crystals using solvothermal synthesis without addition of a terminating amine ligand. Two compounds with layered structures, **3-1** and **3-2** were obtained with little difference on the synthesis conditions that affords different terminating molecules depending on the extent of hydrolysis of the DMF solvent. Framework compounds, **3-3** and **3-4** showed two different nickel-trimer configurations with a slight variation in length of the dicarboxylate linkers and totally

different structures. Another three-dimensional compound **3-5** based on an unprecedented nickel-tetramer building unit was produced by using a dicarboxylate linker with an added functionality and showed a complex structure that contains cavities of varying sizes and shape. Preliminary investigation of their magnetic properties showed different spin interactions at low temperature range with possible long range magnetic ordering present in the nickel cluster systems.

3.5. References

1. Tranchemontagne, D.J.; Ni, Z.; O'Keeffe, M.; Yaghi, O.M. *Angew. Chem. Int. Ed.* **2008**, *47*, 5136–5147.
2. Perry, J.J. IV; Perman, J.A.; Zawarotko, M.J. *Chem. Soc. Rev.* **2009**, *38*, 1400–1417.
3. Yaghi, O.M.; Li, H.; Davis, C.; Richardson, D.; Groy, T.L. *Acc. Chem. Res.* **1998**, *31*, 474–484.
4. Kitagawa, S.; Kitaura, R.; Noro, S. *Angew. Chem. Int. Ed.* **2004**, *43*, 2334–2375.
5. Cheetham, A.K.; Rao, C.N.R.; Feller, R.K. *Chem. Commun.* **2006**, 4780–4795.
6. Yaghi, O.M.; O'Keeffe, M.; Ockwig, N.W.; Chae, H.K.; Eddaoudi, M.; Kim, J. *Nature* **2003**, *423*, 705–714.
7. James, S.L. *Chem. Soc. Rev.* **2003**, *32*, 276–288.
8. Tranchemontagne, D.J.; Mendoza-Cortes, J.L.; O'Keeffe, M.; Yaghi, O.M. *Chem. Soc. Rev.* **2009**, *38*, 1257–1283.
9. Ockwig, N.W.; Delgado-Friedrichs, O.; O'Keeffe, M.; Yaghi, O.M. *Acc. Chem. Res.* **2005**, *38*, 176–182.

10. Rao, C.N.R.; Cheetham, A.K.; Thirumurugan, A. *J. Phys. Condens. Matter* **2008**, *20*, 083202.
11. Kurmoo, M. *Chem. Soc. Rev.* **2009**, *38*, 1353–1379.
12. MasPOCH, D.; Ruiz-Molina, D.; Veciana, J. *Chem. Soc. Rev.* **2007**, *36*, 770–818.
13. Eds: Coronado, E.; Dunbar, K.R. Special Issue for the Forum on Molecular Magnetism: The Role of Inorganic Chemistry. *Inorg. Chem.* **2009**, *48*, 3293–3896.
14. Eds: Rovira, C.; Veciana, J. Special Issue on Crystal Engineering in Molecular Magnetism. *Cryst. Eng. Commun.* **2009**, *11*, 2031–2203.
15. Natarajan, S.; Mahata, P. *Chem. Soc. Rev.* **2009**, *38*, 2304–2318.
16. Cheetham, A.K.; Ferey, G.; Loiseau, T. *Angew. Chem. Int. Ed.* **1999**, *38*, 3268–3292.
17. Eddaoudi, M.; Moler, D.B.; Li, H.; Chen, B.; Reineke, T.M.; O’Keeffe, M.; Yaghi, O.M. *Acc. Chem. Res.* **2001**, *34*, 319–330.
18. Go, Y.B.; Wang, X.; Anokhina, E.V.; Jacobson, A.J. *Inorg. Chem.* **2005**, *44*, 8265–8271.
19. Sun, D.; Cao, R.; Liang, Y.; Shi, Q.; Su, W.; Hong, M. *J. Chem. Soc., Dalton Trans.* **2001**, 2335–2340.
20. *APEX2 User Manual*, Version 1.27; Bruker AXS Inc.: Madison, WI, **2005**.
21. Farrugia, L.J. *J. Appl. Cryst.* **1999**, *32*, 837–838.
22. Brandenburg, K. *DIAMOND*; Crystal Impact GbR, Bonn, Germany, **2006**.
23. Hawxwell, S.M.; Brammer, L. *Cryst. Eng. Commun.* **2006**, *8*, 473–476.
24. Chin, J.; Jubian, V.; Mrejen, K. *J. Chem. Soc., Chem. Commun.* **1990**, 1326–1328.
25. Go, Y.B.; Wang, X.; Anokhina, E.V.; Jacobson, A.J. *Inorg. Chem.* **2004**, *43*, 5360–5367.

26. Yang, G.S.; Lan, Y.Q.; Zang, H.Y.; Shao, K.Z.; Wang, X.L.; Su, Z.M.; Jiang, C.J. *Cryst. Eng. Commun.* **2009**, *11*, 274–277.
27. Lee, Y.K.; Lee, S.W. *Bull. Korean Chem. Soc.* **2003**, *24*, 906–910.
28. Kongshaug, K.O.; Fjellvag, H. *Solid State Sci.* **2003**, *5*, 303–310.
29. Ma, S.; Wang, X.; Manis, E.S.; Collier, C.D.; Zhou, H. *Inorg. Chem.* **2007**, *46*, 3432–3434.
30. Ma, S.; Simmons, J.M.; Yuan, D.; Li, J.; Weng, W.; Liu, D.; Zhou, H. *Chem. Commun.* **2009**, 4049–4051.
31. Kahn, O. *Molecular Magnetism*, Wiley-VCH: New York, **1993**.
32. Bain, G.A.; Berry, J.F. *J. Chem. Educ.* **2008**, *85*, 532–536.
33. Callejo, L.M.; Madariaga, G.; Lezama, L.; Fidalgo, L.; De la Pinta, N.; Cortes, R. *Inorg. Chem.* **2010**, *49*, 5353–5355.
34. Escuer, A.; Esteban, J.; Aliaga-Alcalde, N.; Font-Bardia, M.; Calvet, T.; Roubeau, O.; Teat, S.J. *Inorg. Chem.* **2010**, *49*, 2259–2266.
35. Bu, X.H.; Du, M.; Zhang, L.; Liao, D.Z.; Tang, J.K.; Zhang, R.H.; Shionoya, M. *J. Chem. Soc., Dalton Trans.* **2001**, 593–598.
36. Ding, B.; Yi, L.; Shen, W.Z.; Cheng, P.; Liao, D.Z.; Yan, S.P.; Jiang, Z.H. *J. Mol. Struct.* **2006**, *784*, 138–143.
37. Hui, Y.Y.; Shu, H.M.; Hu, H.M.; Song, J.; Yao, H.L.; Yang, X.L.; Wu, Q.R.; Yang, M.L.; Xue, G.L. *Inorg. Chim. Acta* **2010**, *363*, 3238–3243.
38. Xiao, Y.; Zhang, S.H.; Li, G.Z.; Wang, Y.G.; Feng, C. *Inorg. Chim. Acta* **2011**, *366*, 39–43.

39. Mukherjee, P.; Drew, M.G.B.; Tangoulis, V.; Estrader, M.; Diaz, C.; Ghosh, A. *Polyhedron* **2009**, *28*, 2989–2996.
40. Ginsberg, A.P.; Martin, R.L.; Sherwood, R.C. *Inorg. Chem.* **1968**, *7*, 932–936.
41. Xu, Z.; Thompson, L.K.; Milway, V.A.; Zhao, L.; Kelly, T.; Miller, D.O. *Inorg. Chem.* **2003**, *42*, 2950–2959.
42. Livage, C.; Guillou, N.; Chaigneau, J.; Rabu, P. *MRS Bulletin* **2006**, *41*, 981–986.
43. Wang, Q.; Yang, C.; Qi, L.; Liao, D.Z.; Yang, G.M.; Ren, H.X. *J. Mol. Struct.* **2008**, *892*, 88–92.
44. Efthymiou, C.G.; Raptopoulou, C.P.; Terzis, A.; Perlepes, S.P.; Escuer, A.; Papatriantafyllopoulou, C. *Polyhedron* **2010**, *29*, 627–633.
45. Liu, J.L.; Bao, X.; Herchel, R.; Leng, J.D.; Lin, Z.J.; Tong, M.L. *Aust. J. Chem.* **2010**, *63*, 1111–1115.
46. Biswas, B.; Pieper, U.; Weyhermuller, T.; Chaudhuri, P. *Inorg. Chem.* **2009**, *48*, 6781–6793.
47. Paine, T.K.; Rentschler, E.; Weyhermuller, T.; Chaudhuri, P. *Eur. J. Inorg. Chem.* **2003**, 3167–3178.
48. MAGMUN4.1/OW01.exe is available as a combined package free of charge from the authors (<http://www.ucs.mun.ca/~lthomp/magmun>). MAGMUN has been developed by Dr. Zhiqiang Xu (Memorial University) and OW01.exe by Dr. O. Waldmann. Source codes are not distributed.

Chapter 4

Channeling Chirality: Isoreticular Synthesis of Dicarboxylate-Bridged Frameworks

Based on a Homochiral Chain Compound [Ni₂O(L-Aspartate)(H₂O)₂]

4.1. Introduction

An important subclass of the growing family of metal-organic frameworks (MOFs) are those that are homochiral and porous with potential applications in enantioselective catalysis and separations.¹⁻⁶ Typical strategies for the synthesis of chiral MOFs include the use of optically active ligands as linkers in the framework structure or by induced homochiral crystallization through the incorporation of chiral molecules as templates.¹⁻⁴ For example, the use of natural amino acids as chiral ligands in combination with transition metals has generated a number of coordination polymers that are inherently chiral.⁷⁻¹⁸

In particular, coordination of divalent nickel ions and the aspartic acid ligand leads to the formation of one-dimensional helical chains¹³⁻¹⁴, or three-dimensional networks.¹⁵⁻¹⁸ Most three-dimensional nickel aspartate structures are derived from the one-dimensional nickel aspartate that is based on a mononuclear nickel chain bridged by aspartate ligands.¹⁴ The extended structures are achieved by addition of a subsidiary bridging diamines such as 4,4'-bipyridyl¹⁵, 4,4'-azopyridine¹⁷, bis(4-pyridyl)ethylene¹⁷, 1,4-bis(4-pyridyl)benzene¹⁷, and pyrazine¹⁸, or triamines such as tris(4-pyridyl)-triazine¹⁷ and 3,5-bis(4-pyridyl)pyridine¹⁷. The other nickel aspartate chain synthesized in our group with extended metal to oxygen bonding has a three-dimensional structure with

$(\text{NiAsp}_2)^{2-}$ as the bridging group that links the helices.¹⁵ The latter nickel aspartate structure is the subject of this work.

A synthetic scheme that involves the use of two ligands, a chiral linker, and a rigid spacer has been reported to generate chiral MOFs.⁴ The chiral linker provides the asymmetric center for chirality while the rigid spacer aids the formation of channels by extending the dimensionality of the chiral building units. This approach is used in this study to prepare a series of compounds based on a homochiral $\text{Ni}_2\text{O}(\text{L-Aspartate})$ building unit (**1D Ni-Asp**)¹³ and aromatic dicarboxylate linkers. The building unit used in the work is a metal-oxo helical chain as opposed to usual situation in most chiral MOFs that are based on mononuclear metal centers. The investigation was inspired by three dimensional structure of the **1D Ni-Asp** where $\text{Ni}_2\text{O}(\text{L-aspartate})$ helices are bridged by $(\text{NiAsp}_2)^{2-}$ units through the carboxylates of the aspartate ligand.¹⁵ Substitution of aromatic dicarboxylates of varying lengths provide tunability with respect to the size of the chiral channels in the frameworks.

Four dicarboxylate linkers (Figure 4.1), namely 1,4-benzenedicarboxylic acid (1,4-H₂BDC), 1,4-naphthalenedicarboxylic acid (1,4-H₂NDC), 2,6-naphthalenedicarboxylic acid (2,6-H₂NDC), and 4,4'-biphenyldicarboxylic acid (4,4'-H₂BPDC) were used as rigid spacers to generate an isoreticular series of MOF compounds based on **1D Ni-Asp**. This chapter also discusses the sensitivity of the phases formed to the reaction conditions in this mixed ligand synthetic system. Phase identity of the polycrystalline products was monitored by powder X-ray diffraction (PXRD). An initial evaluation regarding the porosity of the frameworks was also conducted by

successful evacuation and reabsorption of solvent molecules without damaging the integrity of the MOF structure.

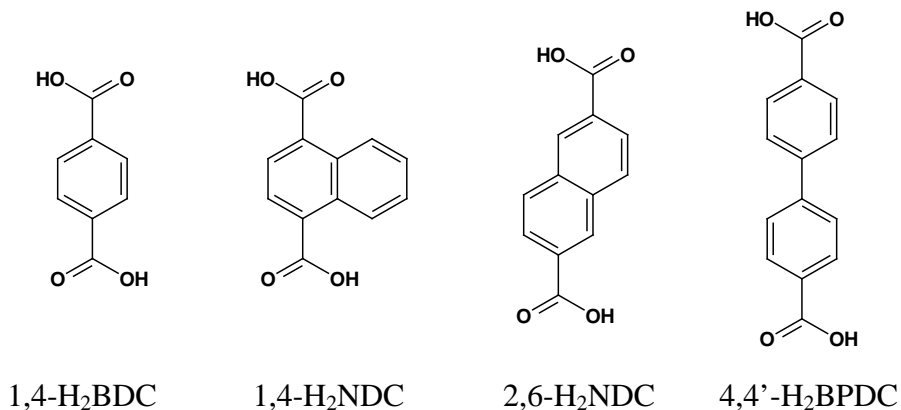


Figure 4.1. Structures of the aromatic dicarboxylate linkers used in the study.

4.2. Experimental Section

Materials and Measurements. All chemicals used in the synthesis were obtained commercially and used without further purification. Solvothermal reactions were carried out in 23-mL Teflon-lined Parr autoclaves at 150 to 180 °C from 4 h to 96 h using mixed N,N-dimethylformamide (DMF) and water as the solvent. Elemental analyses were performed by Galbraith Laboratories (Knoxville, TN). Thermal analyses were conducted on the Hi-Res TGA 2950 thermogravimetric (TG) analyzer from room temperature to 800 °C at a heating rate 0.1 °C min⁻¹ in air.

Synthesis of Ni₂O(L-Aspartate)(1,4-BDC)_{0.5} (4-1). A mixture of 2.15 mL 2M NiCl₂, 1.1 mL 2M (TEA)(L-H₂Asp), 4.3 mL 0.25M 1,4-H₂BDC in DMF, 0.2 mL TEA,

and 5 mL DMF was heated in a 23-mL Teflon-lined Parr autoclave at 150 °C for 48 h followed by slow cooling at a rate 0.5 °C min⁻¹. Light green powder was recovered by filtration, washed with DMF, and dried in air. Anal. Calc. for Ni₂C₈O₇N₁H₁₀: C, 25.2%; H, 2.6%; N, 3.7%; Ni, 30.8%. Found: C, 25.0%; H, 3.5%; N, 4.7%; Ni, 31.3%.

Synthesis of Ni₂O(L-Aspartate)(1,4-NDC)_{0.5} (4-2), Ni₂O(L-Aspartate)(2,6-NDC)_{0.5} (4-3), and Ni₂O(L-Aspartate)(4,4'-BPDC)_{0.5} (4-4). The same preparation described for the synthesis of **4-1** was used but with different dicarboxylic acids [(1,4-H₂NDC for **4-2**, 2,6-H₂NDC for **4-3**, or 4,4'-H₂BPDC for **4-4**] instead of terephthalic acid. Due to the varying solubility of these acids in DMF, they were added to the mixture as powders in the same molar ratio as the preparation of **4-1** with a constant amount of DMF solvent.

X-ray Crystallography. Finely ground samples of the compounds were characterized by powder XRD using the PANalytical X’Pert Pro powder diffractometer with a Cu target ($\lambda = 1.54187 \text{ \AA}$). A Le Bail fit was conducted to confirm that the samples were single phase and to refine the cell parameters of the compounds using the GSAS software.¹⁹

4.3. Results and Discussion

Reticular Chemistry. Four dicarboxylate ligands were used as bridging linkers to form structures derived from the three-dimensional material [Ni_{2.5}(OH)(L-Asp)₂]⁺·6.55H₂O (**3D Ni-Asp**).¹⁵ The linkers have two carboxylate units oriented in a linear conformation with varying degrees of separation between them. They serve to replace the (NiAsp₂)²⁻ bridges found in the **3D Ni-Asp** structure that links Ni₂O(L-Asp)

chains in the framework. The crystal structure of the $\text{Ni}_2\text{O}(\text{L-Asp})(\text{H}_2\text{O})_2$ helices (**1D Ni-Asp**) (Figure 4.2) has been described in detail in literature.¹³ Briefly, the nickel aspartate chains are based on trimers (Figure 4.2b) of nickel octahedra linked via edge- and corner-sharing to generate an extended Ni-O-Ni connectivity in the backbone structure. The helical twist is a consequence of the asymmetric order of the edges of the linked trimer units established by the chiral aspartate ligands. Figure 4.3 shows the transformation of **1D Ni-Asp** to **3D Ni-Asp** upon variation of the reactant stoichiometry or an increase in pH of the reaction system.¹⁵ The structure of **3D Ni-Asp** is presented in Figure 4.4 showing the chiral channels along the *c* axis that are formed from the **1D Ni-Asp** helices bridged by $(\text{NiAsp}_2)^{2-}$ fragments. The linkage is based on the nickel coordination to the bridging aspartate through the carboxylate unit on the side group of the amino acid (Figure 4.4a). This allows direct substitution of any rigid dicarboxylate to function as a bridging linker in the three-dimensional structure. The approach also utilizes the rigidity of the **1D Ni-Asp** building unit that has extended Ni-O-Ni bonding compared to the less condensed phase of one-dimensional nickel aspartate based on mononuclear chains of alternating nickel and aspartate ligands. Furthermore, the variable lengths of the dicarboxylate linkers provide added control on the size of the chiral channels in the structures as they define the separation distances between the **1D Ni-Asp** helices.

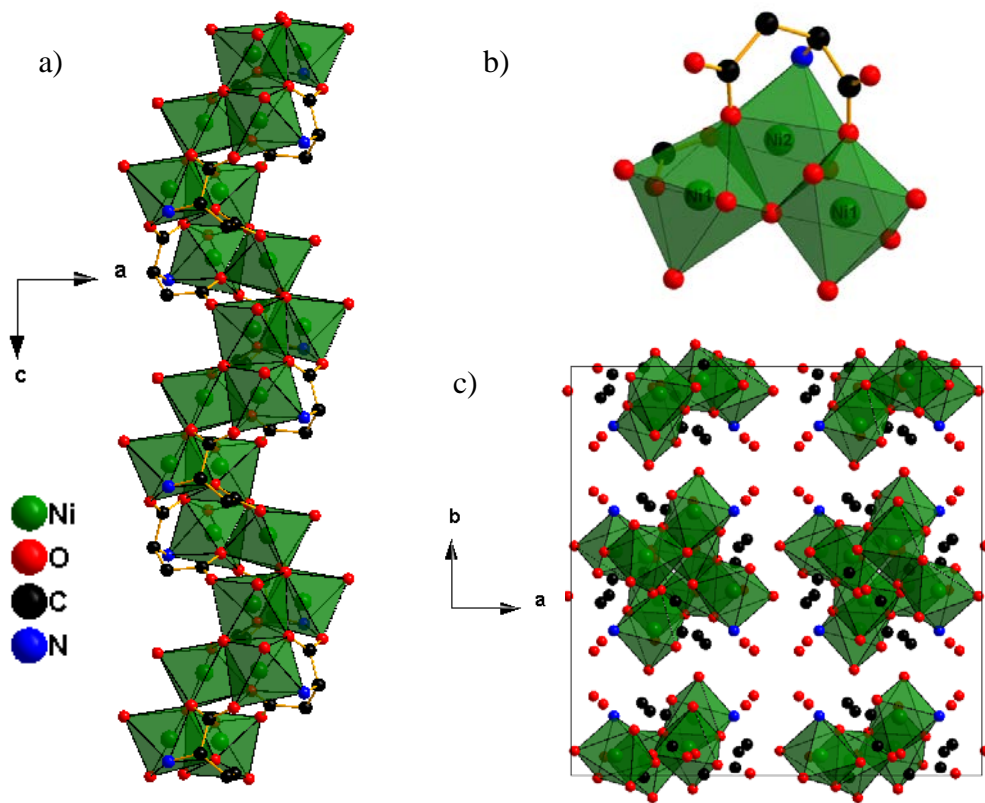


Figure 4.2. a) Helical chain in **1D Ni-Asp**; b) Trimer building unit; c) Unit cell of **1D Ni-Asp** viewed along *c* axis. (Ref. 13)

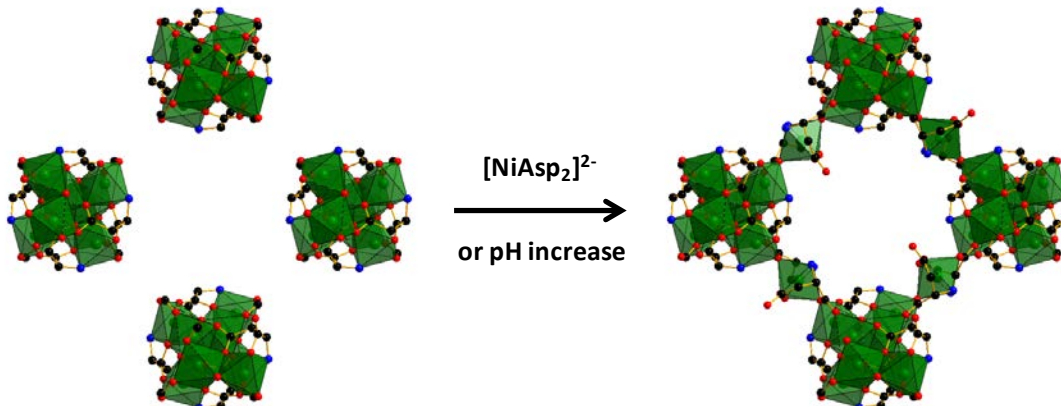


Figure 4.3. Transformation of **1D Ni-Asp** to **3D Ni-Asp** connected by the $(\text{NiAsp}_2)^{2-}$ bridges. (Ref. 15)

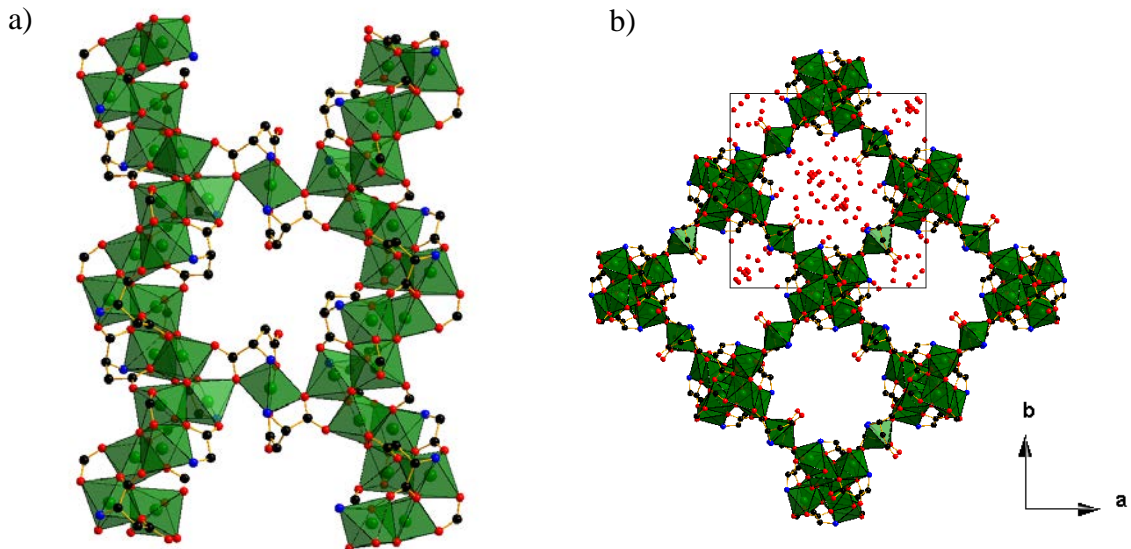


Figure 4.4. Crystal structures of **3D Ni-Asp** a) showing the carboxylate bridging points in the linkages of the **1D Ni-Asp** chains and b) the chiral channels perpendicular to the *c* axis i.e. the direction of the chiral chain. (Ref. 15)

Structures. The unit cell was determined by conventional indexing methods on powder XRD patterns i.e. TREOR, DICVOL04, programs included in the PANalytical X’Pert High Score Plus package.²⁰ Results revealed lattice parameter values of $a \approx b \approx 19 \text{ \AA}$, $c \approx 12 \text{ \AA}$, $\alpha = \beta = \gamma = 90^\circ$ for compound **4-1** which indicates that the structure is similar to that of the **3D Ni-Asp**. A high resolution powder diffraction pattern was refined using Le Bail’s fitting procedure and the lattice parameters determined with the GSAS program (Figure 4.5).¹⁹ The profile fit of the experimental powder pattern is in good agreement with the **3D Ni-Asp** structure with space group $P4_12_12$ with cell

parameters $a = b = 18.940$ (1) Å and $c = 12.135$ (1) Å. The low angle peak was excluded in the profile refinement due to the high asymmetry of the peak shape which lowers the reliability of the fitting process. A Rietveld refinement with a structure model derived from **3D Ni-Asp** was not completely satisfactory and gave some unreasonable bond lengths. This is due to the large number of light atoms present in the structure and the presence of disordered DMF and H₂O solvent molecules. Attempts to replace the solvent molecules with other solvents like CHCl₃ or DMSO proved ineffective and led to degradation in the crystallinity and broader peaks. Powder diffraction patterns of compounds **4-2**, **4-3**, and **4-4** (Figure 4.6) were treated similarly and the refined lattice parameters are summarized in Table 4.1.

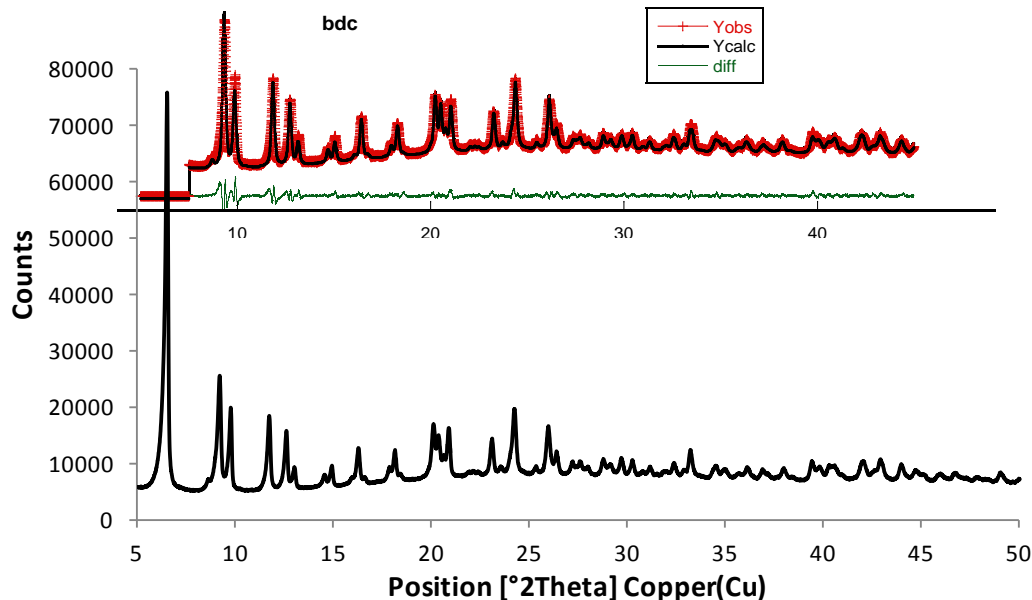


Figure 4.5. Powder diffraction pattern of compound **4-1** and the Le Bail fit to the PXRD pattern of **4-1** using the GSAS.

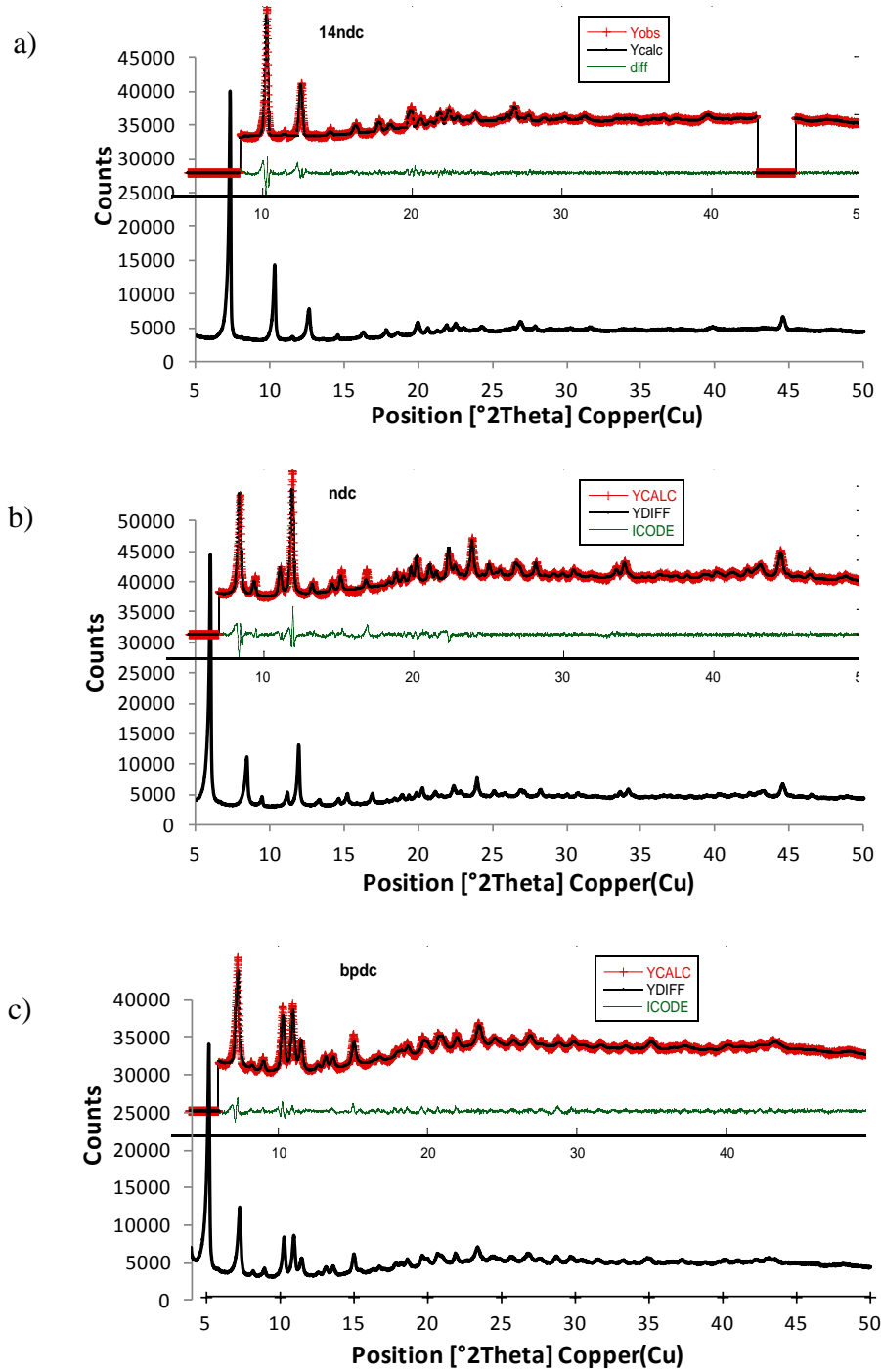


Figure 4.6. Powder diffraction patterns and Le Bail fits (superimposed) of a) compound 4-2, b) compound 4-3, and c) compound 4-4.

Table 4.1. Lattice parameters from the Le Bail fits for compounds **4-1** to **4-4**.

Linker	<i>a</i> (Å)	<i>c</i> (Å)
1,4-BDC	18.940(1)	12.135(1)
1,4-NDC	17.306(4)	12.265(6)
2,6-NDC	21.020(1)	12.044(1)
4,4'-BPDC	24.506(1)	12.156(4)

The structures of compounds **4-1** to **4-4** are isoreticular based on linked chains of Ni₂O[L-Asp] with varying *a* lattice parameters, ranging from 17.31 to 24.51 Å depending on the length of the dicarboxylate linker used. This parameter is directly related to the dimensions of the chiral channels that propagate perpendicular to this direction. The systematic variation of the strongest peak in the patterns with 2θ values of 6.5°, 7.3°, 6.0°, and 5.2° for compounds **4-1** to **4-4** respectively, also affirms this correlation. The *c* lattice parameter value, on the other hand, remains nearly constant at ~12 Å in all the structures since they contain the same **1D Ni-Asp** helix. Overall, they present one of a few examples of isoreticular series of chiral MOFs successfully synthesized by linker substitution and with minimal changes in the synthesis conditions.^{5,17,21-23}

Synthesis of Compound 4-1. The syntheses of the compounds **4-1** to **4-4** were performed under analogous solvothermal conditions as used previously in the synthesis of **1D Ni-Asp** but in a mixed solvent system of DMF and water. The products are sensitive to a number of factors during the synthesis including temperature, solvent

system, pH, and time. The most extensively investigated compound **4-1** was obtained only in two sets of synthesis conditions, (1) from the conditions reported in the experimental section and (2) a 4 h solvothermal reaction at 150 °C of 2.15 mL 2M NiCl₂ and 1.1 mL 2M (TEA)(L-H₂Asp) with 8.6 mL of 0.25M 1,4-H₂BDC in DMF and 0.5 mL TEA, both of which have an initial solution pH of 5-6. Attempts to grow single crystals of the compounds were unsuccessful. Most of the experiments, carried out at room temperature by the test tube layer-diffusion method, yielded blue crystals of nickel aspartate¹⁴ and colorless needles of 1,4-H₂BDC. High temperature reactions, on the other hand, led to the formation of nickel dicarboxylate crystals reported in Chapter 3, as a minor phase.

The appearance of products at different reaction times was monitored by measuring their powder X-ray diffraction patterns shown in Figure 4.7. A prominent feature is the disappearance of phase **4-1** and the appearance of an unidentified phase (**4-X**) as the reaction time is increased. The starting molar ratio used in this series was 2 : 1 : 1 for Ni²⁺ : L-H₂Asp : 1,4-H₂BDC. Peaks belonging to phase **4-X** were observed to emerge starting as early as 12 h (Figure 4.7b) and dominate the system after 3 days (Figure 4.7e) of solvothermal reaction. Further extending the reaction time to 6 d at the same reaction conditions resulted in a mixture of phase **4-X** and traces of nickel metal. (Figure 4.7f) The formation of phase **4-X** can be inhibited by reducing the molar amount of the 1,4-H₂BDC linker at a ratio 2 : 1 : 0.5 for Ni²⁺ : L-H₂Asp : 1,4-H₂BDC to yield compound **4-1** over a reaction period of 2 days.

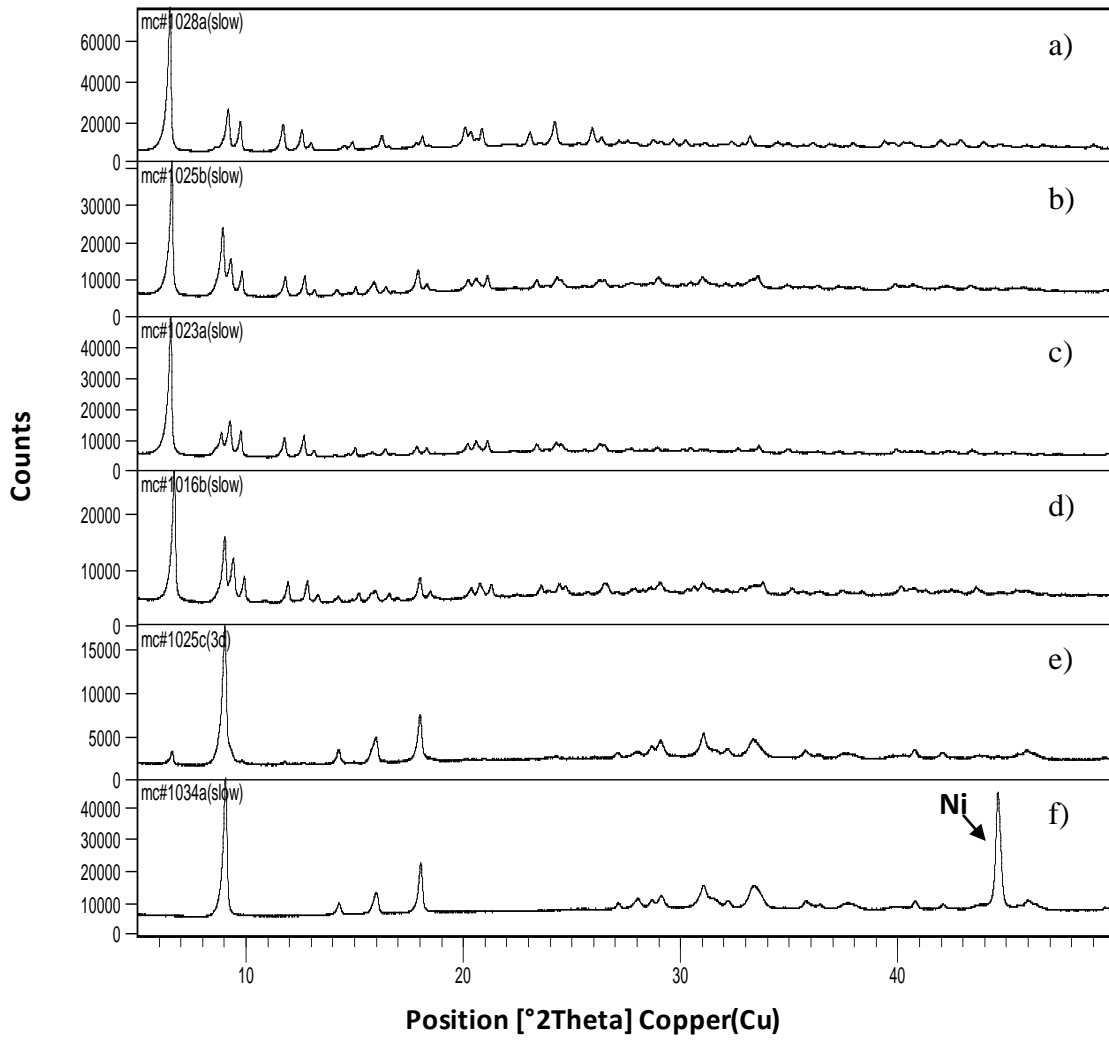


Figure 4.7. Powder diffraction patterns of the products from a 2 : 1 : 1 ratio of Ni^{2+} :L- H_2Asp :1,4-H₂BDC set-ups prepared at a reaction time of a) 4 h, b) 12 h, c) 24 h, d) 48 h, e) 72 h, and f) 144 h.

The reaction is a mixed ligand system of enantiomerically pure aspartic acid and the rigid organic spacer, terephthalic acid. Overall, the two ligands have four carboxylate groups and an amino group for coordination with nickel metal center. These functionalities have different pKa values and may present different coordination behavior depending on the pH of the system. The pH, therefore, has to be controlled during the synthesis because of the complexity of the mixed ligand system and the possibilities of generating multiple-phase products. In this specific case, pH refers to the degree of protonation in the mixed DMF-H₂O solvent system and may be differentiated from the conventional pH definition in aqueous media. It was monitored using the ColorpHast pH indicator strips (EMD Chemicals Inc.) with range 0 to 14. This parameter was varied by adjusting the amount of the TEA base in the reaction mixture and monitored at the beginning of each reaction. PXRD data collected from the samples at different starting pH are summarized in Figure 4.8. Compound **4-1** exclusively forms at a narrow pH range between 5 to 6, which corresponds to a molar ratio of starting ligands to base of 1 : 1.1 (Figure 4.8b). The use of lesser amount of the base results in another unknown phase, while a slight excess of TEA yields a mixture of a known nickel aspartate phase¹⁴ and phase **4-X**. On the other hand, an excess amount of base in the reaction system favors the formation of phase **4-X**.

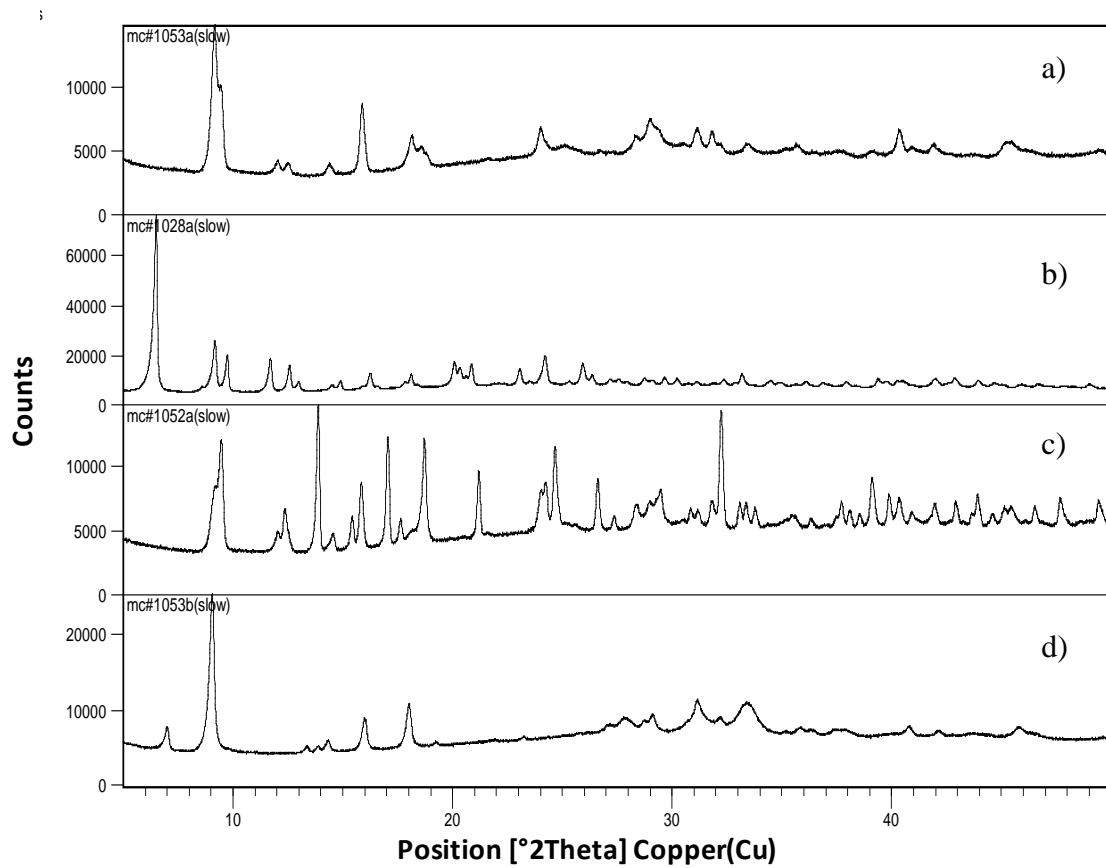


Figure 4.8. Powder diffraction patterns of the products based on compound **4-1** with varying amounts of base at a ligand : TEA ratio of a) 1 : 0.67 (pH 3-4), b) 1 : 1.1 (pH 5-6), c) 1 : 1.4 (pH 6-7), and d) 1 : 5.3 (pH 9-10).

Thermal Analysis of Compound 4-1. The transformation of compound **4-1** with temperature was investigated using PANalytical X’Pert Pro powder diffractometer equipped with the high-temperature measurement system. Figure 4.9 shows a series of PXRD patterns measured at different temperatures using a platinum sample holder. Results showed the generation of a new phase from the **4-1** phase that resembles that of a **1D Ni-Asp** pattern only with broadened peaks. Peak broadening may be due to inhomogeneous transformation and the inclusion of terephthalic acid as an impurity in the sample. The process suggests the loss of carboxylate bridging linkages in the framework structure at high temperature and the presence of remnant **1D Ni-Asp** backbone.

Thermogravimetric analysis of compound **4-1** was measured using a Hi-Res TGA 2950 thermogravimetric analyzer from room temperature to 800 °C at a heating rate of 1 °C min⁻¹ in air after an isothermal step at 150 °C. (Figure 4.10) The TGA data revealed a two-step decomposition process. The first step from the onset of the experiment to 250 °C corresponds to the loss of guest molecules that is comprised of multiple steps due to the different vapor pressures of solvents DMF and H₂O. The second step at 295 °C corresponds to the decomposition of the framework Ni₂O(L-Asp)(BDC)_{0.5} to nickel oxide (43.08% calc., 43.98% expt.). An elemental analysis on a sample, that was evacuated with solvent molecules by 2 h heating at 150 °C and stored in vacuum oven at room T for days, showed composition values consistent with the framework formula and two water molecules per formula of the compound.

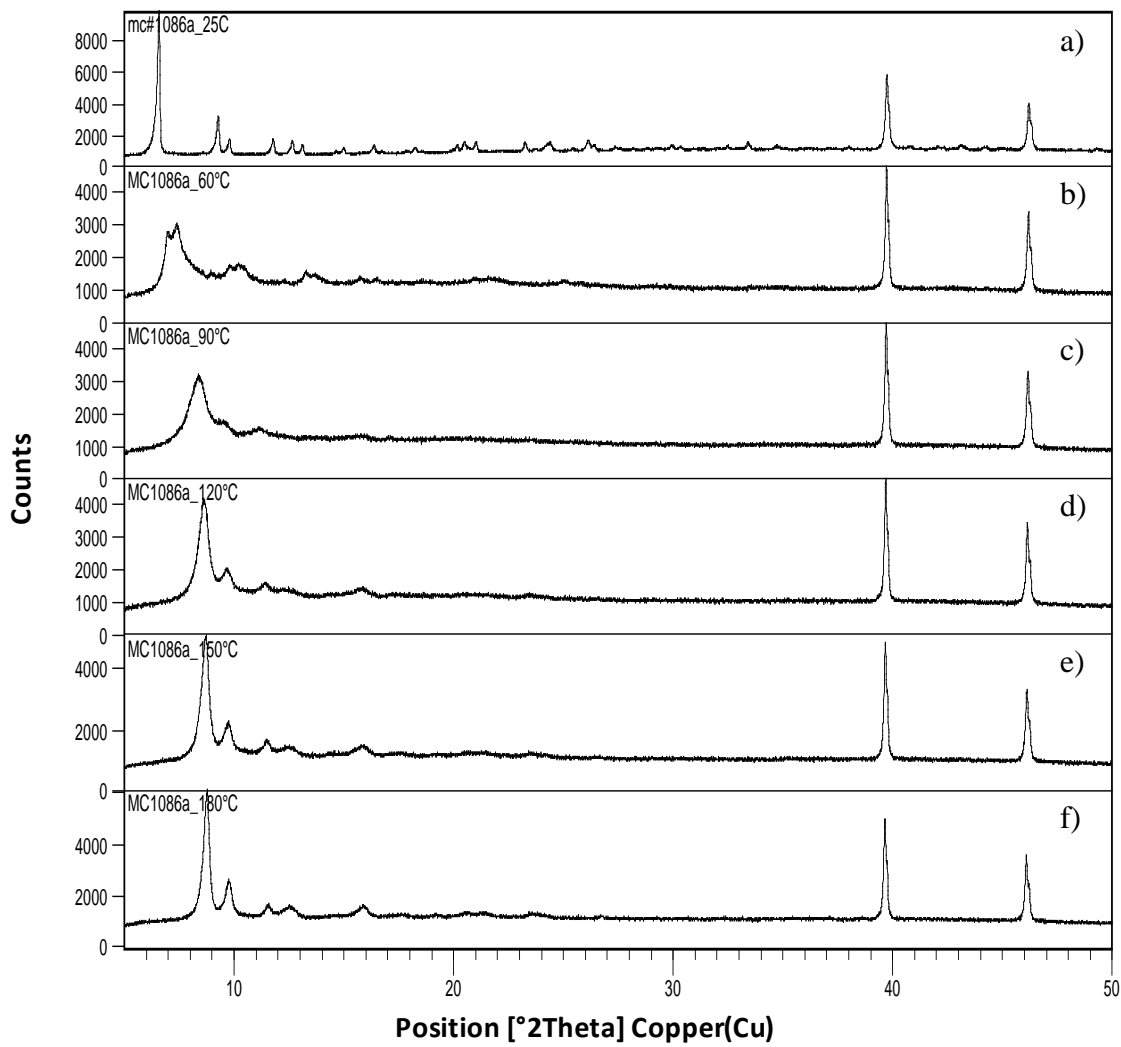


Figure 4.9. PXRD patterns of compound **4-1** measured using the PANalytical X’Pert Pro high temperature measurement system at temperatures of a) 25 °C, b) 60 °C, c) 90 °C, d) 120 °C, e) 160 °C, and f) 180 °C. Sharp peaks at 39.7° and 46.2° are characteristic peaks of the Pt sample holder.

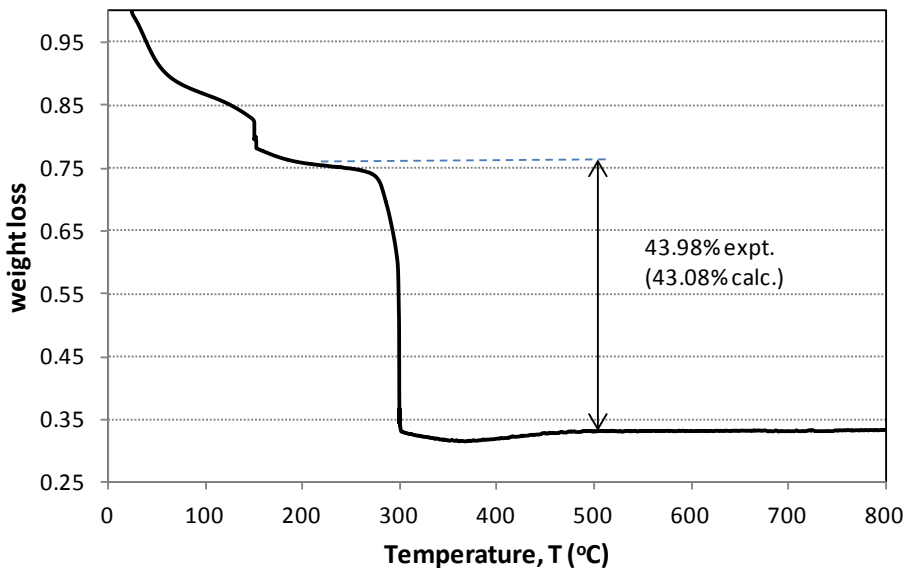


Figure 4.10. Thermogravimetric plot for compound **4-1**.

Solvent Evacuation Study on Compound 4-1. A simple investigation was conducted to study the behavior of the framework channels upon removal and reentry of guest molecules in compound **4-1**. Heat treatment of samples at 180 °C for 30 min showed a substantial difference in the PXRD pattern (Figure 4.11b) compared to the original PXRD pattern of the compound (Figure 4.11a). This implies an adjustment in the lattice parameter of the framework structure once the solvent molecules are taken out of the channels. This process can be reversed upon soaking the evacuated samples in a DMF to H₂O (3 : 1) solvent for 4 h. Powder X-ray diffraction pattern (Figure 4.11c) in this sample shows the presence of **4-1** as the major phase with minor peaks coming from the evacuated phase caused by the incomplete reverse process. The process by which solvent molecules can enter and leave the channels with minor modifications in the structure is a typical to MOFs that have flexible framework structures. This flexible

framework behavior, however, was observed only when the evacuation process proceeds for 30 min, otherwise, more drastic changes in the backbone structure occur and the reverse process cannot be completed as shown by PXRD analysis of the samples heated for longer time periods (Figure 4.12). The framework breaks apart to eventually yield the **1D Ni-Asp** evident from the presence of peaks at around 8.6° , 9.8° , 12.1° , 15.5° , and 21.2° corresponding to the strong peaks of **1D Ni-Asp**.

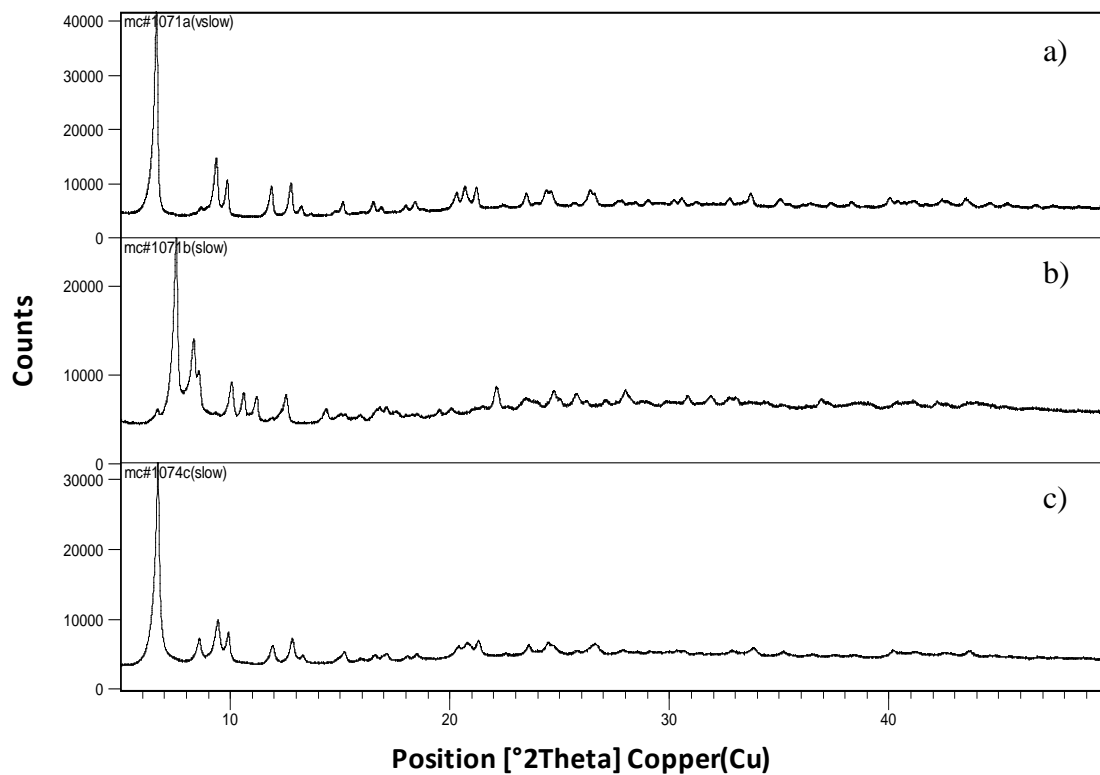


Figure 4.11. a) Powder diffraction pattern of compound **4-1** for base comparison; b) PXRD pattern after heat treatment at $180\text{ }^\circ\text{C}$ for 30 min; c) PXRD pattern after soaking back to DMF- H_2O solvent system.

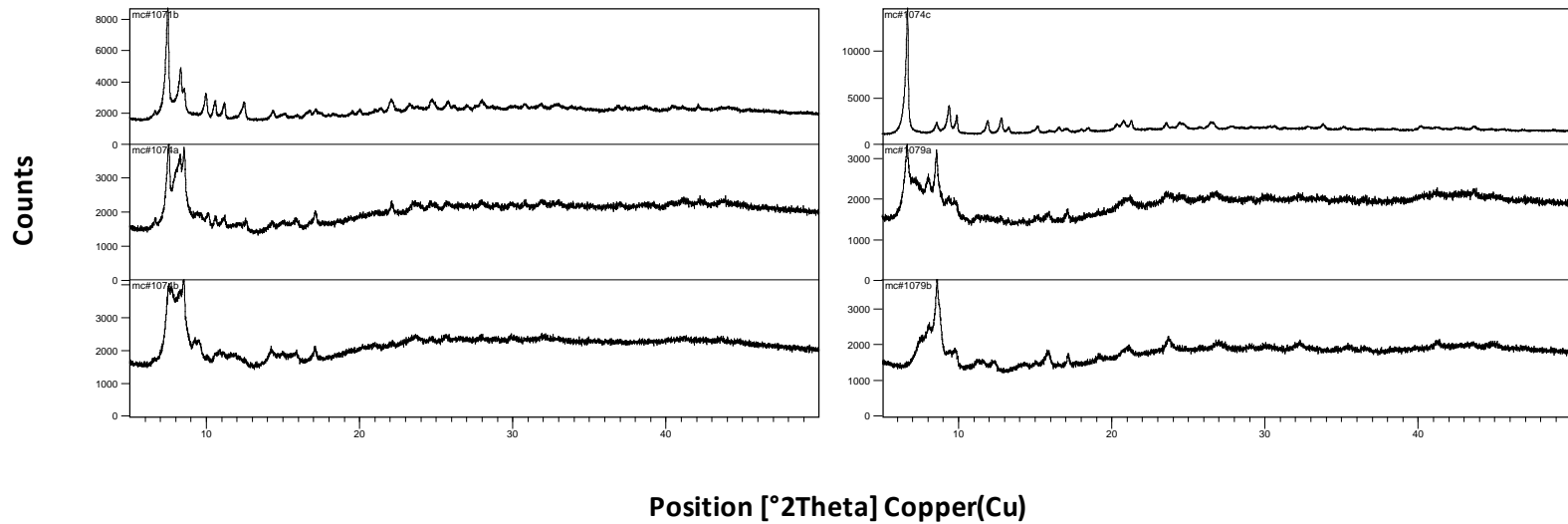


Figure 4.12. PXRD pattern of **4-1** heated at 180 °C (left) then reconditioned in 3 : 1 DMF : H₂O (right) for a) 30 min, b) 60 min, and c) 210 min.

4.4. Conclusion

Reticular chemistry of MOFs offers a promising route to making porous homochiral materials with applications in asymmetric catalysis and enantioselective separation. A rational approach of linking homochiral chains with rigid spacers was utilized to prepare an isoreticular series of chiral frameworks based on Ni₂O(L-aspartate) helices and aromatic dicarboxylate linkers. Four dicarboxylate linkers, namely 1,4-H₂BDC, 1,4-H₂NDC, 2,6-H₂NDC, and 4,4'-H₂BPDC, of varying distances between the carboxylate units were used to provide control on the size of the channels as revealed in the powder diffraction profiles of the compounds. The preparation of compound **4-1** occurs at similar conditions to the synthesis of **1D Ni-Asp** using mixed DMF-H₂O solvent and showed sensitivity to a number of parameters such as reaction time and pH. Furthermore, solvent molecules are observed to leave and reenter the framework channels in **4-1** with a flexible MOF-type behavior.

4.5. References

1. Yoon, M.; Srirambalaji, R.; Kim, K. *Chem. Rev.* **2012**, *112*, 1196–1231.
2. Kim, K.; Banerjee, M.; Yoon, M.; Das, S. *Top Curr. Chem.* **2010**, *293*, 115–153.
3. Ma, L.; Abney, C.; Lin, W. *Chem. Soc. Rev.* **2009**, *38*, 1248–1256.
4. Dybtsev, D.N.; Nuzhdin, A.L.; Chun, H.; Bryliakov, K.P.; Talsi, E.P.; Fedin, V.P.; Kim, K. *Angew. Chem. Int. Ed.* **2006**, *45*, 916–920.
5. Ma, L.; Falkowski, J.M.; Abney, C.; Lin, W. *Nat. Chem.* **2010**, *2*, 838–846.
6. Ingleson, M.J.; Barrio, J.P.; Bacsa, J.; Dickinson, C.; Park, H.; Rosseinsky, M.J. *Chem. Commun.* **2008**, 1287–1289.

7. Rebilly, J.N.; Gradner, P.W.; Darling, G.R.; Bacsa, J.; Rosseinsky, M.J. *Inorg. Chem.* **2008**, *47*, 9390–9399.
8. Ingleson, M.J.; Bacsa, J.; Rosseinsky, M.J. *Chem. Commun.* **2007**, 3036–3038.
9. An, H.Y.; Wang, E.B.; Xiao, D.R.; Li, Y.G.; Su, Z.M.; Xu, L. *Angew. Chem. Int. Ed.* **2006**, *45*, 904–908.
10. Dan, M.; Rao, C.N.R. *Chem. Eur. J.* **2005**, *11*, 7102–7109.
11. Zhang, Y.; Saha, M.K.; Bernal, I. *Cryst. Eng. Comm.* **2003**, *5*, 34–37.
12. Battaglia, L.P.; Corradi, A.B.; Antolini, L.; Marcotrigiano, G.; Menabue, L.; Pellacani, G.C. *J. Am. Chem. Soc.* **1982**, *104*, 2407–2411.
13. Anokhina, E.V.; Jacobson, A.J. *J. Am. Chem. Soc.* **2004**, *126*, 3044–3045.
14. Antolini, L.; Manbue, L.; Pellacani, G.C.; Marcotrigiano, G. *J. Chem. Soc., Dalton Trans.* **1982**, 2541–2543.
15. Anokhina, E.V.; Go, Y.B.; Lee, Y.; Vogt, T.; Jacobson, A.J. *J. Am. Chem. Soc.* **2006**, *128*, 9957–9962.
16. Vaidhyanathan, R.; Bradshaw, D.; Rebilly, J.N.; Barrio, J.P.; Gould, J.A.; Berry, N.G.; Rosseinsky, M.J. *Angew. Chem. Int. Ed.* **2006**, *45*, 6495–6499.
17. Barrio, J.P.; Rebilly, J.N.; Carter, B.; Bradshaw, D.; Bacsa, J.; Ganin, A.Y.; Park, H.; Trewin, A.; Vaidhyanathan, R.; Copper, A.I.; Warren, J.E.; Rosseinsky, M.J. *Chem. Eur. J.* **2008**, *14*, 4521–4532.
18. Ghosh, A.; Sanguramath, R.A. *J. Chem. Sci.* **2008**, *120*, 217–222.
19. Larson, A.C.; Von Dreele, R.B. *General Structure Analysis System (GSAS)*; Report LAUR 86-748, Los Alamos National Laboratory, **1994**.

20. *X’Pert HighScore Plus*, Version 2.2b; PANalytical B.V., Almelo, The Netherlands, **2006**.
21. Song, F.J.; Cheng, W.; Falkowski, J.M.; Ma, L.Q.; Lin, W.B. *J. Am. Chem. Soc.* **2010**, *132*, 15390–15398.
22. Dybtsev, D.N.; Yutkin, M.P.; Peresypkina, E.V.; Virovets, A.V.; Serre, C.; Ferey, G.; Fedin, V.P. *Inorg. Chem.* **2007**, *46*, 6843–6845.
23. Dybtsev, D.N.; Yutkin, M.P.; Samsonenko, D.G.; Fedin, V.P.; Nuzhdin, A.L.; Bezrukov, A.A.; Bryliakov, K.P.; Talsi, E.P.; Belosludov, R.V.; Mizuseki, H.; Kawazoe, Y.; Subbotin, O.S.; Belosludov, V.R. *Chem. Eur. J.* **2010**, *16*, 10348–10356.

Chapter 5

A Tailored Linker: Synthesis and Structures of Metal Dicarboxylates Based on a New Ligand, *meso*-1,4-Phenylenebis(hydroxyacetic acid)

5.1. Introduction

Metal-organic framework (MOF) compounds are constructed from two primary interacting components, namely the connectors and the linkers.¹⁻⁷ Connectors are usually isolated metal cations or metal clusters. The linkers, on the other hand, are polydentate organic ligands such as amines or carboxylates with specific arrangements of functional groups that determine the spatial arrangement of the connectors in the framework structure. While properties such as luminescence and magnetism often originate from the connectors, bulk properties such as chirality are directed by the organic spacers.⁴⁻⁹ Hence, the design of new organic ligands for MOF synthesis in conjunction to the node-and-linker methodology has been a research trend in generating MOFs with targeted properties associated with specific architectures.¹⁰⁻¹²

Studies on MOFs usually use commercially available organic linkers enabling rapid and inexpensive syntheses. The most commonly used linkers are aromatic dicarboxylates which function as rigid spacers leading to porous architectures with good thermal stability.^{7,12-15} Another interesting set of linkers are the α -hydroxycarboxylates such as tartaric acid and mandelic acid which can introduce chirality into MOF structures.¹⁶⁻²⁰ In addition, MOFs based on α -hydroxycarboxylates and transition metal ions form chiral architectures of interest for the study of low-dimensional magnetic systems.¹⁹⁻²² In this work, a non-commercially available ligand that has the structure

displayed in Figure 5.1 has been investigated. This linker has two α -hydroxycarboxylate groups with two chiral carbon centers. This linker has the potential to incorporate the chirality found in metal tartrates with the rigidity of aromatic dicarboxylates in new MOF compounds.

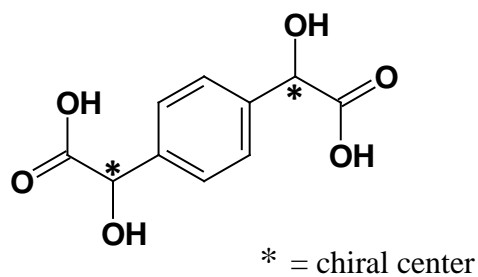


Figure 5.1. Structure of the new linker 1,4-phenylenebis(hydroxyacetic acid) (**H₂L**).

This chapter reports studies on the synthesis of coordination polymers based on **H₂L** as well as the first sets of crystal structure data for MOFs containing this ligand. The preparation and single crystal structures of compounds based on divalent metals and the new linker *meso*-1,4-phenylenebis(hydroxyacetic acid) (**H₂L**) are described. A molecular dimer Ni₂L₂(H₂O)₄ (**5-1**), chain structure compounds CoL·H₂O (**5-2**), ZnL·H₂O (**5-3**), and PbL (**5-4**) were characterized by single crystal X-ray diffraction and infrared spectroscopy.

5.3. Experimental Section

Materials and Measurements. All chemicals were obtained commercially and used without further purification. ^1H -NMR measurements were carried out in a QE-300 (300 MHz) NMR spectrometer using DMSO- d_6 as solvent. Hydrothermal reactions were performed in 23-mL Teflon-lined Parr autoclaves over a range of temperature, 100 to 180 °C for 2 to 7 days. Infrared (IR) measurements were recorded with KBr pellets using a Galaxy Series FTIR 5000 spectrometer in the range 400 to 4000 cm⁻¹. Thermal analyses were conducted on the Hi-Res TGA 2950 thermogravimetric (TG) analyzer from room temperature to 800 °C in air. Powder X-ray diffraction (PXRD) were measured using the PANalytical X’Pert Pro powder diffractometer with a Cu target ($\lambda = 1.54187 \text{ \AA}$). Elemental analyses were conducted by Galbraith Laboratories (Knoxville, TN).

Synthesis of *meso*-1,4-phenylenebis(hydroxyacetic acid) ($\mathbf{H}_2\mathbf{L}$).^{*} The procedure for the synthesis of the ligand $\mathbf{H}_2\mathbf{L}$ was adapted from the literature.²³⁻²⁴ To a mixture of 13.2 mL saturated sodium bisulfite solution and 18 mL water, 3.0 g (0.022 mol) terephthaliccarboxyaldehyde was added. The solution was cooled using an ice bath and 3.18 g (0.065 mol) sodium cyanide in 18 mL water was slowly added (1.5 h) to the mixture while stirring. The stirring was continued for 4 h at a temperature between 5 to 10 °C, followed by solvent extraction with diethyl ether. The ether layer was dried over anhydrous magnesium sulfate and evaporated in vacuo to yield crystals of 1,4-phenylenebis(hydroxyacetonitrile). Concentrated hydrochloric acid was added to the crystals and the mixture stirred for 12 h at room temperature. This was followed by heating for 2 h at 60 to 70 °C almost to dryness. The ammonium chloride was removed

* I thank Professor J. May for advice on the synthesis.

via suction filtration with the product dissolved in 1,4-dioxane. Crystallization was allowed to proceed for 24 h, and the product was collected and dried at 60 °C in a vacuum oven. $^1\text{H-NMR}$ ($\text{DMSO}-d_6$), 300 MHz: δ (ppm) = 3.35 (s, broad; OH), 4.98 (s; CH), 7.37 (s; C_6H_4).

Synthesis of $\text{Ni}_2\text{L}_2(\text{H}_2\text{O})_4$ (5-1). A mixture of 31 mg (0.1 mmol) $\text{Ni}(\text{NO}_3)_2 \cdot 6\text{H}_2\text{O}$, 23 mg (0.1 mmol) H_2L , 0.2 mL (0.2 mmol) 1M KOH and 5 mL H_2O was heated in a Teflon tape-sealed screw-capped glass vial at 80 °C for 2 d. Thin green plates were recovered by filtration, washed with water, and dried in air. Yield: 48% based on Ni. Anal. Calc. for $\text{Ni}_2\text{C}_{20}\text{O}_{16}\text{H}_{20}$: C, 37.9%; H, 3.18%; Ni, 18.5%. Found: C, 37.3%; H, 3.97%; Ni 18.9%.

Synthesis of $\text{CoL}(\text{H}_2\text{O})_2 \cdot \text{H}_2\text{O}$ (5-2). A solution of 45.2 mg (0.2 mmol) H_2L in 4 mL H_2O was allowed to slowly diffuse into a solution of 47.6 mg (0.2 mmol) $\text{CoCl}_2 \cdot 6\text{H}_2\text{O}$ in 4 mL H_2O at room temperature. A few red prismatic crystals of **5-2** were observed at the side of the glass tube after 20 d and were isolated manually from an unknown light red powder matrix.

Synthesis of $\text{ZnL}(\text{H}_2\text{O})_2 \cdot \text{H}_2\text{O}$ (5-3). The procedure was similar to that used in the synthesis of **5-2**, this time using 59.5 mg (0.2 mmol) $\text{Zn}(\text{NO}_3)_2 \cdot 6\text{H}_2\text{O}$ as the metal cation source. Colorless crystals of **5-3** were isolated from an unknown white powder phase after 14 d.

Synthesis of PbL (5-4). A mixture of 77 mg (0.2 mmol) $\text{Pb}(\text{CH}_3\text{COO})_2 \cdot 3\text{H}_2\text{O}$, 44 mg (0.2 mmol) 2,6-H₂NDC, 0.2 mL (0.2 mmol) 1M KOH and 5 mL H_2O was heated in a 23-mL Teflon-lined Parr autoclave at 180 °C for 7 d. Colorless prismatic crystals of **5-4** were isolated from a white powder matrix, washed with water, and dried in air.

Yield: 40% based on Pb. Anal. Calc. for $\text{Pb}_1\text{C}_{10}\text{O}_6\text{H}_6$: C, 28.0%; H, 1.41%; Pb, 48.3%.

Found: C, 27.6%; H, 1.79%; Pb 49.2%.

X-ray Crystallography. Crystals of the M-L compounds with suitable size were carefully selected, picked up with a glass fiber-pin, and mounted on a goniometer on an X-ray machine with a N_2 cold stream operating at 213 K. Measurements were made using monochromated Mo $\text{K}\alpha$ radiation ($\lambda = 0.71073 \text{ \AA}$) on a Siemens SMART platform diffractometer equipped with a CCD area detector. Data collection, cell refinement, and data reduction were performed using the APEX2 system.²⁵ All structures were solved by direct methods using SHELXS97 and refined by difference Fourier techniques using SHELXL97, programs on the WinGX package.²⁶ Molecular graphics and structure representations were done using the DIAMOND visualization software.²⁷ Crystallographic data and structure refinement parameters for the compounds are summarized in Table 5.1.

Table 5.1. Crystallographic data and structure refinement for compounds **5-1** to **5-4**.

Compounds	5-1	5-2	5-3	5-4
Formula	$\text{Ni}_2\text{C}_{20}\text{O}_{16}\text{H}_{20}$	$\text{Co}_1\text{C}_{10}\text{O}_9\text{H}_{12}$	$\text{Zn}_1\text{C}_{10}\text{O}_9\text{H}_{12}$	$\text{Pb}_3\text{C}_{10}\text{O}_6\text{H}_6$
Formula weight	316.89	355.16	361.62	429.34
Crystal system	Orthorhombic	Monoclinic	Monoclinic	Monoclinic
Space group	<i>Pbam</i>	<i>C2/c</i>	<i>C2/c</i>	<i>C2/c</i>
<i>a</i> , Å	9.6142(2)	20.7272(2)	20.7801(1)	10.2009(1)
<i>b</i> , Å	10.1890(2)	12.9346(2)	12.2856(9)	9.779(1)
<i>c</i> , Å	23.7530(5)	10.2502(9)	10.2530(7)	10.1272(1)
α , degrees	90.00	90.00	90.00	90.00
β , degrees	90.00	102.4310(1)	102.6780(1)	101.0470(1)
γ , degrees	90.00	90.00	90.00	90.00
<i>V</i> , Å ³	2362.8(8)	2683.8(4)	2674.3(3)	993.6(2)
Z	8	8	8	4
Temperature, K	223	223	223	223
ρ_c , g cm ⁻³	1.809	1.758	1.796	2.870
μ (Mo K α), mm ⁻¹	1.702	1.329	1.888	16.994
R1, wR2 [I>2σ(I)] ^a	0.0615, 0.1330	0.0249, 0.0708	0.0272, 0.0748	0.0249, 0.0650
R1, wR2 (all data) ^a	0.1458, 0.1570	0.0285, 0.0724	0.0318, 0.0768	0.0279, 0.0665

5.4. Results and Discussion

Syntheses. The synthesis of the ligand, $\mathbf{H}_2\mathbf{L}$ was adapted from the initial steps in the preparation of a complex organic compound reported in literature.²³ The transformation follows a nucleophilic addition to the terephthalaldehyde to produce the nitrile derivative, then the carboxylate is formed by subsequent hydrolysis. The crude product was dried in a vacuum oven to completely remove the 1,4-dioxane solvent and then monitored by $^1\text{H-NMR}$ (Figure 5.2) using a solvent $\text{DMSO}-d_6$ that contains tetramethylsilane (TMS) as internal standard. Peak shifts are assigned accordingly with the aromatic protons at 7.37 ppm and the α -methyl protons at 4.98 ppm. The broad peak at 3.35 ppm is assigned to the hydroxy protons. The FT-IR spectra of the ligand in KBr pellet is presented in Figure 5.3. The data shows the OH stretches at 3447 cm^{-1} typical for alcohols and broad peak at 2914 cm^{-1} for carboxylic acids. The strong C=O stretch at 1723 cm^{-1} is evident, as well as the strong C-O vibrations at 1246 cm^{-1} and 1070 cm^{-1} for acid and alcohol functionalities respectively.

Reactions of the ligand with metal salts yield single crystals of **5-1** and **5-4** by hydrothermal synthesis, and **5-2** and **5-3** by the test tube layer-diffusion method. The optical images of the crystals are shown in Figure 5.4. Among the crystals, only compounds **5-1** and **5-4** were obtained as a pure phase product in high yields. Crystals of **5-2** and **5-3** were isolated as a minor phase product by test tube layer-diffusion but the optimum synthesis conditions are still unknown as most of the replicate tubes did not generate the crystals. Attempts to grow pure phases of **5-2** and **5-3** in single crystalline or powder form were unsuccessful.

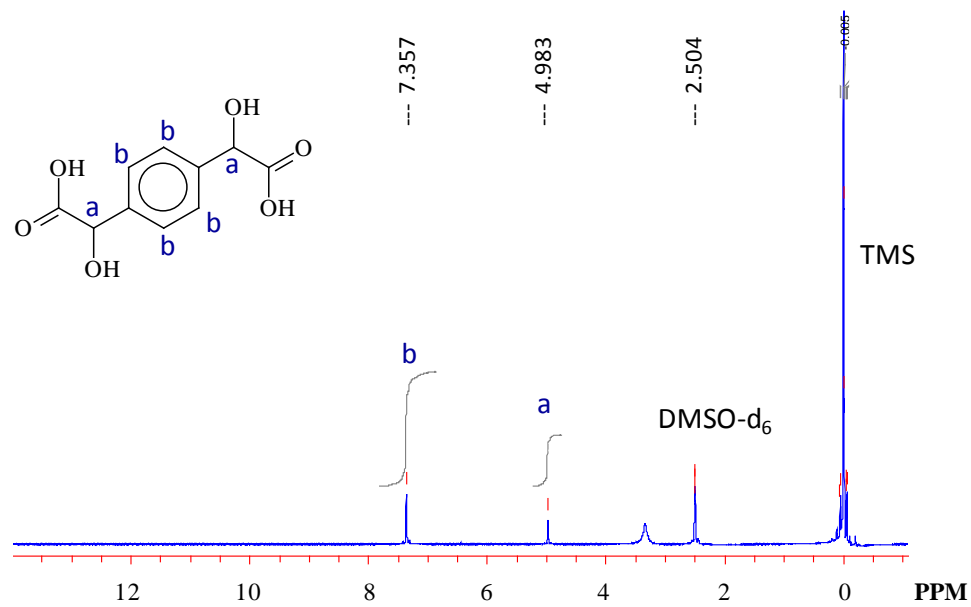


Figure 5.2. ^1H -NMR spectra of H_2L .

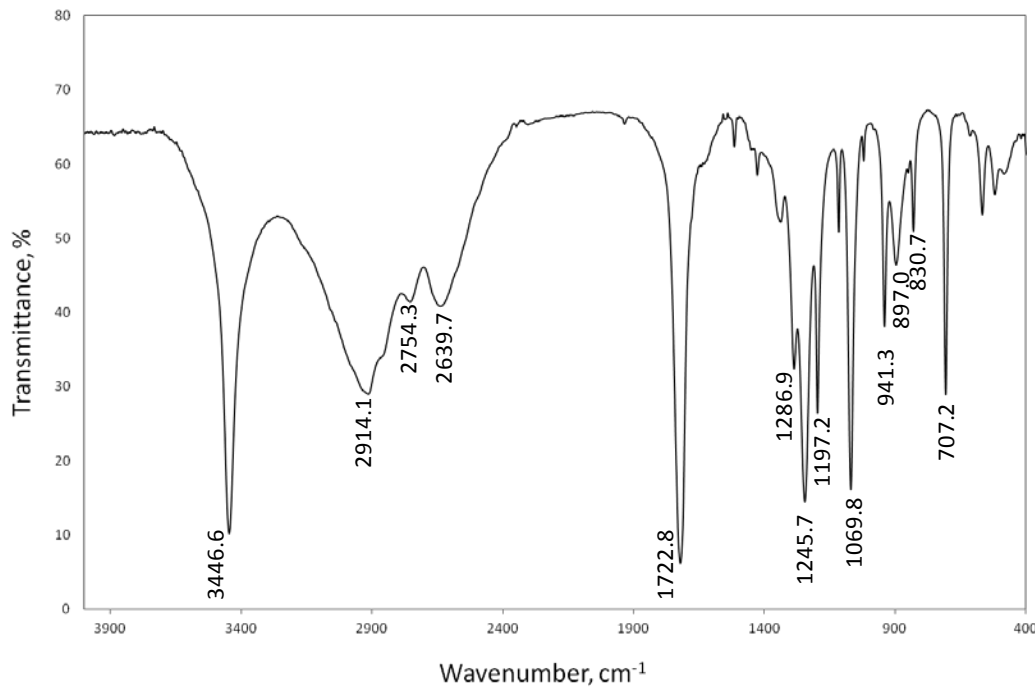


Figure 5.3. FT-IR spectra of H_2L .

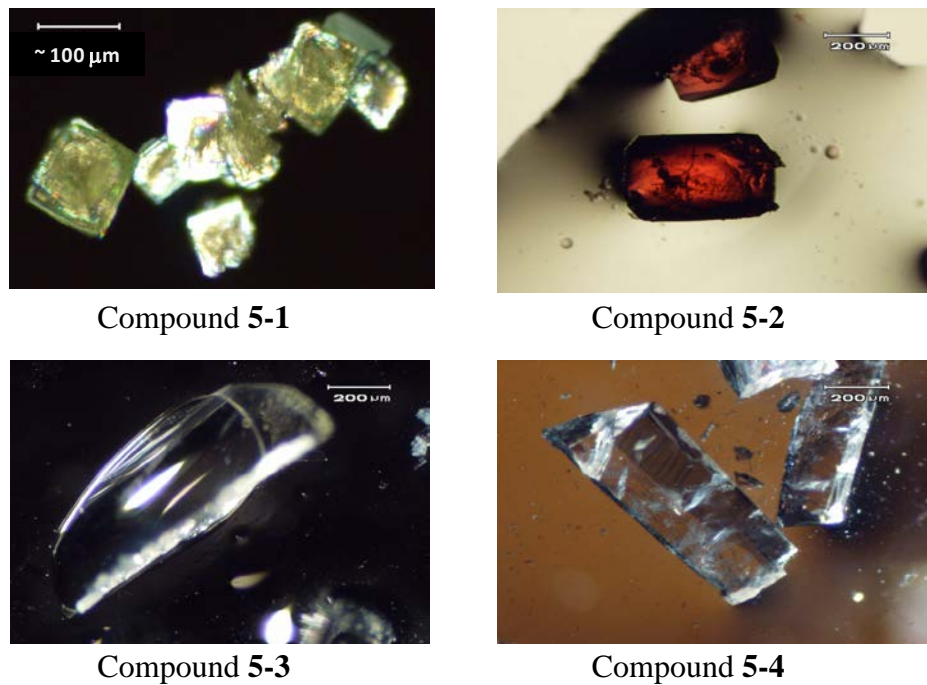


Figure 5.4. Optical Microscope Images of the Crystals **5-1** to **5-4**.

Other metal cations such as Mn^{2+} , Cu^{2+} , Fe^{3+} , Cr^{3+} , Mg^{2+} , Sb^{2+} , Sn^{2+} , La^{3+} , Ce^{3+} , Pr^{3+} , Sm^{3+} , Yb^{3+} , and V^{4+} were tested both solvothermally and by layer-diffusion but failed to yield single crystal products for structure determination. Mixed metal systems of Ni^{2+} combined with Cr^{3+} and Fe^{3+} ions under hydrothermal conditions were also tried. Investigations with temperature variations from ambient, 80 °C, 100 °C, 120 °C, 150 °C, and 180 °C were conducted. Reactions were mostly carried out in water but other solvents like methanol, ethanol, and dimethylformamide were also used. Metal to ligand reactant ratios of 1 : 1, 2 : 1, 1 : 2, and 3 : 2 were used as well as variations of the counterions by using different metal salt sources such as chlorides, nitrates, sulfates,

carbonates, and acetates. In most cases, reactions of metal salts and **H₂L** at different conditions produced less- to non-crystalline phase products.

Nevertheless, these results present the first sets of crystal data reported for compounds involving the ligand **H₂L**. The crystal structure of the complexes showed that the synthesized ligand was in *meso*- form. Since the *meso*- form contains a center of symmetry, it is therefore optically inactive. Attempts to grow optically active products by addition of templating chiral amines to high temperature solvothermal reactions to induce homochirality were not successful.

General Coordination and Hydrogen Bonding. Structures showing the metal coordination environment in the compounds are presented in Figure 5.5. The transition metal (Ni^{2+} , Co^{2+} , Zn^{2+}) complexes adopt octahedral geometry with six coordinated oxygen atoms from two sets of chelating carboxyl and α -hydroxyl oxygen atoms from two distinct ligands and two water molecules. The coordination environment around Pb^{2+} is similar to that of the transition metals except for the missing coordinated water oxygen atoms; a one sided-type of coordination with the four oxygen atoms forming a pyramidal configuration with the metal atom is observed.

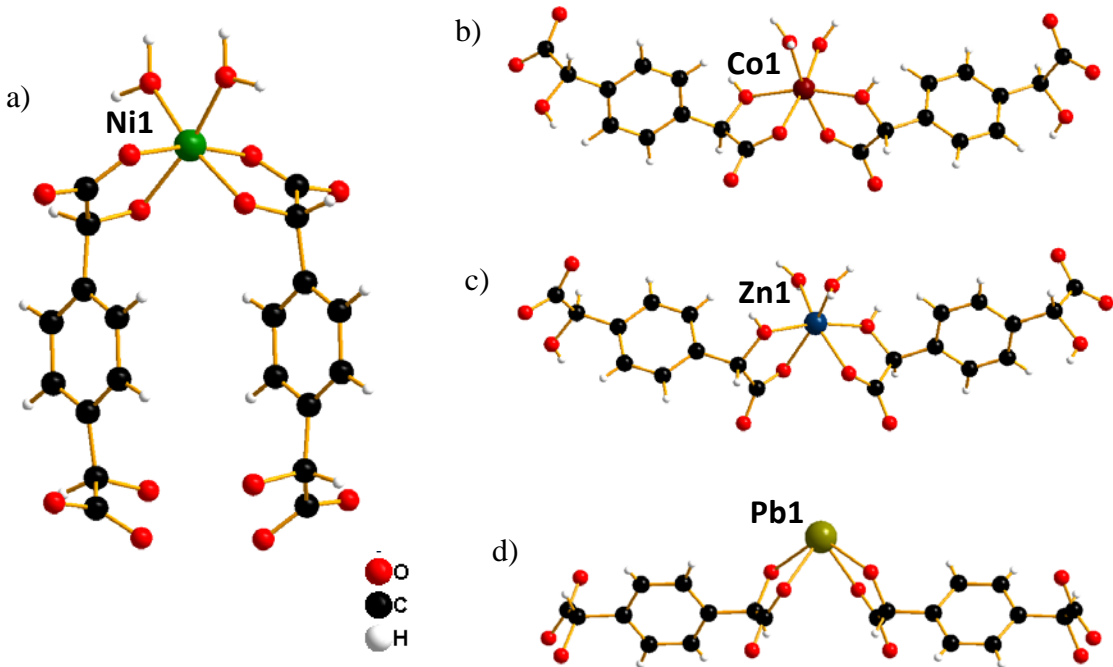


Figure 5.5. The metal coordination environments in compounds **5-1** to **5-4** (a to d, respectively).

The ligand L^{2-} shows only one mode of bridging coordination in all the compounds (Figure 5.6) with one carboxylate and one alkoxy oxygen atoms chelated to the metal cation. This results in one unbound carboxylate oxygen capable of accepting a hydrogen bond from coordinated and/or uncoordinated water molecules or from the protonated alkoxy group of the adjacent ligands. A summary of the hydrogen bonding parameters are outlined in Table 5.2. The presence of several functionalities capable of such interactions results into an extended network of hydrogen bonded layers in **5-1**, **5-2**, and **5-3** (Figure 5.7). Further details of the interactions are provided together with the subsequent crystal structure description for each compound.

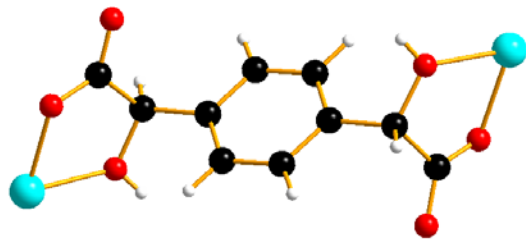


Figure 5.6. Coordination of the linker, \mathbf{L}^{2-} .

Table 5.2. Hydrogen bonding parameters in compounds **5-1** to **5-3**.

	D-H (Å)	D---A (Å)	H---A (Å)	D-H---A (°)
5-1				
O1-H13---O7	1.0117(2)	2.8860(15)	1.9836(3)	147.122(1)
O1-H14---O5	1.0090(2)	2.7496(4)	2.0312(3)	126.129(1)
O7-H12---O2	1.0097(1)	2.7025(3)	1.9260(3)	131.445(8)
5-2				
O1-H16---O9	0.7427(1)	2.7470(3)	2.0100(3)	171.662(1)
O2-H13---O10	0.7759(1)	2.6987(3)	1.9248(2)	175.167(1)
O5-H10---O8	1.0340(1)	2.6870(3)	1.6566(2)	173.985(1)
O5-H11---O4	0.7105(1)	2.8089(4)	2.1049(3)	171.064(2)
O6-H5---O7	0.8911(1)	2.7862(3)	1.9199(2)	163.599(1)
O6-H9---O3	0.8098(1)	2.7217(4)	1.9302(3)	165.487(2)
O9-H6---O7	0.8133(1)	2.8549(3)	2.0698(2)	162.157(1)
O9-H8---O8	0.8648(1)	2.8208(4)	1.9658(3)	169.651(2)
5-3				
O2-H13---O10	0.7727(1)	2.6896(2)	1.9192(2)	174.802(1)
O3-H14---O9	0.6516(1)	2.7483(3)	2.0968(2)	178.630(1)
O5-H6---O4	0.8850(1)	2.7093(3)	1.8335(2)	169.956(1)
O5-H15---O8	0.7299(1)	2.7945(3)	2.0695(2)	172.253(1)
O6-H5---O1	0.7933(1)	2.8026(3)	2.0106(2)	176.142(1)
O6-H16---O7	0.8385(1)	2.6883(3)	1.8498(2)	179.626(1)
O9-H9---O8	0.6647(1)	2.8516(2)	2.2122(2)	161.964(1)
O9-H10---O7	1.0486(1)	2.8177(3)	1.7885(2)	166.134(1)
O10-H11---O8	0.8334(1)	2.9056(3)	2.1097(2)	159.678(1)

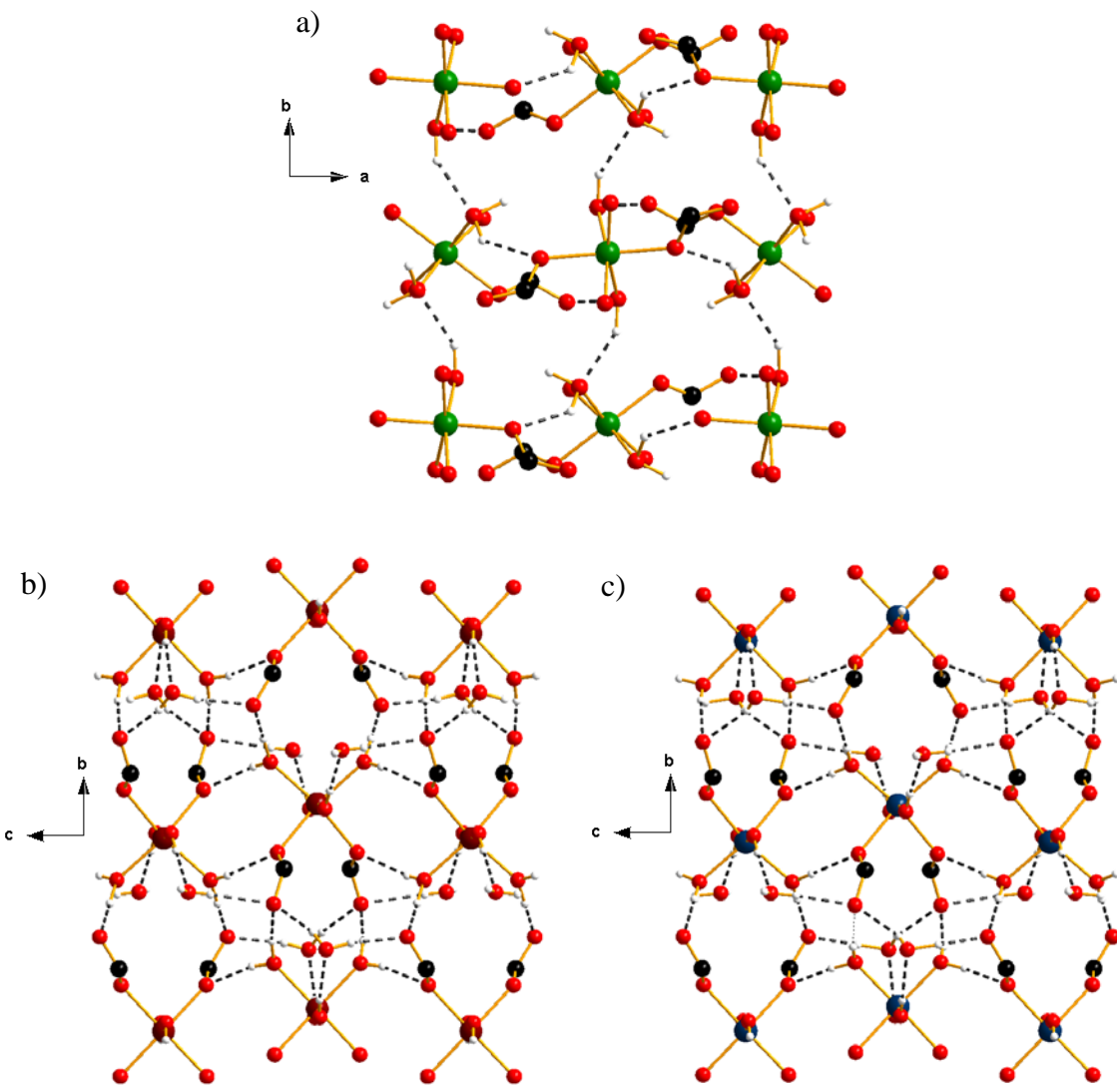


Figure 5.7. Hydrogen bonding layers (top view) in compounds a) **5-1**, b) **5-2**, and c) **5-3**.
Hydrogen bonds are represented by dashed lines (---).

Crystal Structure of $\text{Ni}_2\text{L}_2(\text{H}_2\text{O})_4$ (5-1). Compound **5-1** is a molecular dimer of Ni^{2+} cations bridged by two L^{2-} ligands with the metal chelated to a carboxylate oxygen atom and a hydroxyl oxygen atom of two L^{2-} groups (Figure 5.8). The coordination around the Ni atom is a distorted octahedron with four chelating oxygen atoms from L^{2-} [$\text{Ni}-\text{O}$ distances range from 2.0063(3) to 2.0547(3) Å] and two water molecules occupying the six coordination sites [$\text{Ni}-\text{O}(\text{water})$ distances are 2.0468(3) and 2.0543(3) Å]. The two water molecules and the α -hydroxyl oxygens are situated *cis* to each other, with the carboxylate oxygens occupying the *trans* position. This leaves the free carboxylate oxygens on the four surrounding corners of the dimer available for further linking. This dimer unit configuration is the building unit for several metal tartrates with interesting chiral as well as magnetic properties.²¹

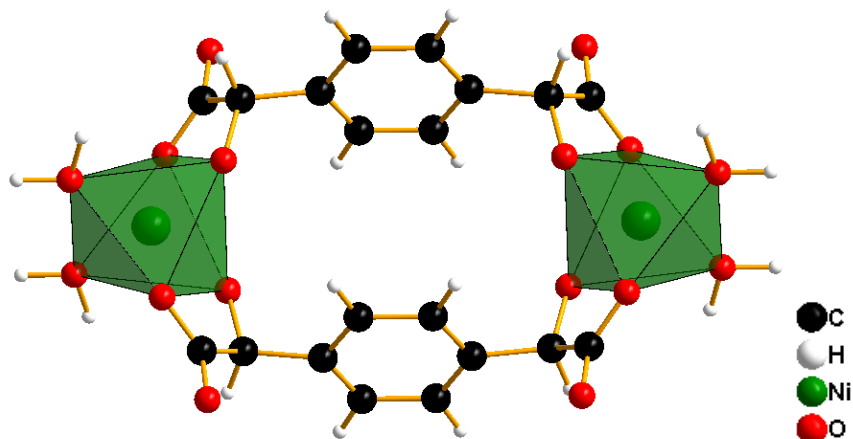


Figure 5.8. Crystal structure of the dimer unit in **5-1**.

The adjacent dimers are held together by hydrogen bonds through the coordinated water molecules and the carboxylate group [donor-O to acceptor-O bond distances vary from 2.7025(3) to 2.8860(2) Å]. The aromatic rings also facilitate the packing of the dimer units and consequently form dimeric layers that are oriented perpendicular to each other (Figure 5.9).

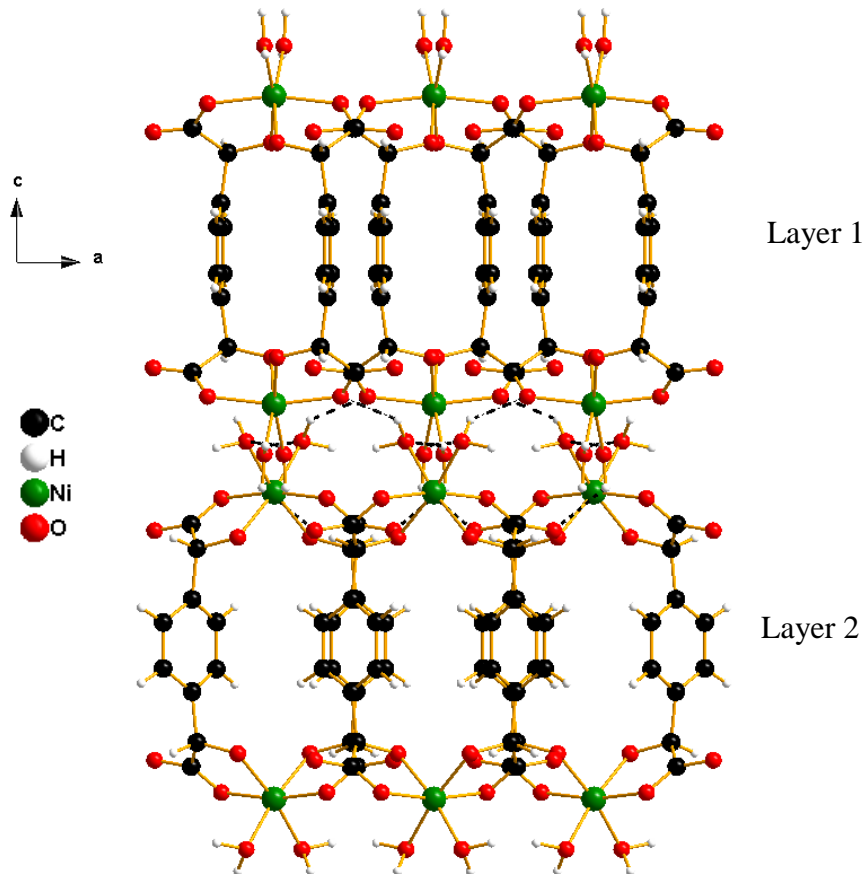


Figure 5.9. Structures of compound **5-1** along *b* showing the perpendicular layers of dimeric units. Hydrogen bonds are represented by dashed lines (---).

The planes of the benzene rings of the ligand are illustrated in Figure 5.10. Within the dimer units, the distance between two parallel planes is 3.5422(1) Å. The shortest distance between two benzene rings of adjacent dimers is 3.3888(5) Å. These values suggest weak π interactions of the aromatic rings. The dihedral angle between the two planes coming from distinct dimers is 9.580(1) $^{\circ}$.

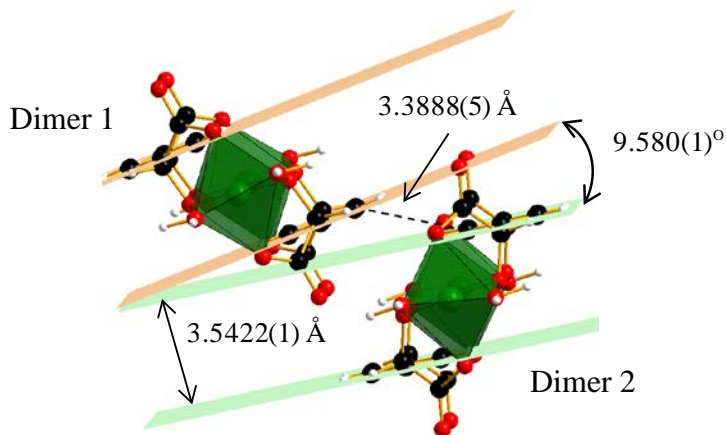


Figure 5.10. Distances and dihedral angle between planes of aromatic rings of adjacent dimers in **5-1**.

Crystal Structures of $\text{CoL}(\text{H}_2\text{O})_2 \cdot \text{H}_2\text{O}$ (5-2) and $\text{ZnL}(\text{H}_2\text{O})_2 \cdot \text{H}_2\text{O}$ (5-3). The crystal structures of **5-2** and **5-3** consist of chains of MO_6 [$\text{M} = \text{Co}^{2+}$ (**5-2**) or Zn^{2+} (**5-3**)] octahedra bridged by L^{2-} through a chelated coordination from the α -hydroxyl oxygen and a carboxylate oxygen of the ligand molecule (Figure 5.11). Two water molecules bound to the metal center are also present in the structure and guest water molecules are located surrounding the chains. Each metal atom is coordinated to six oxygen atoms forming a distorted octahedron with M-O bond distances ranging from 2.0476(3) to 2.1131(3) Å for **5-2** and 2.0320(2) to 2.1362(2) Å for **5-3**. Similar to **5-1**, the coordinated

water molecules are oriented *cis* to each other. The two α -hydroxyl oxygen atoms, however, occupy the *trans* sites leaving the bound carboxylate oxygens *cis* to each other. This results in the unbound carboxylate oxygen atoms oriented perpendicular to the chain capable of hydrogen bonding with neighboring guest or bound water molecules of the adjacent chains. The chains propagating parallel to the *a* direction are stacked together by a complex hydrogen bonding network (Figure 5.12) from several possible combinations of coordinated and uncoordinated water molecules, the α -hydroxy group, and the carboxylate oxygens [donor-O to acceptor-O bond distances range from 2.6870(3) to 2.8549(3) Å for **5-2** and from 2.6883(3) to 2.9056(3) Å for **5-3**].

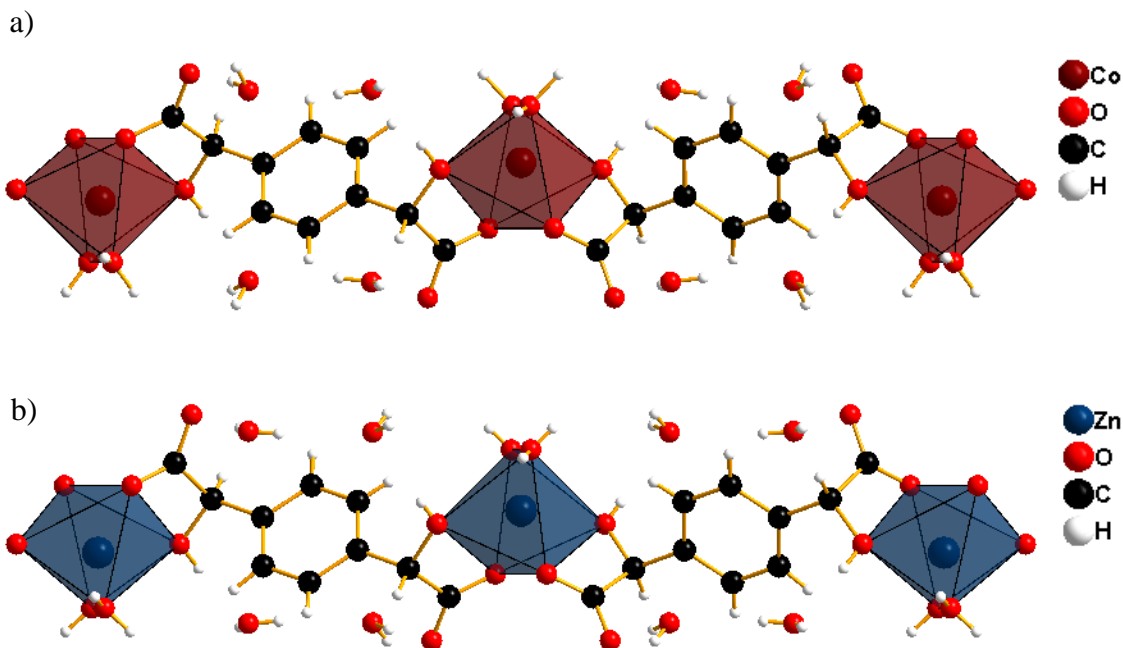


Figure 5.11. Chain structures of a) compound **5-2** and b) compound **5-3** and the guest water molecules surrounding the chains.

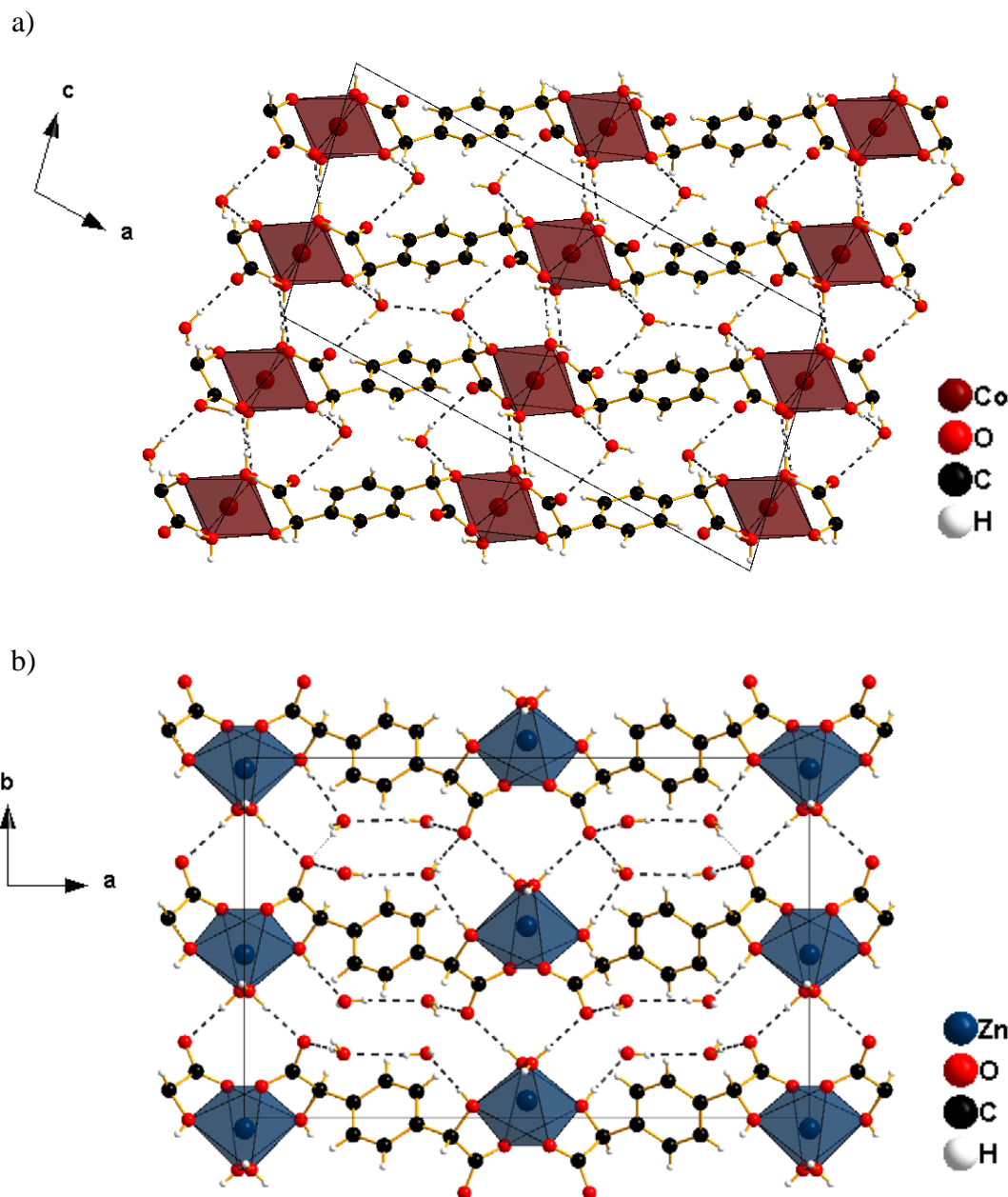


Figure 5.12. Crystal structure of a) compound **5-2** along *b* axis and b) compound **5-3** along *c* axis. H-bonding interaction is represented as dashed lines (---).

Crystal Structure of PbL (5-4). Compound **5-4** is a one dimensional coordination polymer that has a similar chain unit to **5-2** and **5-3** except for the absence of any (bound or guest) water molecules in the structure (Figure 5.13a). The absence of coordinated water molecules leads to an incomplete octahedron around Pb^{2+} and a pyramidal geometry with Pb cation at the apex coordinated to four basal oxygen atoms. The two sets of chelating α -hydroxy and carboxylate oxygens are located on the same side of the Pb atom adopting a hemidirected-type of coordination geometry [Pb-O bond lengths are 2.3153(3) and 2.5012(3) Å]. This type of coordination motif is expected for divalent Pb complexes and suggests the presence of a stereochemically active lone pair at the metal cation.²⁸ The chains are stacked together by weak Pb^{2+} to O interactions [Pb-O distance of 3.0374(3) Å], from the free carboxylate oxygens of the adjacent chains with the nearby Pb atom in the structure (Figure 5.13b).

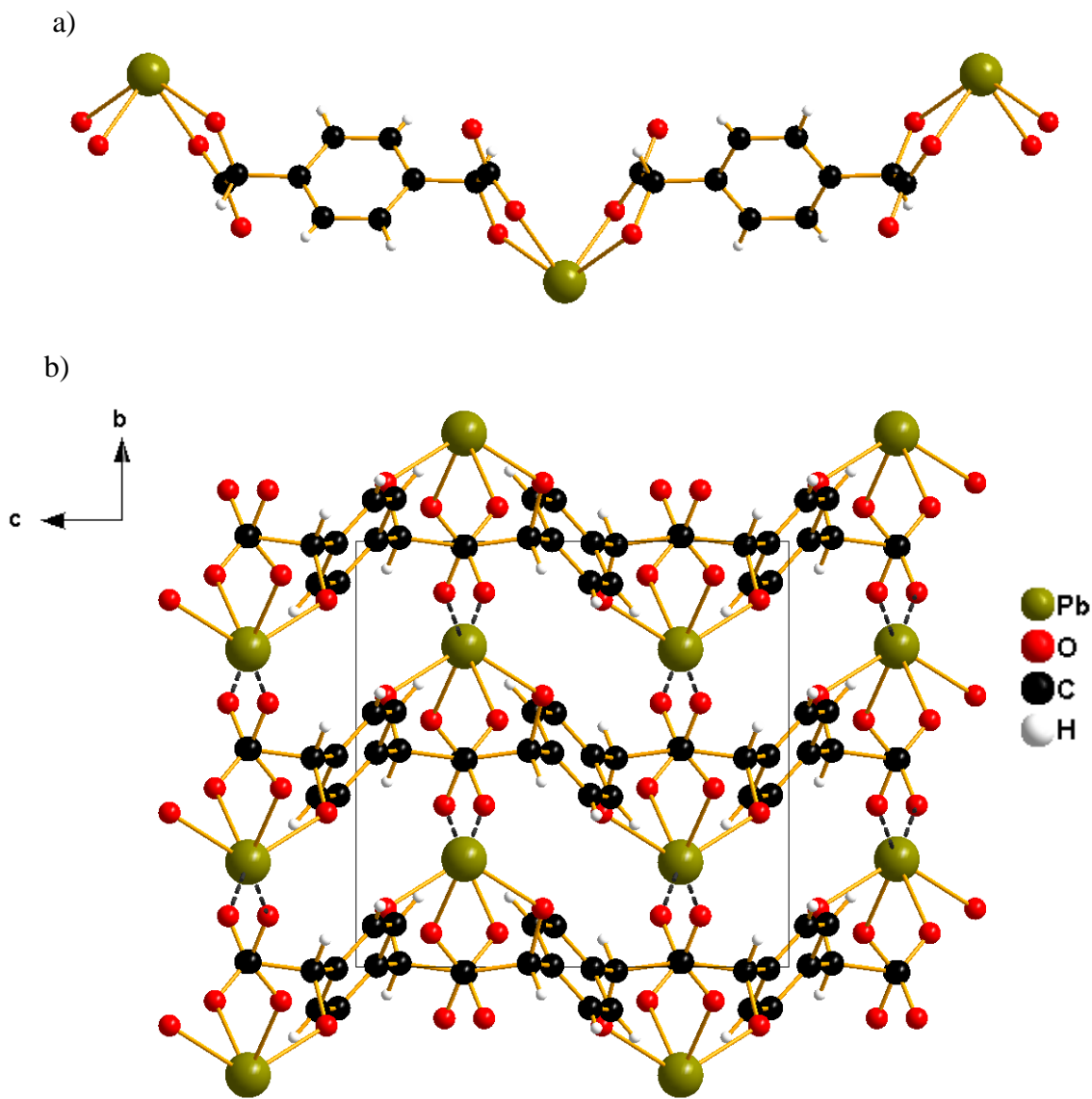


Figure 5.13. Crystal structure of **5-4**: a) 1-D chain unit and b) stacking of chains along *a* showing the weak Pb-O interaction represented as dashed lines (- - -).

FT-IR, PXRD and TGA Characterization. The infrared spectra of compounds **5-1** to **5-4** in the range 400 to 4000 cm⁻¹ are presented in Figure 5.14. Strong broad peaks at around 3400-3200 cm⁻¹ are indicative of O-H stretching due to the presence of water molecules in the structures of **5-1**, **5-2**, and **5-3**. This is clearly not the case for the anhydrous **5-4** as the small hump in this region is caused by surface water. The C-H stretches from the organic linker at around 2900 cm⁻¹ partially overlapping the O-H peaks are observed for all compounds. The collection of strong peaks in the 1700-1100 cm⁻¹ region accounts to several group vibrations including carboxylate symmetric and asymmetric vibrations as well as to the carbonyl frequencies of the alkoxy and carboxylate groups.

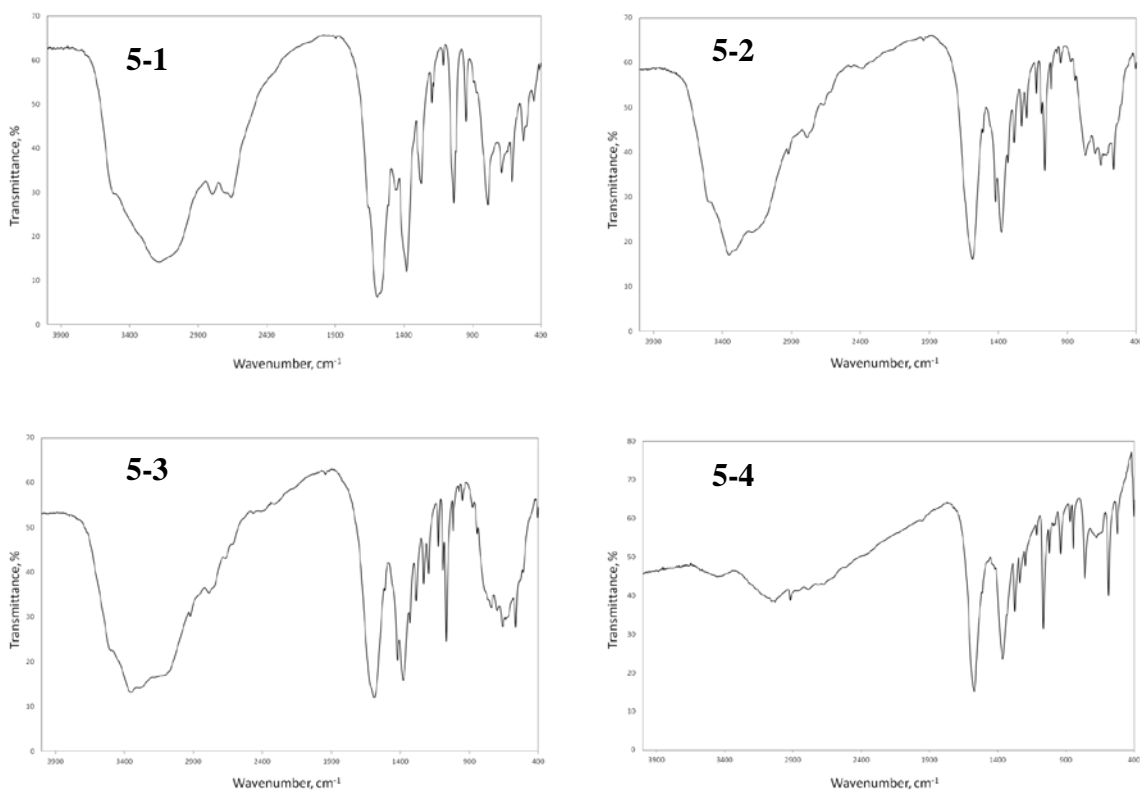


Figure 5.14. FT-IR spectra of compounds **5-1** to **5-4**.

Due to the low yield of **5-2** and **5-3**, no further characterization was conducted for the compounds other than single crystal X-ray diffraction and FT-IR spectroscopy. Compounds **5-1** and **5-4**, however, were generated in substantial yields as pure phase products for thermogravimetric study and powder X-ray diffraction. Powder XRD patterns of compounds **5-1** and **5-4** are displayed in Figure 5.15. The peak positions on the experimental PXRD data are in very good agreement with the simulated patterns. No observable extraneous peaks are present, indicative of the purity of the bulk products. Difference in intensities may be due to the preferred orientation of the powdered materials.

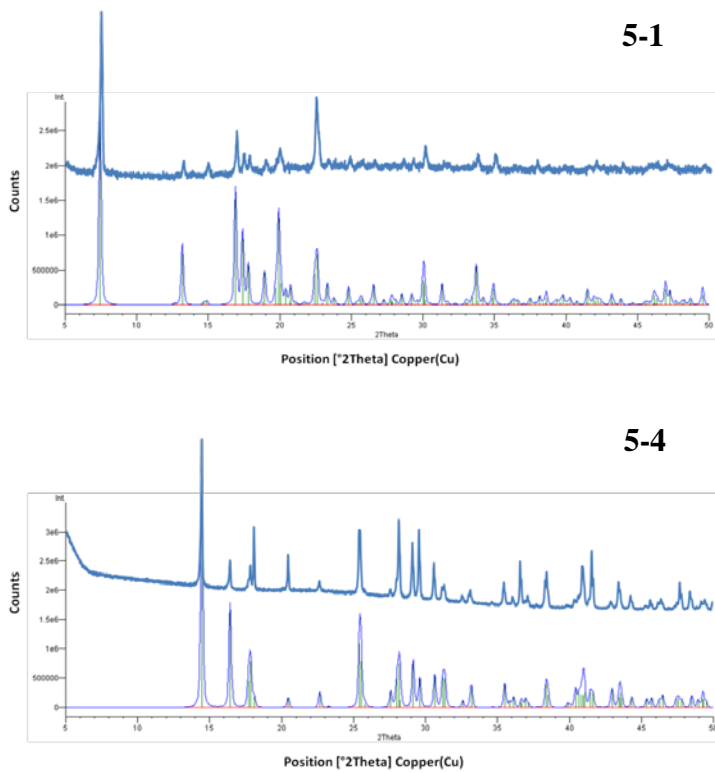


Figure 5.15. PXRD data of compounds **5-1** and **5-4**. The top plots are experimental patterns while the bottom plots are simulated patterns from the single crystal data.

The thermogravimetric results for **5-1** and **5-4** are shown in Figure 5.15. The TG data for compound **5-1** (Figure 5.16a) suggests a decomposition process that occurs in two distinct steps. The first step is a process at 100 °C to 300 °C corresponding to the loss of four coordinated H₂O molecules per dimer formula (11.37% calc., 11.56% expt.). This is followed by the loss of two remaining ligand (**L**²⁻) molecules (65.04% calc., 65.70% expt.) at around 350 °C. On the other hand, the TG plot for compound **5-4** (Figure 5.16b) indicates a two-step loss of the ligand molecule from 300 °C to 450 °C. The total weight loss for this process matches the calculated values for a loss of one ligand molecule per formula unit of the compound (48.02% calc., 48.23% expt.). The residual solids after the analyses were examined by powder X-ray diffraction and identified as nickel oxide (NiO) for **5-1** and lead oxide (PbO) for **5-4**.

5.4. Conclusion

A series of coordination complexes based the ligand, *meso*-1,4-phenylenebis(hydroxyacetic acid) (**H₂L**) and divalent metal cations were successfully prepared and their crystal structures determined by single crystal X-ray crystallography. Compound **5-1** is a molecular dimer based on Ni²⁺ while **5-2** and **5-3** are isostructural chain compounds based on Co²⁺ and Zn²⁺, respectively. Crystal data from these three compounds showed extensive hydrogen bonding responsible for the stacking of the molecular or chain units in the structure. Another chain compound **5-4** based on Pb²⁺ was also prepared and a weak Pb-O interchain interaction accounts for the packing of the chain units. To our knowledge, this is the first report regarding the crystal data of compounds involving the linker **H₂L**.

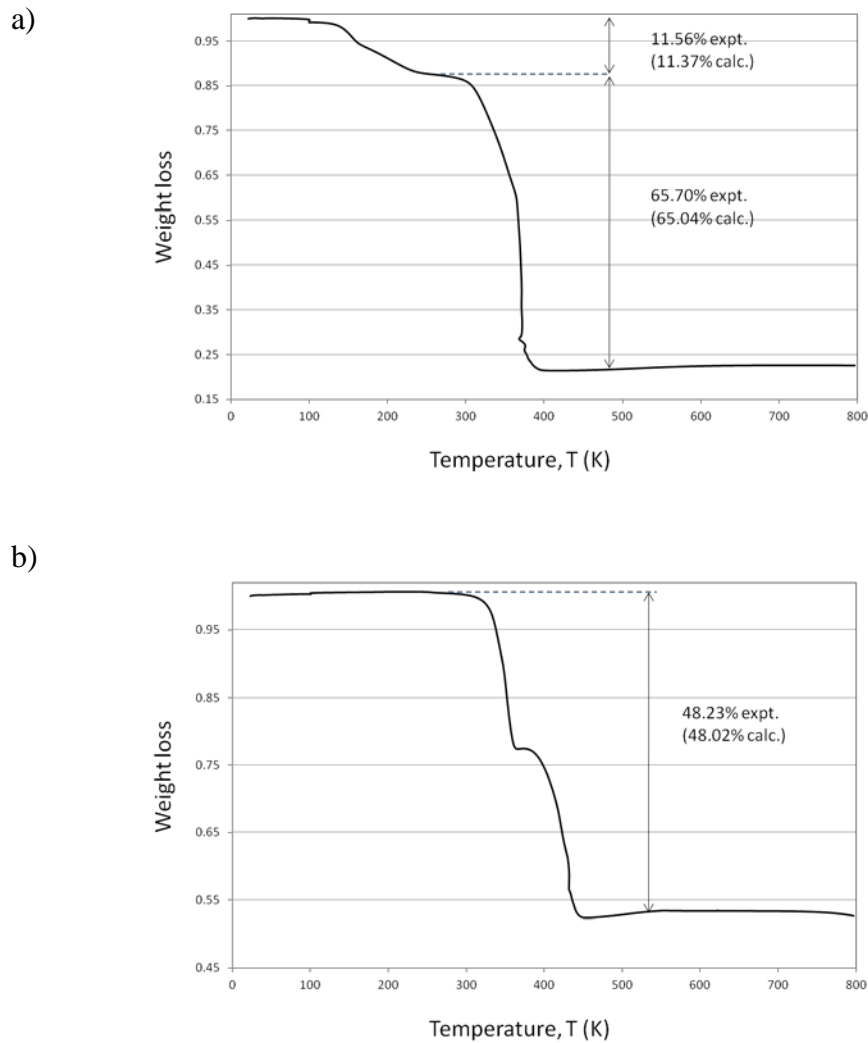


Figure 5.16. TGA plot of compounds a) 5-1 and b) 5-4.

5.5. References

1. Perry IV, J.J.; Perman, J.A.; Zawarotko, M.J. *Chem. Soc. Rev.* **2009**, *38*, 1400–1417.
2. Natarajan, S.; Mahata, P. *Chem. Soc. Rev.* **2009**, *38*, 2304–2318.
3. Tranchemontagne, D.J.; Ni, Z.; O’Keeffe, M.; Yaghi, O.M. *Angew. Chem. Int. Ed.* **2008**, *47*, 5136–5147.
4. Cheetham, A.K.; Rao, C.N.; Feller, R.K. *Chem. Commun.* **2006**, *38*, 4780–4795.
5. Kitagawa, S.; Kitaura, R.; Noro, S. *Angew. Chem. Int. Ed.* **2004**, *43*, 2334–2375.
6. James, S.L. *Chem. Soc. Rev.* **2003**, *32*, 276–288.
7. Eddaoudi, M.; Moler, D.B.; Li, H.; Chen, B.; Reineke, T.M.; O’Keeffe, M.; Yaghi, O.M. *Acc. Chem. Res.* **2001**, *34*, 319–330.
8. Tranchamontagne, D.J.; Mendoza-Cortes, J.L.; O’Keeffe, M.; Yaghi, O.M. *Chem. Soc. Rev.* **2009**, *38*, 1257–1283.
9. Ma, L.; Abney, C.; Lin, W. *Chem. Soc. Rev.* **2009**, *38*, 1248–1256.
10. Lin, W.; Rieter, W.J.; Taylor, K.M.L. *Angew. Chem. Int. Ed.* **2009**, *48*, 650–658.
11. Janiak, C. *Dalton Trans.* **2003**, 2781–2804.
12. Almeida Paz, F.A.; Klinowski, J.; Vilela, S.M.F.; Tome, J.P.C.; Cavaleiro, J.A.S.; Rocha, J. *Chem. Soc. Rev.* **2012**, *41*, 1088–1110.
13. Rao, C.N.R.; Natarajan, S.; Vaidhyanathan, R. *Angew. Chem. Int. Ed.* **2004**, *43*, 1466–1496.
14. Robin, A.Y.; Fromm, K.M. *Coord. Chem. Rev.* **2006**, *250*, 2127–2157.
15. Sudik, A.C.; Cote, A.P.; Wong-Foy, A.G.; O’Keeffe, M.; Yaghi, O.M. *Angew. Chem. Int. Ed.* **2006**, *45*, 2528–2533.

16. Kam, K.C.; Young, K.L.M.; Cheetham, A.K. *Cryst. Growth Des.* **2007**, *7*, 1522–1532.
17. Rood, J.A.; Noll, B.C.; Henderson, K.W. *J. Solid State Chem.* **2010**, *183*, 270–276.
18. Gu, Y.; Yang, M. *Cryst. Res. Technol.* **2008**, *43*, 1331–1334.
19. Train, C.; Gruselle, M.; Verdaguer, M. *Chem. Soc. Rev.* **2011**, *40*, 3297–3312.
20. Beghidja, A.; Rogez, G.; Rabu, P.; Welter, R.; Drillon, M. *J. Mater. Chem.* **2006**, *16*, 2715–2728.
21. Coronado, E.; Galan-Mascaros, J.R.; Gomez-Garcia, C.J.; Murcia-Martinez, A. *Chem. Eur. J.* **2006**, *12*, 3483–3492.
22. Train, C.; Gheorghe, R.; Krstic, V.; Chamoreau, L.M.; Ovanesyan, N.S.; Rikken, G.L.J.A.; Gruselle, M.; Verdaguer, M. *Nat. Mater.* **2008**, *7*, 729–734.
23. Gotthardt, H.; Pflaumbaum, W. *Chem. Ber.* **1987**, *120*, 411–420.
24. Corson, B.B.; Dodge, R.A.; Harris, S.A.; Yeaw, J.S. *Organic Syntheses* **1941**, *Coll. Vol. 1*, 336.
25. *APEX2 User Manual*, Version 1.27; Bruker AXS Inc.: Madison, WI, **2005**.
26. Farrugia, L.J. *J. Appl. Cryst.* **1999**, *32*, 837–838.
27. Brandenburg, K. *DIAMOND*; Crystal Impact GbR, Bonn, Germany, **2006**.
28. Shimon-Livny, L.; Glusker, J.P.; Bock, C.W. *Inorg. Chem.* **1998**, *37*, 1853–1867.

Chapter 6

Assembly at the Surface: Preparation of Metal-Organic Framework Films on Functionalized Gold Surfaces

6.1. Introduction

The novel architectures of metal-organic frameworks (MOFs) have led to numerous studies that provide clues to the general rules for the reticular synthesis of these compounds.¹⁻⁵ Equally important, is their practical application, in particular, the means by which these porous structures can be incorporated in nanodevices.⁶⁻⁹ The controlled deposition of dense, homogenous and highly-oriented porous crystalline MOF thin films presents a significant synthetic challenge. Efforts to address the challenge have been outlined in recent reviews that report several strategies regarding the deposition MOFs on various substrates and their potential applications.¹⁰⁻¹²

MOFs are a class of porous materials based on the combination of metal connectors and organic linkers that have extended connectivity.¹⁻⁴ Their characteristic high surface area is the basis for several applications such as catalysis and gas storage.^{7,9,13-16} The possibility of anchoring MOFs on solid supports further widens their applicability, for example, as separation membranes, functional material coatings, or in chemical sensing devices.

Self-assembled monolayers (SAMs) are organic nano-assemblies that can be used to tailor the functionality of a wide variety of substrates such as metals or metal oxides.¹⁷⁻¹⁸ The relative ease of preparation and the diversity of the functionality introduced on a specific substrate make SAMs the ideal anchor materials for growing crystalline MOF

thin films. Recently, several reports have been published regarding the use of SAMs in the deposition of MOF films on different substrates using various film-fabrication techniques.^{10,19-23}

This work describes a versatile methodology for preparing MOF thin films on SAM-functionalized gold (Au) substrates. The system chosen for study is MOF-5, which has a cubic topology built from a Zn₄O-cluster building unit and a terephthalate linker.²⁴²⁵ The quality of the MOF-5 thin films prepared in this work is described in comparison with the products reported in similar studies using other methods.²¹⁻²² A thiocarboxylate is used to convert the surface of the Au substrate into a COOH-terminated SAM. The terminal carboxylate then serves as an initial point for MOF-5 growth on the Au surface. The crystal growth of micrometer size MOF-5 crystals and the development of dense films on SAM-functionalized Au substrates as well as their stability to moisture are described. Additional experiments with formate-based MOFs are briefly discussed to investigate the generality of the procedure.

6.2. Experimental Section

Materials and Measurements. All chemicals used in the synthesis were obtained commercially and used without further purification. Powder X-ray diffraction (PXRD) pattern of the Au film samples were obtained using a PANalytical X’Pert PRO diffractometer with Cu K α radiation ($\lambda = 1.54180 \text{ \AA}$) and the zero-point error accounted for by using the characteristic Au diffraction peak positions. Optical images of the crystals on films were taken using the Olympus BX41 microscope equipped with an Olympus DP12 digital camera. Image analysis was performed using ImageJ software.²⁶

Substrate Preparation. Gold (Au) films (150 Å) were grown on microscope cover-glass surfaces (Fisher Scientific) by thermal evaporation under ultrahigh vacuum conditions. A thin layer of chromium (30 Å) was deposited first onto the glass surfaces to ensure better adhesion of the gold coating. Prior to use, substrates were cleaned with piranha solution (3:1 H₂SO₄:H₂O₂) then washed with distilled water.

Au-SAM Preparation.¹⁷⁻¹⁸ Self-assembled monolayers (SAMs) of 16-mercaptophexadecanoic acid (SAM16) and 11-mercaptoundecanoic acid (SAM11) were prepared by immersing clean Au substrates in 1 mM ethanolic solutions for 24 h. The substrates were then thoroughly rinsed with ethanol to remove unbound acid thiols from the Au surfaces.

Au-SAM-MOF-5 Preparation. Au-SAM substrates were placed in a solution of 0.178 g (0.6 mmol) Zn(NO₃)₂·6H₂O and 0.033 g (0.2 mmol) terephthalic acid in 5 mL N,N-diethylformamide (DEF). Growth of MOF-5 crystals/films was stopped by removing the substrates from the solution after two to three weeks. Samples were then washed with pure DEF to eliminate crystals that did not adhere to the surface.

Pretreatments of the SAM layers were conducted using two methods; the first method involved high temperature pretreatment by the reaction of Au-SAM with 5% NaOH for 1 h at 90 °C. The sample was then transferred to 10% ZnSO₄ solution for 2 h at 85 °C. This procedure is based on a reported preparation of Zn²⁺ carboxylate esters from alkanoic acids.²⁷ The second method is a mild and direct pretreatment of Au-SAMs by immersing the substrate into a 1 mM ZnCl₂ solution at pH ≈ 8-9 for 24 h. The

substrates were then rinsed with distilled water and conditioned in DEF for 10 min before introduction into the MOF-5 solution.

Au-SAM-Mn(HCOO)₂ Preparation. Au-SAM substrates were placed in a solution of 0.257 g (1.3 mmol) MnCl₂·4H₂O and 0.10 mL (2.6 mmol) formic acid in 5 mL methanol with 0.02 mL triethylamine. A dense film of Au-SAM-Mn(HCOO)₂ was removed from the solution after 20 d and then washed with methanol.

Au-SAM-La(HCOO)₃ Preparation. A solution of containing 1.21 g (2.8 mmol) La(NO₃)₃·6H₂O and 0.32 mL (8.6 mmol) formic acid in 5 mL methanol with 0.02 mL triethylamine was refluxed for 1 h at 60 °C. The solution was cooled and filtered to a vial containing the Au-SAM substrate. The Au-SAM-La(HCOO)₃ film was removed from the crystallization solution after 20 d and then washed with distilled water.

6.3. Results and Discussion

Reticular Chemistry. The functionalization of the surface with SAMs provided a rational scheme for anchoring MOF crystals on the substrate surface by deposition.¹⁰⁻¹² In particular, organothiols that have COOH terminal end groups can initiate the formation of MOFs based on carboxylate linkers. In theory, the terminating COO⁻ of an organocarboxylate SAM participates in the formation of the metal connector building unit of the framework assembly and forms a bridge to the Au film substrate via its thiolate tail. The connectors formed on top of the Au-SAM may serve as nucleation sites for the formation of MOF crystals and eventually dense films on the substrate's surface. The strategy is illustrated schematically in Figure 6.1. The MOF system investigated is

the MOF-5 that is based on the tetrahedral Zn₄O cluster connector and a rigid terephthalate linker. The anchoring SAM is the widely used 16-mercaptophexadecanoic acid (SAM16) or in some experiments, 11-mercaptoundecanoic acid (SAM11).

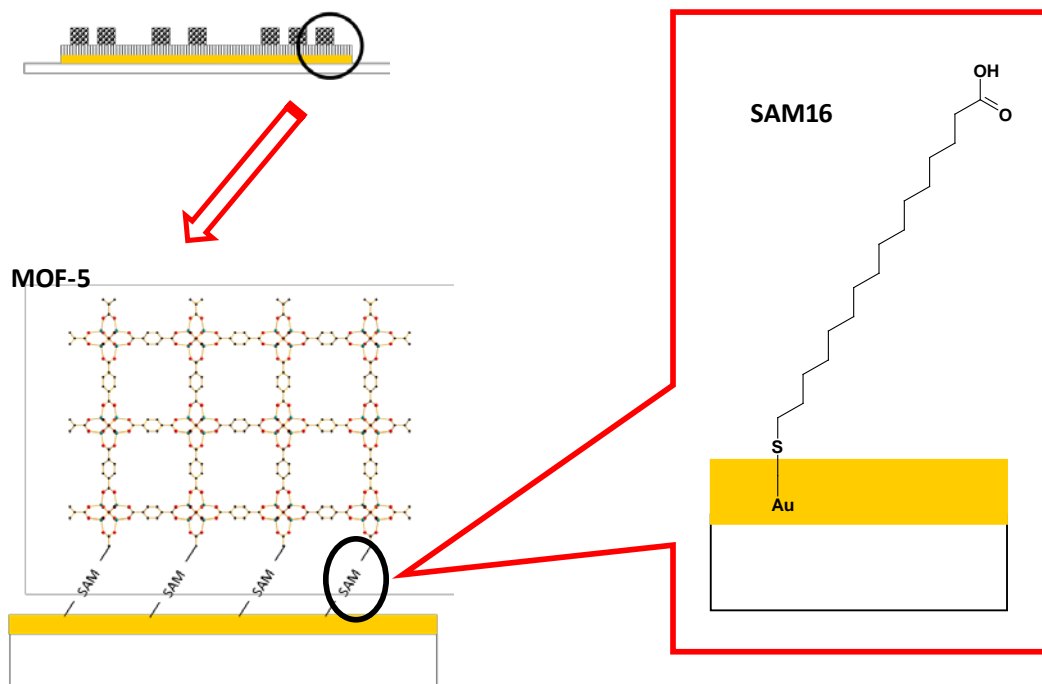


Figure 6.1. Schematic representation of MOF-5 film deposited on Au-SAM substrate.

Au-SAM-MOF-5: Crystallization of pre-heated solution (literature method).

The preparation of MOF-5 on Au-SAM substrate has been reported previously based on a conventional solvothermal method of preparing the crystallization solution by heating at 75 °C for 72 h, then at 105 °C momentarily, and finally cooling to 25 °C. The substrate was immersed in a filtered solution and a dense film of MOF-5 was shown to grow on the region that has been functionalized. The film, however, was observed to be composed of MOF-5 crystallites (100-500 nm in size) that seemed to deposit after homogenous

nucleation in the solution. Nevertheless, the adherence to Au substrate is reported to be selective as the film was observed to deposit only in the region that is COOH-terminated as opposed to bare Au(111)- or CF₃-terminated.²¹

A solution of 0.476 g (1.6 mmol) Zn(NO₃)₂·6H₂O and 0.089 g (0.53 mmol) terephthalic acid in 5 mL N,N-diethylformamide (DEF) was heated for 72 h at 75 °C then the temperature was raised to 105 °C, then filtered into a crystallization vial. The Au-SAM substrate was then immersed in this solution and after a period of 15 d, a white film of MOF-5 crystallites was observed to grow on the Au-SAM substrate (Figure 6.2).

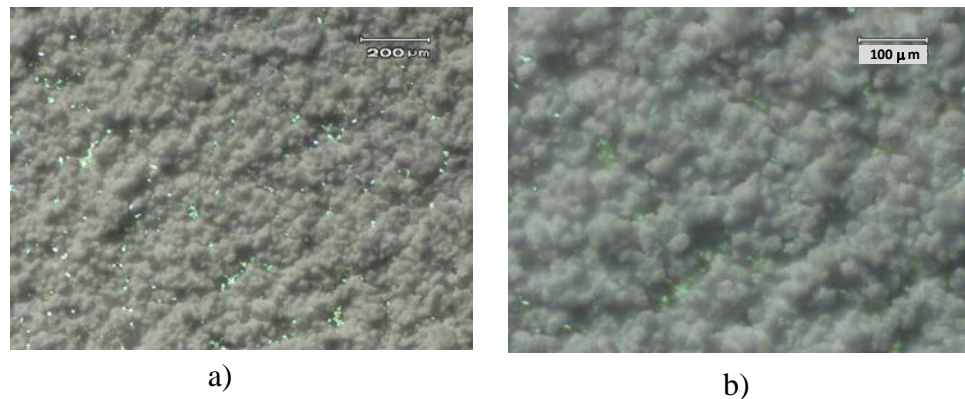


Figure 6.2. Optical images of the Au-SAM-MOF-5 film products obtained by crystallization of pre-heated MOF-5 solution (literature method; Ref. 21) at a) lower magnification and b) higher magnification.

Au-SAM-MOF-5: Room-temperature synthesis without pretreatment of the substrate. The problem of nucleation in solution prior to substrate introduction was addressed by synthesizing MOF-5 at room temperature. The reported room-temperature preparation of MOF-5 uses Zn(CH₃COO)₂ as the metal cation source or by introduction

of a triethylamine as base with metal nitrate as the source.²⁸ Both methods yield powder samples as opposed to the large crystals obtained from the typical synthesis of MOF-5 using Zn(NO₃)₂ at elevated temperature.²⁴ The method employed here used the original recipe with 3 : 1 molar ratio for Zn(NO₃)₂·6H₂O : terephthalic acid in DEF, only at a more dilute condition (~3× than the original procedure) and with the assumption that nucleation will be induced by the COOH-terminal end groups of the Au-SAM substrate. The functionalized substrate, in this case, was introduced after dissolution of the starting components by thorough mixing then filtration. This resulted to a dense film that is comprised of large crystals (*ca* 100 μm average size) displayed in Figure 6.3.

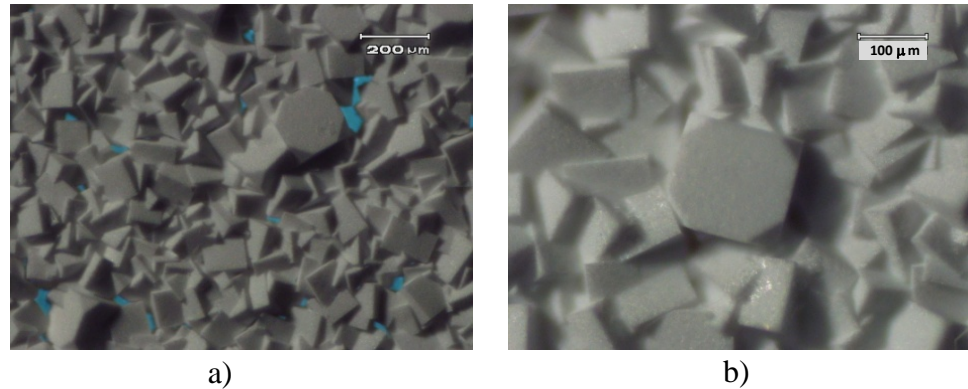


Figure 6.3. Optical images of the Au-SAM-MOF-5 film products obtained by room-temperature synthesis using dilute crystallization solution at a) lower magnification and b) higher magnification.

Au-SAM-MOF-5: Synthesis with substrate pretreatments. To further gain control of nucleation, two pretreatment procedures were applied to the Au-SAM films. In the first (Figure 6.4a), the COOH functionality is converted at high temperature into

the Na^+ -carboxylate salt and the Na^+ ion are displaced by Zn^{2+} to form a Zn^{2+} -terminated Au-SAM substrate.²⁷ This method yielded MOF-5 crystals on the surface that appear to have more regular sizes and shapes, however, the film density of the product was lower (Figure 6.5). This may be due to the instability of the SAMs on gold substrates when subjected to high temperature treatment.²⁹

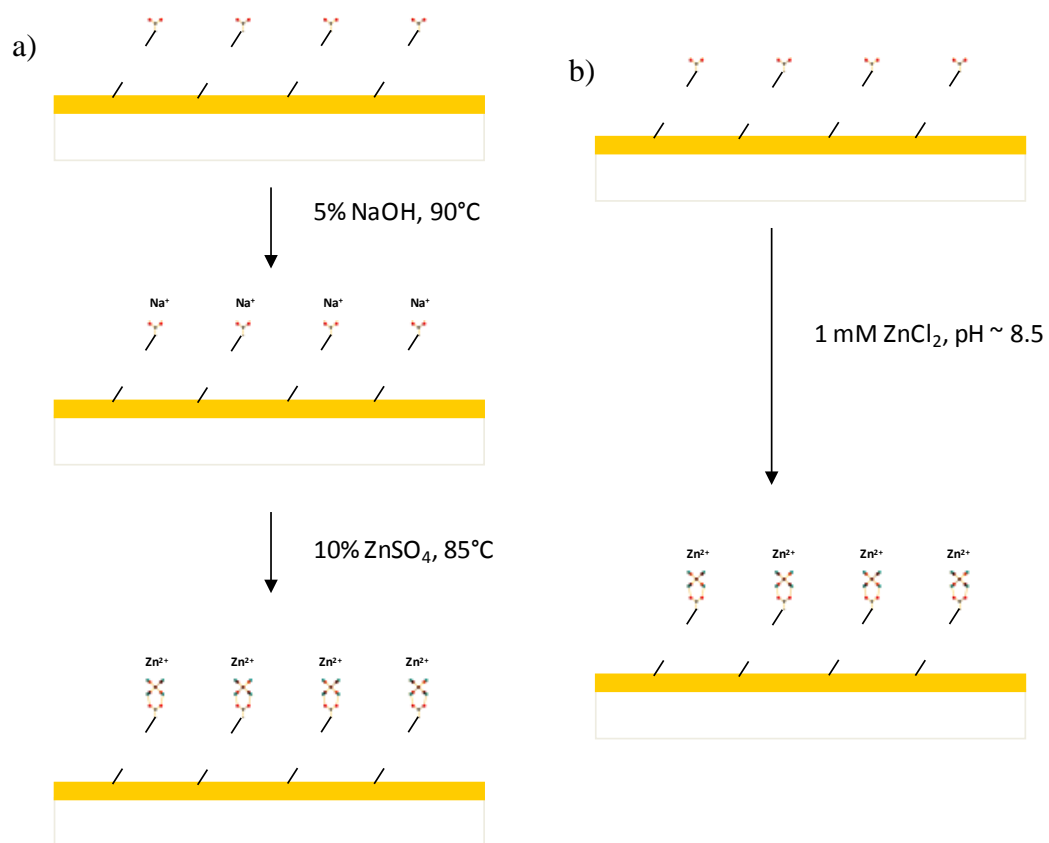


Figure 6.4. Schematic diagram of the pretreatment methods applied to Au-SAM substrate; a) high-temperature pretreatment and b) room-temperature pretreatment.

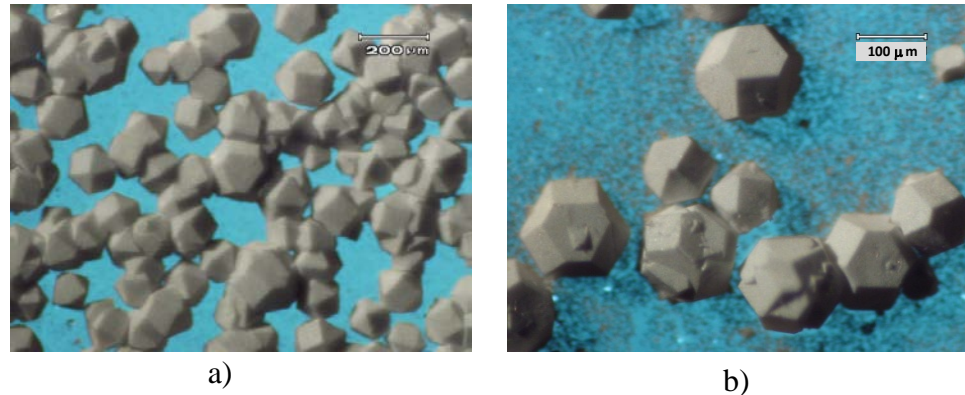


Figure 6.5. Optical images of the Au-SAM-MOF-5 film products obtained by synthesis with substrate pretreatment at high temperature at a) lower magnification and b) higher magnification.

The second pretreatment used was milder (Figure 6.4b). The Au-SAM substrate was immersed in an aqueous zinc chloride solution (1mM) adjusted to pH ~8 to 9 by addition of a few drops of NH₄OH. This method is based on previous studies of the formation of counterion layers on the surface of SAMs and their pH dependency.³⁰ Using this mild pretreatment method, dense films of uniform-size MOF-5 crystals were formed (Figure 6.6a-b). Without adjustment of the pH (at pH ~ 5), however, lower area coverage is observed possibly due to inhomogeneity of the counterion layer as nucleation sites (Figure 6.6c-d)

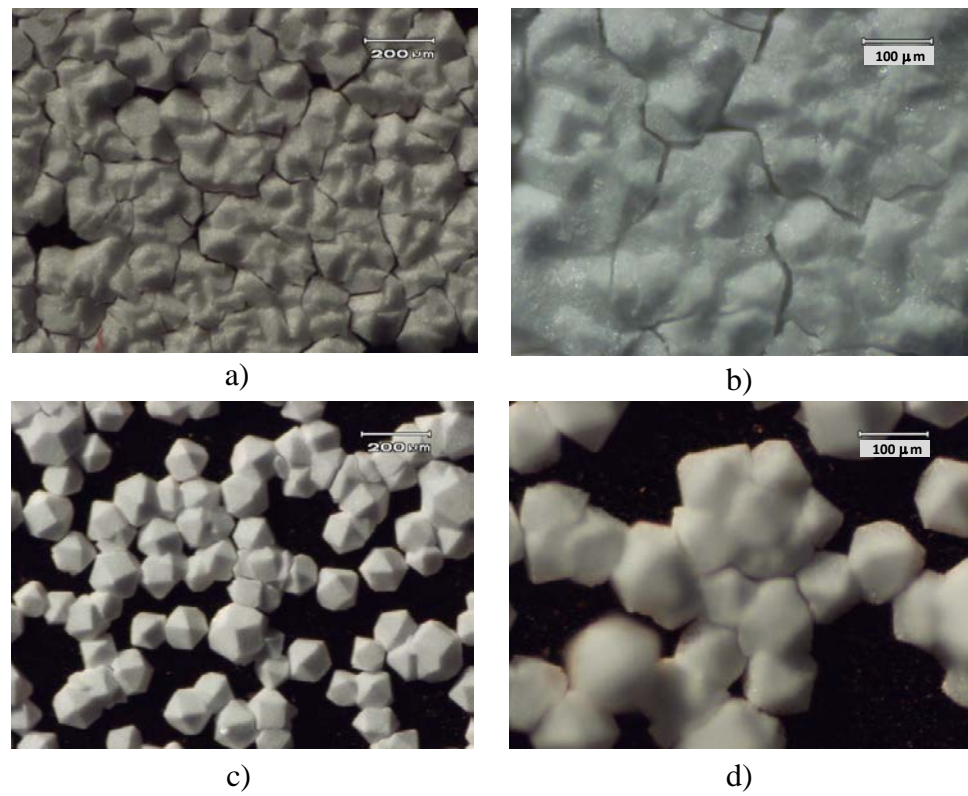


Figure 6.6. Optical images of the Au-SAM-MOF-5 film products obtained by synthesis after substrate pretreatment with pH adjustment ($\text{pH} = 8\text{-}9$) at a) lower magnification and b) higher magnification; without pH adjustment ($\text{pH} = 5$) at c) lower magnification and d) higher magnification.

Au-SAM-MOF-5: Using SAMs of different chain lengths. SAMs with even- (SAM16) and odd- (SAM11) numbered carbon chain were used to investigate the growth of MOF-5 on surfaces with different orientations of the terminal COOH group. A schematic illustration of the conceived orientation with all-*trans* conformer of SAM16 and SAM11 is shown in Figure 6.7. No significant differences either on the crystal sizes or film area coverage were detected for the film products using the two SAMs tested. It is likely that the terminating surfaces of the SAMs are sufficiently flexible to minimize any effects of functional group orientation.

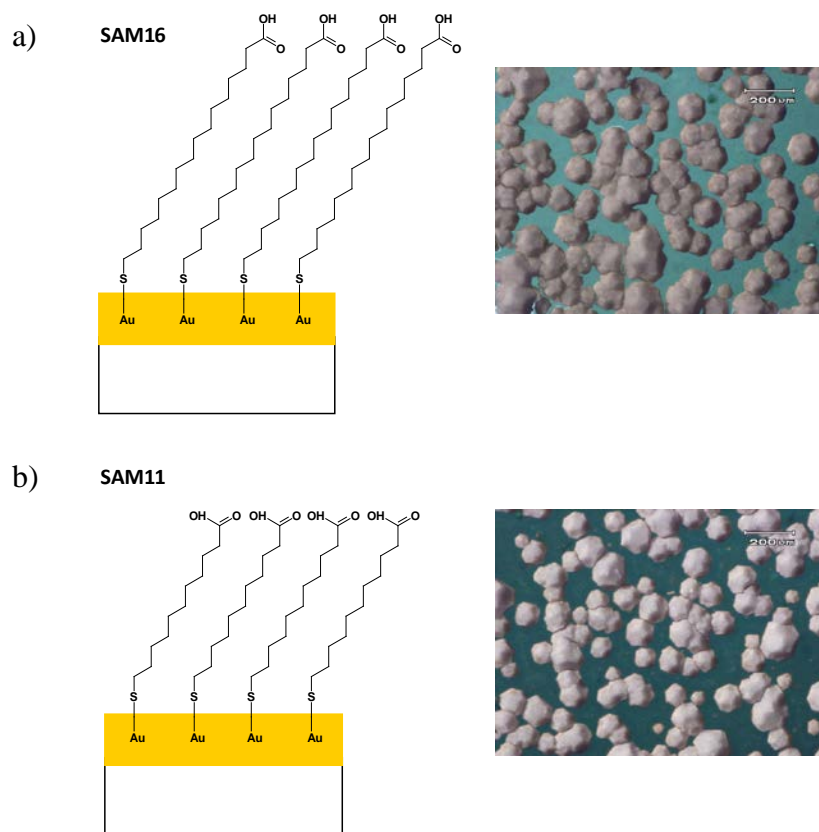


Figure 6.7. Schematic view and optical images of the Au-SAM-MOF-5 films prepared using SAMs of different carbon chain lengths; a) using SAM16 and b) using SAM11.

Au-SAM-MOF-5: Stability to moisture. The film images presented so far are all taken after the samples have been dried in air for at least 24 h. Optical micrographs of the fresh crystals after 1 week of growth are shown in Figure 6.8. The powder XRD pattern confirms the identity of the MOF-5 structure of the fresh films (Figure 6.9a) and shows the orientation preference of the crystal growth. Peaks at $2\theta = 7.09^\circ$, 13.97° and 20.89° corresponding to the (002), (004), and (006) diffraction planes are greatly enhanced compared to the lines coming from other family of planes. This demonstrates the effect of the SAM layer on nucleation and growth of large crystals ($>50 \mu\text{m}$ in size) of MOF-5, which were previously reported to be obtained only at elevated temperature ($>95^\circ\text{C}$). When the films were removed from the supernatant solution, the transparent crystals turned into opaque white solids with the powder pattern shown in Figure 6.9b. Complete transformation occurred after the films were left in the atmosphere at ambient conditions for 24 h. This phase has been previously reported as the hydrolyzed phase of MOF-5 and confirms the sensitivity of MOF-5 to moisture consistent with other previous studies.³¹⁻³²

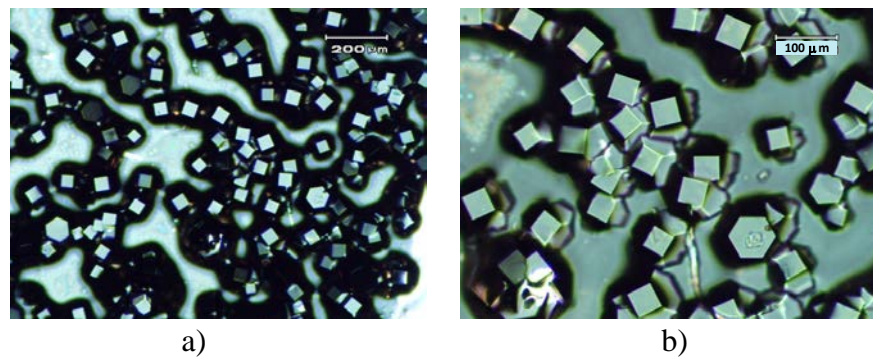


Figure 6.8. Optical images of the Au-SAM-MOF-5 films after a crystal growth period of 1 week at a) lower magnification and b) higher magnification.

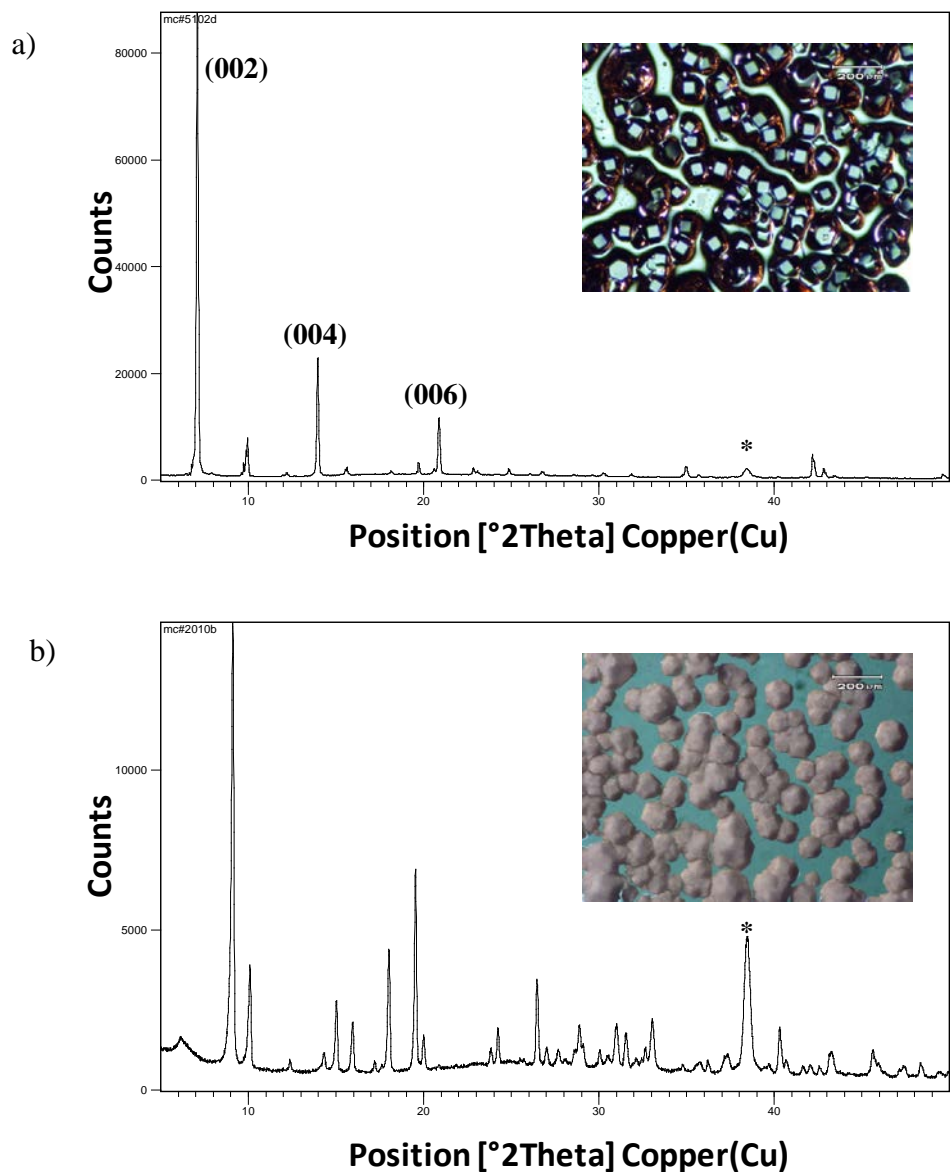


Figure 6.9. PXRD patterns and optical images (inset) of the same Au-SAM-MOF-5 film; a) freshly-prepared and b) after 24 h exposure to air. (* denotes peaks from Au film)

Kinetics of Crystal Growth of MOF-5. The growth of MOF-5 crystals on Au-SAM substrates was studied for a period of 20 days from the start of the crystallization experiment. The method employed for this experiment is the room-temperature synthesis with the Zn^{2+} -substrate pretreatment. The optical images of the films were monitored at different time intervals for crystal growth and are shown in Figure 6.10. An induction period of between 2 to 3 d in the formation of MOF-5 crystals on top of the Au-SAM is observed; the first set of crystals appears only after 3 days. This is confirmed by the PXRD patterns of the films at varying crystallization times (Figure 6.11). An image analysis of the micrographs was performed to study the particle size distribution of MOF-5 during crystal growth. For the size distribution study, three photomicrographs per time interval containing at least twenty crystals per image that have defined grain boundaries were selected and processed using the ImageJ²⁶ software. The cross-sectional areas were measured and collated into histograms with the automatic bins defined by the standard deviation and average area from the set of data (Figure 6.12). For the analysis of results, manual binning of the histograms was carried out to normalize all of the data sets as presented in Figure 6.13. The results indicate saturation of the crystal size at a cross-sectional area of 30000 to 40000 μm^2 corresponding to radii of 98 to 113 μm assuming that the particles are spherical. The histograms also show the decreased number of small size (5000 to 10000 μm^2) crystals from the 3rd day and their disappearance after the 10th day of crystallization. The appearance of large size ($>50000 \mu m^2$) crystals is also observed but the frequency does not significantly increase considering the limited space for expansion over the surface of the Au-SAM substrate.

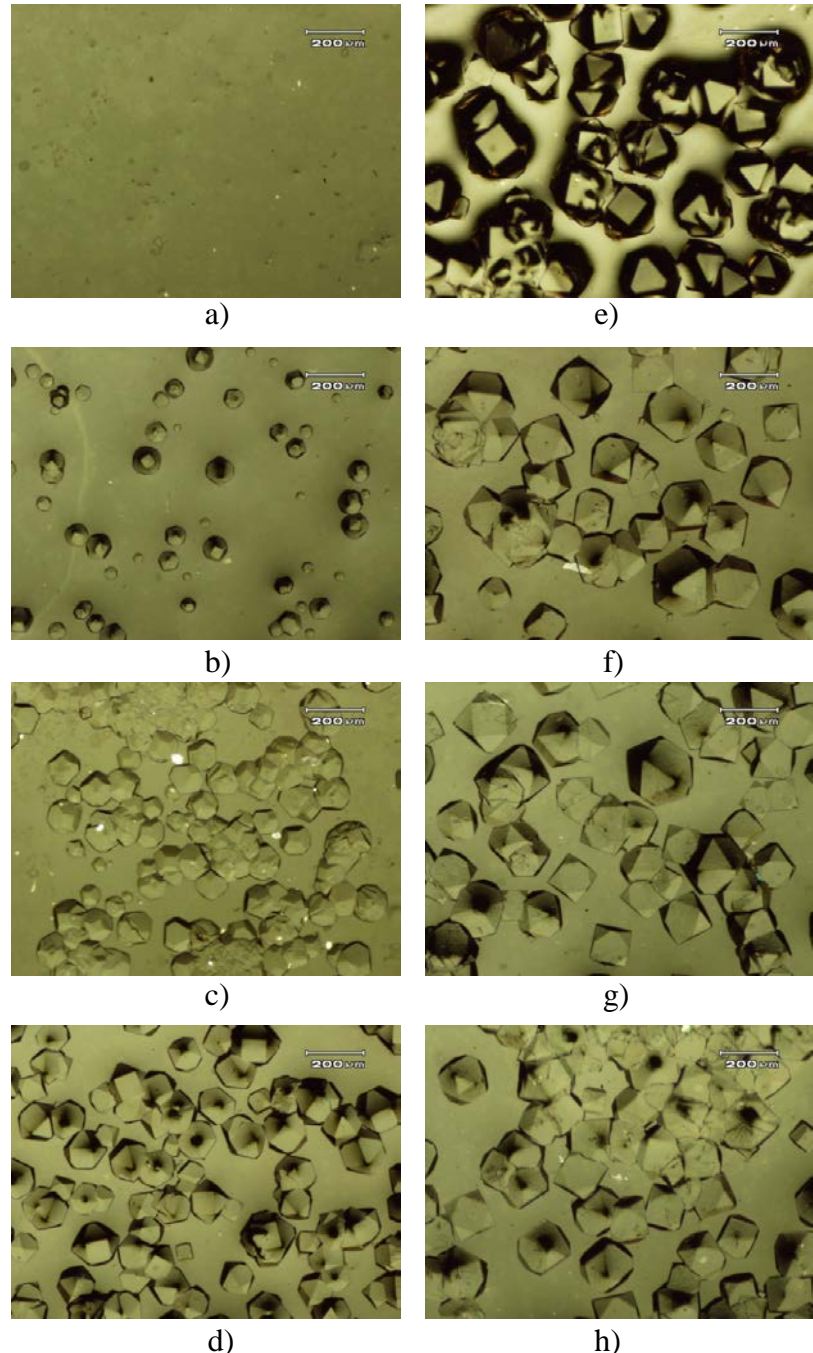


Figure 6.10. Images of the Au-SAM-MOF-5 films at crystal-growth period of: a) 2 days, b) 3 days, c) 4 days, d) 6 days, e) 8 days, f) 12 days, g) 16 days, and h) 20 days.

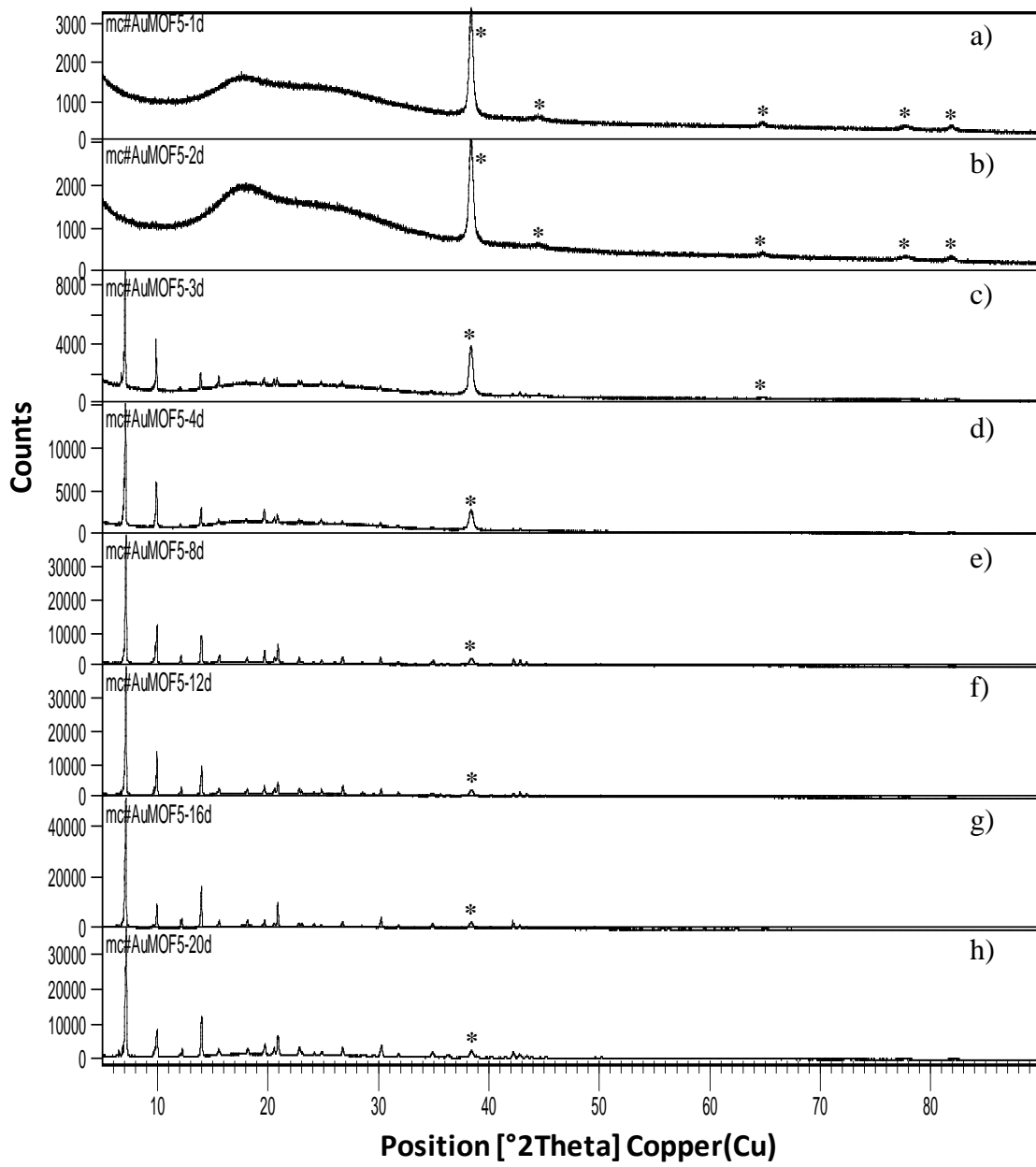


Figure 6.11. PXRD patterns of the Au-SAM-MOF-5 film samples at crystal-growth period of: a) 1 day, b) 2 days, c) 3 days, d) 4 days, e) 8 days, f) 12 days, g) 16 days, and h) 20 days. (* denotes peaks from Au film)

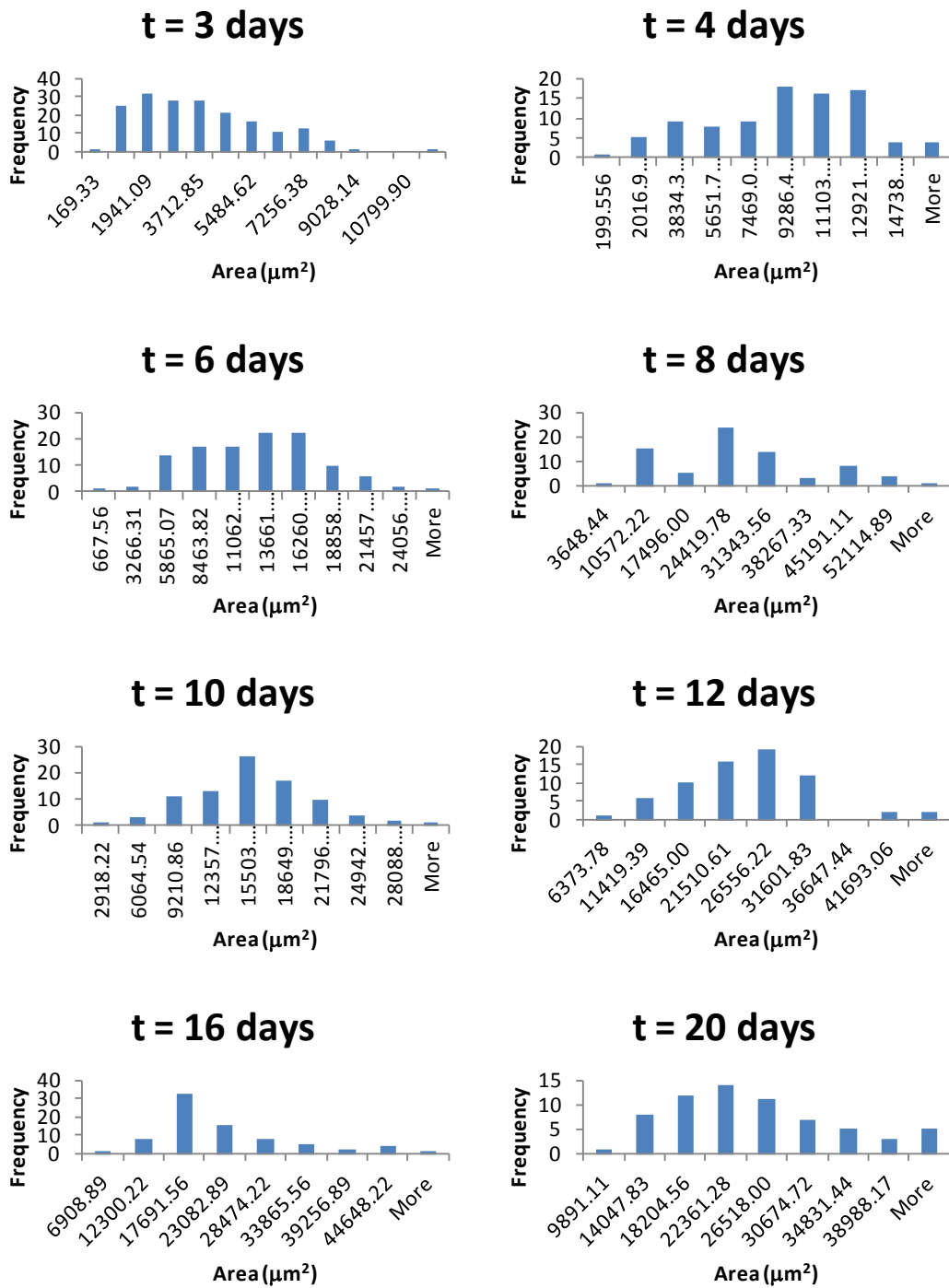


Figure 6.12. Histograms of particle size distribution of Au-SAM-MOF-5 samples at different crystallization times (t) derived from image analysis by automatic binning.

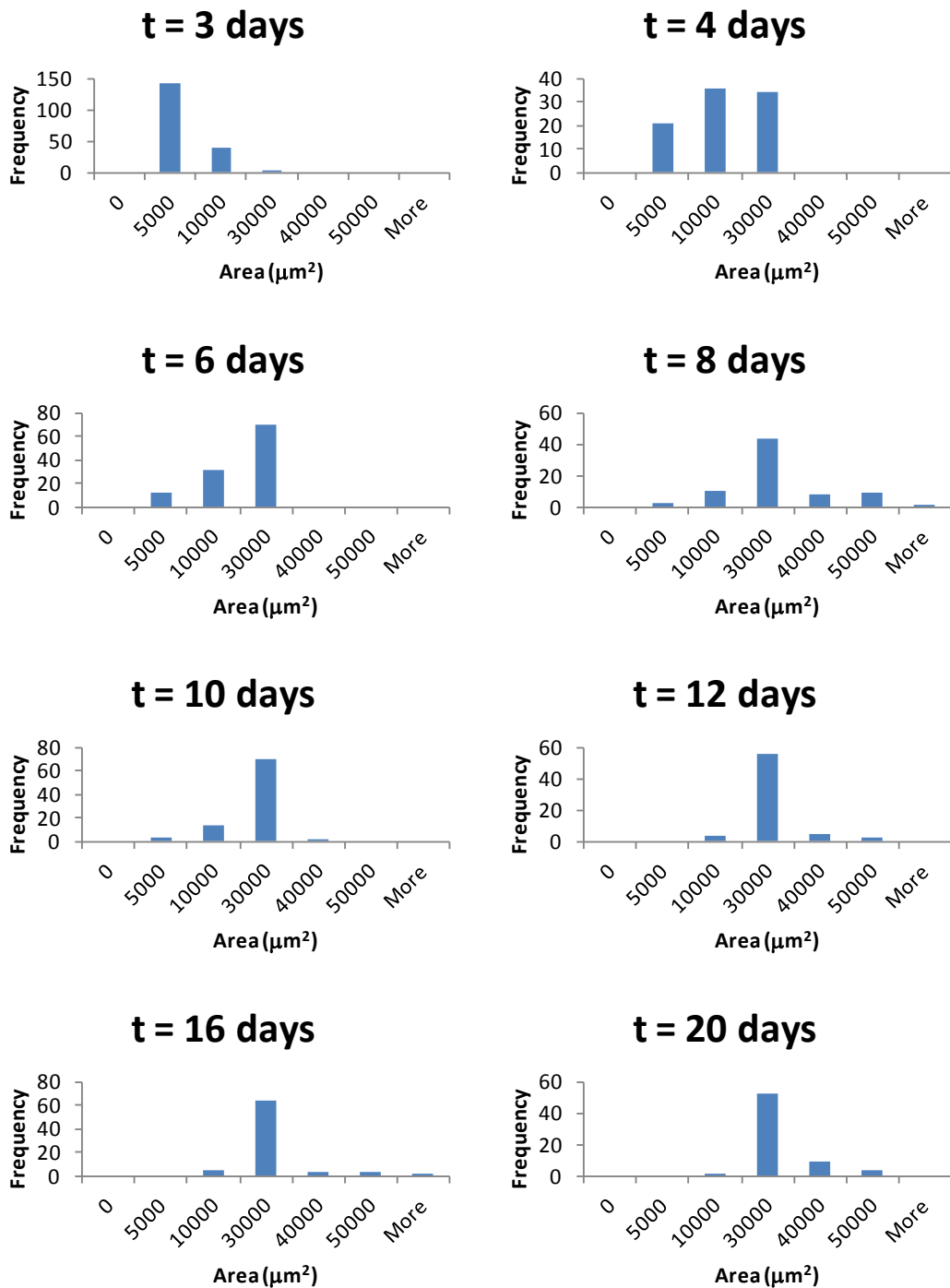


Figure 6.13. Histograms of particle size distribution of Au-SAM-MOF-5 samples at different crystallization times (t) derived from image analysis by manual binning.

Overall, the film coverage of MOF-5 on Au-SAM substrate mostly showed regions of high density crystals intermixed with low density areas. It is important to note that MOF-5 film formation was not limited by the amount of the reagents in the crystallization solution. This is based from the calculated complete coverage of the Au film assuming all the starting materials are converted to MOF-5 crystals. The theoretical thickness expected for total coverage is at ~975 μm and implies that the limiting factor for film growth is the Au-SAM surface. Results were reproduced for at least two replicates but the analysis on the film coverage was not performed since this parameter is largely dependent on the quality of monolayer formation on the Au substrate. Several factors such as defects on the Au film, Au-SAM quality, impurities during SAM formation, and/or MOF-5 crystallization have to be taken into consideration for an in-depth microstructural study on dense MOF-5 film formation.

Experiments on Formate-based MOFs. The generality of the deposition method was extended to metal-formate MOFs, specifically, manganese formate $[\text{Mn}(\text{HCOO})_2]$ and lanthanum formate $[\text{La}(\text{HCOO})_3]$. The reported procedure in the preparation of these two compounds involves syntheses at ambient or slightly elevated temperatures (60 °C). $\text{Mn}(\text{HCOO})_2$, for example, was deposited onto Au-SAM substrate at room temperature for a period of 20 days. The interest in this MOF arises from the reported microporosity and the successful deposition of preferentially-oriented large crystals (~300 μm) on α -alumina and graphite substrates.³³⁻³⁴ In this work, dense films of crystals were found to form on top of the substrate (Figure 6.14a). The film formation, however, is not restricted to only the Au-SAM region but covers the whole area including

the outline of glass substrate that does not contain any Au-films. The film product was identified as the dihydrate phase $[\text{Mn}(\text{HCOO})_2 \cdot 2\text{H}_2\text{O}]^{35}$ using powder X-ray diffraction.

The lanthanum analogue of a gadolinia-doped ceria (GDC, $\text{Ce}_{0.9}\text{Gd}_{0.1}\text{O}_{2-\delta}$) formate precursor that has been of interest because of the high ionic conductivity of the oxide material was also investigated.³⁶ A synthetic route similar to the one reported in literature was used, namely reflux at 60 °C for 1 h. The deposition was conducted on the cooled and filtered solution for a period of 20 days. The PXRD pattern and an image of a dense film of $\text{La}(\text{HCOO})_3$ that was obtained is shown in Figure 6.14b. Interestingly, after drying in air for several weeks, the film can be separated from the Au-SAM substrate as a free-standing membrane. This implies only weak adherence of the $\text{La}(\text{HCOO})_3$ films towards the Au-SAM substrate. The formate film can be transformed to La_2O_3 by heating the free-standing film for 6 h at 600 °C without disintegration of the film membrane.

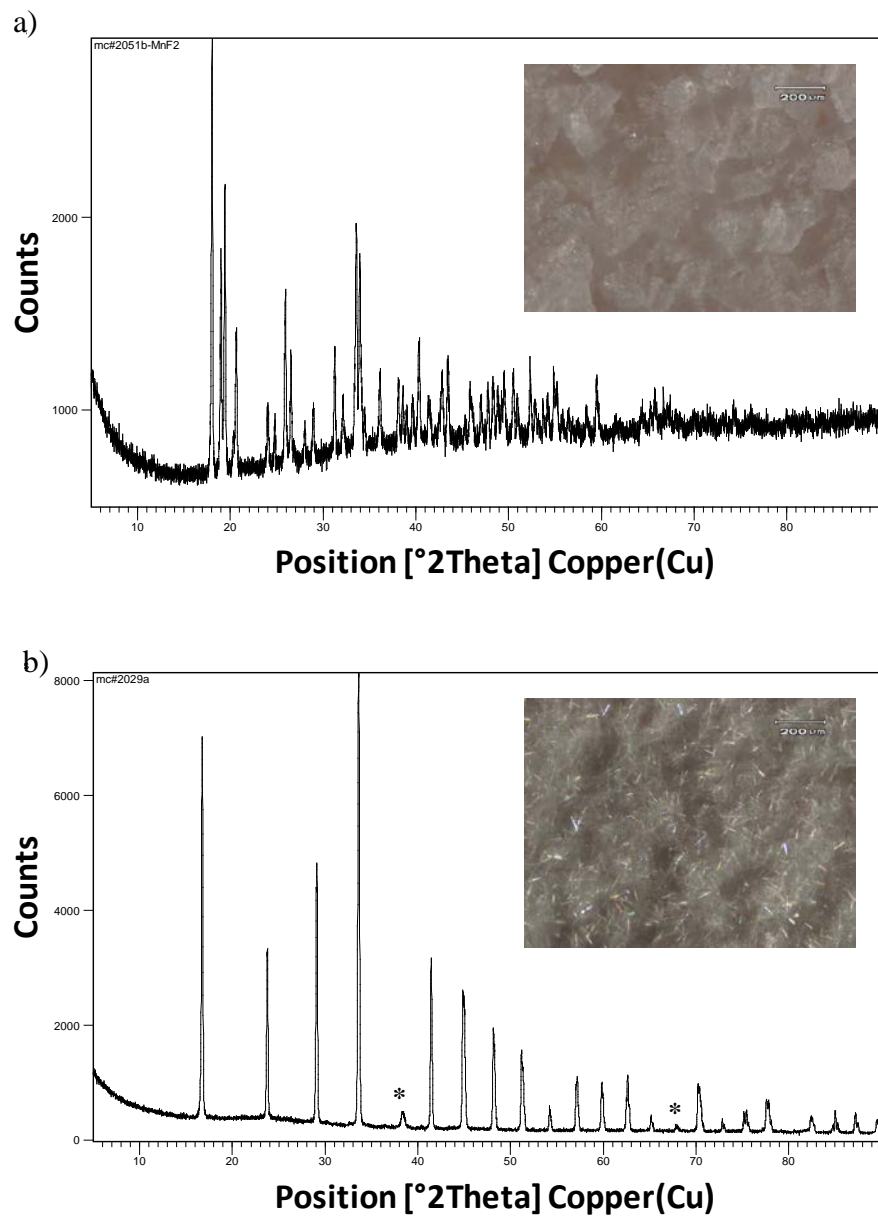


Figure 6.14. PXRD patterns and an optical image (inset) of a) Au-SAM-Mn(HCOO)₂ and b) Au-SAM-La(HCOO)₃. (*) denotes peaks coming from Au film)

6.4. Conclusion

A methodology for depositing MOF films on Au substrates has been investigated based on the idea of using a SAM as the anchor-bridging component. Room-temperature preparation of large single crystals ($\sim 150 \mu\text{m}$) of MOF-5 and dense film formation were successfully achieved by careful control of the nucleation. The nucleation was facilitated by pretreatment of Au-SAM substrate with Zn^{2+} prior to crystal growth in the MOF-5 solution. Kinetics of crystal growth was studied on the film samples by image analysis of the micrographs collected at different times during crystallization. Results showed an induction period of 2 to 3 d and saturation of the crystal size at 30000 to 40000 μm^2 cross sectional area. Experiments on $\text{Mn}(\text{HCOO})_2$ and $\text{La}(\text{HCOO})_3$ deposition, however, showed the non-specificity of the film growth and the influence of the Au-SAM surface remains unclear. Overall, the findings in this work suggest that the deposition process may not be general for all MOF systems. Certain phases only crystallize at high temperature and this limits the applicability of the SAMs on Au substrates. In MOF-5 and other MOF systems where the method works, it certainly provides a new platform to study the fundamental aspects of crystallization important for the development of MOF films for membrane applications.

6.5. References

1. Yaghi, O.M.; Li, H.; Davis, C.; Richardson, D.; Groy, T.L. *Acc. Chem. Res.* **1998**, *31*, 474–484.
2. Kitagawa, S.; Kitaura, R.; Noro, S. *Angew. Chem. Int. Ed.* **2004**, *43*, 2334–2375.
3. Perry IV, J.J.; Perman, J.A.; Zawarotko, M.J. *Chem. Soc. Rev.* **2009**, *38*, 1400–1417.

4. Tranchemontagne, D.J.; Ni, Z.; O'Keeffe, M.; Yaghi, O.M. *Angew. Chem. Int. Ed.* **2008**, *47*, 5136–5147.
5. Farha, O.K.; Hupp, J.T. *Acc. Chem. Res.* **2010**, *43*, 1166–1175.
6. Carne, A.; Carbonell, C.; Imaz, I.; MasPOCH, D. *Chem. Soc. Rev.* **2011**, *40*, 291–305.
7. James, S.L. *Chem. Soc. Rev.* **2003**, *32*, 276–288.
8. Fischer, R.A.; Woll, C. *Angew. Chem. Int. Ed.* **2008**, *47*, 8164–8168.
9. Czaja, A.U.; Trukhan, N.; Muller, U. *Chem. Soc. Rev.* **2009**, *38*, 1284–1293.
10. Betard, A.; Fischer, R.A. *Chem. Rev.* **2012**, *112*, 1055–1083.
11. Shekhah, O.; Liu, J.; Fischer, R.A.; Woll, C. *Chem. Soc. Rev.* **2011**, *40*, 1081–1106.
12. Zacher, D.; Shekhah, O.; Woll, C.; Fischer, R.A. *Chem. Soc. Rev.* **2009**, *38*, 1418–1429.
13. Bureekaew, S.; Kitagawa, S. *Sci. Technol. Adv. Mater.* **2008**, *9*, 014108.
14. Murray, L.J.; Dinca, M.; Long, J.R. *Chem. Soc. Rev.* **2009**, *38*, 1294–1314.
15. Farrusseng, D.; Aguado, S.; Pinel, C. *Angew. Chem. Int. Ed.* **2009**, *48*, 2–14.
16. Li, J.R.; Sculley, J.; Zhou, H.C. *Chem. Rev.* **2012**, *112*, 869–932.
17. Love, J.C.; Estroff, L.A.; Kriebel, J.K.; Nuzzo, R.G.; Whitesides, G.M. *Chem. Rev.* **2005**, *105*, 1103–1169.
18. Barriet, D.; Yam, C.M.; Shmakova, O.E.; Jamison, A.C.; Lee, T.R. *Langmuir* **2007**, *23*, 8866–8875.
19. Scherb, C.; Schodel, A.; Bein, T. *Angew. Chem. Int. Ed.* **2008**, *47*, 5777–5779.
20. Shekhah, O.; Arslan, H.K.; Chen, K.; Schmittel, M.; Maul, R.; Wenzel, W.; Woll, C. *Chem. Commun.* **2011**, *47*, 11210–11212.

21. Hermes, S.; Schroder, F.; Chelmowski, R.; Woll, C.; Fischer, R.A. *J. Am. Chem. Soc.* **2005**, *127*, 13744–13745.
22. Hermes, S.; Zacher, D.; Baunemann, A.; Woll, C.; Fischer, R.A. *Chem. Mater.* **2007**, *19*, 2168–2173.
23. Biemmi, E.; Scherb, C.; Bein, T. *J. Am. Chem. Soc.* **2007**, *129*, 8054–8055.
24. Li, H.; Eddaoudi, M.; O’Keeffe, M.; Yaghi O.M. *Nature* **1999**, *402*, 276–279.
25. Eddaoudi, M.; Kim, J.; Rosi, N.; Vodak, D.; Wachter, J.; O’Keeffe, M.; Yaghi, O.M. *Science* **2002**, *295*, 469–472.
26. Rasband, W.S. ImageJ; U. S. National Institutes of Health, Bethesda, Maryland, USA, <http://imagej.nih.gov/ij/>, 1997-2011.
27. Ekwunife, M.E.; Nwachukwu, M.U.; Rinehart, F.P.; Sime, S.J. *J. Chem. Soc. Faraday Trans. 1* **1975**, *71*, 1432–1446.
28. Tranchemontagne, D.J.; Hunt, J.R.; Yaghi, O.M. *Tetrahedron* **2008**, *64*, 8553–8557.
29. Delamarche, E.; Michel, B.; Kang, H.; Gerber, C. *Langmuir* **1994**, *10*, 4103–4108.
30. Li, J.; Liang, K.S.; Scoles, G.; Ulman, A. *Langmuir* **1995**, *11*, 4418–4427.
31. Kaye. S.S.; Dailly, A.; Yaghi, O.M.; Long, J.R. *J. Am. Chem. Soc.* **2007**, *129*, 14176–14177.
32. Huang, L.; Wang, H.; Chen, J.; Wang, Z.; Sun, J.; Zhao, D.; Yan, Y. *Microporous Mesoporous Mater.* **2003**, *58*, 105–114.
33. Dybtsev, D.N.; Chun, H.; Yoon, S.H.; Kim, D.; Kim, K. *J. Am. Chem. Soc.* **2004**, *126*, 32–33.
34. Arnold, M.; Kortunov, P.; Jones, D.J.; Nedellec, Y.; Karger, J.; Caro, J. *Eur. J. Inorg. Chem.* **2007**, 60–64.

35. Viertelhaus, M.; Henke, H.; Anson, C.E.; Powell, A.K. *Eur. J. Inorg. Chem.* **2003**, 2283–2289.
36. Go, Y.B.; Jacobson, A.J. *Chem. Mater.* **2007**, *19*, 4702–4709.

Chapter 7

Conclusion

Over the past decade, remarkable progress has been made on research pertaining to a group of solids referred to as coordination polymers or metal-organic frameworks (MOFs).¹⁻¹⁸ As new structures and promising properties are continually explored and discovered, the advances in the field are likely to continue to grow. Reticular chemistry, which studies the interplay of the MOF's primary building components, namely metal connectors and organic linkers, has been on the forefront in the design and synthesis of MOFs.¹⁹⁻²⁴ This dissertation investigates certain aspects of reticular chemistry in MOF synthesis with a particular focus on linear dicarboxylate linkers.

The use of aromatic dicarboxylate linkers that have a linear arrangement of the carboxylate linking groups and different lengths has been investigated. A series of MOFs based on clusters of divalent nickel ions with dicarboxylate linkers has been described. (Chapter 3) These include, the layered compounds $\text{Ni}_3(1,4\text{-BDC})_3(\text{DMF})_2(\text{DMA})_2$ (**3-1**) and $\text{Ni}_3(1,4\text{-BDC})_3(\text{DMF})_4$ (**3-2**) [1,4-BDC= terephthalate, DMF= N,N' -dimethylformamide, and DMA= dimethylamine], and compounds with framework structures $\text{Ni}_3(2,6\text{-NDC})_3(\text{DMF})_2(\text{DMA})_2$ (**3-3**) [2,6-NDC= naphthalate], $\text{Ni}_3(\mu_3\text{-O})(4,4'\text{-BPDC})_3(\text{DMA})_3$ (**3-4**) [4,4'-BPDC= 4,4'-biphenyldicarboxylate], and $\text{Ni}_4(\mu_3\text{-O})(1,4\text{-NDC})_4(\text{DMF})_2(\text{DMA})_2$ (**3-5**) [1,4-NDC= 1,4-naphthalenedicarboxylate]. The building units for the compounds are influenced by the various coordination modes of the carboxylate linkers and are remarkably different. Compounds **3-1**, **3-2**, and **3-3** are based on linear trimeric nickel(II) cluster units while **3-4** contains a μ_3 -oxo triangular trimeric

nickel(II) cluster unit and **3-5** is based on an unprecedented tetrameric nickel(II) cluster unit. The compounds are not isoreticular but their synthesis has provided products that have interesting structures for fundamental magnetostructural studies.

The same set of linear dicarboxylate linkers mentioned above, 1,4-BDC, 2,6-NDC, 1,4-NDC, and 4,4'-BPDC were used as bridging rigid units to link an interesting chiral nickel aspartate $[\text{Ni}_2\text{O}(\text{Asp})_2]$ chain compound. (Chapter 4) Isoreticular synthesis in this case proved successful in the synthesis of $\text{Ni}_2\text{O}(\text{Asp})(1,4\text{-BDC})_{0.5}$ (**4-1**), $\text{Ni}_2\text{O}(\text{Asp})(1,4\text{-NDC})_{0.5}$ (**4-2**), $\text{Ni}_2\text{O}(\text{Asp})(2,6\text{-NDC})_{0.5}$ (**4-3**), and $\text{Ni}_2\text{O}(\text{Asp})(4,4'\text{-BPDC})_{0.5}$ (**4-4**). Analysis of powder diffraction data shows that the compounds have closely related structures. The lattice parameter perpendicular to the Ni-aspartate chain systematically increases as the chain length of the dicarboxylate linkers increases. The influence of several factors such as solvent system, reaction time, and pH on the synthesis of **4-1** is reported. The thermal stability of compound **4-1** was also examined as well as the capability of solvent molecules to enter and leave the chiral channels.

An exploratory study of MOF structures based on a new ligand *meso*-1,4-phenylenebis(hydroxyacetic acid) (**H₂L**) was performed. The *meso* ligand was used initially but the ultimate goal is to use one enantiomer to build chiral MOFs containing a chiral rigid linear dicarboxylate linker. (Chapter 5) Four new compounds, $\text{Ni}_2\text{L}_2\cdot(\text{H}_2\text{O})_4$ (**5-1**), $\text{CoL}\cdot\text{H}_2\text{O}$ (**5-2**), $\text{ZnL}\cdot\text{H}_2\text{O}$ (**5-3**), and PbL (**5-4**) were isolated as single crystals and characterized by FT-IR spectroscopy. PXRD, TGA, and elemental analyses for **5-1** and **5-4** were also conducted to support the crystal structure data. Numerous attempts to synthesize other compounds by varying metal cations, solvent system, reaction temperature, and reactant ratios were not successful and illustrate the difficulty of

growing crystals using a dicarboxylate ligand that has some flexibility. The ligand also promotes hydrogen-bonding networks between structural units or with the solvent molecules incorporated in the structure as described for compounds **5-1** to **5-3**.

Growth of MOF films on gold (Au) substrates functionalized with self-assembled monolayers (SAMs) was investigated to develop the use of MOFs as functional membrane materials. (Chapter 6) The idea is to grow metal-carboxylate MOFs on a COOH-terminated Au surface through the widely used thiocarboxylate SAMs. Crystals of zinc terephthalate (MOF-5) were successfully grown using a room-temperature synthesis after pretreatment of the Au-SAM substrate to convert the ends of the chains into a Zn-carboxylate. The top surface of the SAMs then provides the nuclei for crystal growth of the MOF films. The crystal size distribution at different crystallization times was determined using image analysis and the kinetics of crystal growth of MOF-5 on the substrates determined. The procedure used for growing MOF films on Au-SAMs was applied in the preparation of manganese formate and lanthanum formate films to test the generality of the method.

A vast number of combinations of metal connectors and organic linkers can be used to obtain a wide range of MOF architectures. Particular structures and compositions then can be selected to investigate specific applications. More than just making the structures, fundamental studies on how the chemistry responds to different conditions during synthesis is an important aspect of the research. Our studies on metal-organocarboxylate compounds demonstrate the sensitivity of MOF formation towards several synthetic parameters such as temperature, reaction time, solvent system, reactant ratio, and pH. The reticularity of the synthesis towards the preparation of pre-determined

MOF architectures still remain uncertain in many cases. The advantage of knowing the starting building blocks and understanding their behavior at different synthesis conditions, however, is a valuable tool for prediction and design of new structures.

This investigation focuses mainly on the synthesis of metal-carboxylate MOFs and elucidation of their crystal structures through X-ray crystallography. Further characterization using spectroscopic methods to identify the nature of the functional groups and by thermogravimetry to evaluate thermal stability, were also conducted. Physical property measurements such as magnetometry and solvent sorption/desorption experiment were also performed for initial assessment of potential applications.

The characteristic feature of MOFs is their porosity. The crystal structures alone, however, do not determine if these pores are really functional as catalytic cavities or selective permeable membranes. In future work, gas sorption experiments, or in case of compounds **4-1** to **4-4**, enantioselective separation experiments of chiral molecules should be carried out to test their application properties.

The synthesis of **3-1** to **3-5** offers a route to restrict the degree of polymerization of the inorganic component without the addition of chelating amines as terminating ligands. This strategy proved disadvantageous in reducing the stability of the compounds at ambient conditions due to the presence of easily lost solvent molecules that are part of the framework backbone. The molecular weight does not remain constant at ambient conditions which complicates the magnetic property analyses of these materials. An auxiliary molecule to serve as the blocking ligand in place of DMF and DMA molecules may help in fixating the structure, although, the synthesis conditions are expected to be different.

Stability of MOF-5 at ambient conditions is a concern for its application in devices such as chemical sensors. A previous study reported that the extent of hydroxylation lowers the amount of adsorbed gases in MOF-5 accounting for the discrepancies in the values of the sorption capacity published in several papers.²⁵ Our results showed complete transformation of MOF-5 to its hydrolyzed phase after being left at ambient conditions for 24 h implying lower adsorption capacity. This was the motivation for testing the synthesis method with other carboxylate-based MOFs such as the manganese formate and lanthanum formate. Several other MOF systems based on metal-carboxylates can be tested in future studies.

The design and synthesis of new chiral linkers is an open field for the preparation of homochiral porous materials. Collaborative efforts with experts on the organic synthesis of chiral molecules will be needed. Our contributions to the field are structures of compounds **5-1** to **5-4** based on a new linker, designed with the idea of incorporating chiral centers to a rigid structure. The crystal structures of the compounds are achiral due to the *meso* character of the synthesized ligand. The addition of one instead of two chiral centers in the dicarboxylate structure, which would definitely preserve the homochirality in the metal-organic hybrid product, may be a good starting strategy.

References

1. Eds: Zhou, H.C.; Long, J.R.; Yaghi, O.M. Special Issue on Metal-Organic Frameworks. *Chem. Rev.* **2012**, *112*, 673–1268.
2. Eds: Long, J.R.; Yaghi, O.M. Themed Issue on Metal-Organic Frameworks. *Chem. Soc. Rev.* **2009**, *38*, 1201–1508.

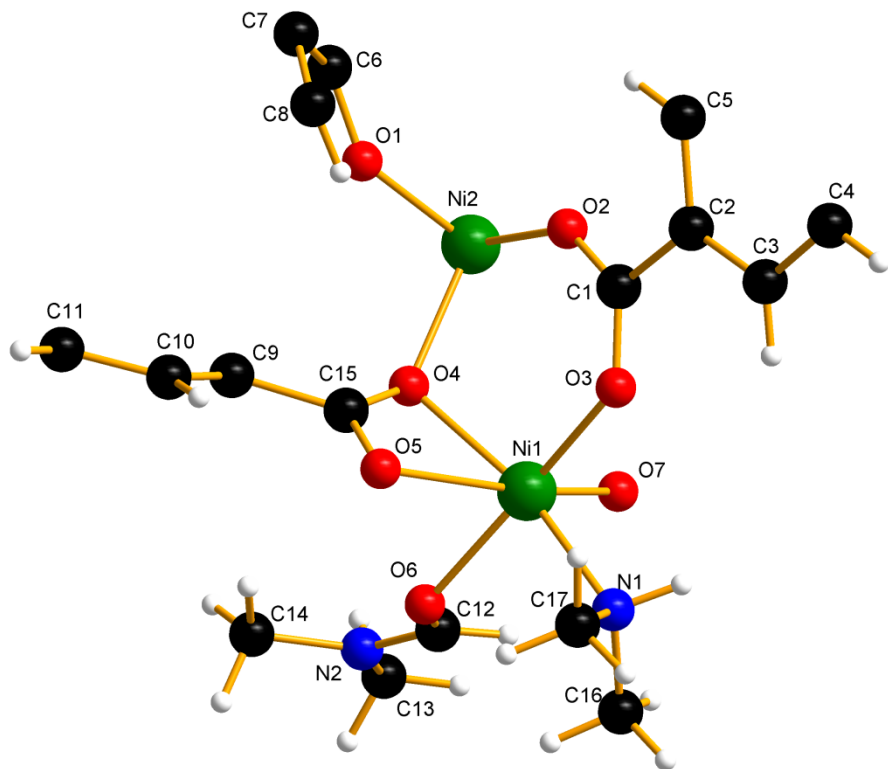
3. Bureekaew, S.; Shimomura, S.; Kitagawa, S. *Sci. Technol. Adv. Mater.* **2008**, *9*, 014108.
4. Carne, A.; Carbonell, C.; Imaz, I.; MasPOCH, D. *Chem. Soc. Rev.* **2011**, *40*, 291–305.
5. Cheetham, A.K.; Ferey, G.; Loiseau, T. *Angew. Chem. Int. Ed.* **1999**, *38*, 3268–3292.
6. Cheetham, A.K.; Rao, C.N.; Feller, R.K. *Chem. Commun.* **2006**, *38*, 4780–4795.
7. Dinca, M.; Long, J.R. *Angew. Chem. Int. Ed.* **2008**, *47*, 6766–6779.
8. Farha, O.K.; Hupp, J.T. *Acc. Chem. Res.* **2010**, *43*, 1166–1175.
9. Farrusseng, D.; Aguado, S.; Pinel, C. *Angew. Chem. Int. Ed.* **2009**, *48*, 7502–7513.
10. James, S.L. *Chem. Soc. Rev.* **2003**, *32*, 276–288.
11. Kitagawa, S.; Kitaura, R.; Noro, S. *Angew. Chem. Int. Ed.* **2004**, *43*, 2334–2375.
12. Lin, W.; Rieter, W.J.; Taylor, K.M.L. *Angew. Chem. Int. Ed.* **2009**, *48*, 650–658.
13. Lu, J.Y. *Coord. Chem. Rev.* **2003**, *246*, 327–347.
14. Moulton, B.; Zawarotko, M.J. *Chem. Rev.* **2001**, *101*, 1629–1658.
15. Rao, C.N.R.; Cheetham, A.K.; Thirumurugan, A. *J. Phys. Condens. Matter* **2008**, *20*, 083202.
16. Robin, A.Y.; Fromm, K.M. *Coord. Chem. Rev.* **2006**, *250*, 2127–2157.
17. Rosi, N.L.; Eddaoudi, M.; Kim, J.; O’Keeffe, M.; Yaghi, O.M. *Cryst. Eng. Comm.* **2002**, *4*, 401–404.
18. Yaghi, O.M.; Li, H.; Davis, C.; Richardson, D.; Groy, T.L. *Acc. Chem. Res.* **1998**, *31*, 474–484.
19. Yaghi, O.M.; O’Keeffe, M.; Ockwig, N.W.; Chae, H.K.; Eddaoudi, M.; Kim, J. *Nature* **2003**, *423*, 705–714.
20. Janiak, C. *Dalton Trans.* **2003**, 2781–2804.

21. Ockwig, N.W.; Delgado-Friedrichs, O.; O'Keeffe, M.; Yaghi, O.M. *Acc. Chem. Res.* **2005**, *38*, 176–182.
22. Perry IV, J.J.; Perman, J.A.; Zawarotko, M.J. *Chem. Soc. Rev.* **2009**, *38*, 1400–1417.
23. Tranchamontagne, D.J.; Mendoza-Cortes, J.L.; O'Keeffe, M.; Yaghi, O.M. *Chem. Soc. Rev.* **2009**, *38*, 1257–1283.
24. Tranchemontagne, D.J.; Ni, Z.; O'Keeffe, M.; Yaghi, O.M. *Angew. Chem. Int. Ed.* **2008**, *47*, 5136–5147.
25. Kaye. S.S.; Dailly, A.; Yaghi, O.M.; Long, J.R. *J. Am. Chem. Soc.* **2007**, *129*, 14176–14177.

Appendix

Crystallographic Information

A3.1. Structural Details for $\text{Ni}_3(1,4\text{-BDC})_3(\text{DMF})_2(\text{DMA})_2$ (**3-1**)



The asymmetric unit contains two nickel centers; Ni1 is surrounded by four oxygen atoms from the bridging carboxylates of the 1,4-BDC linker, an oxygen from DMF, and nitrogen of DMA, while Ni2 is surrounded by six oxygens from carboxylate groups of the linker completing the octahedron around each nickel. All hydrogen atoms are placed in calculated positions, in riding modes. No disorder is modeled in the structure.

A3.2. Crystallographic Information File for Ni₃(1,4-BDC)₃(DMF)₂(DMA)₂ (**3-1**).

```

data_COMPOUND_1_mc3071blt_0m

_audit_creation_method           SHELXL-97
_chemical_name_systematic
;
?
;
_chemical_name_common            ?
_chemical_melting_point         ?
_chemical_formula_moiety        ?
_chemical_formula_sum            'C34 H40 N4 Ni3 O14'
_chemical_formula_weight          904.83

loop_
_atom_type_symbol
_atom_type_description
_atom_type_scat_dispersion_real
_atom_type_scat_dispersion_imag
_atom_type_scat_source
'C'   'C'   0.0033   0.0016
'International Tables Vol C Tables 4.2.6.8 and 6.1.1.4'
'O'   'O'   0.0106   0.0060
'International Tables Vol C Tables 4.2.6.8 and 6.1.1.4'
'Ni'   'Ni'   0.3393   1.1124
'International Tables Vol C Tables 4.2.6.8 and 6.1.1.4'
'N'   'N'   0.0061   0.0033
'International Tables Vol C Tables 4.2.6.8 and 6.1.1.4'
'H'   'H'   0.0000   0.0000
'International Tables Vol C Tables 4.2.6.8 and 6.1.1.4'

_symmetry_cell_setting          ?
_symmetry_space_group_name_H-M   'Pbca'

loop_
_symmetry_equiv_pos_as_xyz
'x, y, z'
'-x+1/2, -y, z+1/2'
'-x, y+1/2, -z+1/2'
'x+1/2, -y+1/2, -z'
'-x, -y, -z'
'x-1/2, y, -z-1/2'
'x, -y-1/2, z-1/2'
'-x-1/2, y-1/2, z'

_cell_length_a                  9.6036(5)
_cell_length_b                  18.2457(9)
_cell_length_c                  21.0411(10)
_cell_angle_alpha                90.00
_cell_angle_beta                 90.00
_cell_angle_gamma                90.00
_cell_volume                     3686.9(3)
_cell_formula_units_Z             4

```

_cell_measurement_temperature	223(2)
_cell_measurement_reflns_used	8193
_cell_measurement_theta_min	2.4
_cell_measurement_theta_max	28.3
_exptl_crystal_description	plate
_exptl_crystal_colour	green
_exptl_crystal_size_max	0.2
_exptl_crystal_size_mid	0.2
_exptl_crystal_size_min	0.05
_exptl_crystal_density_meas	?
_exptl_crystal_density_diffrn	1.630
_exptl_crystal_density_method	'not measured'
_exptl_crystal_F_000	1872
_exptl_absorpt_coefficient_mu	1.590
_exptl_absorpt_correction_type	multi-scan
_exptl_absorpt_correction_T_min	0.217
_exptl_absorpt_correction_T_max	0.270
_exptl_absorpt_process_details	"Blessing, 1995"
_exptl_special_details	
;	
?	
;	
_diffrn_ambient_temperature	223(2)
_diffrn_radiation_wavelength	0.71073
_diffrn_radiation_type	MoK\alpha
_diffrn_radiation_source	'fine-focus sealed tube'
_diffrn_radiation_monochromator	graphite
_diffrn_measurement_device_type	?
_diffrn_measurement_method	?
_diffrn_detector_area_resol_mean	?
_diffrn_standards_number	?
_diffrn_standards_interval_count	?
_diffrn_standards_interval_time	?
_diffrn_standards_decay_%	?
_diffrn_reflns_number	22037
_diffrn_reflns_av_R_equivalents	0.0311
_diffrn_reflns_av_sigmaI/netI	0.0272
_diffrn_reflns_limit_h_min	-7
_diffrn_reflns_limit_h_max	12
_diffrn_reflns_limit_k_min	-24
_diffrn_reflns_limit_k_max	22
_diffrn_reflns_limit_l_min	-28
_diffrn_reflns_limit_l_max	20
_diffrn_reflns_theta_min	1.94
_diffrn_reflns_theta_max	28.30
_reflns_number_total	4289
_reflns_number_gt	3281
_reflns_threshold_expression	>2sigma(I)
_computing_data_collection	?
_computing_cell_refinement	?
_computing_data_reduction	?

```

_computing_structure_solution      'SHELXS-97 (Sheldrick, 1990)'
_computing_structure_refinement   'SHELXL-97 (Sheldrick, 1997)'
_computing_molecular_graphics     ?
_computing_publication_material   ?

_refine_special_details
;
    Refinement of F^2^ against ALL reflections. The weighted R-factor wR
and
    goodness of fit S are based on F^2^, conventional R-factors R are
based
    on F, with F set to zero for negative F^2^. The threshold expression
of
    F^2^ > 2sigma(F^2^) is used only for calculating R-factors(gt) etc.
and is
    not relevant to the choice of reflections for refinement. R-factors
based
    on F^2^ are statistically about twice as large as those based on F,
and R-
    factors based on ALL data will be even larger.
;

_refine_ls_structure_factor_coef  Fsqd
_refine_ls_matrix_type            full
_refine_ls_weighting_scheme       calc
_refine_ls_weighting_details
    'calc w=1/[s^2^(Fo^2^)+(0.0385P)^2^+0.0000P] where
P=(Fo^2^+2Fc^2^)/3'
_refine_ls_solution_primary        direct
_refine_ls_solution_secondary     difmap
_refine_ls_solution_hydrogens      geom
_refine_ls_hydrogen_treatment      constr
_refine_ls_extinction_method      none
_refine_ls_extinction_coef        ?
_refine_ls_number_reflns          4289
_refine_ls_number_parameters      254
_refine_ls_number_restraints      0
_refine_ls_R_factor_all           0.0416
_refine_ls_R_factor_gt             0.0270
_refine_ls_wR_factor_ref          0.0735
_refine_ls_wR_factor_gt            0.0687
_refine_ls_goodness_of_fit_ref     1.081
_refine_ls_restrained_S_all       1.081
_refine_ls_shift/su_max           0.003
_refine_ls_shift/su_mean          0.000

loop_
_atom_site_label
_atom_site_type_symbol
_atom_site_fract_x
_atom_site_fract_y
_atom_site_fract_z
_atom_site_U_iso_or_equiv
_atom_site_adp_type
_atom_site_occupancy

```

`_atom_site_symmetry_multiplicity`
`_atom_site_calc_flag`
`_atom_site_refinement_flags`
`_atom_site_disorder_assembly`
`_atom_site_disorder_group`
 C1 C 1.0761(2) 0.12090(9) 0.59585(8) 0.0186(4) Uani 1 1 d . . .
 C2 C 1.1481(2) 0.19489(9) 0.59942(8) 0.0199(4) Uani 1 1 d . . .
 C3 C 1.1888(2) 0.22601(9) 0.65678(8) 0.0226(4) Uani 1 1 d . . .
 H3 H 1.1725 0.2010 0.6946 0.027 Uiso 1 1 calc R . . .
 C4 C 1.2537(2) 0.29428(9) 0.65824(8) 0.0228(4) Uani 1 1 d . . .
 H4 H 1.2811 0.3143 0.6969 0.027 Uiso 1 1 calc R . . .
 C5 C 1.1733(2) 0.23357(10) 0.54347(9) 0.0306(5) Uani 1 1 d . . .
 H5 H 1.1474 0.2132 0.5047 0.037 Uiso 1 1 calc R . . .
 C6 C 0.8535(2) 0.09439(9) 0.39874(8) 0.0189(4) Uani 1 1 d . . .
 C7 C 0.7776(2) 0.16727(9) 0.39783(8) 0.0211(4) Uani 1 1 d . . .
 C8 C 0.7360(2) 0.19842(10) 0.45525(9) 0.0315(5) Uani 1 1 d . . .
 H8 H 0.7507 0.1731 0.4930 0.038 Uiso 1 1 calc R . . .
 C9 C 0.6152(2) 0.00847(9) 0.53979(8) 0.0196(4) Uani 1 1 d . . .
 C10 C 0.5010(2) 0.05453(10) 0.54566(9) 0.0240(4) Uani 1 1 d . . .
 H10 H 0.5012 0.0912 0.5764 0.029 Uiso 1 1 calc R . . .
 C11 C 0.3868(2) 0.04655(10) 0.50629(9) 0.0249(4) Uani 1 1 d . . .
 H11 H 0.3111 0.0779 0.5105 0.030 Uiso 1 1 calc R . . .
 C12 C 0.8531(3) -0.15990(10) 0.67414(10) 0.0357(5) Uani 1 1 d . . .
 H12 H 0.9441 -0.1671 0.6879 0.043 Uiso 1 1 calc R . . .
 C13 C 0.8508(4) -0.28869(13) 0.64742(15) 0.0869(12) Uani 1 1 d . . .
 H13A H 0.8613 -0.3018 0.6035 0.130 Uiso 1 1 calc R . . .
 H13B H 0.7929 -0.3242 0.6683 0.130 Uiso 1 1 calc R . . .
 H13C H 0.9406 -0.2877 0.6674 0.130 Uiso 1 1 calc R . . .
 C14 C 0.6489(3) -0.2082(2) 0.6260(2) 0.1247(18) Uani 1 1 d . . .
 H14A H 0.5811 -0.2213 0.6575 0.187 Uiso 1 1 calc R . . .
 H14B H 0.6384 -0.2393 0.5895 0.187 Uiso 1 1 calc R . . .
 H14C H 0.6354 -0.1580 0.6137 0.187 Uiso 1 1 calc R . . .
 C15 C 0.7361(2) 0.01452(9) 0.58432(8) 0.0189(4) Uani 1 1 d . . .
 C16 C 0.9574(3) -0.04852(11) 0.79765(10) 0.0441(7) Uani 1 1 d . . .
 H16A H 0.9764 -0.0340 0.8406 0.066 Uiso 1 1 calc R . . .
 H16B H 1.0268 -0.0828 0.7838 0.066 Uiso 1 1 calc R . . .
 H16C H 0.8672 -0.0711 0.7956 0.066 Uiso 1 1 calc R . . .
 C17 C 0.8647(3) 0.07287(14) 0.77937(11) 0.0599(8) Uani 1 1 d . . .
 H17A H 0.7708 0.0548 0.7779 0.090 Uiso 1 1 calc R . . .
 H17B H 0.8726 0.1156 0.7529 0.090 Uiso 1 1 calc R . . .
 H17C H 0.8882 0.0854 0.8224 0.090 Uiso 1 1 calc R . . .
 N1 N 0.95987(19) 0.01611(7) 0.75639(7) 0.0226(4) Uani 1 1 d . . .
 H1 H 1.0469 0.0353 0.7602 0.027 Uiso 1 1 calc R . . .
 N2 N 0.7871(3) -0.21708(10) 0.65199(10) 0.0506(6) Uani 1 1 d . . .
 Ni1 Ni 0.93215(3) -0.003329(10) 0.660747(10) 0.01640(8) Uani 1 1 d . . .
 .
 Ni2 Ni 1.0000 0.0000 0.5000 0.01462(9) Uani 1 2 d S . . .
 O1 O 0.86354(14) 0.06389(6) 0.45155(6) 0.0235(3) Uani 1 1 d . . .
 O2 O 1.06276(14) 0.09493(6) 0.54159(6) 0.0243(3) Uani 1 1 d . . .
 O3 O 1.03474(15) 0.09304(6) 0.64751(6) 0.0239(3) Uani 1 1 d . . .
 O4 O 0.85216(14) -0.01662(6) 0.56988(5) 0.0185(3) Uani 1 1 d . . .
 O5 O 0.72431(14) 0.04499(6) 0.63738(6) 0.0237(3) Uani 1 1 d . . .
 O6 O 0.80609(15) -0.09773(6) 0.67841(6) 0.0283(3) Uani 1 1 d . . .
 O7 O 1.09696(15) -0.07160(6) 0.65353(6) 0.0232(3) Uani 1 1 d . . .

```

loop_
_atom_site_aniso_label
_atom_site_aniso_U_11
_atom_site_aniso_U_22
_atom_site_aniso_U_33
_atom_site_aniso_U_23
_atom_site_aniso_U_13
_atom_site_aniso_U_12
C1 0.0148(11) 0.0146(7) 0.0265(9) -0.0011(6) -0.0007(8) 0.0008(7)
C2 0.0183(12) 0.0149(8) 0.0265(9) -0.0009(6) 0.0009(8) -0.0019(7)
C3 0.0261(13) 0.0183(8) 0.0234(9) 0.0032(6) 0.0010(8) -0.0046(8)
C4 0.0290(13) 0.0180(8) 0.0214(8) -0.0017(6) -0.0015(8) -0.0061(8)
C5 0.0449(16) 0.0237(9) 0.0233(9) -0.0018(7) -0.0010(9) -0.0142(9)
C6 0.0146(11) 0.0151(8) 0.0270(9) 0.0000(6) -0.0022(8) 0.0020(7)
C7 0.0208(12) 0.0162(8) 0.0263(9) -0.0002(6) -0.0018(8) 0.0047(7)
C8 0.0474(16) 0.0237(9) 0.0234(9) 0.0029(7) -0.0011(10) 0.0131(9)
C9 0.0144(11) 0.0222(8) 0.0221(8) 0.0023(6) -0.0008(8) -0.0009(7)
C10 0.0202(13) 0.0254(9) 0.0265(9) -0.0060(7) -0.0012(9) 0.0013(8)
C11 0.0173(13) 0.0267(9) 0.0306(10) -0.0035(7) -0.0026(9) 0.0033(8)
C12 0.0421(16) 0.0235(9) 0.0415(11) 0.0030(8) -0.0010(11) -0.0090(9)
C13 0.150(4) 0.0221(11) 0.089(2) -0.0071(13) 0.021(2) -0.0068(17)
C14 0.048(3) 0.123(3) 0.204(4) -0.110(3) 0.003(3) -0.028(2)
C15 0.0179(12) 0.0144(7) 0.0243(9) 0.0018(6) -0.0002(8) -0.0013(7)
C16 0.070(2) 0.0341(11) 0.0285(11) 0.0052(9) -0.0087(11) -0.0102(12)
C17 0.077(2) 0.0693(17) 0.0336(12) -0.0173(11) -0.0090(13) 0.0431(16)
N1 0.0206(10) 0.0225(7) 0.0248(8) -0.0016(6) -0.0008(7) -0.0021(6)
N2 0.0542(17) 0.0308(9) 0.0667(13) -0.0160(9) 0.0173(12) -0.0176(10)
Ni1 0.01702(16) 0.01223(11) 0.01996(12) -0.00029(8) -0.00066(9)
0.00030(9)
Ni2 0.0159(2) 0.01039(13) 0.01755(15) -0.00022(10) -0.00127(13)
0.00052(12)
O1 0.0220(9) 0.0218(6) 0.0268(6) 0.0061(5) 0.0012(6) 0.0077(6)
O2 0.0296(9) 0.0170(6) 0.0264(7) -0.0041(5) 0.0018(6) -0.0066(5)
O3 0.0285(9) 0.0169(6) 0.0262(6) 0.0008(5) -0.0008(6) -0.0069(5)
O4 0.0139(8) 0.0206(6) 0.0209(6) 0.0014(4) -0.0017(6) 0.0004(5)
O5 0.0205(9) 0.0232(6) 0.0274(6) -0.0043(5) -0.0024(6) 0.0024(6)
O6 0.0295(9) 0.0217(6) 0.0339(7) 0.0009(5) -0.0010(7) -0.0062(6)
O7 0.0257(9) 0.0200(6) 0.0240(6) -0.0010(5) -0.0005(6) 0.0084(5)

_geom_special_details
;
All esds (except the esd in the dihedral angle between two l.s.
planes)
are estimated using the full covariance matrix. The cell esds are
taken
into account individually in the estimation of esds in distances,
angles
and torsion angles; correlations between esds in cell parameters are
only
used when they are defined by crystal symmetry. An approximate
(isotropic)
treatment of cell esds is used for estimating esds involving l.s.
planes.
;
```

```

loop_
  _geom_bond_atom_site_label_1
  _geom_bond_atom_site_label_2
  _geom_bond_distance
  _geom_bond_site_symmetry_2
  _geom_bond_publ_flag
C1 O2 1.243(2) . ?
C1 O3 1.264(2) . ?
C1 C2 1.519(2) . ?
C2 C3 1.390(2) . ?
C2 C5 1.394(2) . ?
C3 C4 1.393(2) . ?
C4 C7 1.392(2) 4_556 ?
C5 C8 1.380(2) 4_556 ?
C6 O1 1.246(2) . ?
C6 O7 1.268(2) 5_756 ?
C6 C7 1.517(2) . ?
C7 C4 1.392(2) 4_456 ?
C7 C8 1.394(2) . ?
C8 C5 1.380(2) 4_456 ?
C9 C10 1.387(3) . ?
C9 C11 1.396(2) 5_656 ?
C9 C15 1.496(3) . ?
C10 C11 1.382(3) . ?
C11 C9 1.396(2) 5_656 ?
C12 O6 1.224(2) . ?
C12 N2 1.307(3) . ?
C13 N2 1.446(3) . ?
C14 N2 1.445(4) . ?
C15 O5 1.2524(19) . ?
C15 O4 1.288(2) . ?
C15 Ni1 2.4974(19) . ?
C16 N1 1.465(2) . ?
C17 N1 1.464(3) . ?
N1 Ni1 2.0607(16) . ?
Ni1 O7 2.0199(13) . ?
Ni1 O3 2.0346(12) . ?
Ni1 O4 2.0746(12) . ?
Ni1 O6 2.1379(13) . ?
Ni1 O5 2.2367(14) . ?
Ni2 O1 2.0287(12) 5_756 ?
Ni2 O1 2.0287(12) . ?
Ni2 O2 2.0321(11) . ?
Ni2 O2 2.0321(11) 5_756 ?
Ni2 O4 2.0664(13) . ?
Ni2 O4 2.0664(13) 5_756 ?
O7 C6 1.268(2) 5_756 ?

```

```

loop_
  _geom_angle_atom_site_label_1
  _geom_angle_atom_site_label_2
  _geom_angle_atom_site_label_3
  _geom_angle
  _geom_angle_site_symmetry_1
  _geom_angle_site_symmetry_3

```

$_geom_angle_publ_flag$
 O2 C1 O3 127.18(16) . . ?
 O2 C1 C2 115.54(15) . . ?
 O3 C1 C2 117.27(15) . . ?
 C3 C2 C5 118.54(16) . . ?
 C3 C2 C1 122.28(15) . . ?
 C5 C2 C1 119.17(15) . . ?
 C2 C3 C4 120.68(16) . . ?
 C7 C4 C3 120.39(16) 4_556 . ?
 C8 C5 C2 120.97(17) 4_556 . ?
 O1 C6 O7 126.69(16) . 5_756 ?
 O1 C6 C7 116.11(15) . . ?
 O7 C6 C7 117.18(15) 5_756 . ?
 C4 C7 C8 118.82(16) 4_456 . ?
 C4 C7 C6 122.15(16) 4_456 . ?
 C8 C7 C6 118.97(15) . . ?
 C5 C8 C7 120.59(17) 4_456 . ?
 C10 C9 C11 119.11(18) . 5_656 ?
 C10 C9 C15 120.87(16) . . ?
 C11 C9 C15 119.93(17) 5_656 . ?
 C11 C10 C9 120.66(17) . . ?
 C10 C11 C9 120.23(18) . 5_656 ?
 O6 C12 N2 125.9(2) . . ?
 O5 C15 O4 118.97(17) . . ?
 O5 C15 C9 121.41(17) . . ?
 O4 C15 C9 119.44(15) . . ?
 O5 C15 Ni1 63.38(10) . . ?
 O4 C15 Ni1 56.06(9) . . ?
 C9 C15 Ni1 168.17(11) . . ?
 C17 N1 C16 111.32(19) . . ?
 C17 N1 Ni1 111.34(13) . . ?
 C16 N1 Ni1 115.98(12) . . ?
 C12 N2 C14 119.4(2) . . ?
 C12 N2 C13 122.7(3) . . ?
 C14 N2 C13 117.7(2) . . ?
 O7 Ni1 O3 98.23(5) . . ?
 O7 Ni1 N1 94.49(6) . . ?
 O3 Ni1 N1 85.54(5) . . ?
 O7 Ni1 O4 98.55(5) . . ?
 O3 Ni1 O4 98.87(5) . . ?
 N1 Ni1 O4 165.44(6) . . ?
 O7 Ni1 O6 87.70(5) . . ?
 O3 Ni1 O6 173.85(5) . . ?
 N1 Ni1 O6 92.41(6) . . ?
 O4 Ni1 O6 81.74(5) . . ?
 O7 Ni1 O5 157.79(5) . . ?
 O3 Ni1 O5 93.52(5) . . ?
 N1 Ni1 O5 105.19(6) . . ?
 O4 Ni1 O5 60.87(5) . . ?
 O6 Ni1 O5 81.40(5) . . ?
 O7 Ni1 C15 128.52(5) . . ?
 O3 Ni1 C15 99.45(5) . . ?
 N1 Ni1 C15 134.73(7) . . ?
 O4 Ni1 C15 30.99(5) . . ?
 O6 Ni1 C15 77.88(5) . . ?

O5 Ni1 C15 30.04(5) . . ?
 O1 Ni2 O1 180.00(6) 5_756 . ?
 O1 Ni2 O2 94.69(5) 5_756 . ?
 O1 Ni2 O2 85.31(5) . . ?
 O1 Ni2 O2 85.31(5) 5_756 5_756 ?
 O1 Ni2 O2 94.69(5) . 5_756 ?
 O2 Ni2 O2 180.00(3) . 5_756 ?
 O1 Ni2 O4 90.11(5) 5_756 . ?
 O1 Ni2 O4 89.89(5) . . ?
 O2 Ni2 O4 91.28(5) . . ?
 O2 Ni2 O4 88.72(5) 5_756 . ?
 O1 Ni2 O4 89.89(5) 5_756 5_756 ?
 O1 Ni2 O4 90.11(5) . 5_756 ?
 O2 Ni2 O4 88.72(5) . 5_756 ?
 O2 Ni2 O4 91.28(5) 5_756 5_756 ?
 O4 Ni2 O4 180.0 . 5_756 ?
 C6 O1 Ni2 138.99(13) . . ?
 C1 O2 Ni2 138.69(11) . . ?
 C1 O3 Ni1 128.13(11) . . ?
 C15 O4 Ni2 134.27(11) . . ?
 C15 O4 Ni1 92.96(10) . . ?
 Ni2 O4 Ni1 112.59(6) . . ?
 C15 O5 Ni1 86.58(11) . . ?
 C12 O6 Ni1 121.66(15) . . ?
 C6 O7 Ni1 124.16(11) 5_756 . ?

 _diff_rn_measured_fraction_theta_max 0.935
 _diff_rn_reflns_theta_full 25.30
 _diff_rn_measured_fraction_theta_full 0.970
 _refine_diff_density_max 0.420
 _refine_diff_density_min -0.424
 _refine_diff_density_rms 0.062

Table A3.1. Selected interatomic distances and angles for

$\text{Ni}_3(1,4\text{-BDC})_3(\text{DMF})_2(\text{DMA})_2$ (**3-1**).

Atoms 1,2	d 1,2 [Å]	Atoms 1,2	d 1,2 [Å]
C1—O2	1.243(2)	C13—N2	1.446(3)
C1—O3	1.264(2)	C14—N2	1.445(4)
C1—C2	1.519(2)	C15—O5	1.2524(19)
C2—C3	1.390(2)	C15—O4	1.288(2)
C2—C5	1.394(2)	C15—Ni1	2.4974(19)
C3—C4	1.393(2)	C16—N1	1.465(2)
C4—C7 ⁱ	1.392(2)	C17—N1	1.464(3)
C5—C8 ⁱ	1.380(2)	N1—Ni1	2.0607(16)
C6—O1	1.246(2)	Ni1—O7	2.0199(13)

Table A3.1 continued

C6—O7 ⁱⁱ	1.268(2)	Ni1—O3	2.0346(12)
C6—C7	1.517(2)	Ni1—O4	2.0746(12)
C7—C4 ⁱⁱⁱ	1.392(2)	Ni1—O6	2.1379(13)
C7—C8	1.394(2)	Ni1—O5	2.2367(14)
C8—C5 ⁱⁱⁱ	1.380(2)	Ni2—O1 ⁱⁱ	2.0287(12)
C9—C10	1.387(3)	Ni2—O1	2.0287(12)
C9—C11 ^{iv}	1.396(2)	Ni2—O2	2.0321(11)
C9—C15	1.496(3)	Ni2—O2 ⁱⁱ	2.0321(11)
C10—C11	1.382(3)	Ni2—O4	2.0664(13)
C11—C9 ^{iv}	1.396(2)	Ni2—O4 ⁱⁱ	2.0664(13)
C12—O6	1.224(2)	O7—C6 ⁱⁱ	1.268(2)
C12—N2	1.307(3)		

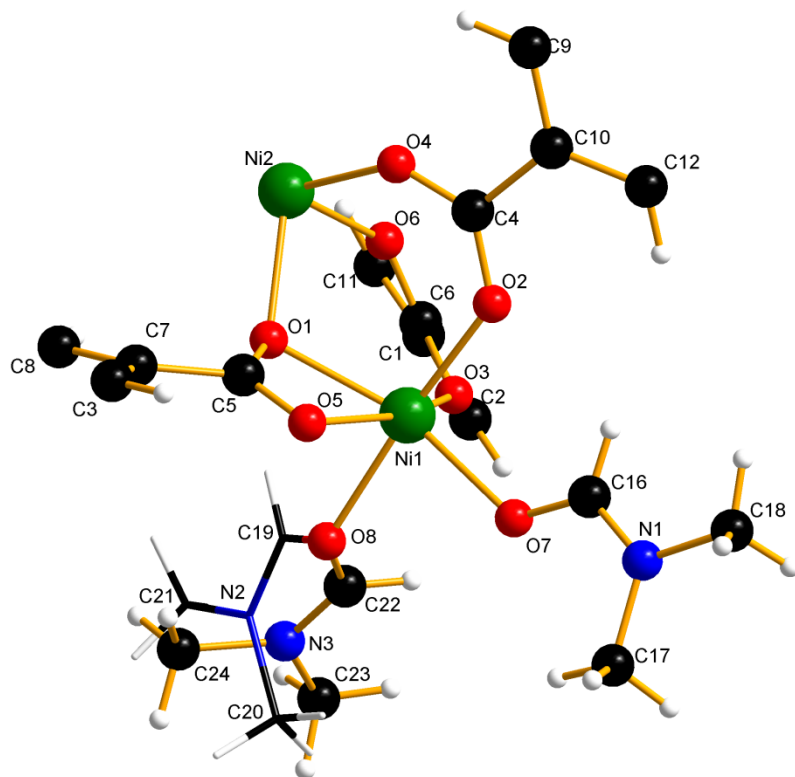
Atoms 1,2,3	Angle 1,2,3 [°]	Atoms 1,2,3	Angle 1,2,3 [°]
O2—C1—O3	127.18(16)	O7—Ni1—O6	87.70(5)
O2—C1—C2	115.54(15)	O3—Ni1—O6	173.85(5)
O3—C1—C2	117.27(15)	N1—Ni1—O6	92.41(6)
C3—C2—C5	118.54(16)	O4—Ni1—O6	81.74(5)
C3—C2—C1	122.28(15)	O7—Ni1—O5	157.79(5)
C5—C2—C1	119.17(15)	O3—Ni1—O5	93.52(5)
C2—C3—C4	120.68(16)	N1—Ni1—O5	105.19(6)
C7 ⁱ —C4—C3	120.39(16)	O4—Ni1—O5	60.87(5)
C8 ⁱ —C5—C2	120.97(17)	O6—Ni1—O5	81.40(5)
O1—C6—O7 ⁱⁱ	126.69(16)	O7—Ni1—C15	128.52(5)
O1—C6—C7	116.11(15)	O3—Ni1—C15	99.45(5)
O7 ⁱⁱ —C6—C7	117.18(15)	N1—Ni1—C15	134.73(7)
C4 ⁱⁱⁱ —C7—C8	118.82(16)	O4—Ni1—C15	30.99(5)
C4 ⁱⁱⁱ —C7—C6	122.15(16)	O6—Ni1—C15	77.88(5)
C8—C7—C6	118.97(15)	O5—Ni1—C15	30.04(5)
C5 ⁱⁱⁱ —C8—C7	120.59(17)	O1 ⁱⁱ —Ni2—O1	180.00(6)
C10—C9—C11 ^{iv}	119.11(18)	O1 ⁱⁱ —Ni2—O2	94.69(5)
C10—C9—C15	120.87(16)	O1—Ni2—O2	85.31(5)
C11 ^{iv} —C9—C15	119.93(17)	O1 ⁱⁱ —Ni2—O2 ⁱⁱ	85.31(5)
C11—C10—C9	120.66(17)	O1—Ni2—O2 ⁱⁱ	94.69(5)
C10—C11—C9 ^{iv}	120.23(18)	O2—Ni2—O2 ⁱⁱ	180.00(3)
O6—C12—N2	125.9(2)	O1 ⁱⁱ —Ni2—O4	90.11(5)

Table A3.1 continued

O5—C15—O4	118.97(17)	O1—Ni2—O4	89.89(5)
O5—C15—C9	121.41(17)	O2—Ni2—O4	91.28(5)
O4—C15—C9	119.44(15)	O2 ⁱⁱ —Ni2—O4	88.72(5)
O5—C15—Ni1	63.38(10)	O1 ⁱⁱ —Ni2—O4 ⁱⁱ	89.89(5)
O4—C15—Ni1	56.06(9)	O1—Ni2—O4 ⁱⁱ	90.11(5)
C9—C15—Ni1	168.17(11)	O2—Ni2—O4 ⁱⁱ	88.72(5)
C17—N1—C16	111.32(19)	O2 ⁱⁱ —Ni2—O4 ⁱⁱ	91.28(5)
C17—N1—Ni1	111.34(13)	O4—Ni2—O4 ⁱⁱ	180.000
C16—N1—Ni1	115.98(12)	C6—O1—Ni2	138.99(13)
C12—N2—C14	119.4(2)	C1—O2—Ni2	138.69(11)
C12—N2—C13	122.7(3)	C1—O3—Ni1	128.13(11)
C14—N2—C13	117.7(2)	C15—O4—Ni2	134.27(11)
O7—Ni1—O3	98.23(5)	C15—O4—Ni1	92.96(10)
O7—Ni1—N1	94.49(6)	Ni2—O4—Ni1	112.59(6)
O3—Ni1—N1	85.54(5)	C15—O5—Ni1	86.58(11)
O7—Ni1—O4	98.55(5)	C12—O6—Ni1	121.66(15)
O3—Ni1—O4	98.87(5)	C6 ⁱⁱ —O7—Ni1	124.16(11)
N1—Ni1—O4	165.44(6)		

Symmetry codes : (i) 0.5+x, 0.5-y, 1-z; (ii) 2-x, -y, 1-z; (iii) -0.5+x, 0.5-y, 1-z;
 (iv) 1-x, -y, 1-z.

A3.3. Structural Details for $\text{Ni}_3(1,4\text{-BDC})_3(\text{DMF})_4$ (**3-2**).



The asymmetric unit contains two nickel centers both coordinated to six oxygen atoms; Ni1 is surrounded by four oxygen atoms from the bridging carboxylates of the 1,4-BDC linker and two oxygens from DMF, while Ni2 is surrounded by six oxygens from carboxylate groups of 1,4-BDC completing the octahedron around each nickel. All hydrogen atoms are placed in calculated positions, in riding modes. A disordered coordinated DMF is modeled in the structure.

A3.4. Crystallographic Information File for Ni₃(1,4-BDC)₃(DMF)₄ (**3-2**).

```
data_COMPOUND_2_mc3117a1

_audit_creation_method           SHELXL-97
_chemical_name_systematic
;
?
;
_chemical_name_common          ?
_chemical_melting_point        ?
_chemical_formula_moiety       ?
_chemical_formula_sum          'C36 H40 N4 Ni3 O16'
_chemical_formula_weight        960.85

loop_
_atom_type_symbol
_atom_type_description
_atom_type_scat_dispersion_real
_atom_type_scat_dispersion_imag
_atom_type_scat_source
'C'   'C'   0.0033  0.0016
'International Tables Vol C Tables 4.2.6.8 and 6.1.1.4'
'H'   'H'   0.0000  0.0000
'International Tables Vol C Tables 4.2.6.8 and 6.1.1.4'
'N'   'N'   0.0061  0.0033
'International Tables Vol C Tables 4.2.6.8 and 6.1.1.4'
'O'   'O'   0.0106  0.0060
'International Tables Vol C Tables 4.2.6.8 and 6.1.1.4'
'Ni'   'Ni'   0.3393  1.1124
'International Tables Vol C Tables 4.2.6.8 and 6.1.1.4'

_symmetry_cell_setting          ?
_symmetry_space_group_name_H-M   'P2(1)/n'

loop_
_symmetry_equiv_pos_as_xyz
'x, y, z'
'-x+1/2, y+1/2, -z+1/2'
'-x, -y, -z'
'x-1/2, -y-1/2, z-1/2'

_cell_length_a                  13.9262(8)
_cell_length_b                  9.6614(6)
_cell_length_c                  16.5066(10)
_cell_angle_alpha               90.00
_cell_angle_beta                108.9890(10)
_cell_angle_gamma               90.00
_cell_volume                    2100.0(2)
_cell_formula_units_Z           2
_cell_measurement_temperature   223(2)
_cell_measurement_reflns_used  7199
_cell_measurement_theta_min    2.6
_cell_measurement_theta_max    28.5
```

_exptl_crystal_description	plate
_exptl_crystal_colour	green
_exptl_crystal_size_max	0.28
_exptl_crystal_size_mid	0.20
_exptl_crystal_size_min	0.08
_exptl_crystal_density_meas	?
_exptl_crystal_density_diffrn	1.520
_exptl_crystal_density_method	'not measured'
_exptl_crystal_F_000	992
_exptl_absorpt_coefficient_mu	1.404
_exptl_absorpt_correction_type	multi-scan
_exptl_absorpt_correction_T_min	0.292
_exptl_absorpt_correction_T_max	0.386
_exptl_absorpt_process_details	"Blessing, 1995"
_exptl_special_details	
;	
?	
;	
_diffrn_ambient_temperature	223(2)
_diffrn_radiation_wavelength	0.71073
_diffrn_radiation_type	MoK\alpha
_diffrn_radiation_source	'fine-focus sealed tube'
_diffrn_radiation_monochromator	graphite
_diffrn_measurement_device_type	?
_diffrn_measurement_method	?
_diffrn_detector_area_resol_mean	?
_diffrn_standards_number	?
_diffrn_standards_interval_count	?
_diffrn_standards_interval_time	?
_diffrn_standards_decay_%	?
_diffrn_reflns_number	12838
_diffrn_reflns_av_R_equivalents	0.0340
_diffrn_reflns_av_sigmaI/netI	0.0309
_diffrn_reflns_limit_h_min	-14
_diffrn_reflns_limit_h_max	18
_diffrn_reflns_limit_k_min	-12
_diffrn_reflns_limit_k_max	12
_diffrn_reflns_limit_l_min	-21
_diffrn_reflns_limit_l_max	18
_diffrn_reflns_theta_min	1.67
_diffrn_reflns_theta_max	28.85
_reflns_number_total	5071
_reflns_number_gt	4367
_reflns_threshold_expression	>2sigma(I)
_computing_data_collection	?
_computing_cell_refinement	?
_computing_data_reduction	?
_computing_structure_solution	'SHELXS-97 (Sheldrick, 1990)'
_computing_structure_refinement	'SHELXL-97 (Sheldrick, 1997)'
_computing_molecular_graphics	?
_computing_publication_material	?

```

_refine_special_details
;
    Refinement of F^2^ against ALL reflections. The weighted R-factor wR
and
    goodness of fit S are based on F^2^, conventional R-factors R are
based
    on F, with F set to zero for negative F^2^. The threshold expression
of
    F^2^ > 2sigma(F^2^) is used only for calculating R-factors(gt) etc.
and is
    not relevant to the choice of reflections for refinement. R-factors
based
    on F^2^ are statistically about twice as large as those based on F,
and R-
    factors based on ALL data will be even larger.
;

_refine_ls_structure_factor_coef   Fsqd
_refine_ls_matrix_type            full
_refine_ls_weighting_scheme      calc
_refine_ls_weighting_details
    'calc w=1/[\s^2^(Fo^2^)+(0.0447P)^2^+0.2439P] where
P=(Fo^2^+2Fc^2^)/3'
_refine_ls_solution_primary       direct
_refine_ls_solution_secondary    difmap
_refine_ls_solution_hydrogens    geom
_refine_ls_hydrogen_treatment    constr
_refine_ls_extinction_method    none
_refine_ls_extinction_coef      ?
_refine_ls_number_reflns        5071
_refine_ls_number_parameters    311
_refine_ls_number_restraints    0
_refine_ls_R_factor_all         0.0345
_refine_ls_R_factor_gt          0.0273
_refine_ls_wR_factor_ref        0.0772
_refine_ls_wR_factor_gt         0.0736
_refine_ls_goodness_of_fit_ref  1.045
_refine_ls_restrained_S_all    1.045
_refine_ls_shift/su_max         0.000
_refine_ls_shift/su_mean        0.000

loop_
_atom_site_label
_atom_site_type_symbol
_atom_site_fract_x
_atom_site_fract_y
_atom_site_fract_z
_atom_site_U_iso_or_equiv
_atom_site_adp_type
_atom_site_occupancy
_atom_site_symmetry_multiplicity
_atom_site_calc_flag
_atom_site_refinement_flags
_atom_site_disorder_assembly

```

`_atom_site_disorder_group`
 Nil Ni 0.323890(14) 0.574689(19) 0.099777(12) 0.02334(7) Uani 1 1 d . A
 .
 Ni2 Ni 0.5000 0.5000 0.0000 0.01942(8) Uani 1 2 d S . . .
 O1 O 0.40385(8) 0.65022(10) 0.02247(7) 0.0256(2) Uani 1 1 d . A .
 O2 O 0.43788(9) 0.47262(13) 0.18696(7) 0.0296(2) Uani 1 1 d . . .
 O3 O 0.25925(9) 0.40813(12) 0.03029(7) 0.0291(3) Uani 1 1 d . . .
 O4 O 0.56031(9) 0.45969(13) 0.12639(7) 0.0320(3) Uani 1 1 d . . .
 O5 O 0.40051(9) 0.77307(12) 0.13254(8) 0.0352(3) Uani 1 1 d . A .
 O6 O 0.38782(8) 0.35844(11) -0.01864(8) 0.0293(2) Uani 1 1 d . . .
 O7 O 0.24559(10) 0.57591(14) 0.18515(9) 0.0409(3) Uani 1 1 d . . .
 O8 O 0.20062(9) 0.68714(13) 0.01887(9) 0.0403(3) Uani 1 1 d . . .
 C1 C 0.22638(11) 0.27089(16) -0.09470(10) 0.0261(3) Uani 1 1 d . . .
 C2 C 0.12628(12) 0.24669(19) -0.10006(11) 0.0336(4) Uani 1 1 d . . .
 H2 H 0.1023 0.2781 -0.0569 0.040 Uiso 1 1 calc R . . .
 C3 C 0.50932(15) 0.99392(17) 0.08608(12) 0.0350(4) Uani 1 1 d . . .
 H3 H 0.5156 0.9896 0.1439 0.042 Uiso 1 1 calc R . . .
 C4 C 0.52503(12) 0.44020(16) 0.18553(10) 0.0258(3) Uani 1 1 d . . .
 C5 C 0.42320(12) 0.76296(16) 0.06546(11) 0.0279(3) Uani 1 1 d . . .
 C6 C 0.29747(11) 0.35230(15) -0.02130(10) 0.0242(3) Uani 1 1 d . . .
 C7 C 0.46522(12) 0.88407(16) 0.03202(11) 0.0288(3) Uani 1 1 d . A .
 C8 C 0.45617(14) 0.89057(17) -0.05420(12) 0.0343(4) Uani 1 1 d . . .
 H8 H 0.4270 0.8174 -0.0905 0.041 Uiso 1 1 calc R A .
 C9 C 0.69528(13) 0.3437(2) 0.26979(12) 0.0420(5) Uani 1 1 d . . .
 H9 H 0.7188 0.3728 0.2259 0.050 Uiso 1 1 calc R . . .
 C10 C 0.59522(12) 0.36902(17) 0.26436(10) 0.0278(3) Uani 1 1 d . . .
 C11 C 0.26030(13) 0.2246(2) -0.15996(13) 0.0427(5) Uani 1 1 d . . .
 H11 H 0.3275 0.2394 -0.1566 0.051 Uiso 1 1 calc R . . .
 C12 C 0.56184(12) 0.3244(2) 0.33029(11) 0.0348(4) Uani 1 1 d . . .
 H12 H 0.4954 0.3423 0.3279 0.042 Uiso 1 1 calc R . . .
 C16 C 0.27916(15) 0.5308(2) 0.25877(13) 0.0404(4) Uani 1 1 d . . .
 H16 H 0.3327 0.4683 0.2706 0.049 Uiso 1 1 calc R . . .
 C17 C 0.1658(3) 0.6632(3) 0.3094(2) 0.0885(10) Uani 1 1 d . . .
 H17A H 0.1395 0.6883 0.2499 0.133 Uiso 1 1 calc R . . .
 H17B H 0.1919 0.7440 0.3431 0.133 Uiso 1 1 calc R . . .
 H17C H 0.1124 0.6236 0.3269 0.133 Uiso 1 1 calc R . . .
 C18 C 0.2876(2) 0.5044(3) 0.40668(15) 0.0651(7) Uani 1 1 d . . .
 H18A H 0.3421 0.4426 0.4082 0.098 Uiso 1 1 calc R . . .
 H18B H 0.2354 0.4542 0.4205 0.098 Uiso 1 1 calc R . . .
 H18C H 0.3127 0.5772 0.4477 0.098 Uiso 1 1 calc R . . .
 N1 N 0.24598(14) 0.56343(16) 0.32158(11) 0.0403(4) Uani 1 1 d . . .
 C19 C 0.1726(4) 0.6712(6) -0.0512(3) 0.0396(14) Uani 0.374(4) 1 d P A 1
 H19 H 0.2162 0.6253 -0.0745 0.048 Uiso 0.374(4) 1 calc PR A 1
 C20 C 0.0089(6) 0.7736(16) -0.0724(6) 0.115(5) Uani 0.374(4) 1 d P A 1
 H20A H 0.0345 0.7731 -0.0110 0.172 Uiso 0.374(4) 1 calc PR A 1
 H20B H -0.0534 0.7219 -0.0917 0.172 Uiso 0.374(4) 1 calc PR A 1
 H20C H -0.0036 0.8672 -0.0926 0.172 Uiso 0.374(4) 1 calc PR A 1
 C21 C 0.0575(7) 0.6964(15) -0.1955(5) 0.112(4) Uani 0.374(4) 1 d P A 1
 H21A H 0.1182 0.6860 -0.2104 0.167 Uiso 0.374(4) 1 calc PR A 1
 H21B H 0.0214 0.7774 -0.2230 0.167 Uiso 0.374(4) 1 calc PR A 1
 H21C H 0.0153 0.6163 -0.2141 0.167 Uiso 0.374(4) 1 calc PR A 1
 N2 N 0.0834(8) 0.7104(13) -0.1060(7) 0.051(2) Uani 0.374(4) 1 d P A 1
 C22 C 0.1187(2) 0.6382(3) -0.0241(2) 0.0421(9) Uani 0.626(4) 1 d P A 2
 H22 H 0.1016 0.5546 -0.0044 0.051 Uiso 0.626(4) 1 calc PR A 2

C23 C -0.0471(3) 0.6238(6) -0.1339(4) 0.0909(19) Uani 0.626(4) 1 d P A
 2
 H23A H -0.0540 0.5436 -0.1018 0.136 Uiso 0.626(4) 1 calc PR A 2
 H23B H -0.0534 0.5969 -0.1913 0.136 Uiso 0.626(4) 1 calc PR A 2
 H23C H -0.0993 0.6894 -0.1351 0.136 Uiso 0.626(4) 1 calc PR A 2
 C24 C 0.0755(5) 0.8121(9) -0.1315(5) 0.140(4) Uani 0.626(4) 1 d P A 2
 H24A H 0.1375 0.8512 -0.0942 0.211 Uiso 0.626(4) 1 calc PR A 2
 H24B H 0.0213 0.8775 -0.1396 0.211 Uiso 0.626(4) 1 calc PR A 2
 H24C H 0.0831 0.7906 -0.1858 0.211 Uiso 0.626(4) 1 calc PR A 2
 N3 N 0.0521(4) 0.6866(8) -0.0934(5) 0.0584(17) Uani 0.626(4) 1 d P A 2

loop_
 _atom_site_aniso_label
 _atom_site_aniso_U_11
 _atom_site_aniso_U_22
 _atom_site_aniso_U_33
 _atom_site_aniso_U_23
 _atom_site_aniso_U_13
 _atom_site_aniso_U_12
 Ni1 0.02184(11) 0.02470(11) 0.02061(11) -0.00098(7) 0.00296(8) -
 0.00031(7)
 Ni2 0.01848(13) 0.02001(13) 0.01681(14) 0.00029(10) 0.00170(10) -
 0.00136(9)
 O1 0.0246(5) 0.0194(5) 0.0309(6) -0.0001(4) 0.0065(4) -0.0004(4)
 O2 0.0251(6) 0.0377(6) 0.0231(6) 0.0050(5) 0.0036(4) 0.0045(5)
 O3 0.0279(6) 0.0316(6) 0.0265(6) -0.0059(5) 0.0069(5) -0.0072(5)
 O4 0.0271(6) 0.0455(7) 0.0200(6) 0.0058(5) 0.0031(5) 0.0046(5)
 O5 0.0422(7) 0.0285(6) 0.0360(7) -0.0055(5) 0.0146(5) -0.0050(5)
 O6 0.0235(5) 0.0254(5) 0.0354(6) -0.0058(5) 0.0049(5) -0.0056(4)
 O7 0.0383(7) 0.0542(8) 0.0327(7) 0.0050(6) 0.0148(6) 0.0088(6)
 O8 0.0308(6) 0.0388(7) 0.0423(8) -0.0003(6) -0.0006(6) 0.0068(5)
 C1 0.0236(7) 0.0293(7) 0.0222(8) -0.0017(6) 0.0031(6) -0.0044(6)
 C2 0.0286(8) 0.0472(10) 0.0248(8) -0.0104(7) 0.0084(7) -0.0073(7)
 C3 0.0449(10) 0.0267(8) 0.0329(9) -0.0031(7) 0.0122(8) -0.0042(7)
 C4 0.0258(8) 0.0267(7) 0.0209(8) 0.0001(6) 0.0020(6) -0.0002(6)
 C5 0.0253(7) 0.0231(7) 0.0324(9) -0.0010(6) 0.0056(6) 0.0012(6)
 C6 0.0234(7) 0.0213(7) 0.0239(8) 0.0013(6) 0.0024(6) -0.0030(6)
 C7 0.0282(8) 0.0205(7) 0.0368(9) -0.0008(6) 0.0092(7) 0.0002(6)
 C8 0.0403(9) 0.0220(7) 0.0380(10) -0.0045(7) 0.0093(8) -0.0045(7)
 C9 0.0302(9) 0.0649(12) 0.0313(9) 0.0196(9) 0.0108(7) 0.0078(9)
 C10 0.0247(7) 0.0325(8) 0.0226(8) 0.0025(6) 0.0027(6) 0.0030(6)
 C11 0.0236(8) 0.0657(13) 0.0386(10) -0.0196(10) 0.0097(7) -0.0102(8)
 C12 0.0224(8) 0.0507(10) 0.0299(9) 0.0097(8) 0.0065(7) 0.0098(7)
 C16 0.0392(10) 0.0447(10) 0.0393(11) 0.0015(9) 0.0153(8) 0.0085(8)
 C17 0.121(3) 0.088(2) 0.080(2) 0.0120(17) 0.065(2) 0.048(2)
 C18 0.0738(17) 0.0845(18) 0.0389(13) 0.0072(12) 0.0210(12) -0.0165(14)
 N1 0.0511(10) 0.0384(8) 0.0362(9) -0.0014(7) 0.0208(8) -0.0030(7)
 C19 0.037(3) 0.050(3) 0.031(3) 0.007(2) 0.011(2) 0.013(2)
 C20 0.058(5) 0.213(13) 0.063(5) 0.007(7) 0.007(4) 0.067(7)
 C21 0.080(6) 0.198(12) 0.042(4) 0.010(6) -0.001(4) 0.048(7)
 N2 0.042(5) 0.068(7) 0.033(3) 0.012(3) -0.003(3) 0.016(4)
 C22 0.0326(16) 0.0364(16) 0.050(2) 0.0054(14) 0.0041(15) 0.0025(13)
 C23 0.044(2) 0.087(3) 0.107(4) -0.015(3) -0.023(2) -0.003(2)
 C24 0.109(5) 0.150(6) 0.103(6) 0.083(5) -0.046(4) -0.040(4)
 N3 0.041(4) 0.059(3) 0.056(3) 0.004(2) -0.011(2) 0.001(3)

```

_geom_special_details
;
All esds (except the esd in the dihedral angle between two l.s.
planes)
are estimated using the full covariance matrix. The cell esds are
taken
into account individually in the estimation of esds in distances,
angles
and torsion angles; correlations between esds in cell parameters are
only
used when they are defined by crystal symmetry. An approximate
(isotropic)
treatment of cell esds is used for estimating esds involving l.s.
planes.
;

loop_
_geom_bond_atom_site_label_1
_geom_bond_atom_site_label_2
_geom_bond_distance
_geom_bond_site_symmetry_2
_geom_bond_publ_flag
N1 O3 2.0108(11) . ?
N1 O2 2.0191(11) . ?
N1 O7 2.0433(13) . ?
N1 O1 2.0798(11) . ?
N1 O8 2.1021(12) . ?
N1 O5 2.1746(12) . ?
N1 C5 2.4601(16) . ?
Ni2 O4 2.0172(11) . ?
Ni2 O4 2.0172(11) 3_665 ?
Ni2 O6 2.0231(10) . ?
Ni2 O6 2.0231(10) 3_665 ?
Ni2 O1 2.0881(10) 3_665 ?
Ni2 O1 2.0881(10) . ?
O1 C5 1.2800(18) . ?
O2 C4 1.261(2) . ?
O3 C6 1.263(2) . ?
O4 C4 1.242(2) . ?
O5 C5 1.250(2) . ?
O6 C6 1.2462(18) . ?
O7 C16 1.231(2) . ?
O8 C19 1.104(5) . ?
O8 C22 1.225(3) . ?
C1 C11 1.384(2) . ?
C1 C2 1.388(2) . ?
C1 C6 1.512(2) . ?
C2 C12 1.388(2) 4_565 ?
C3 C8 1.385(2) 3_675 ?
C3 C7 1.394(2) . ?
C4 C10 1.515(2) . ?
C5 C7 1.492(2) . ?
C7 C8 1.389(3) . ?
C8 C3 1.385(2) 3_675 ?

```

```

C9 C11 1.384(2) 4_666 ?
C9 C10 1.389(2) . ?
C10 C12 1.384(2) . ?
C11 C9 1.384(2) 4_565 ?
C12 C2 1.388(2) 4_666 ?
C16 N1 1.304(3) . ?
C17 N1 1.439(3) . ?
C18 N1 1.451(3) . ?
C19 N2 1.333(12) . ?
C20 N2 1.459(13) . ?
C21 N2 1.409(14) . ?
C22 N3 1.302(8) . ?
C23 N3 1.458(7) . ?
C24 N3 1.450(9) . ?

loop_
_geom_angle_atom_site_label_1
_geom_angle_atom_site_label_2
_geom_angle_atom_site_label_3
_geom_angle
_geom_angle_site_symmetry_1
_geom_angle_site_symmetry_3
_geom_angle_publ_flag
O3 Ni1 O2 96.77(5) . . ?
O3 Ni1 O7 99.07(5) . . ?
O2 Ni1 O7 89.05(5) . . ?
O3 Ni1 O1 99.24(4) . . ?
O2 Ni1 O1 98.91(5) . . ?
O7 Ni1 O1 158.99(5) . . ?
O3 Ni1 O8 85.97(5) . . ?
O2 Ni1 O8 174.48(5) . . ?
O7 Ni1 O8 85.78(5) . . ?
O1 Ni1 O8 85.32(5) . . ?
O3 Ni1 O5 159.98(5) . . ?
O2 Ni1 O5 92.57(5) . . ?
O7 Ni1 O5 98.75(5) . . ?
O1 Ni1 O5 61.71(4) . . ?
O8 Ni1 O5 86.31(5) . . ?
O3 Ni1 C5 129.89(5) . . ?
O2 Ni1 C5 98.90(5) . . ?
O7 Ni1 C5 128.36(5) . . ?
O1 Ni1 C5 31.35(5) . . ?
O8 Ni1 C5 82.86(5) . . ?
O5 Ni1 C5 30.51(5) . . ?
O4 Ni2 O4 180.0 . 3_665 ?
O4 Ni2 O6 93.89(5) . . ?
O4 Ni2 O6 86.11(5) 3_665 . ?
O4 Ni2 O6 86.11(5) . 3_665 ?
O4 Ni2 O6 93.89(5) 3_665 3_665 ?
O6 Ni2 O6 180.0 . 3_665 ?
O4 Ni2 O1 88.52(5) . 3_665 ?
O4 Ni2 O1 91.48(5) 3_665 3_665 ?
O6 Ni2 O1 90.64(4) . 3_665 ?
O6 Ni2 O1 89.36(4) 3_665 3_665 ?
O4 Ni2 O1 91.48(5) . . ?

```

O4 Ni2 O1 88.52(5) 3_665 . ?
 O6 Ni2 O1 89.36(4) . . ?
 O6 Ni2 O1 90.64(4) 3_665 . ?
 O1 Ni2 O1 180.00(6) 3_665 . ?
 C5 O1 Ni1 90.95(10) . . ?
 C5 O1 Ni2 131.18(10) . . ?
 Ni1 O1 Ni2 111.56(5) . . ?
 C4 O2 Ni1 130.26(11) . . ?
 C6 O3 Ni1 121.19(10) . . ?
 C4 O4 Ni2 134.77(11) . . ?
 C5 O5 Ni1 87.47(9) . . ?
 C6 O6 Ni2 139.33(10) . . ?
 C16 O7 Ni1 124.22(12) . . ?
 C19 O8 C22 52.8(3) . . ?
 C19 O8 Ni1 122.0(3) . . ?
 C22 O8 Ni1 125.62(17) . . ?
 C11 C1 C2 119.09(15) . . ?
 C11 C1 C6 119.46(14) . . ?
 C2 C1 C6 121.39(15) . . ?
 C1 C2 C12 120.09(16) . 4_565 ?
 C8 C3 C7 120.36(17) 3_675 . ?
 O4 C4 O2 127.33(15) . . ?
 O4 C4 C10 115.75(14) . . ?
 O2 C4 C10 116.92(14) . . ?
 O5 C5 O1 119.29(15) . . ?
 O5 C5 C7 120.59(14) . . ?
 O1 C5 C7 119.96(15) . . ?
 O5 C5 Ni1 62.02(8) . . ?
 O1 C5 Ni1 57.71(8) . . ?
 C7 C5 Ni1 169.27(12) . . ?
 O6 C6 O3 126.75(14) . . ?
 O6 C6 C1 116.31(14) . . ?
 O3 C6 C1 116.93(13) . . ?
 C8 C7 C3 119.72(16) . . ?
 C8 C7 C5 119.92(15) . . ?
 C3 C7 C5 120.29(16) . . ?
 C3 C8 C7 119.92(16) 3_675 . ?
 C11 C9 C10 120.46(17) 4_666 . ?
 C12 C10 C9 118.76(15) . . ?
 C12 C10 C4 121.94(14) . . ?
 C9 C10 C4 119.27(15) . . ?
 C1 C11 C9 120.69(16) . 4_565 ?
 C10 C12 C2 120.88(15) . 4_666 ?
 O7 C16 N1 125.49(19) . . ?
 C16 N1 C17 120.68(19) . . ?
 C16 N1 C18 122.8(2) . . ?
 C17 N1 C18 116.5(2) . . ?
 O8 C19 N2 127.2(7) . . ?
 C19 N2 C21 123.3(10) . . ?
 C19 N2 C20 118.9(9) . . ?
 C21 N2 C20 117.9(9) . . ?
 O8 C22 N3 129.2(4) . . ?
 C22 N3 C24 119.0(5) . . ?
 C22 N3 C23 123.4(6) . . ?
 C24 N3 C23 117.5(6) . . ?

_diffrn_measured_fraction_theta_max	0.921
_diffrn_reflns_theta_full	25.50
_diffrn_measured_fraction_theta_full	0.998
_refine_diff_density_max	0.399
_refine_diff_density_min	-0.339
_refine_diff_density_rms	0.056

Table A3.2. Selected interatomic distances and angles for

Ni₃(1,4-BDC)₃(DMF)₄ (**3-2**).

Atoms 1,2	d 1,2 [Å]	Atoms 1,2	d 1,2 [Å]
Ni1—O3	2.0108(11)	C1—C2	1.388(2)
Ni1—O2	2.0191(11)	C1—C6	1.512(2)
Ni1—O7	2.0433(13)	C2—C12 ⁱⁱ	1.388(2)
Ni1—O1	2.0798(11)	C3—C8 ⁱⁱⁱ	1.385(2)
Ni1—O8	2.1021(12)	C3—C7	1.394(2)
Ni1—O5	2.1746(12)	C4—C10	1.515(2)
Ni1—C5	2.4601(16)	C5—C7	1.492(2)
Ni2—O4	2.0172(11)	C7—C8	1.389(3)
Ni2—O4 ⁱ	2.0172(11)	C8—C3 ⁱⁱⁱ	1.385(2)
Ni2—O6	2.0231(10)	C9—C11 ^{iv}	1.384(2)
Ni2—O6 ⁱ	2.0231(10)	C9—C10	1.389(2)
Ni2—O1 ⁱ	2.0881(10)	C10—C12	1.384(2)
Ni2—O1	2.0881(10)	C11—C9 ⁱⁱ	1.384(2)
O1—C5	1.2800(18)	C12—C2 ^{iv}	1.388(2)
O2—C4	1.261(2)	C16—N1	1.304(3)
O3—C6	1.263(2)	C17—N1	1.439(3)
O4—C4	1.242(2)	C18—N1	1.451(3)
O5—C5	1.250(2)	C19—N2	1.333(12)
O6—C6	1.2462(18)	C20—N2	1.459(13)
O7—C16	1.231(2)	C21—N2	1.409(14)
O8—C19	1.104(5)	C22—N3	1.302(8)
O8—C22	1.225(3)	C23—N3	1.458(7)
C1—C11	1.384(2)	C24—N3	1.450(9)

Atoms 1,2,3	Angle 1,2,3 [°]	Atoms 1,2,3	Angle 1,2,3 [°]
O3—Ni1—O2	96.77(5)	C16—O7—Ni1	124.22(12)

Table A3.2 continued

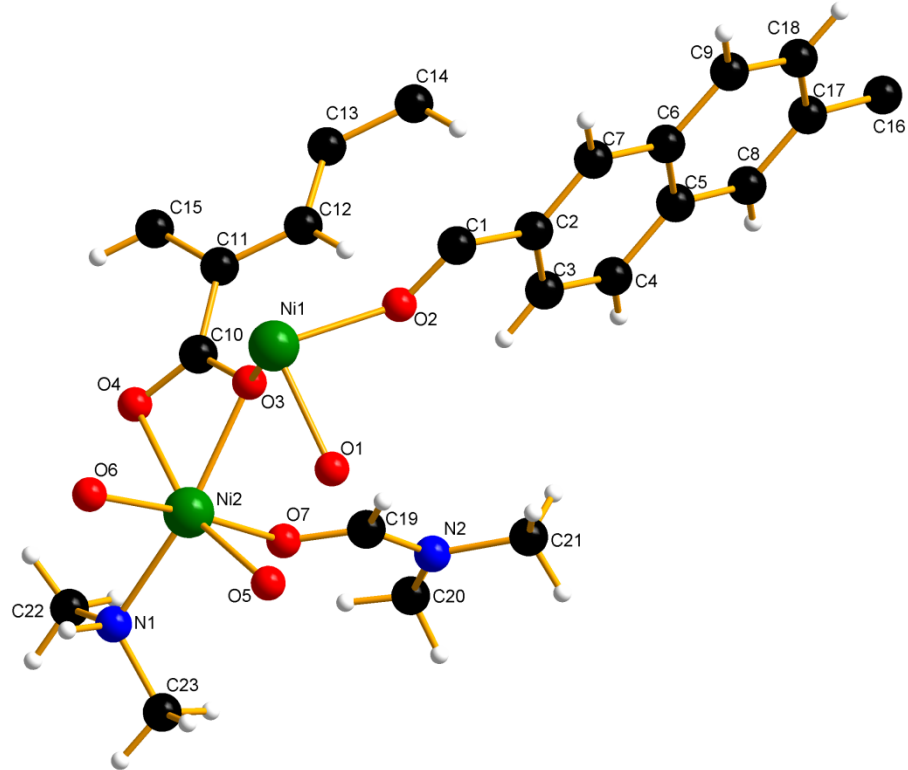
O3—Ni1—O7	99.07(5)	C19—O8—C22	52.8(3)
O2—Ni1—O7	89.05(5)	C19—O8—Ni1	122.0(3)
O3—Ni1—O1	99.24(4)	C22—O8—Ni1	125.62(17)
O2—Ni1—O1	98.91(5)	C11—C1—C2	119.09(15)
O7—Ni1—O1	158.99(5)	C11—C1—C6	119.46(14)
O3—Ni1—O8	85.97(5)	C2—C1—C6	121.39(15)
O2—Ni1—O8	174.48(5)	C1—C2—C12 ⁱⁱ	120.09(16)
O7—Ni1—O8	85.78(5)	C8 ⁱⁱⁱ —C3—C7	120.36(17)
O1—Ni1—O8	85.32(5)	O4—C4—O2	127.33(15)
O3—Ni1—O5	159.98(5)	O4—C4—C10	115.75(14)
O2—Ni1—O5	92.57(5)	O2—C4—C10	116.92(14)
O7—Ni1—O5	98.75(5)	O5—C5—O1	119.29(15)
O1—Ni1—O5	61.71(4)	O5—C5—C7	120.59(14)
O8—Ni1—O5	86.31(5)	O1—C5—C7	119.96(15)
O3—Ni1—C5	129.89(5)	O5—C5—Ni1	62.02(8)
O2—Ni1—C5	98.90(5)	O1—C5—Ni1	57.71(8)
O7—Ni1—C5	128.36(5)	C7—C5—Ni1	169.27(12)
O1—Ni1—C5	31.35(5)	O6—C6—O3	126.75(14)
O8—Ni1—C5	82.86(5)	O6—C6—C1	116.31(14)
O5—Ni1—C5	30.51(5)	O3—C6—C1	116.93(13)
O4—Ni2—O4 ⁱ	180.000	C8—C7—C3	119.72(16)
O4—Ni2—O6	93.89(5)	C8—C7—C5	119.92(15)
O4 ⁱ —Ni2—O6	86.11(5)	C3—C7—C5	120.29(16)
O4—Ni2—O6 ⁱ	86.11(5)	C3 ⁱⁱⁱ —C8—C7	119.92(16)
O4 ⁱ —Ni2—O6 ⁱ	93.89(5)	C11 ^{iv} —C9—C10	120.46(17)
O6—Ni2—O6 ⁱ	180.000	C12—C10—C9	118.76(15)
O4—Ni2—O1 ⁱ	88.52(5)	C12—C10—C4	121.94(14)
O4 ⁱ —Ni2—O1 ⁱ	91.48(5)	C9—C10—C4	119.27(15)
O6—Ni2—O1 ⁱ	90.64(4)	C1—C11—C9 ⁱⁱ	120.69(16)
O6 ⁱ —Ni2—O1 ⁱ	89.36(4)	C10—C12—C2 ^{iv}	120.88(15)
O4—Ni2—O1	91.48(5)	O7—C16—N1	125.49(19)
O4 ⁱ —Ni2—O1	88.52(5)	C16—N1—C17	120.68(19)
O6—Ni2—O1	89.36(4)	C16—N1—C18	122.8(2)
O6 ⁱ —Ni2—O1	90.64(4)	C17—N1—C18	116.5(2)
O1 ⁱ —Ni2—O1	180.00(6)	O8—C19—N2	127.2(7)
C5—O1—Ni1	90.95(10)	C19—N2—C21	123.3(10)

Table A3.2 continued

C5—O1—Ni2	131.18(10)	C19—N2—C20	118.9(9)
Ni1—O1—Ni2	111.56(5)	C21—N2—C20	117.9(9)
C4—O2—Ni1	130.26(11)	O8—C22—N3	129.2(4)
C6—O3—Ni1	121.19(10)	C22—N3—C24	119.0(5)
C4—O4—Ni2	134.77(11)	C22—N3—C23	123.4(6)
C5—O5—Ni1	87.47(9)	C24—N3—C23	117.5(6)
C6—O6—Ni2	139.33(10)		

Symmetry codes : (i) 1-x, 1-y, -z; (ii) -0.5+x, 0.5-y, -0.5+z; (iii) 1-x, 2-y, -z;
(iv) 0.5+x, 0.5-y, 0.5+z.

A3.5. Structural Details for $\text{Ni}_3(2,6\text{-NDC})_3(\text{DMF})_2(\text{DMA})_2$ (**3-3**).



The asymmetric unit contains two nickel centers; Ni1 is surrounded by six oxygens from carboxylate groups of the 2,6-NDC linker, while Ni2 is surrounded by four oxygen atoms from the bridging carboxylates of the linker, an oxygen from DMF, and nitrogen of DMA completing the octahedron around each nickel center. All hydrogen atoms are placed in calculated positions, in riding modes. No disorder is modeled in the structure.

A3.6. Crystallographic Information File for $\text{Ni}_3(2,6\text{-NDC})_3(\text{DMF})_2(\text{DMA})_2$ (**3-3**).

data_COMPOUND_3_mc3061c

_audit_creation_method
_chemical_name_systematic

SHELXL-97

```

;
?
;
_chemical_name_common ?
_chemical_melting_point ?
_chemical_formula_moiety ?
_chemical_formula_sum
'C46 H46 N4 Ni3 O14'
_chemical_formula_weight 1055.00

loop_
_atom_type_symbol
_atom_type_description
_atom_type_scat_dispersion_real
_atom_type_scat_dispersion_imag
_atom_type_scat_source
'C' 'C' 0.0033 0.0016
'International Tables Vol C Tables 4.2.6.8 and 6.1.1.4'
'N' 'N' 0.0061 0.0033
'International Tables Vol C Tables 4.2.6.8 and 6.1.1.4'
'O' 'O' 0.0106 0.0060
'International Tables Vol C Tables 4.2.6.8 and 6.1.1.4'
'Ni' 'Ni' 0.3393 1.1124
'International Tables Vol C Tables 4.2.6.8 and 6.1.1.4'
'H' 'H' 0.0000 0.0000
'International Tables Vol C Tables 4.2.6.8 and 6.1.1.4'

_symmetry_cell_setting ?
_symmetry_space_group_name_H-M 'P2(1)/n'

loop_
_symmetry_equiv_pos_as_xyz
'x, y, z'
'-x+1/2, y+1/2, -z+1/2'
'-x, -y, -z'
'x-1/2, -y-1/2, z-1/2'

_cell_length_a 11.3876(8)
_cell_length_b 19.0717(14)
_cell_length_c 11.6655(8)
_cell_angle_alpha 90.00
_cell_angle_beta 115.4840(10)
_cell_angle_gamma 90.00
_cell_volume 2287.0(3)
_cell_formula_units_Z 2
_cell_measurement_temperature 223(2)
_cell_measurement_reflns_used 7075
_cell_measurement_theta_min 2.2
_cell_measurement_theta_max 28.2

_exptl_crystal_description prism
_exptl_crystal_colour green
_exptl_crystal_size_max 0.40
_exptl_crystal_size_mid 0.25
_exptl_crystal_size_min 0.25

```

```

_exptl_crystal_density_meas      ?
_exptl_crystal_density_diffrn   1.532
_exptl_crystal_density_method    'not measured'
_exptl_crystal_F_000            1092
_exptl_absorpt_coefficient_mu   1.294
_exptl_absorpt_correction_type  multi-scan
_exptl_absorpt_correction_T_min 0.702
_exptl_absorpt_correction_T_max 0.727
_exptl_absorpt_process_details  "Blessing,1995"

_exptl_special_details
;
?
;

_diffrn_ambient_temperature      223(2)
_diffrn_radiation_wavelength     0.71073
_diffrn_radiation_type           MoK\`a
_diffrn_radiation_source         'fine-focus sealed tube'
_diffrn_radiation_monochromator   graphite
_diffrn_measurement_device_type   'Bruker ApexII'
_diffrn_measurement_method        'narrow frame'
_diffrn_detector_area_resol_mean  ?
_diffrn_standards_number          ?
_diffrn_standards_interval_count  ?
_diffrn_standards_interval_time   ?
_diffrn_standards_decay_%          ?
_diffrn_reflns_number             13736
_diffrn_reflns_av_R_equivalents   0.0166
_diffrn_reflns_av_sigmaI/netI     0.0213
_diffrn_reflns_limit_h_min        -8
_diffrn_reflns_limit_h_max        14
_diffrn_reflns_limit_k_min        -22
_diffrn_reflns_limit_k_max        25
_diffrn_reflns_limit_l_min        -15
_diffrn_reflns_limit_l_max        15
_diffrn_reflns_theta_min          2.09
_diffrn_reflns_theta_max          28.30
_reflns_number_total              5331
_reflns_number_gt                 4362
_reflns_threshold_expression      >2sigma(I)

_computing_data_collection        ?
_computing_cell_refinement        ?
_computing_data_reduction         ?
_computing_structure_solution     'SHELXS-97 (Sheldrick, 1990)'
_computing_structure_refinement   'SHELXL-97 (Sheldrick, 1997)'
_computing_molecular_graphics     ?
_computing_publication_material   ?

_refine_special_details
;
Refinement of F^2^ against ALL reflections. The weighted R-factor wR
and

```

goodness of fit S are based on F^2 , conventional R-factors R are based on F , with F set to zero for negative F^2 . The threshold expression of $F^2 > 2\text{sigma}(F^2)$ is used only for calculating R-factors(gt) etc. and is not relevant to the choice of reflections for refinement. R-factors based on F^2 are statistically about twice as large as those based on F, and R-factors based on ALL data will be even larger.
 ;

_refine_ls_structure_factor_coef	Fsqd
_refine_ls_matrix_type	full
_refine_ls_weighting_scheme	calc
_refine_ls_weighting_details	'calc w=1/[s^2^(Fo^2^)+(0.0411P)^2^+0.0000P] where P=(Fo^2^+2Fc^2^)/3'
_atom_sites_solution_primary	direct
_atom_sites_solution_secondary	difmap
_atom_sites_solution_hydrogens	geom
_refine_ls_hydrogen_treatment	constr
_refine_ls_extinction_method	none
_refine_ls_extinction_coeff	?
_refine_ls_number_reflns	5331
_refine_ls_number_parameters	308
_refine_ls_number_restraints	0
_refine_ls_R_factor_all	0.0322
_refine_ls_R_factor_gt	0.0246
_refine_ls_wR_factor_ref	0.0721
_refine_ls_wR_factor_gt	0.0696
_refine_ls_goodness_of_fit_ref	1.074
_refine_ls_restrained_S_all	1.074
_refine_ls_shift/su_max	0.002
_refine_ls_shift/su_mean	0.000

loop_

_atom_site_label	
_atom_site_type_symbol	
_atom_site_fract_x	
_atom_site_fract_y	
_atom_site_fract_z	
_atom_site_U_iso_or_equiv	
_atom_site_adp_type	
_atom_site_occupancy	
_atom_site_symmetry_multiplicity	
_atom_site_calc_flag	
_atom_site_refinement_flags	
_atom_site_disorder_assembly	
_atom_site_disorder_group	

C16 C 0.44087(14) 0.41597(7) 0.19413(14) 0.0214(3) Uani 1 1 d . . .

C17 C 0.35164(14) 0.35883(7) 0.19978(14) 0.0233(3) Uani 1 1 d . . .

C18 C 0.25871(16) 0.32948(8) 0.08543(15) 0.0327(4) Uani 1 1 d . . .

H18 H 0.2512 0.3469 0.0081 0.039 Uiso 1 1 calc R . .

C1 C 0.02772(14) 0.10972(7) 0.32172(13) 0.0197(3) Uani 1 1 d . . .
 C2 C 0.11411(14) 0.16933(7) 0.32007(13) 0.0209(3) Uani 1 1 d . . .
 C3 C 0.20374(15) 0.20003(7) 0.43512(14) 0.0255(3) Uani 1 1 d . . .
 H3 H 0.2083 0.1838 0.5121 0.031 Uiso 1 1 calc R . .
 C4 C 0.28323(16) 0.25312(8) 0.43414(14) 0.0283(3) Uani 1 1 d . . .
 H4 H 0.3414 0.2726 0.5107 0.034 Uiso 1 1 calc R . .
 C5 C 0.27903(15) 0.27924(7) 0.31888(13) 0.0222(3) Uani 1 1 d . . .
 C6 C 0.18825(15) 0.24920(7) 0.20304(14) 0.0243(3) Uani 1 1 d . . .
 C7 C 0.10789(14) 0.19364(7) 0.20727(14) 0.0240(3) Uani 1 1 d . . .
 H7 H 0.0496 0.1732 0.1318 0.029 Uiso 1 1 calc R . .
 C8 C 0.36113(15) 0.33381(7) 0.31366(14) 0.0238(3) Uani 1 1 d . . .
 H8 H 0.4226 0.3530 0.3889 0.029 Uiso 1 1 calc R . .
 C9 C 0.18012(17) 0.27615(9) 0.08671(15) 0.0356(4) Uani 1 1 d . . .
 H9 H 0.1204 0.2572 0.0104 0.043 Uiso 1 1 calc R . .
 C10 C 0.29117(14) -0.02846(7) 0.69721(14) 0.0217(3) Uani 1 1 d . . .
 C11 C 0.37644(14) -0.02862(7) 0.62940(14) 0.0227(3) Uani 1 1 d . . .
 C12 C 0.36023(14) 0.02038(8) 0.53832(15) 0.0246(3) Uani 1 1 d . . .
 H12 H 0.2907 0.0515 0.5132 0.030 Uiso 1 1 calc R . .
 C13 C 0.44796(15) 0.02448(8) 0.48141(14) 0.0236(3) Uani 1 1 d . . .
 C14 C 0.43531(15) 0.07576(8) 0.38856(15) 0.0282(3) Uani 1 1 d . . .
 H14 H 0.3690 0.1088 0.3650 0.034 Uiso 1 1 calc R . .
 C15 C 0.48063(15) -0.07706(8) 0.66648(14) 0.0270(3) Uani 1 1 d . . .
 H15 H 0.4918 -0.1101 0.7290 0.032 Uiso 1 1 calc R . .
 C19 C 0.26575(18) 0.13747(8) 0.82640(16) 0.0348(4) Uani 1 1 d . . .
 H19 H 0.1940 0.1363 0.7477 0.042 Uiso 1 1 calc R . .
 C20 C 0.4432(2) 0.20200(11) 0.9839(2) 0.0609(6) Uani 1 1 d . . .
 H20A H 0.4584 0.1575 1.0264 0.091 Uiso 1 1 calc R . .
 H20B H 0.4298 0.2372 1.0360 0.091 Uiso 1 1 calc R . .
 H20C H 0.5173 0.2144 0.9691 0.091 Uiso 1 1 calc R . .
 C21 C 0.2885(3) 0.25976(9) 0.7828(2) 0.0638(6) Uani 1 1 d . . .
 H21A H 0.3550 0.2722 0.7567 0.096 Uiso 1 1 calc R . .
 H21B H 0.2752 0.2979 0.8296 0.096 Uiso 1 1 calc R . .
 H21C H 0.2089 0.2501 0.7093 0.096 Uiso 1 1 calc R . .
 C22 C 0.3502(2) -0.05150(10) 1.08502(17) 0.0498(5) Uani 1 1 d . . .
 H22A H 0.4099 -0.0154 1.0872 0.075 Uiso 1 1 calc R . .
 H22B H 0.3635 -0.0923 1.0440 0.075 Uiso 1 1 calc R . .
 H22C H 0.3648 -0.0632 1.1702 0.075 Uiso 1 1 calc R . .
 C23 C 0.1867(2) 0.02955(11) 1.08461(17) 0.0452(5) Uani 1 1 d . . .
 H23A H 0.2016 0.0127 1.1673 0.068 Uiso 1 1 calc R . .
 H23B H 0.0973 0.0433 1.0392 0.068 Uiso 1 1 calc R . .
 H23C H 0.2418 0.0692 1.0933 0.068 Uiso 1 1 calc R . .
 N1 N 0.21621(14) -0.02639(7) 1.01418(12) 0.0310(3) Uani 1 1 d . . .
 H1 H 0.1642 -0.0631 1.0120 0.037 Uiso 1 1 calc R . .
 N2 N 0.32871(15) 0.19741(7) 0.86342(14) 0.0411(4) Uani 1 1 d . . .
 Ni1 Ni 0.0000 0.0000 0.5000 0.01514(7) Uani 1 2 d S . .
 Ni2 Ni 0.172720(18) -0.004314(8) 0.826841(17) 0.01873(7) Uani 1 1 d . .
 .
 O1 O -0.07196(11) 0.06838(5) 0.58564(10) 0.0296(2) Uani 1 1 d . . .
 O2 O 0.05156(11) 0.08523(5) 0.42837(10) 0.0287(2) Uani 1 1 d . . .
 O3 O 0.18524(10) 0.00726(5) 0.65360(10) 0.0204(2) Uani 1 1 d . . .
 O4 O 0.32726(10) -0.05872(5) 0.80221(10) 0.0291(2) Uani 1 1 d . . .
 O5 O 0.02136(11) 0.05941(5) 0.79831(10) 0.0291(2) Uani 1 1 d . . .
 O6 O 0.05923(10) -0.09087(5) 0.78371(9) 0.0263(2) Uani 1 1 d . . .
 O7 O 0.29574(11) 0.08270(6) 0.88937(10) 0.0337(3) Uani 1 1 d . .

```

loop_
_atom_site_aniso_label
_atom_site_aniso_U_11
_atom_site_aniso_U_22
_atom_site_aniso_U_33
_atom_site_aniso_U_23
_atom_site_aniso_U_13
_atom_site_aniso_U_12
C16 0.0223(7) 0.0184(6) 0.0277(8) 0.0034(5) 0.0148(6) 0.0007(6)
C17 0.0235(8) 0.0213(7) 0.0278(8) 0.0029(6) 0.0136(7) -0.0036(6)
C18 0.0381(10) 0.0349(9) 0.0244(8) 0.0068(6) 0.0125(7) -0.0122(7)
C1 0.0202(7) 0.0159(6) 0.0277(8) 0.0014(5) 0.0148(6) 0.0005(5)
C2 0.0205(7) 0.0169(6) 0.0277(7) 0.0023(5) 0.0126(6) -0.0009(5)
C3 0.0320(9) 0.0248(7) 0.0231(8) 0.0032(6) 0.0149(7) -0.0050(6)
C4 0.0322(9) 0.0308(8) 0.0223(8) -0.0033(6) 0.0121(7) -0.0123(7)
C5 0.0237(7) 0.0211(7) 0.0241(7) 0.0022(6) 0.0125(6) -0.0032(6)
C6 0.0249(8) 0.0233(7) 0.0248(8) 0.0034(6) 0.0107(7) -0.0046(6)
C7 0.0232(8) 0.0234(7) 0.0235(7) 0.0023(6) 0.0083(6) -0.0054(6)
C8 0.0254(8) 0.0239(7) 0.0237(7) -0.0003(6) 0.0120(6) -0.0063(6)
C9 0.0396(10) 0.0388(9) 0.0233(8) 0.0032(7) 0.0086(8) -0.0180(8)
C10 0.0197(7) 0.0221(7) 0.0263(8) -0.0036(6) 0.0128(6) -0.0028(6)
C11 0.0187(7) 0.0269(7) 0.0259(8) -0.0040(6) 0.0128(6) -0.0017(6)
C12 0.0192(7) 0.0294(7) 0.0295(8) -0.0011(6) 0.0144(7) 0.0030(6)
C13 0.0194(7) 0.0285(7) 0.0256(8) -0.0018(6) 0.0123(6) 0.0011(6)
C14 0.0239(8) 0.0317(8) 0.0336(8) 0.0026(7) 0.0168(7) 0.0059(6)
C15 0.0257(8) 0.0304(8) 0.0292(8) 0.0032(6) 0.0160(7) 0.0025(6)
C19 0.0411(10) 0.0336(9) 0.0337(9) -0.0052(7) 0.0197(8) -0.0127(8)
C20 0.0539(14) 0.0483(12) 0.0712(15) -0.0179(10) 0.0180(12) -0.0221(11)
C21 0.0993(19) 0.0337(10) 0.0668(14) 0.0016(9) 0.0437(13) -0.0181(11)
C22 0.0519(12) 0.0537(11) 0.0353(10) 0.0065(8) 0.0109(9) 0.0158(10)
C23 0.0458(12) 0.0622(12) 0.0312(10) -0.0090(9) 0.0201(9) 0.0008(10)
N1 0.0356(8) 0.0322(7) 0.0263(7) -0.0004(6) 0.0144(6) -0.0058(6)
N2 0.0485(10) 0.0309(7) 0.0488(9) -0.0059(6) 0.0255(8) -0.0153(7)
Ni1 0.01770(14) 0.01311(13) 0.01922(13) -0.00046(8) 0.01232(11) -
0.00047(9)
Ni2 0.01925(11) 0.01782(10) 0.02241(11) -0.00072(7) 0.01209(9) -
0.00049(7)
O1 0.0306(6) 0.0321(6) 0.0285(6) -0.0062(4) 0.0150(5) 0.0110(5)
O2 0.0332(6) 0.0249(5) 0.0286(6) 0.0050(4) 0.0138(5) -0.0101(5)
O3 0.0176(5) 0.0233(5) 0.0242(5) -0.0017(4) 0.0125(4) -0.0001(4)
O4 0.0273(6) 0.0354(6) 0.0310(6) 0.0072(5) 0.0184(5) 0.0067(5)
O5 0.0335(6) 0.0300(6) 0.0286(6) 0.0029(4) 0.0180(5) 0.0123(5)
O6 0.0285(6) 0.0235(5) 0.0276(6) 0.0007(4) 0.0127(5) -0.0086(4)
O7 0.0372(7) 0.0285(6) 0.0356(6) -0.0033(5) 0.0160(5) -0.0095(5)

_geom_special_details
;
All esds (except the esd in the dihedral angle between two l.s.
planes)
are estimated using the full covariance matrix. The cell esds are
taken
into account individually in the estimation of esds in distances,
angles
and torsion angles; correlations between esds in cell parameters are
only

```

used when they are defined by crystal symmetry. An approximate
 (isotropic)
 treatment of cell esds is used for estimating esds involving l.s.
 planes.
;

loop_
 $_geom_bond_atom_site_label_1$
 $_geom_bond_atom_site_label_2$
 $_geom_bond_distance$
 $_geom_bond_site_symmetry_2$
 $_geom_bond_publ_flag$
C16 O1 1.2463(17) 4_665 ?
C16 O5 1.2566(17) 4_665 ?
C16 C17 1.5107(19) . ?
C17 C8 1.3714(19) . ?
C17 C18 1.413(2) . ?
C18 C9 1.359(2) . ?
C1 O2 1.2446(16) . ?
C1 O6 1.2547(16) 3_556 ?
C1 C2 1.5089(18) . ?
C2 C7 1.3680(19) . ?
C2 C3 1.4168(19) . ?
C3 C4 1.361(2) . ?
C4 C5 1.415(2) . ?
C5 C8 1.4177(19) . ?
C5 C6 1.422(2) . ?
C6 C7 1.4146(19) . ?
C6 C9 1.417(2) . ?
C10 O4 1.2525(17) . ?
C10 O3 1.2846(18) . ?
C10 C11 1.493(2) . ?
C10 Ni2 2.4645(15) . ?
C11 C12 1.367(2) . ?
C11 C15 1.417(2) . ?
C12 C13 1.420(2) . ?
C13 C14 1.420(2) . ?
C13 C13 1.422(3) 3_656 ?
C14 C15 1.363(2) 3_656 ?
C15 C14 1.363(2) 3_656 ?
C19 O7 1.2375(19) . ?
C19 N2 1.320(2) . ?
C20 N2 1.452(2) . ?
C21 N2 1.462(2) . ?
C22 N1 1.468(2) . ?
C23 N1 1.471(2) . ?
N1 Ni2 2.0658(13) . ?
Ni1 O1 2.0185(10) . ?
Ni1 O1 2.0185(10) 3_556 ?
Ni1 O2 2.0267(9) 3_556 ?
Ni1 O2 2.0267(9) . ?
Ni1 O3 2.1041(10) 3_556 ?
Ni1 O3 2.1041(10) . ?
Ni2 O5 2.0161(10) . ?
Ni2 O6 2.0222(10) . ?

```

Ni2 O7 2.0902(11) . ?
Ni2 O3 2.0979(10) . ?
Ni2 O4 2.1660(10) . ?
O1 C16 1.2463(17) 4_566 ?
O5 C16 1.2566(16) 4_566 ?
O6 C1 1.2547(16) 3_556 ?

loop_
_geom_angle_atom_site_label_1
_geom_angle_atom_site_label_2
_geom_angle_atom_site_label_3
_geom_angle
_geom_angle_site_symmetry_1
_geom_angle_site_symmetry_3
_geom_angle_publ_flag
O1 C16 O5 127.64(13) 4_665 4_665 ?
O1 C16 C17 115.46(13) 4_665 . ?
O5 C16 C17 116.86(12) 4_665 . ?
C8 C17 C18 119.43(13) . . ?
C8 C17 C16 121.27(13) . . ?
C18 C17 C16 119.28(13) . . ?
C9 C18 C17 121.01(14) . . ?
O2 C1 O6 127.81(13) . 3_556 ?
O2 C1 C2 115.62(12) . . ?
O6 C1 C2 116.57(12) 3_556 . ?
C7 C2 C3 119.28(13) . . ?
C7 C2 C1 120.23(13) . . ?
C3 C2 C1 120.48(12) . . ?
C4 C3 C2 120.66(13) . . ?
C3 C4 C5 121.26(14) . . ?
C4 C5 C8 123.08(13) . . ?
C4 C5 C6 118.34(13) . . ?
C8 C5 C6 118.58(13) . . ?
C7 C6 C9 121.91(14) . . ?
C7 C6 C5 119.04(13) . . ?
C9 C6 C5 119.04(13) . . ?
C2 C7 C6 121.39(14) . . ?
C17 C8 C5 121.23(13) . . ?
C18 C9 C6 120.68(14) . . ?
O4 C10 O3 119.25(13) . . ?
O4 C10 C11 120.17(13) . . ?
O3 C10 C11 120.34(13) . . ?
O4 C10 Ni2 61.44(8) . . ?
O3 C10 Ni2 58.34(7) . . ?
C11 C10 Ni2 167.91(10) . . ?
C12 C11 C15 119.91(14) . . ?
C12 C11 C10 120.63(13) . . ?
C15 C11 C10 119.32(13) . . ?
C11 C12 C13 120.95(14) . . ?
C12 C13 C14 122.26(14) . . ?
C12 C13 C13 118.89(17) . 3_656 ?
C14 C13 C13 118.85(17) . 3_656 ?
C15 C14 C13 120.70(14) 3_656 . ?
C14 C15 C11 120.66(14) 3_656 . ?
O7 C19 N2 124.39(16) . . ?

```

C22 N1 C23 110.75(14) . . ?
 C22 N1 Ni2 112.34(11) . . ?
 C23 N1 Ni2 115.76(11) . . ?
 C19 N2 C20 120.29(16) . . ?
 C19 N2 C21 121.24(17) . . ?
 C20 N2 C21 118.43(16) . . ?
 O1 Ni1 O1 180.0 . 3_556 ?
 O1 Ni1 O2 93.60(5) . 3_556 ?
 O1 Ni1 O2 86.40(5) 3_556 3_556 ?
 O1 Ni1 O2 86.40(5) . . ?
 O1 Ni1 O2 93.60(5) 3_556 . ?
 O2 Ni1 O2 180.00(3) 3_556 . ?
 O1 Ni1 O3 89.56(4) . 3_556 ?
 O1 Ni1 O3 90.44(4) 3_556 3_556 ?
 O2 Ni1 O3 86.34(4) 3_556 3_556 ?
 O2 Ni1 O3 93.66(4) . 3_556 ?
 O1 Ni1 O3 90.44(4) . . ?
 O1 Ni1 O3 89.56(4) 3_556 . ?
 O2 Ni1 O3 93.66(4) 3_556 . ?
 O2 Ni1 O3 86.34(4) . . ?
 O3 Ni1 O3 180.0 3_556 . ?
 O5 Ni2 O6 92.38(4) . . ?
 O5 Ni2 N1 95.52(5) . . ?
 O6 Ni2 N1 86.19(5) . . ?
 O5 Ni2 O7 88.63(5) . . ?
 O6 Ni2 O7 174.62(4) . . ?
 N1 Ni2 O7 88.46(5) . . ?
 O5 Ni2 O3 100.67(4) . . ?
 O6 Ni2 O3 98.47(4) . . ?
 N1 Ni2 O3 162.91(5) . . ?
 O7 Ni2 O3 86.53(4) . . ?
 O5 Ni2 O4 162.28(4) . . ?
 O6 Ni2 O4 92.56(4) . . ?
 N1 Ni2 O4 101.78(5) . . ?
 O7 Ni2 O4 88.04(4) . . ?
 O3 Ni2 O4 61.75(4) . . ?
 O5 Ni2 C10 131.77(5) . . ?
 O6 Ni2 C10 98.90(4) . . ?
 N1 Ni2 C10 131.74(5) . . ?
 O7 Ni2 C10 84.31(5) . . ?
 O3 Ni2 C10 31.42(4) . . ?
 O4 Ni2 C10 30.53(4) . . ?
 C16 O1 Ni1 139.65(10) 4_566 . ?
 C1 O2 Ni1 137.38(9) . . ?
 C10 O3 Ni2 90.24(8) . . ?
 C10 O3 Ni1 136.79(9) . . ?
 Ni2 O3 Ni1 110.77(5) . . ?
 C10 O4 Ni2 88.03(8) . . ?
 C16 O5 Ni2 126.94(9) 4_566 . ?
 C1 O6 Ni2 128.91(9) 3_556 . ?
 C19 O7 Ni2 119.38(11) . . ?

 _diffrn_measured_fraction_theta_max 0.936
 _diffrn_reflns_theta_full 25.50
 _diffrn_measured_fraction_theta_full 0.999

_refine_diff_density_max	0.411
_refine_diff_density_min	-0.350
_refine_diff_density_rms	0.049

Table A3.3. Selected interatomic distances and angles for

Ni₃(2,6-NDC)₃(DMF)₂(DMA)₂ (**3-3**).

Atoms 1,2	d 1,2 [Å]	Atoms 1,2	d 1,2 [Å]
C16—O1 ⁱ	1.2463(17)	C13—C13 ⁱⁱⁱ	1.422(3)
C16—O5 ⁱ	1.2566(17)	C14—C15 ⁱⁱⁱ	1.363(2)
C16—C17	1.5107(19)	C15—C14 ⁱⁱⁱ	1.363(2)
C17—C8	1.3714(19)	C19—O7	1.2375(19)
C17—C18	1.413(2)	C19—N2	1.320(2)
C18—C9	1.359(2)	C20—N2	1.452(2)
C1—O2	1.2446(16)	C21—N2	1.462(2)
C1—O6 ⁱⁱ	1.2547(16)	C22—N1	1.468(2)
C1—C2	1.5089(18)	C23—N1	1.471(2)
C2—C7	1.3680(19)	N1—Ni2	2.0658(13)
C2—C3	1.4168(19)	Ni1—O1	2.0185(10)
C3—C4	1.361(2)	Ni1—O1 ⁱⁱ	2.0185(10)
C4—C5	1.415(2)	Ni1—O2 ⁱⁱ	2.0267(9)
C5—C8	1.4177(19)	Ni1—O2	2.0267(9)
C5—C6	1.422(2)	Ni1—O3 ⁱⁱ	2.1041(10)
C6—C7	1.4146(19)	Ni1—O3	2.1041(10)
C6—C9	1.417(2)	Ni2—O5	2.0161(10)
C10—O4	1.2525(17)	Ni2—O6	2.0222(10)
C10—O3	1.2846(18)	Ni2—O7	2.0902(11)
C10—C11	1.493(2)	Ni2—O3	2.0979(10)
C10—Ni2	2.4645(15)	Ni2—O4	2.166(1)
C11—C12	1.367(2)	O1—C16 ^{iv}	1.2463(17)
C11—C15	1.417(2)	O5—C16 ^{iv}	1.2566(16)
C12—C13	1.420(2)	O6—C1 ⁱⁱ	1.2547(16)
C13—C14	1.420(2)		

Atoms 1,2,3	Angle 1,2,3 [°]	Atoms 1,2,3	Angle 1,2,3 [°]
O1 ⁱ —C16—O5 ⁱ	127.64(13)	O1—Ni1—O1 ⁱⁱ	180.000

Table A3.3 continued

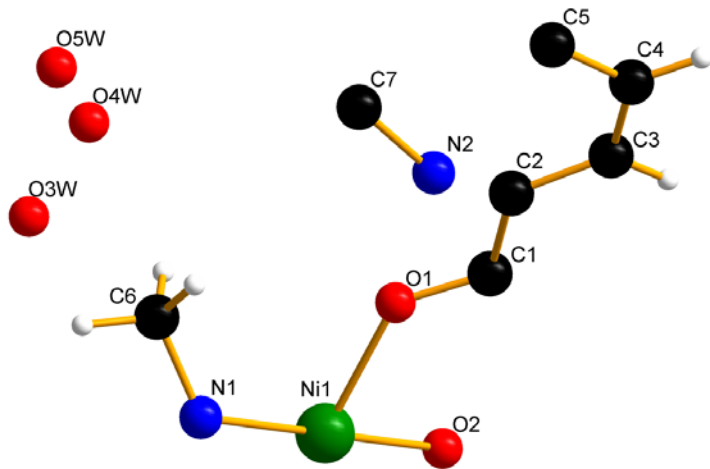
O1 ⁱ —C16—C17	115.46(13)	O1—Ni1—O2 ⁱⁱ	93.60(5)
O5 ⁱ —C16—C17	116.86(12)	O1 ⁱⁱ —Ni1—O2 ⁱⁱ	86.40(5)
C8—C17—C18	119.43(13)	O1—Ni1—O2	86.40(5)
C8—C17—C16	121.27(13)	O1 ⁱⁱ —Ni1—O2	93.60(5)
C18—C17—C16	119.28(13)	O2 ⁱⁱ —Ni1—O2	180.00(3)
C9—C18—C17	121.01(14)	O1—Ni1—O3 ⁱⁱ	89.56(4)
O2—C1—O6 ⁱⁱ	127.81(13)	O1 ⁱⁱ —Ni1—O3 ⁱⁱ	90.44(4)
O2—C1—C2	115.62(12)	O2 ⁱⁱ —Ni1—O3 ⁱⁱ	86.34(4)
O6 ⁱⁱ —C1—C2	116.57(12)	O2—Ni1—O3 ⁱⁱ	93.66(4)
C7—C2—C3	119.28(13)	O1—Ni1—O3	90.44(4)
C7—C2—C1	120.23(13)	O1 ⁱⁱ —Ni1—O3	89.56(4)
C3—C2—C1	120.48(12)	O2 ⁱⁱ —Ni1—O3	93.66(4)
C4—C3—C2	120.66(13)	O2—Ni1—O3	86.34(4)
C3—C4—C5	121.26(14)	O3 ⁱⁱ —Ni1—O3	180.000
C4—C5—C8	123.08(13)	O5—Ni2—O6	92.38(4)
C4—C5—C6	118.34(13)	O5—Ni2—N1	95.52(5)
C8—C5—C6	118.58(13)	O6—Ni2—N1	86.19(5)
C7—C6—C9	121.91(14)	O5—Ni2—O7	88.63(5)
C7—C6—C5	119.04(13)	O6—Ni2—O7	174.62(4)
C9—C6—C5	119.04(13)	N1—Ni2—O7	88.46(5)
C2—C7—C6	121.39(14)	O5—Ni2—O3	100.67(4)
C17—C8—C5	121.23(13)	O6—Ni2—O3	98.47(4)
C18—C9—C6	120.68(14)	N1—Ni2—O3	162.91(5)
O4—C10—O3	119.25(13)	O7—Ni2—O3	86.53(4)
O4—C10—C11	120.17(13)	O5—Ni2—O4	162.28(4)
O3—C10—C11	120.34(13)	O6—Ni2—O4	92.56(4)
O4—C10—Ni2	61.44(8)	N1—Ni2—O4	101.78(5)
O3—C10—Ni2	58.34(7)	O7—Ni2—O4	88.04(4)
C11—C10—Ni2	167.91(10)	O3—Ni2—O4	61.75(4)
C12—C11—C15	119.91(14)	O5—Ni2—C10	131.77(5)
C12—C11—C10	120.63(13)	O6—Ni2—C10	98.90(4)
C15—C11—C10	119.32(13)	N1—Ni2—C10	131.74(5)
C11—C12—C13	120.95(14)	O7—Ni2—C10	84.31(5)
C12—C13—C14	122.26(14)	O3—Ni2—C10	31.42(4)
C12—C13—C13 ⁱⁱⁱ	118.89(17)	O4—Ni2—C10	30.53(4)
C14—C13—C13 ⁱⁱⁱ	118.85(17)	C16 ^{iv} —O1—Ni1	139.65(10)

Table A3.3 continued

C15 ⁱⁱⁱ —C14—C13	120.70(14)	C1—O2—Ni1	137.38(9)
C14 ⁱⁱⁱ —C15—C11	120.66(14)	C10—O3—Ni2	90.24(8)
O7—C19—N2	124.39(16)	C10—O3—Ni1	136.79(9)
C22—N1—C23	110.75(14)	Ni2—O3—Ni1	110.77(5)
C22—N1—Ni2	112.34(11)	C10—O4—Ni2	88.03(8)
C23—N1—Ni2	115.76(11)	C16 ^{iv} —O5—Ni2	126.94(9)
C19—N2—C20	120.29(16)	C1 ⁱⁱ —O6—Ni2	128.91(9)
C19—N2—C21	121.24(17)	C19—O7—Ni2	119.38(11)
C20—N2—C21	118.43(16)		

Symmetry codes : (i) 0.5+x, 0.5-y, -0.5+z; (ii) -x, -y, 1-z; (iii) 1-x, -y, 1-z;
 (iv) -0.5+x, 0.5-y, 0.5+z.

A3.7. Structural Details for $\text{Ni}_3(\mu_3\text{-O})(4,4'\text{-BPDC})_3(\text{DMA})_3$ (**3-4**).



The asymmetric unit contains a nickel center surrounded by five oxygens (one μ_3 -oxo and four oxygens from the 4,4'-BPDC linker) and one nitrogen from coordinated DMA. Water and dimethylamine solvent molecules are located as guests in the structure. All hydrogen atoms are placed in calculated positions, in riding modes. Disordered guests, water and diethylamine are modeled in the structure.

A3.8. Crystallographic Information File for $\text{Ni}_3(\mu_3\text{-O})(4,4'\text{-BPDC})_3(\text{DMA})_3$ (**3-4**).

```
data_COMPOUND_4_mc3075a
_audit_creation_method                               SHELXL-97
_chemical_name_systematic
;
?
;
_chemical_name_common                               ?
_chemical_melting_point                           ?
_chemical_formula_moiety                         ?
_chemical_formula_sum                            'C50 H59 N4 Ni3 O16.50'
```

```

_chemical_formula_weight          1156.14

loop_
_atom_type_symbol
_atom_type_description
_atom_type_scat_dispersion_real
_atom_type_scat_dispersion_imag
_atom_type_scat_source
'C'   'C'   0.0033  0.0016
'International Tables Vol C Tables 4.2.6.8 and 6.1.1.4'
'O'   'O'   0.0106  0.0060
'International Tables Vol C Tables 4.2.6.8 and 6.1.1.4'
'Ni'   'Ni'   0.3393  1.1124
'International Tables Vol C Tables 4.2.6.8 and 6.1.1.4'
'N'   'N'   0.0061  0.0033
'International Tables Vol C Tables 4.2.6.8 and 6.1.1.4'
'H'   'H'   0.0000  0.0000
'International Tables Vol C Tables 4.2.6.8 and 6.1.1.4'

_symmetry_cell_setting      ?
_symmetry_space_group_name_H-M    'P6(3)/mcm'

loop_
_symmetry_equiv_pos_as_xyz
'x, y, z'
'-y, x-y, z'
'-x+y, -x, z'
'-x, -y, z+1/2'
'y, -x+y, z+1/2'
'x-y, x, z+1/2'
'y, x, -z+1/2'
'x-y, -y, -z+1/2'
'-x, -x+y, -z+1/2'
'-y, -x, -z'
'-x+y, y, -z'
'x, x-y, -z'
'-x, -y, -z'
'y, -x+y, -z'
'x-y, x, -z'
'x, y, -z-1/2'
'-y, x-y, -z-1/2'
'-x+y, -x, -z-1/2'
'-y, -x, z-1/2'
'-x+y, y, z-1/2'
'x, x-y, z-1/2'
'y, x, z'
'x-y, -y, z'
'-x, -x+y, z'

_cell_length_a              14.2577(9)
_cell_length_b              14.2577(9)
_cell_length_c              17.3594(11)
_cell_angle_alpha            90.00
_cell_angle_beta             90.00
_cell_angle_gamma            120.00

```

_cell_volume	3056.1(3)
_cell_formula_units_Z	2
_cell_measurement_temperature	223(2)
_cell_measurement_reflns_used	9932
_cell_measurement_theta_min	2.35
_cell_measurement_theta_max	28.24
_exptl_crystal_description	prism
_exptl_crystal_colour	green
_exptl_crystal_size_max	0.55
_exptl_crystal_size_mid	0.23
_exptl_crystal_size_min	0.18
_exptl_crystal_density_meas	?
_exptl_crystal_density_diffrrn	1.256
_exptl_crystal_density_method	'not measured'
_exptl_crystal_F_000	1206
_exptl_absorpt_coefficient_mu	0.977
_exptl_absorpt_correction_type	multi-scan
_exptl_absorpt_correction_T_min	0.497
_exptl_absorpt_correction_T_max	0.545
_exptl_absorpt_process_details	"Blessing,1995"
_exptl_special_details	
;	
?	
;	
_diffrrn_ambient_temperature	223(2)
_diffrrn_radiation_wavelength	0.71073
_diffrrn_radiation_type	MoK\alpha
_diffrrn_radiation_source	'fine-focus sealed tube'
_diffrrn_radiation_monochromator	graphite
_diffrrn_measurement_device_type	'Bruker-ApexII'
_diffrrn_measurement_method	'narrow frame'
_diffrrn_detector_area_resol_mean	?
_diffrrn_standards_number	?
_diffrrn_standards_interval_count	?
_diffrrn_standards_interval_time	?
_diffrrn_standards_decay_%	?
_diffrrn_reflns_number	18243
_diffrrn_reflns_av_R_equivalents	0.0261
_diffrrn_reflns_av_sigmaI/netI	0.0100
_diffrrn_reflns_limit_h_min	-18
_diffrrn_reflns_limit_h_max	16
_diffrrn_reflns_limit_k_min	-18
_diffrrn_reflns_limit_k_max	15
_diffrrn_reflns_limit_l_min	-20
_diffrrn_reflns_limit_l_max	21
_diffrrn_reflns_theta_min	2.86
_diffrrn_reflns_theta_max	28.27
_reflns_number_total	1359
_reflns_number_gt	1208
_reflns_threshold_expression	>2sigma(I)
_computing_data_collection	?

```

_computing_cell_refinement      ?
_computing_data_reduction      ?
_computing_structure_solution   'SHELXS-97 (Sheldrick, 1990)'
_computing_structure_refinement 'SHELXL-97 (Sheldrick, 1997)'
_computing_molecular_graphics  ?
_computing_publication_material ?

_refine_special_details
;
    Refinement of F^2^ against ALL reflections. The weighted R-factor wR
and
    goodness of fit S are based on F^2^, conventional R-factors R are
based
    on F, with F set to zero for negative F^2^. The threshold expression
of
    F^2^ > 2sigma(F^2^) is used only for calculating R-factors(gt) etc.
and is
    not relevant to the choice of reflections for refinement. R-factors
based
    on F^2^ are statistically about twice as large as those based on F,
and R-
    factors based on ALL data will be even larger.
;

_refine_ls_structure_factor_coef  Fsqd
_refine_ls_matrix_type            full
_refine_ls_weighting_scheme       calc
_refine_ls_weighting_details
    'calc w=1/[\s^2^(Fo^2^)+(0.0939P)^2^+3.5425P] where
P=(Fo^2^+2Fc^2^)/3'
_refine_ls_atom_sites_solution_primary direct
_refine_ls_atom_sites_solution_secondary difmap
_refine_ls_atom_sites_solution_hydrogens geom
_refine_ls_refinement_hydrogen_treatment constr
_refine_ls_extinction_method     none
_refine_ls_extinction_coeff      ?
_refine_ls_number_reflns          1359
_refine_ls_number_parameters      93
_refine_ls_number_restraints      1
_refine_ls_R_factor_all           0.0574
_refine_ls_R_factor_gt             0.0530
_refine_ls_wR_factor_ref          0.1626
_refine_ls_wR_factor_gt            0.1579
_refine_ls_goodness_of_fit_ref    1.081
_refine_ls_restrained_S_all       1.082
_refine_ls_shift_su_max           0.001
_refine_ls_shift_su_mean          0.000

loop_
_atom_site_label
_atom_site_type_symbol
_atom_site_fract_x
_atom_site_fract_y
_atom_site_fract_z
_atom_site_U_iso_or_equiv

```

```

_atom_site_adp_type
_atom_site_occupancy
_atom_site_symmetry_multiplicity
_atom_site_calc_flag
_atom_site_refinement_flags
_atom_site_disorder_assembly
_atom_site_disorder_group
N1 Ni 0.85909(4) 0.0000 0.2500 0.0321(3) Uani 1 4 d S . .
O2 O 1.0000 0.0000 0.2500 0.0322(12) Uani 1 12 d S . .
O1 O 0.91039(19) 0.1189(2) 0.16787(17) 0.0678(8) Uani 1 1 d . .
C5 C 1.0000 0.4554(3) 0.0216(3) 0.0496(10) Uani 1 2 d S . .
C1 C 1.0000 0.1970(3) 0.1511(2) 0.0397(8) Uani 1 2 d S . .
C2 C 1.0000 0.2864(3) 0.1053(2) 0.0443(9) Uani 1 2 d S . .
C3 C 1.0927(3) 0.3749(4) 0.0834(4) 0.124(3) Uani 1 1 d . .
H3 H 1.1584 0.3803 0.0965 0.149 Uiso 1 1 calc R . .
C4 C 1.0931(4) 0.4582(4) 0.0418(4) 0.126(3) Uani 1 1 d . .
H4 H 1.1590 0.5175 0.0275 0.152 Uiso 1 1 calc R . .
N1 N 0.7100(4) 0.0000 0.2500 0.077(2) Uani 1 4 d S . .
C6 C 0.6608(5) 0.0000 0.1808(5) 0.119(3) Uani 1 2 d S . .
H6A H 0.6813 -0.0338 0.1415 0.178 Uiso 0.50 1 calc PR . .
H6B H 0.6837 0.0732 0.1660 0.178 Uiso 0.50 1 calc PR . .
H6C H 0.5836 -0.0394 0.1870 0.178 Uiso 0.50 1 calc PR . .
N2 N 1.0000 0.0000 0.0495(9) 0.067(4) Uani 0.50 6 d SPD . .
C7 C 0.9127(12) 0.0000 0.0086(12) 0.115(10) Uani 0.33 2 d SPD . .
O3W O 0.299(3) 0.652(9) 0.229(2) 0.12(2) Uani 0.13 1 d P . .
O4W O 0.353(4) 0.720(5) 0.166(3) 0.14(3) Uani 0.09 1 d P . .
O5W O 0.3333 0.6667 0.120(3) 0.099(12) Uani 0.20 3 d SP . .

loop_
_atom_site_aniso_label
_atom_site_aniso_U_11
_atom_site_aniso_U_22
_atom_site_aniso_U_33
_atom_site_aniso_U_23
_atom_site_aniso_U_13
_atom_site_aniso_U_12
N1 0.0270(3) 0.0251(3) 0.0436(4) 0.000 0.000 0.01255(17)
O2 0.0239(15) 0.0239(15) 0.049(3) 0.000 0.000 0.0120(7)
O1 0.0446(13) 0.0562(14) 0.0942(19) 0.0391(13) -0.0056(12) 0.0189(10)
C5 0.055(2) 0.0409(14) 0.058(3) 0.0155(16) 0.000 0.0274(12)
C1 0.0449(19) 0.0380(13) 0.0386(19) 0.0062(12) 0.000 0.0225(10)
C2 0.048(2) 0.0402(14) 0.047(2) 0.0117(14) 0.000 0.0242(10)
C3 0.048(2) 0.091(3) 0.224(6) 0.101(4) 0.001(3) 0.028(2)
C4 0.053(2) 0.088(3) 0.224(7) 0.104(4) 0.008(3) 0.025(2)
N1 0.054(2) 0.101(5) 0.092(5) 0.000 0.000 0.050(3)
C6 0.070(3) 0.134(7) 0.173(8) 0.000 -0.032(4) 0.067(4)
N2 0.073(6) 0.073(6) 0.056(9) 0.000 0.000 0.036(3)
C7 0.134(14) 0.19(3) 0.040(10) 0.000 -0.016(11) 0.096(14)
O3W 0.10(3) 0.12(4) 0.14(5) 0.05(4) 0.01(2) 0.06(4)
O4W 0.05(2) 0.19(6) 0.16(5) 0.04(5) 0.00(3) 0.05(3)
O5W 0.098(18) 0.098(18) 0.10(3) 0.000 0.000 0.049(9)

_geom_special_details
;

```

All esds (except the esd in the dihedral angle between two l.s. planes) are estimated using the full covariance matrix. The cell esds are taken into account individually in the estimation of esds in distances, angles and torsion angles; correlations between esds in cell parameters are only used when they are defined by crystal symmetry. An approximate (isotropic) treatment of cell esds is used for estimating esds involving l.s. planes.
 ;

```

loop_
  _geom_bond_atom_site_label_1
  _geom_bond_atom_site_label_2
  _geom_bond_distance
  _geom_bond_site_symmetry_2
  _geom_bond_publ_flag
  N1 O2 2.0091(6) . ?
  N1 O1 2.049(2) 23 ?
  N1 O1 2.049(2) 16_556 ?
  N1 O1 2.049(2) . ?
  N1 O1 2.049(2) 8 ?
  N1 N1 2.126(6) . ?
  O2 Ni1 2.0091(6) 3_765 ?
  O2 Ni1 2.0091(6) 2_645 ?
  O1 C1 1.239(3) . ?
  C5 C4 1.354(5) . ?
  C5 C4 1.354(5) 24_765 ?
  C5 C5 1.476(7) 13_765 ?
  C1 O1 1.239(3) 24_765 ?
  C1 C2 1.501(5) . ?
  C2 C3 1.348(5) 24_765 ?
  C2 C3 1.348(5) . ?
  C3 C4 1.387(5) . ?
  N1 C6 1.391(8) . ?
  N1 C6 1.391(8) 16_556 ?
  N2 C7 1.433(10) 2_645 ?
  N2 C7 1.433(10) 3_765 ?
  N2 C7 1.433(10) . ?
  N2 C7 1.60(2) 15_545 ?
  N2 C7 1.60(2) 14_665 ?
  N2 C7 1.60(2) 13_755 ?
  N2 N2 1.72(3) 13_755 ?
  C7 C7 1.28(2) 15_545 ?
  C7 C7 1.28(2) 14_665 ?
  C7 N2 1.60(2) 13_755 ?
  O3W O3W 0.72(8) 16_556 ?
  O3W O3W 0.75(5) 3_565 ?
  O3W O3W 0.75(5) 2_665 ?
  O3W O3W 1.04(7) 18_566 ?
  O3W O3W 1.04(7) 17_666 ?
  O3W O4W 1.14(7) 2_665 ?

```

```

O3W O4W 1.42(8) . ?
O3W O4W 1.50(8) 3_565 ?
O4W O5W 1.03(6) . ?
O4W O4W 1.16(11) 2_665 ?
O4W O4W 1.16(11) 3_565 ?
O4W O3W 1.14(7) 3_565 ?
O4W O3W 1.50(8) 2_665 ?
O5W O4W 1.03(6) 2_665 ?
O5W O4W 1.03(6) 3_565 ?

loop_
    _geom_angle_atom_site_label_1
    _geom_angle_atom_site_label_2
    _geom_angle_atom_site_label_3
    _geom_angle
    _geom_angle_site_symmetry_1
    _geom_angle_site_symmetry_3
    _geom_angle_publ_flag
O2 Ni1 O1 93.24(7) . 23 ?
O2 Ni1 O1 93.24(7) . 16_556 ?
O1 Ni1 O1 173.52(14) 23 16_556 ?
O2 Ni1 O1 93.24(7) . . ?
O1 Ni1 O1 91.47(17) 23 . ?
O1 Ni1 O1 88.16(18) 16_556 . ?
O2 Ni1 O1 93.24(7) . 8 ?
O1 Ni1 O1 88.16(18) 23 8 ?
O1 Ni1 O1 91.47(17) 16_556 8 ?
O1 Ni1 O1 173.52(14) . 8 ?
O2 Ni1 N1 180.000(1) . . ?
O1 Ni1 N1 86.76(7) 23 . ?
O1 Ni1 N1 86.76(7) 16_556 . ?
O1 Ni1 N1 86.76(7) . . ?
O1 Ni1 N1 86.76(7) 8 . ?
Ni1 O2 Ni1 120.0 3_765 . ?
Ni1 O2 Ni1 120.0 3_765 2_645 ?
Ni1 O2 Ni1 120.0 . 2_645 ?
C1 O1 Ni1 133.5(2) . . ?
C4 C5 C4 116.2(4) . 24_765 ?
C4 C5 C5 121.9(2) . 13_765 ?
C4 C5 C5 121.9(2) 24_765 13_765 ?
O1 C1 O1 126.5(3) . 24_765 ?
O1 C1 C2 116.76(17) . . ?
O1 C1 C2 116.76(18) 24_765 . ?
C3 C2 C3 116.2(4) 24_765 . ?
C3 C2 C1 121.9(2) 24_765 . ?
C3 C2 C1 121.9(2) . . ?
C2 C3 C4 122.1(4) . . ?
C5 C4 C3 121.7(4) . . ?
C6 N1 C6 119.5(8) . 16_556 ?
C6 N1 Ni1 120.2(4) . . ?
C6 N1 Ni1 120.2(4) 16_556 . ?
C7 N2 C7 97.6(15) 2_645 3_765 ?
C7 N2 C7 97.6(15) 2_645 . ?
C7 N2 C7 97.6(15) 3_765 . ?
C7 N2 C7 49.5(6) 2_645 15_545 ?

```

C7 N2 C7 111.3(15) 3_765 15_545 ?
 C7 N2 C7 49.5(6) . 15_545 ?
 C7 N2 C7 111.3(15) 2_645 14_665 ?
 C7 N2 C7 49.5(6) 3_765 14_665 ?
 C7 N2 C7 49.5(6) . 14_665 ?
 C7 N2 C7 84.6(11) 15_545 14_665 ?
 C7 N2 C7 49.5(6) 2_645 13_755 ?
 C7 N2 C7 49.5(6) 3_765 13_755 ?
 C7 N2 C7 111.3(15) . 13_755 ?
 C7 N2 C7 84.6(11) 15_545 13_755 ?
 C7 N2 C7 84.6(11) 14_665 13_755 ?
 C7 N2 N2 60.3(12) 2_645 13_755 ?
 C7 N2 N2 60.3(12) 3_765 13_755 ?
 C7 N2 N2 60.3(12) . 13_755 ?
 C7 N2 N2 51.0(7) 15_545 13_755 ?
 C7 N2 N2 51.0(7) 14_665 13_755 ?
 C7 N2 N2 51.0(7) 13_755 13_755 ?
 C7 C7 C7 114.7(13) 15_545 14_665 ?
 C7 C7 N2 72.1(7) 15_545 . ?
 C7 C7 N2 72.1(7) 14_665 . ?
 C7 C7 N2 58.4(10) 15_545 13_755 ?
 C7 C7 N2 58.4(10) 14_665 13_755 ?
 N2 C7 N2 68.7(15) . 13_755 ?
 O3W O3W O3W 90.00(4) 16_556 3_565 ?
 O3W O3W O3W 90.00(4) 16_556 2_665 ?
 O3W O3W O3W 60.00(4) 3_565 2_665 ?
 O3W O3W O3W 46(3) 16_556 18_566 ?
 O3W O3W O3W 44(3) 3_565 18_566 ?
 O3W O3W O3W 68.9(12) 2_665 18_566 ?
 O3W O3W O3W 46(3) 16_556 17_666 ?
 O3W O3W O3W 68.9(12) 3_565 17_666 ?
 O3W O3W O3W 44(3) 2_665 17_666 ?
 O3W O3W O3W 42(2) 18_566 17_666 ?
 O3W O3W O4W 166(5) 16_556 2_665 ?
 O3W O3W O4W 104(4) 3_565 2_665 ?
 O3W O3W O4W 95(7) 2_665 2_665 ?
 O3W O3W O4W 148(6) 18_566 2_665 ?
 O3W O3W O4W 138(9) 17_666 2_665 ?
 O3W O3W O4W 141(4) 16_556 . ?
 O3W O3W O4W 53(6) 3_565 . ?
 O3W O3W O4W 82(8) 2_665 . ?
 O3W O3W O4W 96(6) 18_566 . ?
 O3W O3W O4W 116(8) 17_666 . ?
 O4W O3W O4W 53(5) 2_665 . ?
 O3W O3W O4W 137(3) 16_556 3_565 ?
 O3W O3W O4W 69(7) 3_565 3_565 ?
 O3W O3W O4W 47(3) 2_665 3_565 ?
 O3W O3W O4W 104(6) 18_566 3_565 ?
 O3W O3W O4W 91(4) 17_666 3_565 ?
 O4W O3W O4W 50(5) 2_665 3_565 ?
 O4W O3W O4W 47(4) . 3_565 ?
 O5W O4W O4W 56(3) . 2_665 ?
 O5W O4W O4W 56(3) . 3_565 ?
 O4W O4W O4W 60.000(5) 2_665 3_565 ?
 O5W O4W O3W 127(7) . 3_565 ?

O4W O4W O3W 82(4) 2_665 3_565 ?
 O4W O4W O3W 76(5) 3_565 3_565 ?
 O5W O4W O3W 104(6) . .
 O4W O4W O3W 51(4) 2_665 . ?
 O4W O4W O3W 71(5) 3_565 . ?
 O3W O4W O3W 32(3) 3_565 . ?
 O5W O4W O3W 98(6) . 2_665 ?
 O4W O4W O3W 63(5) 2_665 2_665 ?
 O4W O4W O3W 49(2) 3_565 2_665 ?
 O3W O4W O3W 29(3) 3_565 2_665 ?
 O3W O4W O3W 29(3) . 2_665 ?
 O4W O5W O4W 68(6) . 2_665 ?
 O4W O5W O4W 68(6) . 3_565 ?
 O4W O5W O4W 68(6) 2_665 3_565 ?

_diffrn_measured_fraction_theta_max 0.973
 _diffrn_reflns_theta_full 25.50
 _diffrn_measured_fraction_theta_full 0.984
 _refine_diff_density_max 0.433
 _refine_diff_density_min -0.394
 _refine_diff_density_rms 0.097

Table A3.4. Selected interatomic distances and angles for

$\text{Ni}_3(\mu_3\text{-O})(4,4'\text{-BPDC})_3(\text{DMA})_3$ (**3-4**).

Atoms 1,2	d 1,2 [Å]	Atoms 1,2	d 1,2 [Å]
Ni1—O2	2.0091(6)	N2—C7 ^{vii}	1.60(2)
Ni1—O1 ⁱ	2.049(2)	N2—C7 ^{ix}	1.60(2)
Ni1—O1 ⁱⁱ	2.049(2)	N2—C7 ^x	1.60(2)
Ni1—O1	2.049(2)	N2—N2 ^x	1.72(3)
Ni1—O1 ⁱⁱⁱ	2.049(2)	C7—C7 ^{viii}	1.28(2)
Ni1—N1	2.126(6)	C7—C7 ^{ix}	1.28(2)
O2—Ni1 ^{iv}	2.0091(6)	C7—N2 ^x	1.60(2)
O2—Ni1 ^v	2.0091(6)	O3W—O3W ⁱⁱ	0.72(8)
O1—C1	1.239(3)	O3W—O3W ^{xi}	0.75(5)
C5—C4	1.354(5)	O3W—O3W ^{xii}	0.75(5)
C5—C4 ^{vi}	1.354(5)	O3W—O3W ^{xiii}	1.04(7)
C5—C5 ^{vii}	1.476(7)	O3W—O3W ^{xiv}	1.04(7)
C1—O1 ^{vi}	1.239(3)	O3W—O4W ^{xii}	1.14(7)
C1—C2	1.501(5)	O3W—O4W	1.42(8)
C2—C3 ^{vi}	1.348(5)	O3W—O4W ^{xi}	1.50(8)
C2—C3	1.348(5)	O4W—O5W	1.03(6)

Table A3.4 continued

C3—C4	1.387(5)	O4W—O4W ^{xii}	1.16(11)
N1—C6	1.391(8)	O4W—O4W ^{xi}	1.16(11)
N1—C6 ⁱⁱ	1.391(8)	O4W—O3W ^{xi}	1.14(7)
N2—C7 ^v	1.433(10)	O4W—O3W ^{xii}	1.50(8)
N2—C7 ^{iv}	1.433(10)	O5W—O4W ^{xii}	1.03(6)
N2—C7	1.433(10)	O5W—O4W ^{xi}	1.03(6)

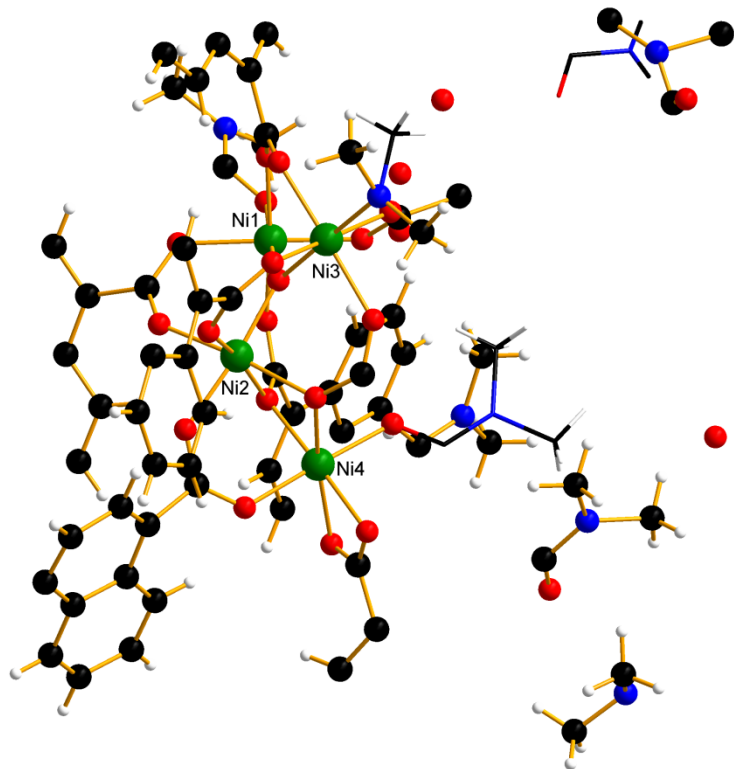
Atoms 1,2,3	Angle 1,2,3 [°]	Atoms 1,2,3	Angle 1,2,3 [°]
O2—Ni1—O1 ⁱ	93.24(7)	C7 ^x —N2—N2 ^x	51.0(7)
O2—Ni1—O1 ⁱⁱ	93.24(7)	C7 ^{viii} —C7—C7 ^{ix}	114.7(13)
O1 ⁱ —Ni1—O1 ⁱⁱ	173.52(14)	C7 ^{viii} —C7—N2	72.1(7)
O2—Ni1—O1	93.24(7)	C7 ^{ix} —C7—N2	72.1(7)
O1 ⁱ —Ni1—O1	91.47(17)	C7 ^{viii} —C7—N2 ^x	58.4(10)
O1 ⁱⁱ —Ni1—O1	88.16(18)	C7 ^{ix} —C7—N2 ^x	58.4(10)
O2—Ni1—O1 ⁱⁱⁱ	93.24(7)	N2—C7—N2 ^x	68.7(15)
O1 ⁱ —Ni1—O1 ⁱⁱⁱ	88.16(18)	O3W ⁱⁱ —O3W—O3W ^{xi}	90.00(4)
O1 ⁱⁱ —Ni1—O1 ⁱⁱⁱ	91.47(17)	O3W ⁱⁱ —O3W—O3W ^{xii}	90.00(4)
O1—Ni1—O1 ⁱⁱⁱ	173.52(14)	O3W ^{xi} —O3W—O3W ^{xii}	60.00(4)
O2—Ni1—N1	180.000(1)	O3W ⁱⁱ —O3W—O3W ^{xiii}	46.(3)
O1 ⁱ —Ni1—N1	86.76(7)	O3W ^{xi} —O3W—O3W ^{xiii}	44.(3)
O1 ⁱⁱ —Ni1—N1	86.76(7)	O3W ^{xii} —O3W—O3W ^{xiii}	68.9(12)
O1—Ni1—N1	86.76(7)	O3W ⁱⁱ —O3W—O3W ^{xiv}	46.(3)
O1 ⁱⁱⁱ —Ni1—N1	86.76(7)	O3W ^{xi} —O3W—O3W ^{xiv}	68.9(12)
Ni1 ^{iv} —O2—Ni1	120.000	O3W ^{xii} —O3W—O3W ^{xiv}	44.(3)
Ni1 ^{iv} —O2—Ni1 ^v	120.000	O3W ^{xiii} —O3W—O3W ^{xiv}	42.(2)
Ni1—O2—Ni1 ^v	120.000	O3W ⁱⁱ —O3W—O4W ^{xii}	166.(5)
C1—O1—Ni1	133.5(2)	O3W ^{xi} —O3W—O4W ^{xii}	104.(4)
C4—C5—C4 ^{vi}	116.2(4)	O3W ^{xii} —O3W—O4W ^{xii}	95.(7)
C4—C5—C5 ^{vii}	121.9(2)	O3W ^{xiii} —O3W—O4W ^{xii}	148.(6)
C4 ^{vi} —C5—C5 ^{vii}	121.9(2)	O3W ^{xiv} —O3W—O4W ^{xii}	138.(9)
O1—C1—O1 ^{vi}	126.5(3)	O3W ⁱⁱ —O3W—O4W	141.(4)
O1—C1—C2	116.76(17)	O3W ^{xi} —O3W—O4W	53.(6)
O1 ^{vi} —C1—C2	116.76(18)	O3W ^{xii} —O3W—O4W	82.(8)
C3 ^{vi} —C2—C3	116.2(4)	O3W ^{xiii} —O3W—O4W	96.(6)
C3 ^{vi} —C2—C1	121.9(2)	O3W ^{xiv} —O3W—O4W	116.(8)
C3—C2—C1	121.9(2)	O4W ^{xii} —O3W—O4W	53.(5)

Table A3.4 continued

C2—C3—C4	122.1(4)	O3W ⁱⁱ —O3W—O4W ^{xi}	137.(3)
C5—C4—C3	121.7(4)	O3W ^{xi} —O3W—O4W ^{xi}	69.(7)
C6—N1—C6 ⁱⁱ	119.5(8)	O3W ^{xii} —O3W—O4W ^{xi}	47.(3)
C6—N1—Ni1	120.2(4)	O3W ^{xiii} —O3W—O4W ^{xi}	104.(6)
C6 ⁱⁱ —N1—Ni1	120.2(4)	O3W ^{xiv} —O3W—O4W ^{xi}	91.(4)
C7 ^v —N2—C7 ^{iv}	97.6(15)	O4W ^{xii} —O3W—O4W ^{xi}	50.(5)
C7 ^v —N2—C7	97.6(15)	O4W—O3W—O4W ^{xi}	47.(4)
C7 ^{iv} —N2—C7	97.6(15)	O5W—O4W—O4W ^{xii}	56.(3)
C7 ^v —N2—C7 ^{viii}	49.5(6)	O5W—O4W—O4W ^{xi}	56.(3)
C7 ^{iv} —N2—C7 ^{viii}	111.3(15)	O4W ^{xii} —O4W—O4W ^{xi}	60.000(5)
C7—N2—C7 ^{viii}	49.5(6)	O5W—O4W—O3W ^{xi}	127.(7)
C7 ^v —N2—C7 ^{ix}	111.3(15)	O4W ^{xii} —O4W—O3W ^{xi}	82.(4)
C7 ^{iv} —N2—C7 ^{ix}	49.5(6)	O4W ^{xi} —O4W—O3W ^{xi}	76.(5)
C7—N2—C7 ^{ix}	49.5(6)	O5W—O4W—O3W	104.(6)
C7 ^{viii} —N2—C7 ^{ix}	84.6(11)	O4W ^{xii} —O4W—O3W	51.(4)
C7 ^v —N2—C7 ^x	49.5(6)	O4W ^{xi} —O4W—O3W	71.(5)
C7 ^{iv} —N2—C7 ^x	49.5(6)	O3W ^{xi} —O4W—O3W	32.(3)
C7—N2—C7 ^x	111.3(15)	O5W—O4W—O3W ^{xii}	98.(6)
C7 ^{viii} —N2—C7 ^x	84.6(11)	O4W ^{xii} —O4W—O3W ^{xii}	63.(5)
C7 ^{ix} —N2—C7 ^x	84.6(11)	O4W ^{xi} —O4W—O3W ^{xii}	49.(2)
C7 ^v —N2—N2 ^x	60.3(12)	O3W ^{xi} —O4W—O3W ^{xii}	29.(3)
C7 ^{iv} —N2—N2 ^x	60.3(12)	O3W—O4W—O3W ^{xii}	29.(3)
C7—N2—N2 ^x	60.3(12)	O4W—O5W—O4W ^{xii}	68.(6)
C7 ^{viii} —N2—N2 ^x	51.0(7)	O4W—O5W—O4W ^{xi}	68.(6)
C7 ^{ix} —N2—N2 ^x	51.0(7)	O4W ^{xii} —O5W—O4W ^{xi}	68.(6)

Symmetry codes : (i) x-y, -y, z; (ii) x, y, 0.5-z; (iii) x-y, -y, 0.5-z;
 (iv) 2-x+y, 1-x, z; (v) 1-y, -1+x-y, z; (vi) 2-x, 1-x+y, z; (vii) 2-x, 1-y, -z;
 (viii) x-y, -1+x, -z; (ix) 1+y, 1-x+y, -z; (x) 2-x, -y, -z; (xi) -x+y, 1-x, z;
 (xii) 1-y, 1+x-y, z; (xiii) -x+y, 1-x, 0.5-z; (xiv) 1-y, 1+x-y, 0.5-z.

A3.9. Structural Details for $\text{Ni}_4(\mu_3\text{-O})(1,4\text{-NDC})_4(\text{DMF})_2(\text{DMA})_2$ (**3-5**).



The asymmetric unit contains four nickel centers; Ni1 is surrounded by six oxygens (one μ_3 -oxo, four from the 1,4-NDC linker, and one from DMF), Ni2 by six oxygens (five from bridging 1,4-NDC linker and one μ_3 -oxo), Ni3 by five oxygens (one μ_3 -oxo and four from the linker) and one nitrogen from DMA, and Ni4 by five oxygens from the linker and one nitrogen from DMA. Water, DMF, and DMA solvent molecules are located as guests in the structure. All hydrogen atoms are placed in calculated positions, in riding modes. Disordered solvent molecules DMF and DMA are modeled in the structure.

A3.10. Crystallographic Information File for $\text{Ni}_4(\mu_3\text{-O})(1,4\text{-NDC})_4(\text{DMF})_2(\text{DMA})_2$
(3-5).

```

data_COMPOUND_5_mc3114d

_audit_creation_method           SHELXL-97
_chemical_name_systematic
;
?
;
_chemical_name_common          ?
_chemical_melting_point        ?
_chemical_formula_moiety       ?
_chemical_formula_sum          'C62.50 H64 N5.50 Ni4 O21.28'
_chemical_formula_weight        1467.48

loop_
_atom_type_symbol
_atom_type_description
_atom_type_scat_dispersion_real
_atom_type_scat_dispersion_imag
_atom_type_scat_source
'C'   'C'   0.0033  0.0016
'International Tables Vol C Tables 4.2.6.8 and 6.1.1.4'
'O'   'O'   0.0106  0.0060
'International Tables Vol C Tables 4.2.6.8 and 6.1.1.4'
'Ni'   'Ni'   0.3393  1.1124
'International Tables Vol C Tables 4.2.6.8 and 6.1.1.4'
'N'   'N'   0.0061  0.0033
'International Tables Vol C Tables 4.2.6.8 and 6.1.1.4'
'H'   'H'   0.0000  0.0000
'International Tables Vol C Tables 4.2.6.8 and 6.1.1.4'

_symmetry_cell_setting          ?
_symmetry_space_group_name_H-M   'R-3'

loop_
_symmetry_equiv_pos_as_xyz
'x, y, z'
'-y, x-y, z'
'-x+y, -x, z'
'x+2/3, y+1/3, z+1/3'
'-y+2/3, x-y+1/3, z+1/3'
'-x+y+2/3, -x+1/3, z+1/3'
'x+1/3, y+2/3, z+2/3'
'-y+1/3, x-y+2/3, z+2/3'
'-x+y+1/3, -x+2/3, z+2/3'
'-x, -y, -z'
'y, -x+y, -z'
'x-y, x, -z'
'-x+2/3, -y+1/3, -z+1/3'

```

```

'y+2/3, -x+y+1/3, -z+1/3'
'x-y+2/3, x+1/3, -z+1/3'
'-x+1/3, -y+2/3, -z+2/3'
'y+1/3, -x+y+2/3, -z+2/3'
'x-y+1/3, x+2/3, -z+2/3'

_cell_length_a          48.857(7)
_cell_length_b          48.857(7)
_cell_length_c          14.858(2)
_cell_angle_alpha        90.00
_cell_angle_beta         90.00
_cell_angle_gamma       120.00
_cell_volume            30713(7)
_cell_formula_units_Z    18
_cell_measurement_temperature 223(2)
_cell_measurement_reflns_used 9965
_cell_measurement_theta_min 2.2
_cell_measurement_theta_max 26.6

_exptl_crystal_description      prism
_exptl_crystal_colour          green
_exptl_crystal_size_max        0.32
_exptl_crystal_size_mid        0.24
_exptl_crystal_size_min        0.20
_exptl_crystal_density_meas     ?
_exptl_crystal_density_diffrn  1.428
_exptl_crystal_density_method   'not measured'
_exptl_crystal_F_000           13675
_exptl_absorpt_coefficient_mu   1.163
_exptl_absorpt_correction_type  multi-scan
_exptl_absorpt_correction_T_min 0.657
_exptl_absorpt_correction_T_max 0.809
_exptl_absorpt_process_details  "Blessing, 1995"

_exptl_special_details
;
?
;

_diffrn_ambient_temperature    223(2)
_diffrn_radiation_wavelength   0.71073
_diffrn_radiation_type          MoK\alpha
_diffrn_radiation_source        'fine-focus sealed tube'
_diffrn_radiation_monochromator graphite
_diffrn_measurement_device_type 'Bruker-ApexII'
_diffrn_measurement_method      'narrow frame'
_diffrn_detector_area_resol_mean ?
_diffrn_standards_number        ?
_diffrn_standards_interval_count ?
_diffrn_standards_interval_time  ?
_diffrn_standards_decay_%       ?
_diffrn_reflns_number          62878
_diffrn_reflns_av_R_equivalents 0.0627
_diffrn_reflns_av_sigmaI/netI   0.0864
_diffrn_reflns_limit_h_min      -65

```

```

_diffrn_reflns_limit_h_max      62
_diffrn_reflns_limit_k_min     -62
_diffrn_reflns_limit_k_max      64
_diffrn_reflns_limit_l_min     -15
_diffrn_reflns_limit_l_max       19
_diffrn_reflns_theta_min        1.67
_diffrn_reflns_theta_max       28.35
_reflns_number_total           16325
_reflns_number_gt              9858
_reflns_threshold_expression    >2\s(I)

_computing_data_collection      ?
_computing_cell_refinement      ?
_computing_data_reduction       ?
_computing_structure_solution    ?
_computing_structure_refinement 'SHELXL-97 (Sheldrick, 2008)'
_computing_molecular_graphics    ?
_computing_publication_material   ?

_refine_special_details
;
  Refinement of F^2^ against ALL reflections. The weighted R-factor wR
and
  goodness of fit S are based on F^2^, conventional R-factors R are
based
  on F, with F set to zero for negative F^2^. The threshold expression
of
  F^2^ > 2\s(F^2^) is used only for calculating R-factors(gt) etc. and
is
  not relevant to the choice of reflections for refinement. R-factors
based
  on F^2^ are statistically about twice as large as those based on F,
and R-
  factors based on ALL data will be even larger.
;

_refine_ls_structure_factor_coef  Fsqd
_refine_ls_matrix_type            full
_refine_ls_weighting_scheme       calc
_refine_ls_weighting_details
  'calc w=1/[\s^2^(Fo^2^)+(0.0753P)^2^+0.0000P] where
P=(Fo^2^+2Fc^2^)/3'
_refine_ls_solution_primary        direct
_refine_ls_solution_secondary      difmap
_refine_ls_solution_hydrogens      geom
_refine_ls_hydrogen_treatment      constr
_refine_ls_extinction_method      none
_refine_ls_extinction_coeff       ?
_refine_ls_number_reflns          16325
_refine_ls_number_parameters       992
_refine_ls_number_restraints       190
_refine_ls_R_factor_all            0.0856
_refine_ls_R_factor_gt             0.0444
_refine_ls_wR_factor_ref           0.1292
_refine_ls_wR_factor_gt            0.1150

```

```

_refine_ls_goodness_of_fit_ref      0.845
_refine_ls_restrained_S_all       0.850
_refine_ls_shift/su_max          0.002
_refine_ls_shift/su_mean          0.000

loop_
_atom_site_label
_atom_site_type_symbol
_atom_site_fract_x
_atom_site_fract_y
_atom_site_fract_z
_atom_site_U_iso_or_equiv
_atom_site_adp_type
_atom_site_occupancy
_atom_site_symmetry_multiplicity
_atom_site_calc_flag
_atom_site_refinement_flags
_atom_site_disorder_assembly
_atom_site_disorder_group

C1 C 0.70638(8) 0.08904(8) 0.1151(2) 0.0257(7) Uani 1 1 d . A 1
C2 C 0.72800(8) 0.07915(8) 0.0724(2) 0.0259(7) Uani 1 1 d . A 1
C3 C 0.76051(8) 0.09228(8) 0.0945(2) 0.0258(7) Uani 1 1 d . A 1
C4 C 0.77486(9) 0.11343(9) 0.1676(3) 0.0385(9) Uani 1 1 d . A 1
H4 H 0.7626 0.1185 0.2045 0.046 Uiso 1 1 calc R A 1
C5 C 0.80654(9) 0.12653(10) 0.1844(3) 0.0500(11) Uani 1 1 d . A 1
H5 H 0.8157 0.1404 0.2325 0.060 Uiso 1 1 calc R A 1
C6 C 0.82531(9) 0.11909(10) 0.1293(3) 0.0509(12) Uani 1 1 d . A 1
H6 H 0.8468 0.1280 0.1413 0.061 Uiso 1 1 calc R A 1
C7 C 0.81247(8) 0.09909(9) 0.0590(3) 0.0393(9) Uani 1 1 d . A 1
H7 H 0.8253 0.0946 0.0232 0.047 Uiso 1 1 calc R A 1
C8 C 0.77972(7) 0.08472(8) 0.0386(2) 0.0263(7) Uani 1 1 d . A 1
C9 C 0.76524(7) 0.06262(7) -0.0332(2) 0.0244(7) Uani 1 1 d . . 1
C10 C 0.73369(7) 0.04810(8) -0.0457(2) 0.0283(8) Uani 1 1 d . A 1
H10 H 0.7241 0.0320 -0.0880 0.034 Uiso 1 1 calc R A 1
C11 C 0.71526(8) 0.05725(8) 0.0054(2) 0.0299(8) Uani 1 1 d . A 1
H11 H 0.6938 0.0481 -0.0070 0.036 Uiso 1 1 calc R A 1
C12 C 0.60972(8) 0.06017(7) 0.2296(2) 0.0240(7) Uani 1 1 d . . 1
C13 C 0.60198(8) 0.04626(8) -0.0182(2) 0.0263(7) Uani 1 1 d . B 1
C14 C 0.59511(7) 0.01855(8) -0.0779(2) 0.0266(8) Uani 1 1 d . B 1
C15 C 0.61100(7) 0.00093(7) -0.0676(2) 0.0248(7) Uani 1 1 d . B 1
C16 C 0.63161(8) 0.00596(8) 0.0057(2) 0.0330(8) Uani 1 1 d . B 1
H16 H 0.6348 0.0209 0.0493 0.040 Uiso 1 1 calc R B 1
C17 C 0.64708(9) -0.01124(9) 0.0129(3) 0.0425(10) Uani 1 1 d . B 1
H17 H 0.6606 -0.0077 0.0610 0.051 Uiso 1 1 calc R B 1
C18 C 0.64240(10) -0.03385(9) -0.0517(3) 0.0437(10) Uani 1 1 d . B 1
H18 H 0.6535 -0.0447 -0.0472 0.052 Uiso 1 1 calc R B 1
C19 C 0.62191(9) -0.04034(8) -0.1212(3) 0.0365(9) Uani 1 1 d . B 1
H19 H 0.6188 -0.0559 -0.1629 0.044 Uiso 1 1 calc R B 1
C20 C 0.60512(8) -0.02349(7) -0.1308(2) 0.0266(7) Uani 1 1 d . B 1
C21 C 0.72066(8) 0.08415(8) 0.4663(2) 0.0269(7) Uani 1 1 d . . 1
C22 C 0.75292(8) 0.09952(8) 0.4600(3) 0.0343(9) Uani 1 1 d . . 1
H22 H 0.7631 0.1145 0.4150 0.041 Uiso 1 1 calc R . 1
C23 C 0.57381(8) 0.01130(8) -0.1457(3) 0.0339(9) Uani 1 1 d . B 1
H23 H 0.5635 0.0228 -0.1517 0.041 Uiso 1 1 calc R B 1
C24 C 0.70355(8) 0.09220(8) 0.3971(2) 0.0272(8) Uani 1 1 d . C 1

```

C25 C 0.57061(8) 0.12488(8) -0.0367(2) 0.0274(8) Uani 1 1 d . D 1
 C26 C 0.55151(8) 0.13035(8) -0.1065(2) 0.0295(8) Uani 1 1 d . D 1
 C27 C 0.53792(8) 0.11049(8) -0.1836(2) 0.0314(8) Uani 1 1 d . D 1
 C28 C 0.54300(11) 0.08478(10) -0.2043(3) 0.0502(12) Uani 1 1 d . D 1
 H28 H 0.5546 0.0797 -0.1650 0.060 Uiso 1 1 calc R D 1
 C29 C 0.53109(13) 0.06774(12) -0.2807(3) 0.0686(15) Uani 1 1 d . D 1
 H29 H 0.5347 0.0511 -0.2930 0.082 Uiso 1 1 calc R D 1
 C30 C 0.77222(10) 0.18020(12) 0.0079(3) 0.0601(13) Uani 1 1 d . . 1
 H30 H 0.7762 0.1723 0.0601 0.072 Uiso 1 1 calc R . 1
 C31 C 0.74236(9) 0.17465(9) -0.0094(3) 0.0404(10) Uani 1 1 d . . 1
 H31 H 0.7262 0.1631 0.0315 0.049 Uiso 1 1 calc R . 1
 C32 C 0.73571(8) 0.18618(8) -0.0885(2) 0.0282(8) Uani 1 1 d . . 1
 C33 C 0.70462(8) 0.18072(8) -0.1088(2) 0.0294(8) Uani 1 1 d . . 1
 C34 C 0.69991(9) 0.19470(9) -0.1821(3) 0.0412(10) Uani 1 1 d . . 1
 H34 H 0.6799 0.1917 -0.1934 0.049 Uiso 1 1 calc R . 1
 C35 C 0.54685(9) 0.15534(9) -0.0928(3) 0.0404(10) Uani 1 1 d . D 1
 H35 H 0.5563 0.1686 -0.0438 0.048 Uiso 1 1 calc R D 1
 C36 C 0.67663(8) 0.15954(8) -0.0520(2) 0.0252(7) Uani 1 1 d . . 1
 C37 C 0.68478(7) 0.16389(7) 0.1918(2) 0.0225(7) Uani 1 1 d . . 1
 C38 C 0.70742(7) 0.18483(7) 0.2623(2) 0.0229(7) Uani 1 1 d . . 1
 C39 C 0.70218(8) 0.20669(8) 0.3130(2) 0.0298(8) Uani 1 1 d . . 1
 C40 C 0.67363(9) 0.20777(10) 0.3062(3) 0.0464(11) Uani 1 1 d . . 1
 H40 H 0.6576 0.1938 0.2681 0.056 Uiso 1 1 calc R . 1
 C41 C 0.66961(10) 0.22909(11) 0.3548(3) 0.0649(15) Uani 1 1 d . . 1
 H41 H 0.6510 0.2298 0.3485 0.078 Uiso 1 1 calc R . 1
 C42 C 0.69293(11) 0.24987(11) 0.4140(4) 0.0688(16) Uani 1 1 d . . 1
 H42 H 0.6899 0.2645 0.4461 0.083 Uiso 1 1 calc R . 1
 C43 C 0.71994(9) 0.24893(10) 0.4253(3) 0.0488(11) Uani 1 1 d . . 1
 H43 H 0.7349 0.2625 0.4665 0.059 Uiso 1 1 calc R . 1
 C44 C 0.72583(8) 0.22742(8) 0.3747(2) 0.0293(8) Uani 1 1 d . . 1
 C45 C 0.55837(7) 0.13798(8) 0.2803(2) 0.0256(7) Uani 1 1 d . D 1
 C46 C 0.75743(8) 0.20367(8) 0.3369(2) 0.0278(8) Uani 1 1 d . . 1
 H46 H 0.7755 0.2021 0.3451 0.033 Uiso 1 1 calc R . 1
 C47 C 0.73497(7) 0.18406(8) 0.2744(2) 0.0261(7) Uani 1 1 d . . 1
 H47 H 0.7386 0.1702 0.2403 0.031 Uiso 1 1 calc R . 1
 C48 C 0.57734(8) 0.13197(8) 0.2105(2) 0.0245(7) Uani 1 1 d . D 1
 C52 C 0.51882(12) 0.02116(15) 0.1686(5) 0.125(3) Uani 1 1 d . E 1
 H52A H 0.4966 0.0062 0.1676 0.188 Uiso 1 1 calc R E 1
 H52B H 0.5245 0.0316 0.2259 0.188 Uiso 1 1 calc R E 1
 H52C H 0.5304 0.0102 0.1592 0.188 Uiso 1 1 calc R E 1
 C53 C 0.5046(2) 0.0556(3) 0.0800(9) 0.078(5) Uani 0.494(10) 1 d P E 1
 H53A H 0.5118 0.0687 0.0274 0.117 Uiso 0.494(10) 1 calc PR E 1
 H53B H 0.5040 0.0677 0.1301 0.117 Uiso 0.494(10) 1 calc PR E 1
 H53C H 0.4837 0.0381 0.0693 0.117 Uiso 0.494(10) 1 calc PR E 1
 C531 C 0.5093(2) 0.0327(3) 0.0196(7) 0.078(4) Uani 0.506(10) 1 d P E 2
 H53D H 0.5227 0.0318 -0.0260 0.117 Uiso 0.506(10) 1 calc PR E 2
 H53E H 0.5023 0.0470 0.0009 0.117 Uiso 0.506(10) 1 calc PR E 2
 H53F H 0.4914 0.0121 0.0286 0.117 Uiso 0.506(10) 1 calc PR E 2
 N3 N 0.64943(13) 0.14633(13) 0.4635(3) 0.0598(16) Uani 0.795(7) 1 d P C 1
 C55 C 0.66477(14) 0.13471(14) 0.4176(3) 0.0410(14) Uani 0.795(7) 1 d P C 1
 C56 C 0.6176(2) 0.1391(3) 0.4368(10) 0.072(3) Uani 0.795(7) 1 d P C 1
 H56A H 0.6089 0.1217 0.3954 0.108 Uiso 0.795(7) 1 calc PR C 1
 H56B H 0.6187 0.1573 0.4083 0.108 Uiso 0.795(7) 1 calc PR C 1

H56C H 0.6044 0.1336 0.4891 0.108 Uiso 0.795(7) 1 calc PR C 1
 C57 C 0.6664(2) 0.16977(18) 0.5377(5) 0.099(3) Uani 0.795(7) 1 d P C 1
 H57A H 0.6858 0.1702 0.5513 0.149 Uiso 0.795(7) 1 calc PR C 1
 H57B H 0.6533 0.1637 0.5904 0.149 Uiso 0.795(7) 1 calc PR C 1
 H57C H 0.6710 0.1904 0.5186 0.149 Uiso 0.795(7) 1 calc PR C 1
 C58 C 0.67795(15) 0.07484(15) 0.8267(4) 0.113(3) Uani 1 1 d . . .
 H58A H 0.6628 0.0778 0.7933 0.169 Uiso 1 1 calc R . .
 H58B H 0.6673 0.0593 0.8729 0.169 Uiso 1 1 calc R . .
 H58C H 0.6886 0.0677 0.7868 0.169 Uiso 1 1 calc R . .
 C59 C 0.73337(14) 0.11550(14) 0.8362(4) 0.0891(19) Uani 1 1 d . . .
 H59A H 0.7384 0.0990 0.8440 0.134 Uiso 1 1 calc R . .
 H59B H 0.7477 0.1336 0.8710 0.134 Uiso 1 1 calc R . .
 H59C H 0.7352 0.1212 0.7737 0.134 Uiso 1 1 calc R . .
 N1 N 0.52622(7) 0.04352(7) 0.1002(2) 0.0364(8) Uani 1 1 d . . .
 N4 N 0.70055(11) 0.10414(10) 0.8669(3) 0.0739(13) Uani 1 1 d . . .
 Ni1 Ni 0.629332(9) 0.158116(9) 0.07660(3) 0.01953(10) Uani 1 1 d . D .
 Ni2 Ni 0.653724(9) 0.103432(9) 0.07955(3) 0.01778(10) Uani 1 1 d . . .
 Ni3 Ni 0.574454(9) 0.079494(9) 0.09097(3) 0.02004(10) Uani 1 1 d . . .
 Ni4 Ni 0.678095(10) 0.102690(10) 0.27281(3) 0.02237(11) Uani 1 1 d . . .
 .
 O1 O 0.61966(5) 0.11365(5) 0.0841(2) 0.0393(7) Uani 1 1 d . . .
 O2 O 0.60541(5) 0.15297(5) 0.19480(16) 0.0291(5) Uani 1 1 d . . .
 O3 O 0.59202(5) 0.14953(5) -0.00023(17) 0.0328(6) Uani 1 1 d . . .
 O4 O 0.67090(5) 0.17448(5) 0.14615(16) 0.0273(5) Uani 1 1 d . . .
 O5 O 0.65666(5) 0.16804(5) -0.03767(16) 0.0305(6) Uani 1 1 d . . .
 O6 O 0.64019(6) 0.20551(6) 0.07658(19) 0.0374(6) Uani 1 1 d D . .
 C49 C 0.6421(2) 0.21805(15) 0.0042(6) 0.136(3) Uani 1 1 d D D .
 N2 N 0.6417(3) 0.24573(18) -0.0043(5) 0.278(7) Uani 1 1 d D . .
 C50 C 0.6505(2) 0.26738(18) 0.0764(7) 0.190(5) Uani 1 1 d D D .
 H50A H 0.6628 0.2627 0.1177 0.285 Uiso 1 1 calc R . .
 H50B H 0.6316 0.2642 0.1058 0.285 Uiso 1 1 calc R . .
 H50C H 0.6627 0.2890 0.0570 0.285 Uiso 1 1 calc R . .
 C51 C 0.6441(6) 0.2594(4) -0.0949(8) 0.492(18) Uani 1 1 d D D .
 H51A H 0.6564 0.2539 -0.1334 0.738 Uiso 1 1 calc R . .
 H51B H 0.6542 0.2820 -0.0903 0.738 Uiso 1 1 calc R . .
 H51C H 0.6233 0.2512 -0.1197 0.738 Uiso 1 1 calc R . .
 O7 O 0.67479(5) 0.13388(5) -0.02654(15) 0.0277(5) Uani 1 1 d . . .
 O8 O 0.68174(5) 0.13634(5) 0.17949(14) 0.0221(5) Uani 1 1 d . . .
 O9 O 0.63073(5) 0.06637(5) -0.00589(16) 0.0308(6) Uani 1 1 d . . .
 O10 O 0.63789(5) 0.07578(5) 0.19670(14) 0.0213(5) Uani 1 1 d . . .
 O11 O 0.68953(5) 0.09383(5) 0.06027(15) 0.0268(5) Uani 1 1 d . . .
 O12 O 0.56369(6) 0.09690(6) -0.02050(17) 0.0352(6) Uani 1 1 d . . .
 O13 O 0.56257(5) 0.10498(5) 0.17501(16) 0.0311(6) Uani 1 1 d . . .
 O14 O 0.57877(5) 0.04746(6) 0.01168(18) 0.0374(6) Uani 1 1 d . . .
 O15 O 0.58654(5) 0.06193(5) 0.20311(17) 0.0330(6) Uani 1 1 d . . .
 O17 O 0.70590(6) 0.09144(6) 0.19925(16) 0.0348(6) Uani 1 1 d . A .
 O18 O 0.65247(6) 0.11624(6) 0.35197(17) 0.0347(6) Uani 1 1 d . C .
 O19 O 0.71614(5) 0.12021(5) 0.36700(16) 0.0309(6) Uani 1 1 d . C .
 O20 O 0.67700(5) 0.07122(5) 0.36727(16) 0.0320(6) Uani 1 1 d . C .
 O21 O 0.6909(2) 0.1314(2) 0.7044(7) 0.123(5) Uani 0.524(6) 1 d PD F 1
 C60 C 0.6704(3) 0.1131(3) 0.6593(11) 0.152(9) Uani 0.524(6) 1 d PD F 1
 N5 N 0.6375(3) 0.0982(3) 0.6760(8) 0.126(5) Uani 0.524(6) 1 d PD F 1
 C61 C 0.6254(3) 0.1051(3) 0.7662(11) 0.126(6) Uani 0.524(6) 1 d PD F 1
 H61A H 0.6146 0.0861 0.8010 0.189 Uiso 0.524(6) 1 calc PR F 1
 H61B H 0.6111 0.1127 0.7528 0.189 Uiso 0.524(6) 1 calc PR F 1

H61C H 0.6430 0.1208 0.7999 0.189 Uiso 0.524(6) 1 calc PR F 1
 C62 C 0.6138(4) 0.0755(4) 0.6148(13) 0.179(9) Uani 0.524(6) 1 d PD F 1
 H62A H 0.6237 0.0755 0.5589 0.269 Uiso 0.524(6) 1 calc PR F 1
 H62B H 0.5980 0.0813 0.6040 0.269 Uiso 0.524(6) 1 calc PR F 1
 H62C H 0.6042 0.0548 0.6411 0.269 Uiso 0.524(6) 1 calc PR F 1
 N31 N 0.6242(5) 0.1130(6) 0.4767(12) 0.070(7) Uani 0.205(7) 1 d PU C 2
 C551 C 0.6438(7) 0.1063(8) 0.4300(16) 0.075(9) Uani 0.205(7) 1 d PU C 2
 C561 C 0.6049(14) 0.1275(14) 0.441(5) 0.132(19) Uani 0.205(7) 1 d PU C 2
 H56D H 0.6077 0.1303 0.3769 0.199 Uiso 0.205(7) 1 calc PR C 2
 H56E H 0.6119 0.1476 0.4690 0.199 Uiso 0.205(7) 1 calc PR C 2
 H56F H 0.5829 0.1136 0.4541 0.199 Uiso 0.205(7) 1 calc PR C 2
 C571 C 0.6158(7) 0.1031(11) 0.574(2) 0.127(15) Uani 0.205(7) 1 d PU C 2
 H57D H 0.6111 0.0817 0.5813 0.190 Uiso 0.205(7) 1 calc PR C 2
 H57E H 0.5976 0.1047 0.5905 0.190 Uiso 0.205(7) 1 calc PR C 2
 H57F H 0.6332 0.1168 0.6120 0.190 Uiso 0.205(7) 1 calc PR C 2
 O22 O 0.5797(5) 0.3467(3) 0.6706(10) 0.375(13) Uani 0.679(10) 1 d PDU G 1
 C63 C 0.5894(5) 0.3660(4) 0.6170(11) 0.188(7) Uani 0.679(10) 1 d PDU G 1
 N6 N 0.5932(5) 0.3946(4) 0.6313(11) 0.176(6) Uani 0.679(10) 1 d PDU G 1
 C64 C 0.5734(7) 0.3986(5) 0.7071(13) 0.363(17) Uani 0.679(10) 1 d PDU G 1
 C65 C 0.6035(5) 0.4179(4) 0.5608(14) 0.232(11) Uani 0.679(10) 1 d PDU G 1
 O221 O 0.6214(10) 0.3737(9) 0.517(3) 0.36(2) Uani 0.321(10) 1 d PDU G 2
 C631 C 0.6125(9) 0.3923(7) 0.5167(18) 0.209(13) Uani 0.321(10) 1 d PDU G 2
 N61 N 0.5986(9) 0.3946(5) 0.5939(17) 0.163(9) Uani 0.321(10) 1 d PDU G 2
 C641 C 0.6013(14) 0.3791(10) 0.681(2) 0.276(18) Uani 0.321(10) 1 d PDU G 2
 C651 C 0.6013(12) 0.4254(7) 0.610(3) 0.166(13) Uani 0.321(10) 1 d PDU G 2
 O23W O 0.6667 0.3333 0.3333 0.103(11) Uani 0.31 6 d SP . 4
 O24W O 0.49693(17) 0.0873(2) 0.1443(6) 0.072(3) Uani 0.38 1 d P H 4
 O25W O 0.6943(12) 0.3421(17) 0.384(4) 0.23(4) Uani 0.13 1 d P I 4
 O26W O 0.6329(5) 0.2066(4) 0.8663(11) 0.088(6) Uani 0.21 1 d P J 4

loop_
 _atom_site_aniso_label
 _atom_site_aniso_U_11
 _atom_site_aniso_U_22
 _atom_site_aniso_U_33
 _atom_site_aniso_U_23
 _atom_site_aniso_U_13
 _atom_site_aniso_U_12
 C1 0.0253(17) 0.0243(17) 0.032(2) 0.0016(15) 0.0030(15) 0.0157(15)
 C2 0.0278(18) 0.0290(18) 0.0264(18) 0.0025(15) 0.0056(15) 0.0184(15)
 C3 0.0281(18) 0.0276(18) 0.0260(18) -0.0016(15) 0.0005(15) 0.0171(15)
 C4 0.044(2) 0.047(2) 0.034(2) -0.0123(18) -0.0004(18) 0.030(2)
 C5 0.044(2) 0.062(3) 0.047(3) -0.031(2) -0.016(2) 0.029(2)
 C6 0.026(2) 0.070(3) 0.053(3) -0.026(2) -0.010(2) 0.021(2)
 C7 0.0277(19) 0.050(2) 0.045(2) -0.017(2) -0.0033(18) 0.0226(18)
 C8 0.0229(17) 0.0273(18) 0.032(2) -0.0014(15) 0.0005(15) 0.0148(15)

C9 0.0242(17) 0.0247(17) 0.0284(19) 0.0008(14) 0.0061(14) 0.0152(14)
 C10 0.0220(17) 0.0283(18) 0.034(2) -0.0042(16) -0.0007(15) 0.0125(15)
 C11 0.0225(17) 0.0315(19) 0.039(2) -0.0043(16) 0.0012(16) 0.0156(15)
 C12 0.0274(18) 0.0213(16) 0.0233(18) 0.0025(14) 0.0010(14) 0.0124(14)
 C13 0.0262(18) 0.0263(18) 0.0251(19) -0.0050(15) -0.0026(15) 0.0122(15)
 C14 0.0210(16) 0.0231(17) 0.031(2) -0.0078(15) -0.0011(15) 0.0072(14)
 C15 0.0222(17) 0.0197(16) 0.0276(19) -0.0034(14) -0.0004(14) 0.0068(14)
 C16 0.035(2) 0.0291(19) 0.030(2) -0.0054(16) -0.0059(16) 0.0120(16)
 C17 0.046(2) 0.042(2) 0.041(2) -0.0024(19) -0.0174(19) 0.023(2)
 C18 0.053(3) 0.039(2) 0.051(3) -0.004(2) -0.012(2) 0.032(2)
 C19 0.047(2) 0.031(2) 0.038(2) -0.0069(17) -0.0051(19) 0.0239(18)
 C20 0.0278(18) 0.0231(17) 0.0280(19) -0.0028(15) 0.0002(15) 0.0120(15)
 C21 0.0298(18) 0.0267(18) 0.0293(19) 0.0014(15) -0.0049(15) 0.0178(15)
 C22 0.0303(19) 0.0291(19) 0.040(2) 0.0142(17) -0.0008(17) 0.0120(16)
 C23 0.032(2) 0.0315(19) 0.044(2) -0.0126(17) -0.0094(17) 0.0203(17)
 C24 0.0299(19) 0.035(2) 0.0235(18) 0.0000(16) -0.0027(15) 0.0214(17)
 C25 0.0268(18) 0.034(2) 0.0241(18) 0.0008(16) -0.0032(15) 0.0176(16)
 C26 0.0267(18) 0.0317(19) 0.030(2) 0.0002(16) -0.0077(15) 0.0144(16)
 C27 0.037(2) 0.038(2) 0.0265(19) -0.0016(16) -0.0047(16) 0.0245(18)
 C28 0.074(3) 0.067(3) 0.039(2) -0.015(2) -0.019(2) 0.057(3)
 C29 0.106(4) 0.087(4) 0.057(3) -0.031(3) -0.032(3) 0.082(4)
 C30 0.046(3) 0.089(4) 0.038(3) 0.026(3) 0.000(2) 0.028(3)
 C31 0.031(2) 0.051(2) 0.031(2) 0.0121(19) 0.0047(17) 0.0145(19)
 C32 0.0267(18) 0.0282(18) 0.0269(19) 0.0054(15) 0.0055(15) 0.0115(15)
 C33 0.0276(18) 0.0271(18) 0.033(2) 0.0066(16) 0.0097(16) 0.0132(15)
 C34 0.029(2) 0.052(2) 0.046(2) 0.026(2) 0.0115(18) 0.0232(19)
 C35 0.050(2) 0.035(2) 0.042(2) -0.0107(18) -0.026(2) 0.0251(19)
 C36 0.0260(17) 0.0272(18) 0.0211(18) 0.0029(14) 0.0011(14) 0.0124(15)
 C37 0.0186(16) 0.0209(16) 0.0266(18) -0.0018(14) -0.0006(14) 0.0088(14)
 C38 0.0223(16) 0.0205(16) 0.0256(18) -0.0015(14) -0.0057(14) 0.0106(14)
 C39 0.0268(18) 0.0302(19) 0.036(2) -0.0097(16) -0.0102(16) 0.0170(16)
 C40 0.032(2) 0.054(3) 0.059(3) -0.028(2) -0.019(2) 0.026(2)
 C41 0.043(3) 0.081(3) 0.093(4) -0.051(3) -0.032(3) 0.048(3)
 C42 0.054(3) 0.076(3) 0.098(4) -0.059(3) -0.033(3) 0.048(3)
 C43 0.040(2) 0.054(3) 0.059(3) -0.032(2) -0.021(2) 0.028(2)
 C44 0.0265(18) 0.0299(18) 0.033(2) -0.0100(16) -0.0093(16) 0.0150(15)
 C45 0.0229(17) 0.0296(18) 0.0257(18) -0.0032(15) 0.0020(14) 0.0142(15)
 C46 0.0224(17) 0.0274(18) 0.034(2) -0.0050(16) -0.0081(15) 0.0128(15)
 C47 0.0236(17) 0.0251(17) 0.031(2) -0.0048(15) -0.0043(15) 0.0129(14)
 C48 0.0252(17) 0.0305(18) 0.0212(17) -0.0016(15) 0.0010(14) 0.0164(15)
 C52 0.041(3) 0.107(5) 0.146(6) 0.078(5) -0.010(4) -0.025(3)
 C53 0.026(5) 0.074(8) 0.127(12) 0.028(8) 0.010(6) 0.020(5)
 C531 0.032(5) 0.086(8) 0.070(8) -0.022(6) -0.003(5) -0.004(5)
 N3 0.075(4) 0.078(4) 0.047(3) -0.020(3) 0.002(3) 0.054(3)
 C55 0.060(4) 0.049(3) 0.025(3) 0.001(2) 0.004(2) 0.035(3)
 C56 0.054(4) 0.097(7) 0.085(6) -0.024(5) 0.008(4) 0.053(5)
 C57 0.148(8) 0.110(6) 0.063(5) -0.030(5) 0.005(5) 0.082(6)
 C58 0.099(5) 0.113(5) 0.072(4) -0.012(4) 0.023(4) 0.012(4)
 C59 0.108(5) 0.084(4) 0.085(4) 0.019(4) 0.031(4) 0.055(4)
 N1 0.0214(15) 0.0317(17) 0.049(2) -0.0050(15) -0.0007(15) 0.0082(13)
 N4 0.092(3) 0.060(3) 0.069(3) -0.017(2) 0.004(3) 0.038(3)
 Ni1 0.0173(2) 0.0194(2) 0.0229(2) 0.00012(17) -0.00136(17) 0.00992(17)
 Ni2 0.0171(2) 0.0172(2) 0.0196(2) -0.00054(16) 0.00041(16) 0.00897(16)
 Ni3 0.0179(2) 0.0192(2) 0.0233(2) -0.00125(17) -0.00020(17) 0.00959(17)
 Ni4 0.0245(2) 0.0283(2) 0.0201(2) 0.00011(18) -0.00156(18) 0.01753(19)

O1 0.0172(12) 0.0169(12) 0.086(2) 0.0116(13) 0.0087(13) 0.0101(10)
 O2 0.0216(12) 0.0296(13) 0.0304(14) -0.0062(11) 0.0026(10) 0.0086(10)
 O3 0.0294(13) 0.0289(13) 0.0408(15) -0.0002(11) -0.0123(12) 0.0151(11)
 O4 0.0254(12) 0.0227(12) 0.0346(14) -0.0021(10) -0.0107(11) 0.0126(10)
 O5 0.0315(13) 0.0350(13) 0.0296(14) 0.0099(11) 0.0095(11) 0.0201(12)
 O6 0.0392(15) 0.0246(13) 0.0505(18) 0.0060(12) -0.0004(13) 0.0176(12)
 C49 0.183(8) 0.072(5) 0.168(9) 0.042(5) 0.032(7) 0.074(5)
 N2 0.64(2) 0.138(7) 0.131(7) 0.065(6) 0.082(10) 0.256(11)
 C50 0.235(11) 0.091(6) 0.235(12) 0.001(7) 0.096(10) 0.074(7)
 C51 1.13(6) 0.323(19) 0.193(14) 0.162(14) 0.19(2) 0.49(3)
 O7 0.0300(13) 0.0248(12) 0.0292(13) 0.0082(10) 0.0100(11) 0.0142(10)
 O8 0.0252(12) 0.0200(11) 0.0223(12) -0.0009(9) -0.0031(10) 0.0122(10)
 O9 0.0228(12) 0.0280(13) 0.0352(14) -0.0139(11) -0.0005(11) 0.0078(10)
 O10 0.0215(11) 0.0214(11) 0.0215(12) 0.0039(9) 0.0024(9) 0.0111(9)
 O11 0.0260(12) 0.0342(13) 0.0263(13) 0.0007(11) 0.0014(10) 0.0195(11)
 O12 0.0381(14) 0.0326(14) 0.0340(15) -0.0002(12) -0.0143(12) 0.0171(12)
 O13 0.0265(12) 0.0283(13) 0.0375(15) -0.0068(11) 0.0067(11) 0.0129(11)
 O14 0.0257(13) 0.0325(14) 0.0507(17) -0.0165(12) 0.0008(12) 0.0121(11)
 O15 0.0230(12) 0.0371(14) 0.0384(15) 0.0144(12) 0.0010(11) 0.0147(11)
 O17 0.0412(15) 0.0548(16) 0.0264(14) 0.0015(12) 0.0038(12) 0.0375(14)
 O18 0.0385(15) 0.0442(15) 0.0299(15) -0.0034(12) 0.0026(12) 0.0269(13)
 O19 0.0335(13) 0.0307(13) 0.0311(14) 0.0047(11) -0.0054(11) 0.0180(11)
 O20 0.0318(13) 0.0336(13) 0.0317(14) 0.0019(11) -0.0070(11) 0.0173(12)
 O21 0.152(9) 0.081(6) 0.137(8) -0.047(6) -0.108(7) 0.059(6)
 C60 0.172(18) 0.125(14) 0.21(2) 0.119(14) 0.116(16) 0.116(14)
 N5 0.169(13) 0.094(9) 0.099(10) -0.003(7) -0.046(10) 0.054(9)
 C61 0.081(9) 0.095(10) 0.176(17) 0.017(11) 0.009(10) 0.024(8)
 C62 0.192(19) 0.133(15) 0.21(2) -0.043(15) -0.125(17) 0.080(14)
 N31 0.094(16) 0.14(2) 0.027(9) -0.003(11) 0.002(9) 0.101(16)
 C551 0.095(19) 0.14(3) 0.040(12) -0.021(15) -0.013(12) 0.102(19)
 C561 0.20(5) 0.19(5) 0.12(3) -0.03(4) -0.02(4) 0.18(4)
 C571 0.08(2) 0.26(4) 0.049(14) 0.02(2) 0.014(15) 0.09(3)
 O22 0.70(3) 0.136(10) 0.246(16) 0.036(9) -0.121(18) 0.177(16)
 C63 0.279(17) 0.117(10) 0.151(14) -0.015(8) -0.066(12) 0.087(12)
 N6 0.258(13) 0.096(8) 0.145(12) 0.002(8) -0.065(11) 0.066(9)
 C64 0.65(4) 0.22(2) 0.164(17) -0.101(14) 0.047(19) 0.18(2)
 C65 0.163(14) 0.108(11) 0.27(2) 0.091(14) -0.032(16) -0.049(11)
 O221 0.45(5) 0.27(4) 0.41(5) -0.15(3) -0.09(3) 0.21(3)
 C631 0.30(3) 0.094(19) 0.164(19) -0.052(17) -0.044(19) 0.047(18)
 N61 0.273(19) 0.045(10) 0.112(15) -0.034(10) -0.090(15) 0.036(12)
 C641 0.44(4) 0.15(3) 0.18(2) 0.05(2) -0.09(3) 0.11(3)
 C651 0.19(3) 0.065(14) 0.20(3) -0.040(16) -0.08(2) 0.039(16)
 O23W 0.109(18) 0.109(18) 0.09(3) 0.000 0.000 0.055(9)
 O24W 0.034(4) 0.090(7) 0.076(6) -0.036(5) -0.002(4) 0.019(4)
 O25W 0.21(6) 0.32(10) 0.29(9) 0.18(8) 0.11(6) 0.23(7)
 O26W 0.139(16) 0.087(12) 0.063(11) 0.053(10) 0.034(11) 0.076(12)

```

_geom_special_details
;
All s.u.'s (except the s.u. in the dihedral angle between two l.s.
planes)
are estimated using the full covariance matrix. The cell s.u.'s are
taken
into account individually in the estimation of s.u.'s in distances,
angles

```

and torsion angles; correlations between s.u.'s in cell parameters are
 only
 used when they are defined by crystal symmetry. An approximate
 (isotropic)
 treatment of cell s.u.'s is used for estimating s.u.'s involving l.s.
 planes.
 ;

```

loop_
  _geom_bond_atom_site_label_1
  _geom_bond_atom_site_label_2
  _geom_bond_distance
  _geom_bond_site_symmetry_2
  _geom_bond_publ_flag
C1 O17 1.257(4) . ?
C1 O11 1.261(4) . ?
C1 C2 1.504(4) . ?
C2 C11 1.363(5) . ?
C2 C3 1.423(4) . ?
C3 C4 1.419(5) . ?
C3 C8 1.433(4) . ?
C4 C5 1.370(5) . ?
C5 C6 1.407(5) . ?
C6 C7 1.351(5) . ?
C7 C8 1.422(5) . ?
C8 C9 1.429(5) . ?
C9 C10 1.349(4) . ?
C9 C12 1.499(4) 9_654 ?
C10 C11 1.410(4) . ?
C12 O15 1.242(4) . ?
C12 O10 1.290(4) . ?
C12 C9 1.498(4) 5_545 ?
C13 O14 1.247(4) . ?
C13 O9 1.262(4) . ?
C13 C14 1.509(4) . ?
C14 C23 1.361(5) . ?
C14 C15 1.427(4) . ?
C15 C16 1.419(5) . ?
C15 C20 1.430(4) . ?
C16 C17 1.387(5) . ?
C17 C18 1.393(5) . ?
C18 C19 1.361(5) . ?
C19 C20 1.430(5) . ?
C20 C21 1.427(5) 5_544 ?
C21 C22 1.369(5) . ?
C21 C20 1.427(5) 9_655 ?
C21 C24 1.497(4) . ?
C22 C23 1.406(5) 9_655 ?
C23 C22 1.406(5) 5_544 ?
C24 O20 1.265(4) . ?
C24 O19 1.268(4) . ?
C24 Ni4 2.420(3) . ?
C25 O3 1.256(4) . ?
C25 O12 1.256(4) . ?
C25 C26 1.506(4) . ?

```

C26 C35 1.364(5) . ?
C26 C27 1.433(5) . ?
C27 C32 1.425(4) 17_554 ?
C27 C28 1.430(5) . ?
C28 C29 1.354(6) . ?
C29 C30 1.396(6) 17_554 ?
C30 C31 1.369(5) . ?
C30 C29 1.396(6) 18_544 ?
C31 C32 1.409(5) . ?
C32 C27 1.425(4) 18_544 ?
C32 C33 1.437(5) . ?
C33 C34 1.365(5) . ?
C33 C36 1.496(4) . ?
C34 C35 1.401(5) 18_544 ?
C35 C34 1.401(5) 17_554 ?
C36 O5 1.255(4) . ?
C36 O7 1.269(4) . ?
C37 O4 1.240(4) . ?
C37 O8 1.292(4) . ?
C37 C38 1.496(4) . ?
C38 C47 1.377(4) . ?
C38 C39 1.430(4) . ?
C39 C40 1.425(5) . ?
C39 C44 1.426(5) . ?
C40 C41 1.361(5) . ?
C41 C42 1.395(6) . ?
C42 C43 1.353(5) . ?
C43 C44 1.434(5) . ?
C44 C45 1.435(4) 18_545 ?
C45 C46 1.361(4) 17 ?
C45 C44 1.435(4) 17 ?
C45 C48 1.514(4) . ?
C46 C45 1.361(4) 18_545 ?
C46 C47 1.390(4) . ?
C48 O2 1.257(4) . ?
C48 O13 1.260(4) . ?
C52 N1 1.400(6) . ?
C53 N1 1.477(10) . ?
C531 N1 1.400(10) . ?
N3 C55 1.332(6) . ?
N3 C56 1.466(12) . ?
N3 C57 1.505(8) . ?
C55 O18 1.259(6) . ?
C58 N4 1.430(7) . ?
C59 N4 1.482(7) . ?
N1 Ni3 2.126(3) . ?
Ni1 O1 1.982(2) . ?
Ni1 O3 2.009(2) . ?
Ni1 O4 2.051(2) . ?
Ni1 O2 2.054(2) . ?
Ni1 O5 2.062(2) . ?
Ni1 O6 2.101(2) . ?
Ni2 O1 1.963(2) . ?
Ni2 O9 2.029(2) . ?
Ni2 O11 2.045(2) . ?

Ni2 O7 2.056(2) . ?
 Ni2 O10 2.099(2) . ?
 Ni2 O8 2.113(2) . ?
 Ni3 O1 1.997(2) . ?
 Ni3 O13 2.042(2) . ?
 Ni3 O12 2.047(2) . ?
 Ni3 O14 2.052(2) . ?
 Ni3 O15 2.090(2) . ?
 Ni4 O17 2.022(2) . ?
 Ni4 O18 2.054(2) . ?
 Ni4 O20 2.063(2) . ?
 Ni4 O10 2.070(2) . ?
 Ni4 O8 2.089(2) . ?
 Ni4 O19 2.134(2) . ?
 O6 C49 1.217(8) . ?
 C49 N2 1.368(8) . ?
 N2 C51 1.481(11) . ?
 N2 C50 1.513(10) . ?
 O18 C551 1.25(3) . ?
 O21 C60 1.164(15) . ?
 C60 N5 1.414(13) . ?
 N5 C62 1.453(13) . ?
 N5 C61 1.571(13) . ?
 N31 C551 1.35(3) . ?
 N31 C571 1.52(3) . ?
 N31 C561 1.53(6) . ?
 O22 C63 1.141(15) . ?
 C63 N6 1.332(14) . ?
 N6 C65 1.439(14) . ?
 N6 C64 1.559(16) . ?
 O221 C631 1.187(18) . ?
 C631 N61 1.366(17) . ?
 N61 C651 1.464(16) . ?
 N61 C641 1.531(18) . ?
 O23W O25W 1.41(5) 16_655 ?
 O23W O25W 1.41(5) 18_545 ?
 O23W O25W 1.41(5) . ?
 O23W O25W 1.41(5) 3_665 ?
 O23W O25W 1.41(5) 2_655 ?
 O23W O25W 1.41(5) 17 ?

loop_
 _geom_angle_atom_site_label_1
 _geom_angle_atom_site_label_2
 _geom_angle_atom_site_label_3
 _geom_angle
 _geom_angle_site_symmetry_1
 _geom_angle_site_symmetry_3
 _geom_angle_publ_flag
 O17 C1 O11 125.5(3) . . ?
 O17 C1 C2 119.9(3) . . ?
 O11 C1 C2 114.6(3) . . ?
 C11 C2 C3 119.4(3) . . ?
 C11 C2 C1 116.2(3) . . ?
 C3 C2 C1 124.3(3) . . ?

C4 C3 C2 122.6(3) . . ?
 C4 C3 C8 118.9(3) . . ?
 C2 C3 C8 118.5(3) . . ?
 C5 C4 C3 120.7(3) . . ?
 C4 C5 C6 120.2(4) . . ?
 C7 C6 C5 120.7(4) . . ?
 C6 C7 C8 121.6(3) . . ?
 C7 C8 C9 122.9(3) . . ?
 C7 C8 C3 118.0(3) . . ?
 C9 C8 C3 119.1(3) . . ?
 C10 C9 C8 120.2(3) . . ?
 C10 C9 C12 116.4(3) . 9_654 ?
 C8 C9 C12 123.0(3) . 9_654 ?
 C9 C10 C11 120.2(3) . . ?
 C2 C11 C10 121.9(3) . . ?
 O15 C12 O10 125.4(3) . . ?
 O15 C12 C9 117.5(3) . 5_545 ?
 O10 C12 C9 116.9(3) . 5_545 ?
 O14 C13 O9 126.6(3) . . ?
 O14 C13 C14 116.9(3) . . ?
 O9 C13 C14 116.5(3) . . ?
 C23 C14 C15 119.9(3) . . ?
 C23 C14 C13 117.8(3) . . ?
 C15 C14 C13 122.3(3) . . ?
 C16 C15 C14 122.1(3) . . ?
 C16 C15 C20 118.5(3) . . ?
 C14 C15 C20 119.4(3) . . ?
 C17 C16 C15 120.6(3) . . ?
 C16 C17 C18 120.3(4) . . ?
 C19 C18 C17 121.2(4) . . ?
 C18 C19 C20 120.5(3) . . ?
 C21 C20 C15 118.4(3) 5_544 . ?
 C21 C20 C19 122.8(3) 5_544 . ?
 C15 C20 C19 118.8(3) . . ?
 C22 C21 C20 120.5(3) . 9_655 ?
 C22 C21 C24 116.8(3) . . ?
 C20 C21 C24 122.8(3) 9_655 . ?
 C21 C22 C23 120.5(3) . 9_655 ?
 C14 C23 C22 121.3(3) . 5_544 ?
 O20 C24 O19 119.9(3) . . ?
 O20 C24 C21 120.6(3) . . ?
 O19 C24 C21 119.5(3) . . ?
 O20 C24 Ni4 58.48(17) . . ?
 O19 C24 Ni4 61.72(17) . . ?
 C21 C24 Ni4 173.6(2) . . ?
 O3 C25 O12 127.1(3) . . ?
 O3 C25 C26 114.8(3) . . ?
 O12 C25 C26 118.1(3) . . ?
 C35 C26 C27 119.8(3) . . ?
 C35 C26 C25 116.9(3) . . ?
 C27 C26 C25 123.3(3) . . ?
 C32 C27 C28 118.0(3) 17_554 . ?
 C32 C27 C26 119.2(3) 17_554 . ?
 C28 C27 C26 122.8(3) . . ?
 C29 C28 C27 120.7(4) . . ?

C28 C29 C30 121.2(4) . 17_554 ?
 C31 C30 C29 120.1(4) . 18_544 ?
 C30 C31 C32 120.9(4) . . ?
 C31 C32 C27 119.2(3) . 18_544 ?
 C31 C32 C33 122.3(3) . . ?
 C27 C32 C33 118.6(3) 18_544 . ?
 C34 C33 C32 120.1(3) . . ?
 C34 C33 C36 118.1(3) . . ?
 C32 C33 C36 121.8(3) . . ?
 C33 C34 C35 120.9(3) . 18_544 ?
 C26 C35 C34 121.3(3) . 17_554 ?
 O5 C36 O7 126.4(3) . . ?
 O5 C36 C33 117.4(3) . . ?
 O7 C36 C33 116.1(3) . . ?
 O4 C37 O8 123.8(3) . . ?
 O4 C37 C38 118.0(3) . . ?
 O8 C37 C38 118.2(3) . . ?
 C47 C38 C39 119.6(3) . . ?
 C47 C38 C37 118.1(3) . . ?
 C39 C38 C37 122.1(3) . . ?
 C40 C39 C44 118.7(3) . . ?
 C40 C39 C38 122.3(3) . . ?
 C44 C39 C38 119.0(3) . . ?
 C41 C40 C39 120.6(4) . . ?
 C40 C41 C42 120.9(4) . . ?
 C43 C42 C41 120.6(4) . . ?
 C42 C43 C44 121.1(4) . . ?
 C39 C44 C43 118.0(3) . . ?
 C39 C44 C45 119.0(3) . 18_545 ?
 C43 C44 C45 122.9(3) . 18_545 ?
 C46 C45 C44 119.5(3) 17 17 ?
 C46 C45 C48 117.7(3) 17 . ?
 C44 C45 C48 122.7(3) 17 . ?
 C45 C46 C47 121.9(3) 18_545 . ?
 C38 C47 C46 120.9(3) . . ?
 O2 C48 O13 126.7(3) . . ?
 O2 C48 C45 119.5(3) . . ?
 O13 C48 C45 113.8(3) . . ?
 C55 N3 C56 120.8(7) . . ?
 C55 N3 C57 119.0(5) . . ?
 C56 N3 C57 119.8(7) . . ?
 O18 C55 N3 122.3(5) . . ?
 C531 N1 C52 117.0(6) . . ?
 C531 N1 C53 64.6(6) . . ?
 C52 N1 C53 120.1(5) . . ?
 C531 N1 Ni3 117.2(4) . . ?
 C52 N1 Ni3 116.0(3) . . ?
 C53 N1 Ni3 112.1(4) . . ?
 C58 N4 C59 113.3(5) . . ?
 O1 Ni1 O3 96.26(10) . . ?
 O1 Ni1 O4 92.62(9) . . ?
 O3 Ni1 O4 170.27(9) . . ?
 O1 Ni1 O2 90.50(10) . . ?
 O3 Ni1 O2 93.37(10) . . ?
 O4 Ni1 O2 90.51(9) . . ?

O1 Ni1 O5 94.33(10) . . ?
 O3 Ni1 O5 89.69(10) . . ?
 O4 Ni1 O5 85.67(9) . . ?
 O2 Ni1 O5 173.98(9) . . ?
 O1 Ni1 O6 176.71(12) . . ?
 O3 Ni1 O6 86.14(10) . . ?
 O4 Ni1 O6 85.15(9) . . ?
 O2 Ni1 O6 87.11(10) . . ?
 O5 Ni1 O6 87.92(10) . . ?
 O1 Ni2 O9 94.99(10) . . ?
 O1 Ni2 O11 173.81(11) . . ?
 O9 Ni2 O11 82.13(9) . . ?
 O1 Ni2 O7 91.37(10) . . ?
 O9 Ni2 O7 91.11(10) . . ?
 O11 Ni2 O7 83.23(9) . . ?
 O1 Ni2 O10 92.79(10) . . ?
 O9 Ni2 O10 94.76(9) . . ?
 O11 Ni2 O10 92.91(8) . . ?
 O7 Ni2 O10 172.48(9) . . ?
 O1 Ni2 O8 95.25(10) . . ?
 O9 Ni2 O8 167.89(9) . . ?
 O11 Ni2 O8 88.28(8) . . ?
 O7 Ni2 O8 95.09(9) . . ?
 O10 Ni2 O8 78.29(8) . . ?
 O1 Ni3 O13 93.14(10) . . ?
 O1 Ni3 O12 91.04(10) . . ?
 O13 Ni3 O12 91.77(10) . . ?
 O1 Ni3 O14 96.63(10) . . ?
 O13 Ni3 O14 170.06(9) . . ?
 O12 Ni3 O14 89.89(10) . . ?
 O1 Ni3 O15 87.84(10) . . ?
 O13 Ni3 O15 89.30(10) . . ?
 O12 Ni3 O15 178.49(10) . . ?
 O14 Ni3 O15 89.24(10) . . ?
 O1 Ni3 N1 179.02(12) . . ?
 O13 Ni3 N1 85.91(10) . . ?
 O12 Ni3 N1 89.25(11) . . ?
 O14 Ni3 N1 84.31(11) . . ?
 O15 Ni3 N1 91.89(11) . . ?
 O17 Ni4 O18 176.23(11) . . ?
 O17 Ni4 O20 86.31(10) . . ?
 O18 Ni4 O20 93.31(10) . . ?
 O17 Ni4 O10 94.89(9) . . ?
 O18 Ni4 O10 88.84(9) . . ?
 O20 Ni4 O10 103.63(9) . . ?
 O17 Ni4 O8 92.91(9) . . ?
 O18 Ni4 O8 87.27(9) . . ?
 O20 Ni4 O8 176.83(9) . . ?
 O10 Ni4 O8 79.50(8) . . ?
 O17 Ni4 O19 83.94(10) . . ?
 O18 Ni4 O19 92.54(10) . . ?
 O20 Ni4 O19 62.97(9) . . ?
 O10 Ni4 O19 166.58(9) . . ?
 O8 Ni4 O19 113.90(9) . . ?
 O17 Ni4 C24 82.44(10) . . ?

O18 Ni4 C24 95.28(11) . . ?
 O20 Ni4 C24 31.52(10) . . ?
 O10 Ni4 C24 135.03(10) . . ?
 O8 Ni4 C24 145.33(10) . . ?
 O19 Ni4 C24 31.55(10) . . ?
 Ni2 O1 Ni1 120.60(11) . . ?
 Ni2 O1 Ni3 120.89(11) . . ?
 Ni1 O1 Ni3 118.46(10) . . ?
 C48 O2 Ni1 125.5(2) . . ?
 C25 O3 Ni1 132.7(2) . . ?
 C37 O4 Ni1 139.0(2) . . ?
 C36 O5 Ni1 125.5(2) . . ?
 C49 O6 Ni1 117.9(4) . . ?
 O6 C49 N2 122.9(8) . . ?
 C49 N2 C51 119.6(9) . . ?
 C49 N2 C50 118.6(8) . . ?
 C51 N2 C50 118.3(8) . . ?
 C36 O7 Ni2 134.9(2) . . ?
 C37 O8 Ni4 130.3(2) . . ?
 C37 O8 Ni2 125.85(19) . . ?
 Ni4 O8 Ni2 95.72(8) . . ?
 C13 O9 Ni2 133.6(2) . . ?
 C12 O10 Ni4 124.1(2) . . ?
 C12 O10 Ni2 129.5(2) . . ?
 Ni4 O10 Ni2 96.71(8) . . ?
 C1 O11 Ni2 131.7(2) . . ?
 C25 O12 Ni3 128.4(2) . . ?
 C48 O13 Ni3 134.9(2) . . ?
 C13 O14 Ni3 133.1(2) . . ?
 C12 O15 Ni3 137.4(2) . . ?
 C1 O17 Ni4 127.6(2) . . ?
 C551 O18 C55 60.3(15) . . ?
 C551 O18 Ni4 123.4(11) . . ?
 C55 O18 Ni4 121.7(3) . . ?
 C24 O19 Ni4 86.73(19) . . ?
 C24 O20 Ni4 90.0(2) . . ?
 O21 C60 N5 128.1(16) . . ?
 C60 N5 C62 123.4(14) . . ?
 C60 N5 C61 119.5(11) . . ?
 C62 N5 C61 117.1(13) . . ?
 C551 N31 C571 122(2) . . ?
 C551 N31 C561 128(3) . . ?
 C571 N31 C561 110(3) . . ?
 O18 C551 N31 122(2) . . ?
 O22 C63 N6 122.4(18) . . ?
 C63 N6 C65 121.5(18) . . ?
 C63 N6 C64 118.6(15) . . ?
 C65 N6 C64 114.8(16) . . ?
 O221 C631 N61 117(3) . . ?
 C631 N61 C651 116(2) . . ?
 C631 N61 C641 120(2) . . ?
 C651 N61 C641 112(2) . . ?
 O25W O23W O25W 94(3) 16_655 18_545 ?
 O25W O23W O25W 179.992(16) 16_655 . ?
 O25W O23W O25W 86(3) 18_545 . ?

O25W O23W O25W 86(3) 16_655 3_665 ?
 O25W O23W O25W 179.99(2) 18_545 3_665 ?
 O25W O23W O25W 94(3) . 3_665 ?
 O25W O23W O25W 86(3) 16_655 2_655 ?
 O25W O23W O25W 86(3) 18_545 2_655 ?
 O25W O23W O25W 94(3) . 2_655 ?
 O25W O23W O25W 94(3) 3_665 2_655 ?
 O25W O23W O25W 94(3) 16_655 17 ?
 O25W O23W O25W 94(3) 18_545 17 ?
 O25W O23W O25W 86(3) . 17 ?
 O25W O23W O25W 86(3) 3_665 17 ?
 O25W O23W O25W 180(2) 2_655 17 ?

_diff_rn_measured_fraction_theta_max 0.958
 _diff_rn_reflns_theta_full 25.50
 _diff_rn_measured_fraction_theta_full 0.999
 _refine_diff_density_max 0.800
 _refine_diff_density_min -0.878
 _refine_diff_density_rms 0.083

Table A3.5. Selected interatomic distances and angles for

$\text{Ni}_4(\mu_3\text{-O})(1,4\text{-NDC})_4(\text{DMF})_2(\text{DMA})_2$ (**3-5**).

Atoms 1,2	d 1,2 [Å]	Atoms 1,2	d 1,2 [Å]
C1—O17	1.257(4)	C43—C44	1.434(5)
C1—O11	1.261(4)	C44—C45 ^{vii}	1.435(4)
C1—C2	1.504(4)	C45—C46 ^{viii}	1.361(4)
C2—C11	1.363(5)	C45—C44 ^{viii}	1.435(4)
C2—C3	1.423(4)	C45—C48	1.514(4)
C3—C4	1.419(5)	C46—C45 ^{vii}	1.361(4)
C3—C8	1.433(4)	C46—C47	1.390(4)
C4—C5	1.370(5)	C48—O2	1.257(4)
C5—C6	1.407(5)	C48—O13	1.260(4)
C6—C7	1.351(5)	C52—N1	1.400(6)
C7—C8	1.422(5)	C53—N1	1.477(10)
C8—C9	1.429(5)	C531—N1	1.40(1)
C9—C10	1.349(4)	N3—C55	1.332(6)
C9—C12 ⁱ	1.499(4)	N3—C56	1.466(12)
C10—C11	1.410(4)	N3—C57	1.505(8)
C12—O15	1.242(4)	C55—O18	1.259(6)
C12—O10	1.290(4)	C58—N4	1.430(7)

Table A3.5 continued

C12—C9 ⁱⁱ	1.498(4)	C59—N4	1.482(7)
C13—O14	1.247(4)	N1—Ni3	2.126(3)
C13—O9	1.262(4)	Ni1—O1	1.982(2)
C13—C14	1.509(4)	Ni1—O3	2.009(2)
C14—C23	1.361(5)	Ni1—O4	2.051(2)
C14—C15	1.427(4)	Ni1—O2	2.054(2)
C15—C16	1.419(5)	Ni1—O5	2.062(2)
C15—C20	1.430(4)	Ni1—O6	2.101(2)
C16—C17	1.387(5)	Ni2—O1	1.963(2)
C17—C18	1.393(5)	Ni2—O9	2.029(2)
C18—C19	1.361(5)	Ni2—O11	2.045(2)
C19—C20	1.430(5)	Ni2—O7	2.056(2)
C20—C21 ⁱⁱⁱ	1.427(5)	Ni2—O10	2.099(2)
C21—C22	1.369(5)	Ni2—O8	2.113(2)
C21—C20 ^{iv}	1.427(5)	Ni3—O1	1.997(2)
C21—C24	1.497(4)	Ni3—O13	2.042(2)
C22—C23 ^{iv}	1.406(5)	Ni3—O12	2.047(2)
C23—C22 ⁱⁱⁱ	1.406(5)	Ni3—O14	2.052(2)
C24—O20	1.265(4)	Ni3—O15	2.090(2)
C24—O19	1.268(4)	Ni4—O17	2.022(2)
C24—Ni4	2.420(3)	Ni4—O18	2.054(2)
C25—O3	1.256(4)	Ni4—O20	2.063(2)
C25—O12	1.256(4)	Ni4—O10	2.070(2)
C25—C26	1.506(4)	Ni4—O8	2.089(2)
C26—C35	1.364(5)	Ni4—O19	2.134(2)
C26—C27	1.433(5)	O6—C49	1.217(8)
C27—C32 ^v	1.425(4)	C49—N2	1.368(8)
C27—C28	1.430(5)	N2—C51	1.481(11)
C28—C29	1.354(6)	N2—C50	1.513(10)
C29—C30 ^v	1.396(6)	O18—C551	1.25(3)
C30—C31	1.369(5)	O21—C60	1.164(15)
C30—C29 ^{vi}	1.396(6)	C60—N5	1.414(13)
C31—C32	1.409(5)	N5—C62	1.453(13)
C32—C27 ^{vi}	1.425(4)	N5—C61	1.571(13)
C32—C33	1.437(5)	N31—C551	1.35(3)
C33—C34	1.365(5)	N31—C571	1.52(3)

Table A3.5 continued

C33—C36	1.496(4)	N31—C561	1.53(6)
C34—C35 ^{vi}	1.401(5)	O22—C63	1.141(15)
C35—C34 ^v	1.401(5)	C63—N6	1.332(14)
C36—O5	1.255(4)	N6—C65	1.439(14)
C36—O7	1.269(4)	N6—C64	1.559(16)
C37—O4	1.240(4)	O221—C631	1.187(18)
C37—O8	1.292(4)	C631—N61	1.366(17)
C37—C38	1.496(4)	N61—C651	1.464(16)
C38—C47	1.377(4)	N61—C641	1.531(18)
C38—C39	1.430(4)	O23W—O25W ^{ix}	1.41(5)
C39—C40	1.425(5)	O23W—O25W ^{vii}	1.41(5)
C39—C44	1.426(5)	O23W—O25W	1.41(5)
C40—C41	1.361(5)	O23W—O25W ^x	1.41(5)
C41—C42	1.395(6)	O23W—O25W ^{xi}	1.41(5)
C42—C43	1.353(5)	O23W—O25W ^{viii}	1.41(5)

Atoms 1,2,3	Angle 1,2,3 [°]	Atoms 1,2,3	Angle 1,2,3 [°]
O17—C1—O11	125.5(3)	O2—Ni1—O5	173.98(9)
O17—C1—C2	119.9(3)	O1—Ni1—O6	176.71(12)
O11—C1—C2	114.6(3)	O3—Ni1—O6	86.14(10)
C11—C2—C3	119.4(3)	O4—Ni1—O6	85.15(9)
C11—C2—C1	116.2(3)	O2—Ni1—O6	87.11(10)
C3—C2—C1	124.3(3)	O5—Ni1—O6	87.92(10)
C4—C3—C2	122.6(3)	O1—Ni2—O9	94.99(10)
C4—C3—C8	118.9(3)	O1—Ni2—O11	173.81(11)
C2—C3—C8	118.5(3)	O9—Ni2—O11	82.13(9)
C5—C4—C3	120.7(3)	O1—Ni2—O7	91.37(10)
C4—C5—C6	120.2(4)	O9—Ni2—O7	91.11(10)
C7—C6—C5	120.7(4)	O11—Ni2—O7	83.23(9)
C6—C7—C8	121.6(3)	O1—Ni2—O10	92.79(10)
C7—C8—C9	122.9(3)	O9—Ni2—O10	94.76(9)
C7—C8—C3	118.0(3)	O11—Ni2—O10	92.91(8)
C9—C8—C3	119.1(3)	O7—Ni2—O10	172.48(9)
C10—C9—C8	120.2(3)	O1—Ni2—O8	95.25(10)
C10—C9—C12 ⁱ	116.4(3)	O9—Ni2—O8	167.89(9)
C8—C9—C12 ⁱ	123.0(3)	O11—Ni2—O8	88.28(8)

Table A3.5 continued

C9—C10—C11	120.2(3)	O7—Ni2—O8	95.09(9)
C2—C11—C10	121.9(3)	O10—Ni2—O8	78.29(8)
O15—C12—O10	125.4(3)	O1—Ni3—O13	93.14(10)
O15—C12—C9 ⁱⁱ	117.5(3)	O1—Ni3—O12	91.04(10)
O10—C12—C9 ⁱⁱ	116.9(3)	O13—Ni3—O12	91.77(10)
O14—C13—O9	126.6(3)	O1—Ni3—O14	96.63(10)
O14—C13—C14	116.9(3)	O13—Ni3—O14	170.06(9)
O9—C13—C14	116.5(3)	O12—Ni3—O14	89.89(10)
C23—C14—C15	119.9(3)	O1—Ni3—O15	87.84(10)
C23—C14—C13	117.8(3)	O13—Ni3—O15	89.3(1)
C15—C14—C13	122.3(3)	O12—Ni3—O15	178.49(10)
C16—C15—C14	122.1(3)	O14—Ni3—O15	89.24(10)
C16—C15—C20	118.5(3)	O1—Ni3—N1	179.02(12)
C14—C15—C20	119.4(3)	O13—Ni3—N1	85.91(10)
C17—C16—C15	120.6(3)	O12—Ni3—N1	89.25(11)
C16—C17—C18	120.3(4)	O14—Ni3—N1	84.31(11)
C19—C18—C17	121.2(4)	O15—Ni3—N1	91.89(11)
C18—C19—C20	120.5(3)	O17—Ni4—O18	176.23(11)
C21 ⁱⁱⁱ —C20—C15	118.4(3)	O17—Ni4—O20	86.31(10)
C21 ⁱⁱⁱ —C20—C19	122.8(3)	O18—Ni4—O20	93.31(10)
C15—C20—C19	118.8(3)	O17—Ni4—O10	94.89(9)
C22—C21—C20 ^{iv}	120.5(3)	O18—Ni4—O10	88.84(9)
C22—C21—C24	116.8(3)	O20—Ni4—O10	103.63(9)
C20 ^{iv} —C21—C24	122.8(3)	O17—Ni4—O8	92.91(9)
C21—C22—C23 ^{iv}	120.5(3)	O18—Ni4—O8	87.27(9)
C14—C23—C22 ⁱⁱⁱ	121.3(3)	O20—Ni4—O8	176.83(9)
O20—C24—O19	119.9(3)	O10—Ni4—O8	79.50(8)
O20—C24—C21	120.6(3)	O17—Ni4—O19	83.94(10)
O19—C24—C21	119.5(3)	O18—Ni4—O19	92.54(10)
O20—C24—Ni4	58.48(17)	O20—Ni4—O19	62.97(9)
O19—C24—Ni4	61.72(17)	O10—Ni4—O19	166.58(9)
C21—C24—Ni4	173.6(2)	O8—Ni4—O19	113.90(9)
O3—C25—O12	127.1(3)	O17—Ni4—C24	82.44(10)
O3—C25—C26	114.8(3)	O18—Ni4—C24	95.28(11)
O12—C25—C26	118.1(3)	O20—Ni4—C24	31.52(10)
C35—C26—C27	119.8(3)	O10—Ni4—C24	135.03(10)

Table A3.5 continued

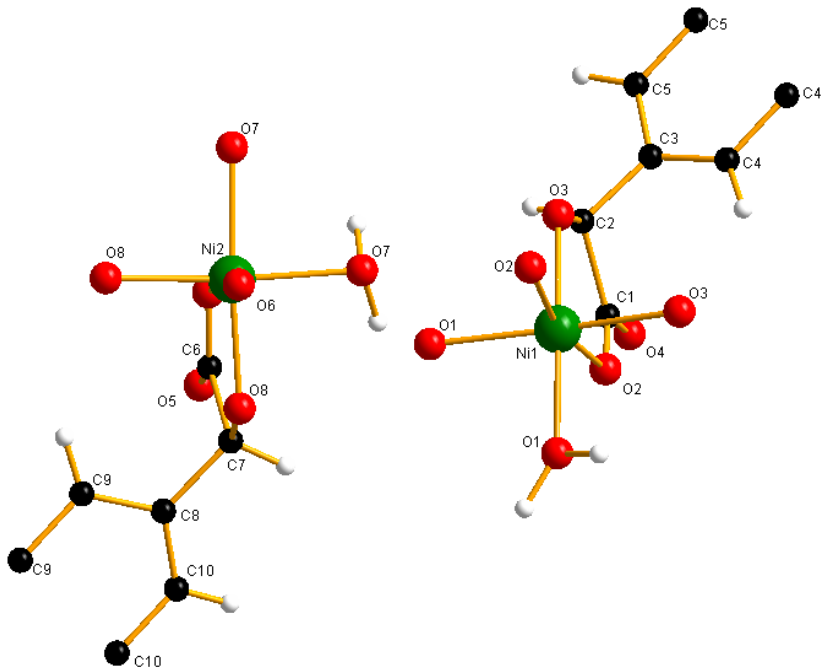
C35—C26—C25	116.9(3)	O8—Ni4—C24	145.33(10)
C27—C26—C25	123.3(3)	O19—Ni4—C24	31.55(10)
C32 ^v —C27—C28	118.0(3)	Ni2—O1—Ni1	120.60(11)
C32 ^v —C27—C26	119.2(3)	Ni2—O1—Ni3	120.89(11)
C28—C27—C26	122.8(3)	Ni1—O1—Ni3	118.46(10)
C29—C28—C27	120.7(4)	C48—O2—Ni1	125.5(2)
C28—C29—C30 ^v	121.2(4)	C25—O3—Ni1	132.7(2)
C31—C30—C29 ^{vi}	120.1(4)	C37—O4—Ni1	139.0(2)
C30—C31—C32	120.9(4)	C36—O5—Ni1	125.5(2)
C31—C32—C27 ^{vi}	119.2(3)	C49—O6—Ni1	117.9(4)
C31—C32—C33	122.3(3)	O6—C49—N2	122.9(8)
C27 ^{vi} —C32—C33	118.6(3)	C49—N2—C51	119.6(9)
C34—C33—C32	120.1(3)	C49—N2—C50	118.6(8)
C34—C33—C36	118.1(3)	C51—N2—C50	118.3(8)
C32—C33—C36	121.8(3)	C36—O7—Ni2	134.9(2)
C33—C34—C35 ^{vi}	120.9(3)	C37—O8—Ni4	130.3(2)
C26—C35—C34 ^v	121.3(3)	C37—O8—Ni2	125.85(19)
O5—C36—O7	126.4(3)	Ni4—O8—Ni2	95.72(8)
O5—C36—C33	117.4(3)	C13—O9—Ni2	133.6(2)
O7—C36—C33	116.1(3)	C12—O10—Ni4	124.1(2)
O4—C37—O8	123.8(3)	C12—O10—Ni2	129.5(2)
O4—C37—C38	118.0(3)	Ni4—O10—Ni2	96.71(8)
O8—C37—C38	118.2(3)	C1—O11—Ni2	131.7(2)
C47—C38—C39	119.6(3)	C25—O12—Ni3	128.4(2)
C47—C38—C37	118.1(3)	C48—O13—Ni3	134.9(2)
C39—C38—C37	122.1(3)	C13—O14—Ni3	133.1(2)
C40—C39—C44	118.7(3)	C12—O15—Ni3	137.4(2)
C40—C39—C38	122.3(3)	C1—O17—Ni4	127.6(2)
C44—C39—C38	119.0(3)	C551—O18—C55	60.3(15)
C41—C40—C39	120.6(4)	C551—O18—Ni4	123.4(11)
C40—C41—C42	120.9(4)	C55—O18—Ni4	121.7(3)
C43—C42—C41	120.6(4)	C24—O19—Ni4	86.73(19)
C42—C43—C44	121.1(4)	C24—O20—Ni4	90.0(2)
C39—C44—C43	118.0(3)	O21—C60—N5	128.1(16)
C39—C44—C45 ^{vii}	119.0(3)	C60—N5—C62	123.4(14)
C43—C44—C45 ^{vii}	122.9(3)	C60—N5—C61	119.5(11)

Table A3.5 continued

C46 ^{viii} —C45—C44 ^{viii}	119.5(3)	C62—N5—C61	117.1(13)
C46 ^{viii} —C45—C48	117.7(3)	C551—N31—C571	122.(2)
C44 ^{viii} —C45—C48	122.7(3)	C551—N31—C561	128.(3)
C45 ^{vii} —C46—C47	121.9(3)	C571—N31—C561	110.(3)
C38—C47—C46	120.9(3)	O18—C551—N31	122.(2)
O2—C48—O13	126.7(3)	O22—C63—N6	122.4(18)
O2—C48—C45	119.5(3)	C63—N6—C65	121.5(18)
O13—C48—C45	113.8(3)	C63—N6—C64	118.6(15)
C55—N3—C56	120.8(7)	C65—N6—C64	114.8(16)
C55—N3—C57	119.0(5)	O221—C631—N61	117.(3)
C56—N3—C57	119.8(7)	C631—N61—C651	116.(2)
O18—C55—N3	122.3(5)	C631—N61—C641	120.(2)
C531—N1—C52	117.0(6)	C651—N61—C641	112.(2)
C531—N1—C53	64.6(6)	O25W ^{ix} —O23W—O25W ^{vii}	94.(3)
C52—N1—C53	120.1(5)	O25W ^{ix} —O23W—O25W	179.992(16)
C531—N1—Ni3	117.2(4)	O25W ^{vii} —O23W—O25W	86.(3)
C52—N1—Ni3	116.0(3)	O25W ^{ix} —O23W—O25W ^x	86.(3)
C53—N1—Ni3	112.1(4)	O25W ^{vii} —O23W—O25W ^x	179.99(2)
C58—N4—C59	113.3(5)	O25W—O23W—O25W ^x	94.(3)
O1—Ni1—O3	96.26(10)	O25W ^{ix} —O23W—O25W ^{xi}	86.(3)
O1—Ni1—O4	92.62(9)	O25W ^{vii} —O23W—O25W ^{xi}	86.(3)
O3—Ni1—O4	170.27(9)	O25W—O23W—O25W ^{xi}	94.(3)
O1—Ni1—O2	90.5(1)	O25W ^x —O23W—O25W ^{xi}	94.(3)
O3—Ni1—O2	93.37(10)	O25W ^{ix} —O23W—O25W ^{viii}	94.(3)
O4—Ni1—O2	90.51(9)	O25W ^{vii} —O23W—O25W ^{viii}	94.(3)
O1—Ni1—O5	94.33(10)	O25W—O23W—O25W ^{viii}	86.(3)
O3—Ni1—O5	89.69(10)	O25W ^x —O23W—O25W ^{viii}	86.(3)
O4—Ni1—O5	85.67(9)	O25W ^{xi} —O23W—O25W ^{viii}	180.(2)

Symmetry codes : (i) 1.33-x+y, 0.67-x, -0.33+z; (ii) 0.67-y, -0.67+x-y, 0.33+z;
 (iii) 0.67-y, -0.67+x-y, -0.67+z; (iv) 1.33-x+y, 0.67-x, 0.67+z;
 (v) 0.33+y, 0.67-x+y, -0.33-z; (vi) 0.33+x-y, -0.33+x, -0.33-z;
 (vii) 0.33+x-y, -0.33+x, 0.67-z; (viii) 0.33+y, 0.67-x+y, 0.67-z;
 (ix) 1.33-x, 0.67-y, 0.67-z; (x) 1-x+y, 1-x, z; (xi) 1-y, x-y, z.

A5.1. Structural Details for $\text{Ni}_2(\text{C}_{10}\text{H}_8\text{O}_6)_2(\text{H}_2\text{O})_4$ (**5-1**).



The asymmetric unit contains two nickel centers, each surrounded by four oxygens from the organic linker and two water oxygens completing the octahedron. All hydrogen atoms are placed in calculated positions, in riding modes. No disorder is modeled in the structure.

A5.2. Crystallographic Information File for $\text{Ni}_2(\text{C}_{10}\text{H}_8\text{O}_6)_2(\text{H}_2\text{O})_4$ (**5-1**).

```
data_mc4056d

_audit_creation_method           SHELXL-97
_chemical_name_systematic
;
?
;
_chemical_name_common            ?
_chemical_melting_point          ?
_chemical_formula_moiety         ?
_chemical_formula_sum             'C10 H10 Ni O8'
_chemical_formula_weight          316.89
```

```

loop_
_atom_type_symbol
_atom_type_description
_atom_type_scat_dispersion_real
_atom_type_scat_dispersion_imag
_atom_type_scat_source
'C' 'C' 0.0033 0.0016
'International Tables Vol C Tables 4.2.6.8 and 6.1.1.4'
'Ni' 'Ni' 0.3393 1.1124
'International Tables Vol C Tables 4.2.6.8 and 6.1.1.4'
'O' 'O' 0.0106 0.0060
'International Tables Vol C Tables 4.2.6.8 and 6.1.1.4'
'H' 'H' 0.0000 0.0000
'International Tables Vol C Tables 4.2.6.8 and 6.1.1.4'

_symmetry_cell_setting ?
_symmetry_space_group_name_H-M ?

loop_
_symmetry_equiv_pos_as_xyz
'x, y, z'
'-x, -y, z'
'x+1/2, -y+1/2, -z'
'-x+1/2, y+1/2, -z'
'-x, -y, -z'
'x, y, -z'
'-x-1/2, y-1/2, z'
'x-1/2, -y-1/2, z'

_cell_length_a 9.6142(19)
_cell_length_b 10.189(2)
_cell_length_c 23.753(5)
_cell_angle_alpha 90.00
_cell_angle_beta 90.00
_cell_angle_gamma 90.00
_cell_volume 2326.8(8)
_cell_formula_units_Z 8
_cell_measurement_temperature 293(2)
_cell_measurement_reflns_used ?
_cell_measurement_theta_min ?
_cell_measurement_theta_max ?

_exptl_crystal_description ?
_exptl_crystal_colour ?
_exptl_crystal_size_max ?
_exptl_crystal_size_mid ?
_exptl_crystal_size_min ?
_exptl_crystal_density_meas ?
_exptl_crystal_density_diffrn 1.809
_exptl_crystal_density_method 'not measured'
_exptl_crystal_F_000 1296
_exptl_absorpt_coefficient_mu 1.702
_exptl_absorpt_correction_type ?
_exptl_absorpt_correction_T_min ?

```

```

_exptl_absorpt_correction_T_max      ?
_exptl_absorpt_process_details      ?

_exptl_special_details
;
?
;

_diffrn_ambient_temperature          293(2)
_diffrn_radiation_wavelength        0.71073
_diffrn_radiation_type              MoK\alpha
_diffrn_radiation_source            'fine-focus sealed tube'
_diffrn_radiation_monochromator     graphite
_diffrn_measurement_device_type     ?
_diffrn_measurement_method          ?
_diffrn_detector_area_resol_mean    ?
_diffrn_standards_number            ?
_diffrn_standards_interval_count    ?
_diffrn_standards_interval_time     ?
_diffrn_standards_decay_%           ?
_diffrn_reflns_number               8172
_diffrn_reflns_av_R_equivalents    0.1369
_diffrn_reflns_av_sigmaI/netI       0.1238
_diffrn_reflns_limit_h_min          -10
_diffrn_reflns_limit_h_max          8
_diffrn_reflns_limit_k_min          -10
_diffrn_reflns_limit_k_max          10
_diffrn_reflns_limit_l_min          -24
_diffrn_reflns_limit_l_max          21
_diffrn_reflns_theta_min            1.71
_diffrn_reflns_theta_max            21.82
_reflns_number_total                1439
_reflns_number_gt                  654
_reflns_threshold_expression        >2sigma(I)

_computing_data_collection          ?
_computing_cell_refinement          ?
_computing_data_reduction           ?
_computing_structure_solution       ?
_computing_structure_refinement     'SHELXL-97 (Sheldrick, 1997)'
_computing_molecular_graphics       ?
_computing_publication_material     ?

_refine_special_details
;
Refinement of F^2^ against ALL reflections. The weighted R-factor wR
and
goodness of fit S are based on F^2^, conventional R-factors R are
based
on F, with F set to zero for negative F^2^. The threshold expression
of
F^2^ > 2sigma(F^2^) is used only for calculating R-factors(gt) etc.
and is
not relevant to the choice of reflections for refinement. R-factors
based

```

on F²⁻ are statistically about twice as large as those based on F,
 and R-
 factors based on ALL data will be even larger.
;

_refine_ls_structure_factor_coef	Fsqd
_refine_ls_matrix_type	full
_refine_ls_weighting_scheme	calc
_refine_ls_weighting_details	
'calc w=1/[s^2^(Fo^2^)+(0.0657P)^2^+0.0000P] where P=(Fo^2^+2Fc^2^)/3'	
_atom_sites_solution_primary	direct
_atom_sites_solution_secondary	difmap
_atom_sites_solution_hydrogens	geom
_refine_ls_hydrogen_treatment	mixed
_refine_ls_extinction_method	none
_refine_ls_extinction_coeff	?
_refine_ls_number_reflns	1439
_refine_ls_number_parameters	185
_refine_ls_number_restraints	6
_refine_ls_R_factor_all	0.1458
_refine_ls_R_factor_gt	0.0615
_refine_ls_wR_factor_ref	0.1570
_refine_ls_wR_factor_gt	0.1330
_refine_ls_goodness_of_fit_ref	0.978
_refine_ls_restrained_S_all	0.976
_refine_ls_shift/su_max	0.002
_refine_ls_shift/su_mean	0.000

loop_

_atom_site_label	
_atom_site_type_symbol	
_atom_site_fract_x	
_atom_site_fract_y	
_atom_site_fract_z	
_atom_site_U_iso_or_equiv	
_atom_site_adp_type	
_atom_site_occularity	
_atom_site_symmetry_multiplicity	
_atom_site_calc_flag	
_atom_site_refinement_flags	
_atom_site_disorder_assembly	
_atom_site_disorder_group	

C1 C 0.2580(14)	0.1083(12)	0.3451(5)	0.035(3)	Uani	1	1	d	.	.	.
C2 C 0.1460(12)	0.1917(10)	0.3775(4)	0.031(3)	Uani	1	1	d	.	.	.
H2 H 0.1540	0.2824	0.3641	0.038	Uiso	1	1	calc	R	.	.
C3 C 0.1690(12)	0.1936(11)	0.4405(5)	0.032(3)	Uani	1	1	d	.	.	.
C4 C 0.173(3)	0.0895(16)	0.4710(6)	0.31(2)	Uani	1	1	d	.	.	.
H4 H 0.1761	0.0088	0.4527	0.376	Uiso	1	1	calc	R	.	.
C5 C 0.159(3)	0.2965(15)	0.4709(6)	0.205(14)	Uani	1	1	d	.	.	.
H5 H 0.1514	0.3769	0.4526	0.246	Uiso	1	1	calc	R	.	.
C6 C 0.2625(17)	0.5824(10)	0.1525(6)	0.042(4)	Uani	1	1	d	.	.	.
C7 C 0.2425(14)	0.4497(10)	0.1224(5)	0.043(4)	Uani	1	1	d	.	.	.
H7 H 0.3140	0.3891	0.1360	0.051	Uiso	1	1	calc	R	.	.
C8 C 0.2584(14)	0.4627(9)	0.0590(6)	0.040(3)	Uani	1	1	d	.	.	.

```

C9 C 0.180(2) 0.5457(19) 0.0299(6) 0.188(12) Uani 1 1 d . .
H9 H 0.1245 0.6053 0.0491 0.226 Uiso 1 1 calc R . .
C10 C 0.3474(17) 0.4031(18) 0.0289(6) 0.126(8) Uani 1 1 d . .
H10 H 0.4171 0.3564 0.0472 0.151 Uiso 1 1 calc R . .
Nil Ni 0.0000 0.0000 0.30463(9) 0.0357(6) Uani 1 2 d S . .
Ni2 Ni 0.0000 0.5000 0.19407(9) 0.0452(7) Uani 1 2 d S . .
O1 O 0.0306(8) -0.1345(7) 0.2420(3) 0.039(2) Uani 1 1 d D . .
H13 H -0.012(9) -0.218(4) 0.257(3) 0.047 Uiso 1 1 d D . .
H14 H 0.039(9) -0.154(7) 0.2004(9) 0.047 Uiso 1 1 d D . .
O2 O 0.2101(7) 0.0154(7) 0.3144(3) 0.035(2) Uani 1 1 d . .
O3 O 0.0102(8) 0.1477(6) 0.3640(3) 0.0326(18) Uani 1 1 d . .
O4 O 0.3810(9) 0.1322(8) 0.3510(3) 0.051(2) Uani 1 1 d . .
O5 O 0.3766(9) 0.6432(7) 0.1449(4) 0.047(2) Uani 1 1 d . .
O6 O 0.1676(9) 0.6188(7) 0.1858(3) 0.045(2) Uani 1 1 d . .
O7 O 0.0894(15) 0.3913(12) 0.2574(5) 0.152(6) Uani 1 1 d D . .
H11 H 0.182(9) 0.363(16) 0.242(8) 0.182 Uiso 1 1 d D . .
H12 H 0.115(15) 0.471(10) 0.280(6) 0.182 Uiso 1 1 d D . .
O8 O 0.1107(8) 0.3972(6) 0.1364(3) 0.037(2) Uani 1 1 d . .

loop_
_atom_site_aniso_label
_atom_site_aniso_U_11
_atom_site_aniso_U_22
_atom_site_aniso_U_33
_atom_site_aniso_U_23
_atom_site_aniso_U_13
_atom_site_aniso_U_12
C1 0.036(9) 0.050(8) 0.020(8) 0.005(7) -0.002(7) -0.002(8)
C2 0.042(9) 0.020(6) 0.032(7) 0.005(5) 0.002(6) -0.014(6)
C3 0.029(8) 0.036(7) 0.030(8) 0.009(6) 0.011(6) -0.005(6)
C4 0.83(7) 0.087(13) 0.025(11) -0.013(10) -0.01(2) 0.19(2)
C5 0.53(4) 0.053(10) 0.032(10) -0.006(8) 0.010(15) -0.026(17)
C6 0.059(12) 0.011(8) 0.057(11) 0.013(7) -0.026(9) 0.007(8)
C7 0.053(10) 0.019(7) 0.056(9) 0.000(6) -0.015(8) 0.006(6)
C8 0.037(9) 0.010(6) 0.074(10) -0.004(7) -0.008(8) -0.005(6)
C9 0.27(3) 0.24(2) 0.052(12) 0.000(12) 0.007(12) 0.25(2)
C10 0.102(15) 0.189(17) 0.087(14) 0.006(11) -0.006(10) 0.111(14)
Nil 0.0360(14) 0.0423(12) 0.0289(13) 0.000 0.000 -0.0036(14)
Ni2 0.084(2) 0.0280(11) 0.0232(13) 0.000 0.000 -0.0173(15)
O1 0.041(6) 0.044(5) 0.033(5) -0.008(4) -0.004(4) -0.012(4)
O2 0.033(5) 0.035(5) 0.036(5) -0.015(5) 0.000(4) -0.010(4)
O3 0.021(4) 0.040(4) 0.037(4) -0.007(4) -0.002(4) -0.012(4)
O4 0.031(6) 0.069(6) 0.054(6) -0.023(5) 0.000(5) -0.020(5)
O5 0.052(6) 0.026(5) 0.063(6) 0.015(5) -0.022(5) -0.005(5)
O6 0.070(7) 0.030(5) 0.035(5) 0.000(4) -0.015(5) -0.012(5)
O7 0.267(17) 0.094(8) 0.094(10) 0.066(7) -0.117(10) -0.123(10)
O8 0.028(5) 0.032(4) 0.052(5) 0.005(4) -0.001(4) -0.007(4)

_geom_special_details
;
All esds (except the esd in the dihedral angle between two l.s.
planes)
are estimated using the full covariance matrix. The cell esds are
taken

```

into account individually in the estimation of esds in distances,
 angles
 and torsion angles; correlations between esds in cell parameters are
 only
 used when they are defined by crystal symmetry. An approximate
 (isotropic)
 treatment of cell esds is used for estimating esds involving l.s.
 planes.
 ;

```

loop_
  _geom_bond_atom_site_label_1
  _geom_bond_atom_site_label_2
  _geom_bond_distance
  _geom_bond_site_symmetry_2
  _geom_bond_publ_flag
C1 O4 1.216(14) . ?
C1 O2 1.279(12) . ?
C1 C2 1.573(15) . ?
C2 O3 1.417(12) . ?
C2 C3 1.513(13) . ?
C2 H2 0.9800 . ?
C3 C5 1.276(15) . ?
C3 C4 1.286(17) . ?
C4 C4 1.38(3) 6_556 ?
C4 H4 0.9300 . ?
C5 C5 1.38(3) 6_556 ?
C5 H5 0.9300 . ?
C6 O6 1.263(15) . ?
C6 O5 1.272(14) . ?
C6 C7 1.541(15) . ?
C7 O8 1.415(13) . ?
C7 C8 1.520(15) . ?
C7 H7 0.9800 . ?
C8 C10 1.269(16) . ?
C8 C9 1.324(16) . ?
C9 C9 1.42(3) 6 ?
C9 H9 0.9300 . ?
C10 C10 1.37(3) 6 ?
C10 H10 0.9300 . ?
Ni1 O2 2.040(7) 2 ?
Ni1 O2 2.040(7) . ?
Ni1 O1 2.044(7) . ?
Ni1 O1 2.044(7) 2 ?
Ni1 O3 2.064(6) . ?
Ni1 O3 2.064(6) 2 ?
Ni2 O8 2.026(7) 2_565 ?
Ni2 O8 2.026(7) . ?
Ni2 O6 2.025(8) . ?
Ni2 O6 2.025(8) 2_565 ?
Ni2 O7 2.055(11) . ?
Ni2 O7 2.055(11) 2_565 ?
O1 H13 1.010(11) . ?
O1 H14 1.010(11) . ?
O7 H11 1.010(11) . ?

```

```

O7 H12 1.010(11) . ?

loop_
_geom_angle_atom_site_label_1
_geom_angle_atom_site_label_2
_geom_angle_atom_site_label_3
_geom_angle
_geom_angle_site_symmetry_1
_geom_angle_site_symmetry_3
_geom_angle_publ_flag
O4 C1 O2 124.4(12) . . ?
O4 C1 C2 120.0(11) . . ?
O2 C1 C2 115.6(11) . . ?
O3 C2 C3 111.2(9) . . ?
O3 C2 C1 110.4(9) . . ?
C3 C2 C1 113.0(10) . . ?
O3 C2 H2 107.3 . . ?
C3 C2 H2 107.3 . . ?
C1 C2 H2 107.3 . . ?
C5 C3 C4 111.1(13) . . ?
C5 C3 C2 124.0(11) . . ?
C4 C3 C2 123.5(12) . . ?
C3 C4 C4 124.3(9) . 6_556 ?
C3 C4 H4 117.8 . . ?
C4 C4 H4 117.8 6_556 . ?
C3 C5 C5 124.5(8) . 6_556 ?
C3 C5 H5 117.8 . . ?
C5 C5 H5 117.8 6_556 . ?
O6 C6 O5 124.6(12) . . ?
O6 C6 C7 117.2(13) . . ?
O5 C6 C7 118.0(13) . . ?
O8 C7 C8 110.9(10) . . ?
O8 C7 C6 109.5(11) . . ?
C8 C7 C6 111.8(10) . . ?
O8 C7 H7 108.2 . . ?
C8 C7 H7 108.2 . . ?
C6 C7 H7 108.2 . . ?
C10 C8 C9 113.2(14) . . ?
C10 C8 C7 125.7(13) . . ?
C9 C8 C7 121.0(12) . . ?
C8 C9 C9 121.4(8) . 6 ?
C8 C9 H9 119.3 . . ?
C9 C9 H9 119.3 6 . ?
C8 C10 C10 124.3(9) . 6 ?
C8 C10 H10 117.9 . . ?
C10 C10 H10 117.9 6 . ?
O2 Ni1 O2 166.9(4) 2 . ?
O2 Ni1 O1 100.0(3) 2 . ?
O2 Ni1 O1 89.6(3) . . ?
O2 Ni1 O1 89.6(3) 2 2 ?
O2 Ni1 O1 100.0(3) . 2 ?
O1 Ni1 O1 86.6(4) . 2 ?
O2 Ni1 O3 91.4(3) 2 . ?
O2 Ni1 O3 79.6(3) . . ?
O1 Ni1 O3 168.2(3) . . ?

```

O1 Ni1 O3 90.9(3) 2 . ?
 O2 Ni1 O3 79.6(3) 2 2 ?
 O2 Ni1 O3 91.4(3) . 2 ?
 O1 Ni1 O3 90.9(3) . 2 ?
 O1 Ni1 O3 168.2(3) 2 2 ?
 O3 Ni1 O3 93.9(4) . 2 ?
 O8 Ni2 O8 95.0(4) 2_565 . ?
 O8 Ni2 O6 92.5(3) 2_565 . ?
 O8 Ni2 O6 79.9(3) . . ?
 O8 Ni2 O6 79.9(3) 2_565 2_565 ?
 O8 Ni2 O6 92.5(3) . 2_565 ?
 O6 Ni2 O6 168.9(5) . 2_565 ?
 O8 Ni2 O7 173.0(5) 2_565 . ?
 O8 Ni2 O7 89.8(5) . . ?
 O6 Ni2 O7 93.4(4) . . ?
 O6 Ni2 O7 94.7(4) 2_565 . ?
 O8 Ni2 O7 89.8(5) 2_565 2_565 ?
 O8 Ni2 O7 173.0(5) . 2_565 ?
 O6 Ni2 O7 94.7(4) . 2_565 ?
 O6 Ni2 O7 93.4(4) 2_565 2_565 ?
 O7 Ni2 O7 86.0(10) . 2_565 ?
 Ni1 O1 H13 105(4) . . ?
 Ni1 O1 H14 149(4) . . ?
 H13 O1 H14 102.0(14) . . ?
 C1 O2 Ni1 118.6(8) . . ?
 C2 O3 Ni1 115.4(6) . . ?
 C6 O6 Ni2 117.4(8) . . ?
 Ni2 O7 H11 105(10) . . ?
 Ni2 O7 H12 94(10) . . ?
 H11 O7 H12 102.0(14) . . ?
 C7 O8 Ni2 115.7(6) . . ?

 _diffrn_measured_fraction_theta_max 0.995
 _diffrn_reflns_theta_full 21.82
 _diffrn_measured_fraction_theta_full 0.995
 _refine_diff_density_max 0.669
 _refine_diff_density_min -0.449
 _refine_diff_density_rms 0.099

Table A5.1. Selected interatomic distances and angles for $\text{Ni}_2(\text{C}_{10}\text{H}_8\text{O}_6)_2(\text{H}_2\text{O})_4$ (**5-1**).

Atoms 1,2	d 1,2 [Å]	Atoms 1,2	d 1,2 [Å]
C1—O4	1.216(14)	C9—C9 ⁱⁱ	1.42(3)
C1—O2	1.279(12)	C9—H9	0.9300
C1—C2	1.573(15)	C10—C10 ⁱⁱ	1.37(3)
C2—O3	1.417(12)	C10—H10	0.9300
C2—C3	1.513(13)	Ni1—O2 ⁱⁱⁱ	2.040(7)
C2—H2	0.9800	Ni1—O2	2.040(7)

Table A5.1 continued

C3—C5	1.276(15)	Ni1—O1	2.044(7)
C3—C4	1.286(17)	Ni1—O1 ⁱⁱⁱ	2.044(7)
C4—C4 ⁱ	1.38(3)	Ni1—O3	2.064(6)
C4—H4	0.9300	Ni1—O3 ⁱⁱⁱ	2.064(6)
C5—C5 ⁱ	1.38(3)	Ni2—O8 ^{iv}	2.026(7)
C5—H5	0.9300	Ni2—O8	2.026(7)
C6—O6	1.263(15)	Ni2—O6	2.025(8)
C6—O5	1.272(14)	Ni2—O6 ^{iv}	2.025(8)
C6—C7	1.541(15)	Ni2—O7	2.055(11)
C7—O8	1.415(13)	Ni2—O7 ^{iv}	2.055(11)
C7—C8	1.520(15)	O1—H13	1.010(11)
C7—H7	0.9800	O1—H14	1.010(11)
C8—C10	1.269(16)	O7—H11	1.010(11)
C8—C9	1.324(16)	O7—H12	1.010(11)

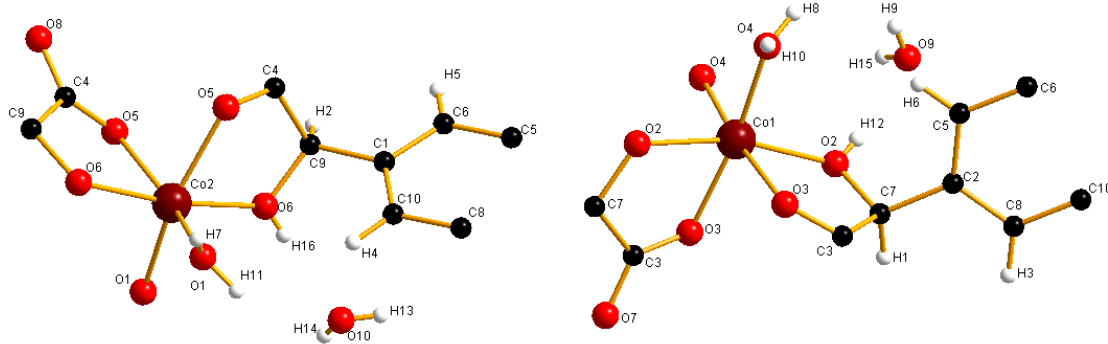
Atoms 1,2,3	Angle 1,2,3 [°]	Atoms 1,2,3	Angle 1,2,3 [°]
O4—C1—O2	124.4(12)	O2—Ni1—O1	89.6(3)
O4—C1—C2	120.0(11)	O2 ⁱⁱⁱ —Ni1—O1 ⁱⁱⁱ	89.6(3)
O2—C1—C2	115.6(11)	O2—Ni1—O1 ⁱⁱⁱ	100.0(3)
O3—C2—C3	111.2(9)	O1—Ni1—O1 ⁱⁱⁱ	86.6(4)
O3—C2—C1	110.4(9)	O2 ⁱⁱⁱ —Ni1—O3	91.4(3)
C3—C2—C1	113.(1)	O2—Ni1—O3	79.6(3)
O3—C2—H2	107.300	O1—Ni1—O3	168.2(3)
C3—C2—H2	107.300	O1 ⁱⁱⁱ —Ni1—O3	90.9(3)
C1—C2—H2	107.300	O2 ⁱⁱⁱ —Ni1—O3 ⁱⁱⁱ	79.6(3)
C5—C3—C4	111.1(13)	O2—Ni1—O3 ⁱⁱⁱ	91.4(3)
C5—C3—C2	124.0(11)	O1—Ni1—O3 ⁱⁱⁱ	90.9(3)
C4—C3—C2	123.5(12)	O1 ⁱⁱⁱ —Ni1—O3 ⁱⁱⁱ	168.2(3)
C3—C4—C4 ⁱ	124.3(9)	O3—Ni1—O3 ⁱⁱⁱ	93.9(4)
C3—C4—H4	117.800	O8 ^{iv} —Ni2—O8	95.0(4)
C4 ⁱ —C4—H4	117.800	O8 ^{iv} —Ni2—O6	92.5(3)
C3—C5—C5 ⁱ	124.5(8)	O8—Ni2—O6	79.9(3)
C3—C5—H5	117.800	O8 ^{iv} —Ni2—O6 ^{iv}	79.9(3)
C5 ⁱ —C5—H5	117.800	O8—Ni2—O6 ^{iv}	92.5(3)
O6—C6—O5	124.6(12)	O6—Ni2—O6 ^{iv}	168.9(5)
O6—C6—C7	117.2(13)	O8 ^{iv} —Ni2—O7	173.0(5)

Table A5.1 continued

O5—C6—C7	118.0(13)	O8—Ni2—O7	89.8(5)
O8—C7—C8	110.9(10)	O6—Ni2—O7	93.4(4)
O8—C7—C6	109.5(11)	O6 ^{iv} —Ni2—O7	94.7(4)
C8—C7—C6	111.8(10)	O8 ^{iv} —Ni2—O7 ^{iv}	89.8(5)
O8—C7—H7	108.200	O8—Ni2—O7 ^{iv}	173.0(5)
C8—C7—H7	108.200	O6—Ni2—O7 ^{iv}	94.7(4)
C6—C7—H7	108.200	O6 ^{iv} —Ni2—O7 ^{iv}	93.4(4)
C10—C8—C9	113.2(14)	O7—Ni2—O7 ^{iv}	86.(1)
C10—C8—C7	125.7(13)	Ni1—O1—H13	105.(4)
C9—C8—C7	121.0(12)	Ni1—O1—H14	149.(4)
C8—C9—C9 ⁱⁱ	121.4(8)	H13—O1—H14	102.0(14)
C8—C9—H9	119.300	C1—O2—Ni1	118.6(8)
C9 ⁱⁱ —C9—H9	119.300	C2—O3—Ni1	115.4(6)
C8—C10—C10 ⁱⁱ	124.3(9)	C6—O6—Ni2	117.4(8)
C8—C10—H10	117.900	Ni2—O7—H11	105.(10)
C10 ⁱⁱ —C10—H10	117.900	Ni2—O7—H12	94.(10)
O2 ⁱⁱⁱ —Ni1—O2	166.9(4)	H11—O7—H12	102.0(14)
O2 ⁱⁱⁱ —Ni1—O1	100.0(3)	C7—O8—Ni2	115.7(6)

Symmetry codes : (i) x, y, 1-z; (ii) x, y, -z; (iii) -x, -y, z; (iv) -x, 1-y, z.

A5.3. Structural Details for $\text{Co}(\text{C}_{10}\text{H}_8\text{O}_6)(\text{H}_2\text{O})_2 \cdot \text{H}_2\text{O}$ (**5-2**).



The asymmetric unit contains two cobalt centers, each surrounded by four oxygens from the organic linker and two water oxygens completing the octahedron. Water molecules are located as guests surrounding the chains. All hydrogen atoms are found from difference maps. No disorder is modeled in the structure.

A5.4. Crystallographic Information File for $\text{Co}(\text{C}_{10}\text{H}_8\text{O}_6)(\text{H}_2\text{O})_2 \cdot \text{H}_2\text{O}$ (**5-2**).

```
data_mc4087dlt

_audit_creation_method           SHELXL-97
_chemical_name_systematic
;
?
;
_chemical_name_common            ?
_chemical_melting_point          ?
_chemical_formula_moiety         ?
_chemical_formula_sum             'C10 H16 Co O10'
_chemical_formula_weight          355.16

loop_
_atom_type_symbol
_atom_type_description
_atom_type_scat_dispersion_real
_atom_type_scat_dispersion_imag
_atom_type_scat_source
'C'   'C'   0.0030   0.0020
'International Tables Vol C Tables 4.2.6.8 and 6.1.1.4'
'H'   'H'   0.0000   0.0000
'International Tables Vol C Tables 4.2.6.8 and 6.1.1.4'
```

```

'O'  'O'  0.0110  0.0060
'International Tables Vol C Tables 4.2.6.8 and 6.1.1.4'
'Co'  'Co'  0.3490  0.9720
'International Tables Vol C Tables 4.2.6.8 and 6.1.1.4'

_symmetry_cell_setting      ?
_symmetry_space_group_name_H-M    'C 2/c'

loop_
_symmetry_equiv_pos_as_xyz
'x, y, z'
'-x, y, -z+1/2'
'x+1/2, y+1/2, z'
'-x+1/2, y+1/2, -z+1/2'
'-x, -y, -z'
'x, -y, z-1/2'
'-x+1/2, -y+1/2, -z'
'x+1/2, -y+1/2, z-1/2'

_cell_length_a          20.7272(18)
_cell_length_b          12.9346(11)
_cell_length_c          10.2507(9)
_cell_angle_alpha        90.00
_cell_angle_beta         102.4310(10)
_cell_angle_gamma        90.00
_cell_volume            2683.8(4)
_cell_formula_units_Z   8
_cell_measurement_temperature 296(2)
_cell_measurement_reflns_used 5233
_cell_measurement_theta_min 2.60
_cell_measurement_theta_max 28.43

_exptl_crystal_description prism
_exptl_crystal_colour red
_exptl_crystal_size_max 0.23
_exptl_crystal_size_mid 0.20
_exptl_crystal_size_min 0.075
_exptl_crystal_density_meas ?
_exptl_crystal_density_diffrn 1.758
_exptl_crystal_density_method 'not measured'
_exptl_crystal_F_000 1464
_exptl_absorpt_coefficient_mu 1.329
_exptl_absorpt_correction_type 'multi-scan'
_exptl_absorpt_correction_T_min 0.571
_exptl_absorpt_correction_T_max 0.629
_exptl_absorpt_process_details 'Blessings, 1995'

_exptl_special_details
;
?;
;

_diffrn_ambient_temperature 296(2)
_diffrn_radiation_wavelength 0.71073
_diffrn_radiation_type MoK\`a

```

```

_diffrn_radiation_source      'fine-focus sealed tube'
_diffrn_radiation_monochromator graphite
_diffrn_measurement_device_type ?
_diffrn_measurement_method ?
_diffrn_detector_area_resol_mean ?
_diffrn_standards_number ?
_diffrn_standards_interval_count ?
_diffrn_standards_interval_time ?
_diffrn_standards_decay_% ?
_diffrn_reflns_number          8184
_diffrn_reflns_av_R_equivalents 0.0385
_diffrn_reflns_av_sigmaI/netI   0.0295
_diffrn_reflns_limit_h_min     -26
_diffrn_reflns_limit_h_max     27
_diffrn_reflns_limit_k_min     -13
_diffrn_reflns_limit_k_max     17
_diffrn_reflns_limit_l_min     -13
_diffrn_reflns_limit_l_max     13
_diffrn_reflns_theta_min       1.87
_diffrn_reflns_theta_max       28.71
_reflns_number_total          3204
_reflns_number_gt              2858
_reflns_threshold_expression   >2sigma(I)

_computing_data_collection    ?
_computing_cell_refinement    ?
_computing_data_reduction     ?
_computing_structure_solution  ?
_computing_structure_refinement 'SHELXL-97 (Sheldrick, 1997)'
_computing_molecular_graphics  ?
_computing_publication_material ?

_refine_special_details
;
    Refinement of F^2^ against ALL reflections. The weighted R-factor wR
and
    goodness of fit S are based on F^2^, conventional R-factors R are
based
    on F, with F set to zero for negative F^2^. The threshold expression
of
    F^2^ > 2sigma(F^2^) is used only for calculating R-factors(gt) etc.
and is
    not relevant to the choice of reflections for refinement. R-factors
based
    on F^2^ are statistically about twice as large as those based on F,
and R-
    factors based on ALL data will be even larger.
;

_refine_ls_structure_factor_coef  Fsqd
_refine_ls_matrix_type           full
_refine_ls_weighting_scheme      calc
_refine_ls_weighting_details
    'calc w=1/[s^2^(Fo^2^)+(0.0452P)^2^+0.0478P] where
P=(Fo^2^+2Fc^2^)/3'

```

```

_atom_sites_solution_primary      direct
_atom_sites_solution_secondary    difmap
_atom_sites_solution_hydrogens    geom
_refine_ls_hydrogen_treatment    mixed
_refine_ls_extinction_method    none
_refine_ls_extinction_coef      ?
_refine_ls_number_reflns        3204
_refine_ls_number_parameters    255
_refine_ls_number_restraints    0
_refine_ls_R_factor_all         0.0285
_refine_ls_R_factor_gt          0.0249
_refine_ls_wR_factor_ref        0.0724
_refine_ls_wR_factor_gt         0.0708
_refine_ls_goodness_of_fit_ref   1.077
_refine_ls_restrained_S_all     1.077
_refine_ls_shift/su_max         0.001
_refine_ls_shift/su_mean        0.000

loop_
_atom_site_label
_atom_site_type_symbol
_atom_site_fract_x
_atom_site_fract_y
_atom_site_fract_z
_atom_site_U_iso_or_equiv
_atom_site_adp_type
_atom_site_occupancy
_atom_site_symmetry_multiplicity
_atom_site_calc_flag
_atom_site_refinement_flags
_atom_site_disorder_assembly
_atom_site_disorder_group
Co1 Co 0.0000 0.028174(18) 0.2500 0.01501(9) Uani 1 2 d S . .
Co2 Co -0.5000 -0.043283(19) -0.2500 0.01599(9) Uani 1 2 d S . .
O1 O -0.48970(6) -0.14861(9) -0.09693(11) 0.0269(2) Uani 1 1 d . .
O2 O 0.09990(5) 0.00695(8) 0.24172(10) 0.0194(2) Uani 1 1 d . .
O3 O -0.02978(5) -0.08806(7) 0.11099(9) 0.0200(2) Uani 1 1 d . .
O4 O 0.01457(6) 0.14270(9) 0.39141(11) 0.0285(3) Uani 1 1 d . .
O5 O -0.53904(5) 0.07958(7) -0.37949(9) 0.0206(2) Uani 1 1 d . .
O6 O -0.40372(5) -0.03064(8) -0.27668(11) 0.0211(2) Uani 1 1 d . .
O7 O -0.10634(5) -0.20846(7) 0.04125(10) 0.0222(2) Uani 1 1 d . .
O8 O -0.61153(5) 0.20864(7) -0.39247(10) 0.0215(2) Uani 1 1 d . .
O9 O 0.17638(6) 0.17641(9) 0.22211(12) 0.0258(2) Uani 1 1 d . .
O10 O -0.32253(7) -0.17840(10) -0.33038(13) 0.0295(3) Uani 1 1 d . .
C1 C -0.30480(6) 0.01879(10) -0.11312(13) 0.0156(3) Uani 1 1 d . .
C2 C 0.19386(6) -0.04114(10) 0.42111(13) 0.0162(3) Uani 1 1 d . .
C3 C -0.08584(6) -0.12855(10) 0.10509(13) 0.0167(3) Uani 1 1 d . .
C4 C -0.59082(6) 0.11937(10) -0.35734(12) 0.0166(3) Uani 1 1 d . .
C5 C 0.19232(7) 0.04859(10) 0.49554(14) 0.0192(3) Uani 1 1 d . .
C6 C -0.24759(7) 0.07833(10) -0.09052(13) 0.0182(3) Uani 1 1 d . .
C7 C 0.13348(6) -0.07619(10) 0.31998(13) 0.0163(3) Uani 1 1 d . .
C8 C 0.25087(7) -0.10108(10) 0.44507(13) 0.0192(3) Uani 1 1 d . .
C9 C -0.36549(6) 0.05399(10) -0.21427(13) 0.0163(3) Uani 1 1 d . .
C10 C -0.30606(7) -0.07133(11) -0.04012(14) 0.0199(3) Uani 1 1 d . .
H1 H 0.1441(6) -0.1291(10) 0.2640(14) 0.008(3) Uiso 1 1 d . .

```

```

H2 H -0.3532(7) 0.0966(11) -0.2857(14) 0.012(3) Uiso 1 1 d . . .
H3 H 0.2509(8) -0.1648(13) 0.3965(16) 0.025(4) Uiso 1 1 d . . .
H4 H -0.3446(9) -0.1153(13) -0.0570(17) 0.033(5) Uiso 1 1 d . . .
H5 H -0.2467(8) 0.1378(12) -0.1419(17) 0.025(4) Uiso 1 1 d . . .
H6 H 0.1537(9) 0.0897(14) 0.4776(18) 0.036(5) Uiso 1 1 d . . .
H7 H -0.5024(10) -0.1339(14) -0.041(2) 0.034(6) Uiso 1 1 d . . .
H8 H 0.0404(11) 0.1933(14) 0.3987(19) 0.033(5) Uiso 1 1 d . . .
H9 H 0.1595(12) 0.2135(15) 0.260(2) 0.056(7) Uiso 1 1 d . . .
H10 H 0.0058(10) 0.1302(15) 0.464(2) 0.043(6) Uiso 1 1 d . . .
H11 H -0.4591(11) -0.1977(14) -0.079(2) 0.037(5) Uiso 1 1 d . . .
H12 H 0.1220(10) 0.0462(14) 0.2412(19) 0.029(6) Uiso 1 1 d . . .
H13 H -0.2862(13) -0.1707(16) -0.305(2) 0.052(7) Uiso 1 1 d . . .
H14 H -0.3302(11) -0.1888(16) -0.403(2) 0.049(7) Uiso 1 1 d . . .
H15 H 0.1623(12) 0.1909(16) 0.141(2) 0.052(7) Uiso 1 1 d . . .
H16 H -0.3841(12) -0.0689(17) -0.285(2) 0.051(7) Uiso 1 1 d . . .

loop_
_atom_site_aniso_label
_atom_site_aniso_U_11
_atom_site_aniso_U_22
_atom_site_aniso_U_33
_atom_site_aniso_U_23
_atom_site_aniso_U_13
_atom_site_aniso_U_12
Co1 0.01266(14) 0.01620(14) 0.01620(14) 0.000 0.00317(10) 0.000
Co2 0.01338(15) 0.01666(14) 0.01751(14) 0.000 0.00236(10) 0.000
O1 0.0332(6) 0.0276(6) 0.0229(5) 0.0065(4) 0.0129(5) 0.0147(5)
O2 0.0134(5) 0.0218(5) 0.0223(5) 0.0063(4) 0.0021(4) -0.0020(4)
O3 0.0157(5) 0.0232(5) 0.0221(5) -0.0052(4) 0.0059(4) -0.0014(4)
O4 0.0391(7) 0.0267(6) 0.0240(5) -0.0076(4) 0.0161(5) -0.0147(5)
O5 0.0171(5) 0.0231(5) 0.0228(5) 0.0048(4) 0.0070(4) 0.0018(4)
O6 0.0127(5) 0.0234(5) 0.0264(5) -0.0103(4) 0.0022(4) 0.0007(4)
O7 0.0193(5) 0.0173(5) 0.0287(5) -0.0042(4) 0.0022(4) 0.0012(4)
O8 0.0205(5) 0.0172(5) 0.0265(5) 0.0032(4) 0.0047(4) 0.0000(4)
O9 0.0287(6) 0.0247(5) 0.0246(6) 0.0000(4) 0.0068(5) 0.0009(4)
O10 0.0280(7) 0.0346(6) 0.0255(6) -0.0055(5) 0.0049(5) 0.0059(5)
C1 0.0115(6) 0.0176(6) 0.0175(6) -0.0025(5) 0.0026(5) 0.0023(5)
C2 0.0124(6) 0.0188(6) 0.0174(6) 0.0020(5) 0.0033(5) -0.0013(5)
C3 0.0161(6) 0.0164(6) 0.0169(6) 0.0029(5) 0.0021(5) 0.0030(5)
C4 0.0148(6) 0.0189(6) 0.0150(6) -0.0010(5) 0.0006(5) -0.0035(5)
C5 0.0132(7) 0.0204(6) 0.0233(7) -0.0002(5) 0.0021(5) 0.0033(5)
C6 0.0158(7) 0.0171(6) 0.0216(6) 0.0024(5) 0.0036(5) -0.0009(5)
C7 0.0126(6) 0.0177(6) 0.0187(6) 0.0001(5) 0.0034(5) -0.0008(5)
C8 0.0168(7) 0.0178(6) 0.0232(6) -0.0021(5) 0.0047(5) 0.0015(5)
C9 0.0121(6) 0.0196(6) 0.0168(6) -0.0023(5) 0.0020(5) -0.0005(5)
C10 0.0150(7) 0.0201(6) 0.0240(7) -0.0012(5) 0.0030(5) -0.0046(5)

_geom_special_details
;
All esds (except the esd in the dihedral angle between two l.s.
planes)
are estimated using the full covariance matrix. The cell esds are
taken
into account individually in the estimation of esds in distances,
angles

```

and torsion angles; correlations between esds in cell parameters are
 only
 used when they are defined by crystal symmetry. An approximate
 (isotropic)
 treatment of cell esds is used for estimating esds involving l.s.
 planes.
;

```

loop_
  _geom_bond_atom_site_label_1
  _geom_bond_atom_site_label_2
  _geom_bond_distance
  _geom_bond_site_symmetry_2
  _geom_bond_publ_flag
Co1 O4 2.0489(11) . ?
Co1 O4 2.0489(11) 2 ?
Co1 O3 2.0720(9) . ?
Co1 O3 2.0720(9) 2 ?
Co1 O2 2.1085(10) 2 ?
Co1 O2 2.1086(10) . ?
Co2 O1 2.0541(11) 2_454 ?
Co2 O1 2.0541(11) . ?
Co2 O6 2.0782(11) . ?
Co2 O6 2.0782(11) 2_454 ?
Co2 O5 2.1165(10) 2_454 ?
Co2 O5 2.1165(10) . ?
O2 C7 1.4297(16) . ?
O3 C3 1.2642(16) . ?
O5 C4 1.2542(16) . ?
O6 C9 1.4202(16) . ?
O7 C3 1.2479(15) . ?
O8 C4 1.2573(15) . ?
C1 C10 1.3885(18) . ?
C1 C6 1.3908(18) . ?
C1 C9 1.5177(18) . ?
C2 C8 1.3902(18) . ?
C2 C5 1.3931(18) . ?
C2 C7 1.5127(18) . ?
C3 C7 1.5330(17) 2 ?
C4 C9 1.5363(17) 2_454 ?
C5 C6 1.3886(19) 2 ?
C6 C5 1.3886(19) 2 ?
C7 C3 1.5330(17) 2 ?
C8 C10 1.3878(19) 2 ?
C9 C4 1.5363(17) 2_454 ?
C10 C8 1.3878(19) 2 ?

loop_
  _geom_angle_atom_site_label_1
  _geom_angle_atom_site_label_2
  _geom_angle_atom_site_label_3
  _geom_angle
  _geom_angle_site_symmetry_1
  _geom_angle_site_symmetry_3
  _geom_angle_publ_flag

```

O4 Co1 O4 87.40(7) . 2 ?
 O4 Co1 O3 171.06(4) . . ?
 O4 Co1 O3 93.52(5) 2 . ?
 O4 Co1 O3 93.52(5) . 2 ?
 O4 Co1 O3 171.06(4) 2 2 ?
 O3 Co1 O3 86.96(6) . 2 ?
 O4 Co1 O2 93.56(4) . 2 ?
 O4 Co1 O2 97.25(4) 2 2 ?
 O3 Co1 O2 77.50(4) . 2 ?
 O3 Co1 O2 91.58(4) 2 2 ?
 O4 Co1 O2 97.25(4) . . ?
 O4 Co1 O2 93.56(4) 2 . ?
 O3 Co1 O2 91.58(4) . . ?
 O3 Co1 O2 77.50(4) 2 . ?
 O2 Co1 O2 165.04(6) 2 . ?
 O1 Co2 O1 96.90(7) 2_454 . ?
 O1 Co2 O6 84.06(4) 2_454 . ?
 O1 Co2 O6 102.00(5) . . ?
 O1 Co2 O6 102.00(5) 2_454 2_454 ?
 O1 Co2 O6 84.06(4) . 2_454 ?
 O6 Co2 O6 170.97(6) . 2_454 ?
 O1 Co2 O5 160.03(4) 2_454 2_454 ?
 O1 Co2 O5 93.22(4) . 2_454 ?
 O6 Co2 O5 77.01(4) . 2_454 ?
 O6 Co2 O5 96.12(4) 2_454 2_454 ?
 O1 Co2 O5 93.22(4) 2_454 . ?
 O1 Co2 O5 160.03(4) . . ?
 O6 Co2 O5 96.12(4) . . ?
 O6 Co2 O5 77.01(4) 2_454 . ?
 O5 Co2 O5 82.67(5) 2_454 . ?
 C7 O2 Co1 116.04(8) . . ?
 C3 O3 Co1 117.92(8) . . ?
 C4 O5 Co2 114.90(8) . . ?
 C9 O6 Co2 117.37(8) . . ?
 C10 C1 C6 119.29(12) . . ?
 C10 C1 C9 120.74(12) . . ?
 C6 C1 C9 119.95(11) . . ?
 C8 C2 C5 119.13(13) . . ?
 C8 C2 C7 120.02(11) . . ?
 C5 C2 C7 120.79(12) . . ?
 O7 C3 O3 125.03(12) . . ?
 O7 C3 C7 116.44(12) . 2 ?
 O3 C3 C7 118.52(11) . 2 ?
 O5 C4 O8 125.29(12) . . ?
 O5 C4 C9 118.43(11) . 2_454 ?
 O8 C4 C9 116.25(11) . 2_454 ?
 C6 C5 C2 120.13(12) 2 . ?
 C5 C6 C1 120.57(12) 2 . ?
 O2 C7 C2 112.96(11) . . ?
 O2 C7 C3 108.98(10) . 2 ?
 C2 C7 C3 108.43(10) . 2 ?
 C10 C8 C2 120.67(12) 2 . ?
 O6 C9 C1 112.12(11) . . ?
 O6 C9 C4 108.08(10) . 2_454 ?
 C1 C9 C4 109.02(10) . 2_454 ?

C8 C10 C1 120.19(12) 2 . ?

_diffrn_measured_fraction_theta_max	0.921
_diffrn_reflns_theta_full	25.50
_diffrn_measured_fraction_theta_full	0.997
_refine_diff_density_max	0.403
_refine_diff_density_min	-0.351
_refine_diff_density_rms	0.058

Table A5.2. Selected interatomic distances and angles for

$\text{Co}(\text{C}_{10}\text{H}_8\text{O}_6)(\text{H}_2\text{O})_2\cdot\text{H}_2\text{O}$ (**5-2**).

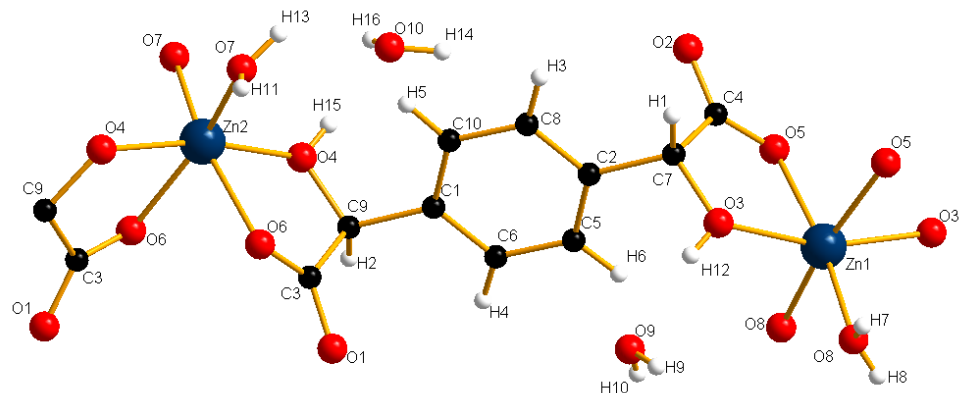
Atoms 1,2	d 1,2 [Å]	Atoms 1,2	d 1,2 [Å]
Co1—O4	2.0489(11)	O7—C3	1.2479(15)
Co1—O4 ⁱ	2.0489(11)	O8—C4	1.2573(15)
Co1—O3	2.0720(9)	C1—C10	1.3885(18)
Co1—O3 ⁱ	2.0720(9)	C1—C6	1.3908(18)
Co1—O2 ⁱ	2.1085(10)	C1—C9	1.5177(18)
Co1—O2	2.1086(10)	C2—C8	1.3902(18)
Co2—O1 ⁱⁱ	2.0541(11)	C2—C5	1.3931(18)
Co2—O1	2.0541(11)	C2—C7	1.5127(18)
Co2—O6	2.0782(11)	C3—C7 ⁱ	1.5330(17)
Co2—O6 ⁱⁱ	2.0782(11)	C4—C9 ⁱⁱ	1.5363(17)
Co2—O5 ⁱⁱ	2.1165(10)	C5—C6 ⁱ	1.3886(19)
Co2—O5	2.1165(10)	C6—C5 ⁱ	1.3886(19)
O2—C7	1.4297(16)	C7—C3 ⁱ	1.5330(17)
O3—C3	1.2642(16)	C8—C10 ⁱ	1.3878(19)
O5—C4	1.2542(16)	C9—C4 ⁱⁱ	1.5363(17)
O6—C9	1.4202(16)	C10—C8 ⁱ	1.3878(19)
Atoms 1,2,3	Angle 1,2,3 [°]	Atoms 1,2,3	Angle 1,2,3 [°]
O4—Co1—O4 ⁱ	87.40(7)	O6 ⁱⁱ —Co2—O5	77.01(4)
O4—Co1—O3	171.06(4)	O5 ⁱⁱ —Co2—O5	82.67(5)
O4 ⁱ —Co1—O3	93.52(5)	C7—O2—Co1	116.04(8)
O4—Co1—O3 ⁱ	93.52(5)	C3—O3—Co1	117.92(8)
O4 ⁱ —Co1—O3 ⁱ	171.06(4)	C4—O5—Co2	114.90(8)
O3—Co1—O3 ⁱ	86.96(6)	C9—O6—Co2	117.37(8)
O4—Co1—O2 ⁱ	93.56(4)	C10—C1—C6	119.29(12)
O4 ⁱ —Co1—O2 ⁱ	97.25(4)	C10—C1—C9	120.74(12)
O3—Co1—O2 ⁱ	77.50(4)	C6—C1—C9	119.95(11)
O3 ⁱ —Co1—O2 ⁱ	91.58(4)	C8—C2—C5	119.13(13)
O4—Co1—O2	97.25(4)	C8—C2—C7	120.02(11)
O4 ⁱ —Co1—O2	93.56(4)	C5—C2—C7	120.79(12)

Table A5.2 continued

O3—Co1—O2	91.58(4)	O7—C3—O3	125.03(12)
O3 ⁱ —Co1—O2	77.50(4)	O7—C3—C7 ⁱ	116.44(12)
O2 ⁱ —Co1—O2	165.04(6)	O3—C3—C7 ⁱ	118.52(11)
O1 ⁱⁱ —Co2—O1	96.90(7)	O5—C4—O8	125.29(12)
O1 ⁱⁱ —Co2—O6	84.06(4)	O5—C4—C9 ⁱⁱ	118.43(11)
O1—Co2—O6	102.00(5)	O8—C4—C9 ⁱⁱ	116.25(11)
O1 ⁱⁱ —Co2—O6 ⁱⁱ	102.00(5)	C6 ⁱ —C5—C2	120.13(12)
O1—Co2—O6 ⁱⁱ	84.06(4)	C5 ⁱ —C6—C1	120.57(12)
O6—Co2—O6 ⁱⁱ	170.97(6)	O2—C7—C2	112.96(11)
O1 ⁱⁱ —Co2—O5 ⁱⁱ	160.03(4)	O2—C7—C3 ⁱ	108.98(10)
O1—Co2—O5 ⁱⁱ	93.22(4)	C2—C7—C3 ⁱ	108.43(10)
O6—Co2—O5 ⁱⁱ	77.01(4)	C10 ⁱ —C8—C2	120.67(12)
O6 ⁱⁱ —Co2—O5 ⁱⁱ	96.12(4)	O6—C9—C1	112.12(11)
O1 ⁱⁱ —Co2—O5	93.22(4)	O6—C9—C4 ⁱⁱ	108.08(10)
O1—Co2—O5	160.03(4)	C1—C9—C4 ⁱⁱ	109.02(10)
O6—Co2—O5	96.12(4)	C8 ⁱ —C10—C1	120.19(12)

Symmetry codes : (i) -x, y, 0.5-z; (ii) -1-x, y, -0.5-z.

A5.5. Structural Details for $\text{Zn}(\text{C}_{10}\text{H}_8\text{O}_6)(\text{H}_2\text{O})_2 \cdot \text{H}_2\text{O}$ (**5-3**).



The asymmetric unit contains two zinc centers, each surrounded by four oxygens from the organic linker and two water oxygens completing the octahedron. Water molecules are located as guests surrounding the chains. All hydrogen atoms are located from difference maps. No disorder is modeled in the structure.

A5.6. Crystallographic Information File for $\text{Zn}(\text{C}_{10}\text{H}_8\text{O}_6)(\text{H}_2\text{O})_2 \cdot \text{H}_2\text{O}$ (**5-3**).

```

data_mc4087flt

_audit_creation_method           SHELLXL-97
_chemical_name_systematic
;
?
;
_chemical_name_common            ?
_chemical_melting_point          ?
_chemical_formula_moiety         ?
_chemical_formula_sum             'C10 H16 O10 Zn'
_chemical_formula_weight          361.62

loop_
_atom_type_symbol
_atom_type_description
_atom_type_scat_dispersion_real
_atom_type_scat_dispersion_imag
_atom_type_scat_source
'C'   'C'   0.0030   0.0020
'International Tables Vol C Tables 4.2.6.8 and 6.1.1.4'
'H'   'H'   0.0000   0.0000

```

```

'International Tables Vol C Tables 4.2.6.8 and 6.1.1.4'
'O'    'O'    0.0110    0.0060
'International Tables Vol C Tables 4.2.6.8 and 6.1.1.4'
'Zn'   'Zn'   0.2840    1.4300
'International Tables Vol C Tables 4.2.6.8 and 6.1.1.4'

_symmetry_cell_setting      ?
_symmetry_space_group_name_H-M   'C2/c'

loop_
_symmetry_equiv_pos_as_xyz
'x, y, z'
'-x, y, -z+1/2'
'x+1/2, y+1/2, z'
'-x+1/2, y+1/2, -z+1/2'
'-x, -y, -z'
'x, -y, z-1/2'
'-x+1/2, -y+1/2, -z'
'x+1/2, -y+1/2, z-1/2'

_cell_length_a          20.7801(14)
_cell_length_b          12.8656(9)
_cell_length_c          10.2531(7)
_cell_angle_alpha        90.00
_cell_angle_beta         102.6780(10)
_cell_angle_gamma        90.00
_cell_volume            2674.3(3)
_cell_formula_units_Z   8
_cell_measurement_temperature 293(2)
_cell_measurement_reflns_used 4504
_cell_measurement_theta_min 2.6
_cell_measurement_theta_max 28.6

_exptl_crystal_description     'prism'
_exptl_crystal_colour         'colorless'
_exptl_crystal_size_max       0.3
_exptl_crystal_size_mid       0.1
_exptl_crystal_size_min       0.1
_exptl_crystal_density_meas   ?
_exptl_crystal_density_diffrn 1.796
_exptl_crystal_density_method 'not measured'
_exptl_crystal_F_000          1488
_exptl_absorpt_coefficient_mu 1.888
_exptl_absorpt_correction_type 'multi-scan'
_exptl_absorpt_correction_T_min 0.497
_exptl_absorpt_correction_T_max 0.689
_exptl_absorpt_process_details 'Blessings, 1995'

_exptl_special_details
;
?
;

_diffrn_ambient_temperature 293(2)
_diffrn_radiation_wavelength 0.71073

```

```

_diffrn_radiation_type MoK\alpha
_diffrn_radiation_source 'fine-focus sealed tube'
_diffrn_radiation_monochromator graphite
_diffrn_measurement_device_type ?
_diffrn_measurement_method ?
_diffrn_detector_area_resol_mean ?
_diffrn_standards_number ?
_diffrn_standards_interval_count ?
_diffrn_standards_interval_time ?
_diffrn_standards_decay_% ?
_diffrn_reflns_number 8196
_diffrn_reflns_av_R_equivalents 0.0699
_diffrn_reflns_av_sigmaI/netI 0.0511
_diffrn_reflns_limit_h_min -25
_diffrn_reflns_limit_h_max 27
_diffrn_reflns_limit_k_min -11
_diffrn_reflns_limit_k_max 17
_diffrn_reflns_limit_l_min -13
_diffrn_reflns_limit_l_max 12
_diffrn_reflns_theta_min 1.87
_diffrn_reflns_theta_max 28.73
_reflns_number_total 3166
_reflns_number_gt 2746
_reflns_threshold_expression >2sigma(I)

_computing_data_collection ?
_computing_cell_refinement ?
_computing_data_reduction ?
_computing_structure_solution ?
_computing_structure_refinement 'SHELXL-97 (Sheldrick, 1997)'
_computing_molecular_graphics ?
_computing_publication_material ?

_refine_special_details
;
    Refinement of F^2 against ALL reflections. The weighted R-factor wR
and
    goodness of fit S are based on F^2, conventional R-factors R are
based
    on F, with F set to zero for negative F^2. The threshold expression
of
    F^2 > 2sigma(F^2) is used only for calculating R-factors(gt) etc.
and is
    not relevant to the choice of reflections for refinement. R-factors
based
    on F^2 are statistically about twice as large as those based on F,
and R-
    factors based on ALL data will be even larger.
;

_refine_ls_structure_factor_coef Fsqd
_refine_ls_matrix_type full
_refine_ls_weighting_scheme calc
_refine_ls_weighting_details

```

```

'calc w=1/[s^2^(Fo^2^)+(0.0373P)^2^+0.0000P] where
P=(Fo^2^+2Fc^2^)/3'
_atom_sites_solution_primary      direct
_atom_sites_solution_secondary    difmap
_atom_sites_solution_hydrogens   geom
_refine_ls_hydrogen_treatment    mixed
_refine_ls_extinction_method    SHELXL
_refine_ls_extinction_coef      0.00031(10)
_refine_ls_extinction_expression
'Fc^*^=kFc[1+0.001xFc^2^l^3^/sin(2\q)]^-1/4^'
_refine_ls_number_reflns        3166
_refine_ls_number_parameters    256
_refine_ls_number_restraints    0
_refine_ls_R_factor_all         0.0318
_refine_ls_R_factor_gt          0.0272
_refine_ls_wR_factor_ref        0.0768
_refine_ls_wR_factor_gt         0.0748
_refine_ls_goodness_of_fit_ref  1.008
_refine_ls_restrained_S_all    1.008
_refine_ls_shift/su_max         0.015
_refine_ls_shift/su_mean        0.001

loop_
_atom_site_label
_atom_site_type_symbol
_atom_site_fract_x
_atom_site_fract_y
_atom_site_fract_z
_atom_site_U_iso_or_equiv
_atom_site_adp_type
_atom_site_occupancy
_atom_site_symmetry_multiplicity
_atom_site_calc_flag
_atom_site_refinement_flags
_atom_site_disorder_assembly
_atom_site_disorder_group
Zn1 Zn 0.0000 0.46869(2) 0.2500 0.01557(10) Uani 1 2 d S . .
Zn2 Zn -0.5000 0.54716(2) -0.2500 0.01643(10) Uani 1 2 d S . .
O1 O -0.38891(6) 0.29075(8) -0.10892(13) 0.0214(3) Uani 1 1 d . .
O2 O -0.10565(6) 0.71018(8) 0.04332(12) 0.0215(3) Uani 1 1 d . .
O3 O -0.09958(6) 0.49308(10) 0.25903(12) 0.0186(3) Uani 1 1 d . .
O4 O -0.40344(6) 0.53152(10) -0.27720(13) 0.0202(3) Uani 1 1 d . .
O5 O -0.03005(5) 0.58703(10) 0.11077(11) 0.0191(3) Uani 1 1 d . .
O6 O -0.53962(5) 0.42171(10) -0.37933(11) 0.0199(3) Uani 1 1 d . .
O7 O -0.49237(7) 0.64996(11) -0.09745(14) 0.0249(3) Uani 1 1 d . .
O8 O 0.01178(7) 0.35473(11) 0.39049(14) 0.0268(3) Uani 1 1 d . .
O9 O -0.17574(7) 0.32343(12) 0.27924(15) 0.0257(3) Uani 1 1 d . .
O10 O -0.32155(8) 0.67856(12) -0.33131(16) 0.0292(3) Uani 1 1 d . .
C1 C -0.30456(8) 0.48144(13) -0.11309(16) 0.0159(3) Uani 1 1 d . .
C2 C -0.19355(8) 0.54153(12) 0.07892(16) 0.0163(3) Uani 1 1 d . .
C3 C -0.59096(7) 0.38108(13) -0.35655(15) 0.0159(3) Uani 1 1 d . .
C4 C -0.08551(8) 0.62879(13) 0.10597(15) 0.0160(3) Uani 1 1 d . .
C5 C -0.19203(8) 0.45156(13) 0.00496(17) 0.0193(4) Uani 1 1 d . .
C6 C -0.24742(8) 0.42155(13) -0.09109(16) 0.0180(3) Uani 1 1 d . .
C7 C -0.13311(8) 0.57689(13) 0.18101(16) 0.0166(3) Uani 1 1 d . .

```

```

C8 C -0.25037(8) 0.60187(13) 0.05527(17) 0.0189(3) Uani 1 1 d . . .
C9 C -0.36532(8) 0.44615(13) -0.21489(16) 0.0163(3) Uani 1 1 d . . .
C10 C -0.30570(8) 0.57202(14) -0.04059(17) 0.0196(3) Uani 1 1 d . . .
H1 H -0.1455(8) 0.6293(12) 0.2345(16) 0.010(4) Uiso 1 1 d . . .
H2 H -0.3521(7) 0.4030(13) -0.2850(16) 0.008(4) Uiso 1 1 d . . .
H3 H -0.2490(9) 0.6658(15) 0.1014(18) 0.022(5) Uiso 1 1 d . . .
H4 H -0.2484(9) 0.3619(14) -0.1426(18) 0.022(5) Uiso 1 1 d . . .
H5 H -0.3451(10) 0.6161(15) -0.0556(18) 0.028(5) Uiso 1 1 d . . .
H6 H -0.1514(10) 0.4114(16) 0.025(2) 0.036(6) Uiso 1 1 d . . .
H7 H 0.0073(11) 0.3756(17) 0.467(2) 0.038(7) Uiso 1 1 d . . .
H8 H 0.0355(12) 0.3089(16) 0.395(2) 0.024(6) Uiso 1 1 d . . .
H9 H -0.1632(15) 0.306(2) 0.363(3) 0.069(10) Uiso 1 1 d . . .
H10 H -0.1608(12) 0.2909(16) 0.237(2) 0.033(7) Uiso 1 1 d . . .
H11 H -0.5006(13) 0.6276(19) -0.039(3) 0.046(8) Uiso 1 1 d . . .
H13 H -0.4640(14) 0.6991(18) -0.078(3) 0.051(8) Uiso 1 1 d . . .
H14 H -0.2789(19) 0.678(3) -0.294(3) 0.099(11) Uiso 1 1 d . . .
H15 H -0.3788(12) 0.576(2) -0.291(2) 0.044(7) Uiso 1 1 d . . .
H16 H -0.3281(12) 0.6849(19) -0.403(3) 0.040(8) Uiso 1 1 d . . .
H12 H -0.1233(12) 0.4493(18) 0.262(2) 0.035(7) Uiso 1 1 d . . .

loop_
_atom_site_aniso_label
_atom_site_aniso_U_11
_atom_site_aniso_U_22
_atom_site_aniso_U_33
_atom_site_aniso_U_23
_atom_site_aniso_U_13
_atom_site_aniso_U_12
Zn1 0.01269(15) 0.01801(16) 0.01619(15) 0.000 0.00352(10) 0.000
Zn2 0.01318(15) 0.01858(16) 0.01740(16) 0.000 0.00311(10) 0.000
O1 0.0205(6) 0.0180(6) 0.0256(7) 0.0035(5) 0.0051(5) 0.0008(5)
O2 0.0185(6) 0.0183(6) 0.0270(7) 0.0044(5) 0.0036(5) -0.0004(4)
O3 0.0134(6) 0.0223(7) 0.0199(6) 0.0061(5) 0.0032(5) -0.0013(5)
O4 0.0131(6) 0.0239(7) 0.0232(7) 0.0098(5) 0.0031(5) -0.0002(5)
O5 0.0141(6) 0.0228(6) 0.0212(6) 0.0054(5) 0.0056(4) 0.0014(5)
O6 0.0154(6) 0.0240(6) 0.0217(6) -0.0039(5) 0.0074(5) -0.0003(5)
O7 0.0305(7) 0.0250(7) 0.0220(7) -0.0058(6) 0.0117(6) -0.0124(6)
O8 0.0363(8) 0.0253(7) 0.0228(7) 0.0065(6) 0.0156(6) 0.0133(6)
O9 0.0291(7) 0.0264(7) 0.0230(7) -0.0005(6) 0.0088(6) 0.0019(6)
O10 0.0289(8) 0.0346(8) 0.0236(8) 0.0048(6) 0.0047(6) -0.0055(6)
C1 0.0122(8) 0.0197(8) 0.0159(8) 0.0023(6) 0.0033(6) -0.0014(6)
C2 0.0137(8) 0.0196(8) 0.0161(8) 0.0009(6) 0.0042(6) -0.0010(6)
C3 0.0125(8) 0.0198(8) 0.0138(7) 0.0016(6) -0.0005(6) 0.0026(6)
C4 0.0154(8) 0.0185(8) 0.0136(7) -0.0025(6) 0.0018(6) -0.0035(6)
C5 0.0134(8) 0.0211(9) 0.0231(9) -0.0003(7) 0.0037(7) 0.0031(6)
C6 0.0167(8) 0.0169(8) 0.0205(8) -0.0019(7) 0.0041(6) 0.0013(6)
C7 0.0125(7) 0.0186(8) 0.0183(8) -0.0006(7) 0.0023(6) -0.0003(6)
C8 0.0172(8) 0.0175(8) 0.0224(8) -0.0022(7) 0.0052(6) 0.0013(6)
C9 0.0121(8) 0.0196(8) 0.0167(8) 0.0016(7) 0.0020(6) 0.0005(6)
C10 0.0148(8) 0.0208(8) 0.0232(9) 0.0015(7) 0.0041(6) 0.0050(7)

_geom_special_details
;
All esds (except the esd in the dihedral angle between two l.s.
planes)

```

are estimated using the full covariance matrix. The cell esds are taken into account individually in the estimation of esds in distances, angles and torsion angles; correlations between esds in cell parameters are only used when they are defined by crystal symmetry. An approximate (isotropic) treatment of cell esds is used for estimating esds involving l.s. planes.
 ;

```

loop_
  _geom_bond_atom_site_label_1
  _geom_bond_atom_site_label_2
  _geom_bond_distance
  _geom_bond_site_symmetry_2
  _geom_bond_publ_flag
Zn1 O8 2.0322(14) 2 ?
Zn1 O8 2.0322(14) . ?
Zn1 O5 2.0868(12) 2 ?
Zn1 O5 2.0868(12) . ?
Zn1 O3 2.1150(12) . ?
Zn1 O3 2.1150(12) 2 ?
Zn2 O7 2.0278(13) . ?
Zn2 O7 2.0278(13) 2_454 ?
Zn2 O4 2.0952(13) 2_454 ?
Zn2 O4 2.0952(13) . ?
Zn2 O6 2.1358(12) . ?
Zn2 O6 2.1358(12) 2_454 ?
O1 C3 1.2594(19) 2_454 ?
O2 C4 1.2515(19) . ?
O3 C7 1.429(2) . ?
O4 C9 1.4213(19) . ?
O5 C4 1.2627(19) . ?
O6 C3 1.255(2) . ?
C1 C10 1.385(2) . ?
C1 C6 1.392(2) . ?
C1 C9 1.520(2) . ?
C2 C5 1.388(2) . ?
C2 C8 1.389(2) . ?
C2 C7 1.518(2) . ?
C3 O1 1.2594(19) 2_454 ?
C3 C9 1.535(2) 2_454 ?
C4 C7 1.533(2) . ?
C5 C6 1.395(2) . ?
C8 C10 1.393(2) . ?
C9 C3 1.535(2) 2_454 ?

loop_
  _geom_angle_atom_site_label_1
  _geom_angle_atom_site_label_2
  _geom_angle_atom_site_label_3
  _geom_angle
  _geom_angle_site_symmetry_1

```

```

_geom_angle_site_symmetry_3
_geom_angle_publ_flag
O8 Zn1 O8 87.64(9) 2 . ?
O8 Zn1 O5 169.33(5) 2 2 ?
O8 Zn1 O5 94.02(6) . 2 ?
O8 Zn1 O5 94.02(6) 2 . ?
O8 Zn1 O5 169.33(5) . . ?
O5 Zn1 O5 86.29(7) 2 . ?
O8 Zn1 O3 99.86(5) 2 . ?
O8 Zn1 O3 92.45(5) . . ?
O5 Zn1 O3 90.61(5) 2 . ?
O5 Zn1 O3 76.88(5) . . ?
O8 Zn1 O3 92.45(5) 2 2 ?
O8 Zn1 O3 99.86(5) . 2 ?
O5 Zn1 O3 76.88(5) 2 2 ?
O5 Zn1 O3 90.61(5) . 2 ?
O3 Zn1 O3 162.94(7) . 2 ?
O7 Zn2 O7 98.58(9) . 2_454 ?
O7 Zn2 O4 82.82(5) . 2_454 ?
O7 Zn2 O4 104.49(5) 2_454 2_454 ?
O7 Zn2 O4 104.49(5) . . ?
O7 Zn2 O4 82.82(5) 2_454 . ?
O4 Zn2 O4 168.98(7) 2_454 . ?
O7 Zn2 O6 157.82(5) . . ?
O7 Zn2 O6 93.42(5) 2_454 . ?
O4 Zn2 O6 76.12(5) 2_454 . ?
O4 Zn2 O6 95.44(5) . . ?
O7 Zn2 O6 93.42(5) . 2_454 ?
O7 Zn2 O6 157.82(5) 2_454 2_454 ?
O4 Zn2 O6 95.44(5) 2_454 2_454 ?
O4 Zn2 O6 76.12(5) . 2_454 ?
O6 Zn2 O6 81.84(6) . 2_454 ?
C7 O3 Zn1 116.66(10) . . ?
C9 O4 Zn2 118.03(10) . . ?
C4 O5 Zn1 118.07(11) . . ?
C3 O6 Zn2 115.26(10) . . ?
C10 C1 C6 119.55(15) . . ?
C10 C1 C9 120.68(15) . . ?
C6 C1 C9 119.76(15) . . ?
C5 C2 C8 119.40(15) . . ?
C5 C2 C7 120.81(15) . . ?
C8 C2 C7 119.74(15) . . ?
O6 C3 O1 125.14(16) . 2_454 ?
O6 C3 C9 118.56(14) . 2_454 ?
O1 C3 C9 116.27(14) 2_454 2_454 ?
O2 C4 O5 125.13(16) . . ?
O2 C4 C7 116.24(14) . . ?
O5 C4 C7 118.62(14) . . ?
C2 C5 C6 120.16(16) . . ?
C1 C6 C5 120.23(16) . . ?
O3 C7 C2 112.82(13) . . ?
O3 C7 C4 108.70(13) . . ?
C2 C7 C4 108.17(13) . . ?
C2 C8 C10 120.50(16) . . ?
O4 C9 C1 112.01(13) . . ?

```

O4 C9 C3 107.83(13) . 2_454 ?
 C1 C9 C3 108.95(13) . 2_454 ?
 C1 C10 C8 120.13(16) . . ?

 _diffrn_measured_fraction_theta_max 0.910
 _diffrn_reflns_theta_full 28.73
 _diffrn_measured_fraction_theta_full 0.910
 _refine_diff_density_max 0.430
 _refine_diff_density_min -0.423
 _refine_diff_density_rms 0.072

Table A5.3. Selected interatomic distances and angles for

Zn(C₁₀H₈O₆)(H₂O)₂·H₂O (**5-3**).

Atoms 1,2	d 1,2 [Å]	Atoms 1,2	d 1,2 [Å]
Zn1—O8 ⁱ	2.0322(14)	O4—C9	1.4213(19)
Zn1—O8	2.0322(14)	O5—C4	1.2627(19)
Zn1—O5 ⁱ	2.0868(12)	O6—C3	1.255(2)
Zn1—O5	2.0868(12)	C1—C10	1.385(2)
Zn1—O3	2.1150(12)	C1—C6	1.392(2)
Zn1—O3 ⁱ	2.1150(12)	C1—C9	1.520(2)
Zn2—O7	2.0278(13)	C2—C5	1.388(2)
Zn2—O7 ⁱⁱ	2.0278(13)	C2—C8	1.389(2)
Zn2—O4 ⁱⁱ	2.0952(13)	C2—C7	1.518(2)
Zn2—O4	2.0952(13)	C3—O1 ⁱⁱ	1.2594(19)
Zn2—O6	2.1358(12)	C3—C9 ⁱⁱ	1.535(2)
Zn2—O6 ⁱⁱ	2.1358(12)	C4—C7	1.533(2)
O1—C3 ⁱⁱ	1.2594(19)	C5—C6	1.395(2)
O2—C4	1.2515(19)	C8—C10	1.393(2)
O3—C7	1.429(2)	C9—C3 ⁱⁱ	1.535(2)

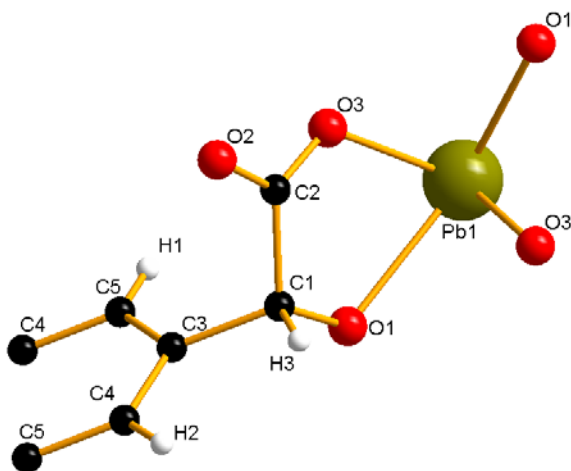
Atoms 1,2,3	Angle 1,2,3 [°]	Atoms 1,2,3	Angle 1,2,3 [°]
O8 ⁱ —Zn1—O8	87.64(9)	O4—Zn2—O6 ⁱⁱ	76.12(5)
O8 ⁱ —Zn1—O5 ⁱ	169.33(5)	O6—Zn2—O6 ⁱⁱ	81.84(6)
O8—Zn1—O5 ⁱ	94.02(6)	C7—O3—Zn1	116.66(10)
O8 ⁱ —Zn1—O5	94.02(6)	C9—O4—Zn2	118.03(10)
O8—Zn1—O5	169.33(5)	C4—O5—Zn1	118.07(11)
O5 ⁱ —Zn1—O5	86.29(7)	C3—O6—Zn2	115.26(10)
O8 ⁱ —Zn1—O3	99.86(5)	C10—C1—C6	119.55(15)
O8—Zn1—O3	92.45(5)	C10—C1—C9	120.68(15)
O5 ⁱ —Zn1—O3	90.61(5)	C6—C1—C9	119.76(15)
O5—Zn1—O3	76.88(5)	C5—C2—C8	119.40(15)
O8 ⁱ —Zn1—O3 ⁱ	92.45(5)	C5—C2—C7	120.81(15)
O8—Zn1—O3 ⁱ	99.86(5)	C8—C2—C7	119.74(15)

Table A5.3 continued

O5 ⁱ —Zn1—O3 ⁱ	76.88(5)	O6—C3—O1 ⁱⁱ	125.14(16)
O5—Zn1—O3 ⁱ	90.61(5)	O6—C3—C9 ⁱⁱ	118.56(14)
O3—Zn1—O3 ⁱ	162.94(7)	O1 ⁱⁱ —C3—C9 ⁱⁱ	116.27(14)
O7—Zn2—O7 ⁱⁱ	98.58(9)	O2—C4—O5	125.13(16)
O7—Zn2—O4 ⁱⁱ	82.82(5)	O2—C4—C7	116.24(14)
O7 ⁱⁱ —Zn2—O4 ⁱⁱ	104.49(5)	O5—C4—C7	118.62(14)
O7—Zn2—O4	104.49(5)	C2—C5—C6	120.16(16)
O7 ⁱⁱ —Zn2—O4	82.82(5)	C1—C6—C5	120.23(16)
O4 ⁱⁱ —Zn2—O4	168.98(7)	O3—C7—C2	112.82(13)
O7—Zn2—O6	157.82(5)	O3—C7—C4	108.70(13)
O7 ⁱⁱ —Zn2—O6	93.42(5)	C2—C7—C4	108.17(13)
O4 ⁱⁱ —Zn2—O6	76.12(5)	C2—C8—C10	120.50(16)
O4—Zn2—O6	95.44(5)	O4—C9—C1	112.01(13)
O7—Zn2—O6 ⁱⁱ	93.42(5)	O4—C9—C3 ⁱⁱ	107.83(13)
O7 ⁱⁱ —Zn2—O6 ⁱⁱ	157.82(5)	C1—C9—C3 ⁱⁱ	108.95(13)
O4 ⁱⁱ —Zn2—O6 ⁱⁱ	95.44(5)	C1—C10—C8	120.13(16)

Symmetry codes : (i) -x, y, 0.5-z; (ii) -1-x, y, -0.5-z.

A5.7. Structural Details for Pb(C₁₀H₈O₆) (**5-4**).



The asymmetric unit contains a lead center surrounded by four oxygens from the organic linker. All hydrogen atoms are located from difference maps. No disorder is modeled in the structure.

A5.8. Crystallographic Information File for Pb(C₁₀H₈O₆) (**5-4**).

```
data_mc4044hk3

_audit_creation_method           SHELXL-97
_chemical_name_systematic
;
?
;
_chemical_name_common            ?
_chemical_melting_point          ?
_chemical_formula_moiety         ?
_chemical_formula_sum             'C10 H6 O6 Pb'
_chemical_formula_weight          429.34

loop_
_atom_type_symbol
_atom_type_description
_atom_type_scat_dispersion_real
_atom_type_scat_dispersion_imag
_atom_type_scat_source
'C'   'C'   0.0033   0.0016
'International Tables Vol C Tables 4.2.6.8 and 6.1.1.4'
'H'   'H'   0.0000   0.0000
```

```

'International Tables Vol C Tables 4.2.6.8 and 6.1.1.4'
'O'    'O'    0.0106   0.0060
'International Tables Vol C Tables 4.2.6.8 and 6.1.1.4'
'Pb'   'Pb'   -3.3944  10.1111
'International Tables Vol C Tables 4.2.6.8 and 6.1.1.4'

_symmetry_cell_setting      ?
_symmetry_space_group_name_H-M  ?

loop_
_symmetry_equiv_pos_as_xyz
'x, y, z'
'-x, y, -z+1/2'
'x+1/2, y+1/2, z'
'-x+1/2, y+1/2, -z+1/2'
'-x, -y, -z'
'x, -y, z-1/2'
'-x+1/2, -y+1/2, -z'
'x+1/2, -y+1/2, z-1/2'

_cell_length_a              10.2009(12)
_cell_length_b              9.7997(11)
_cell_length_c              10.1272(12)
_cell_angle_alpha            90.00
_cell_angle_beta             101.0470(10)
_cell_angle_gamma            90.00
_cell_volume                 993.6(2)
_cell_formula_units_Z        4
_cell_measurement_temperature 293(2)
_cell_measurement_reflns_used ?
_cell_measurement_theta_min  ?
_cell_measurement_theta_max  ?

_exptl_crystal_description  ?
_exptl_crystal_colour        ?
_exptl_crystal_size_max      ?
_exptl_crystal_size_mid      ?
_exptl_crystal_size_min      ?
_exptl_crystal_density_meas  ?
_exptl_crystal_density_diffrn 2.870
_exptl_crystal_density_method 'not measured'
_exptl_crystal_F_000          784
_exptl_absorpt_coefficient_mu 16.994
_exptl_absorpt_correction_type ?
_exptl_absorpt_correction_T_min ?
_exptl_absorpt_correction_T_max ?
_exptl_absorpt_process_details ?

_exptl_special_details
;
?
;

_diffrn_ambient_temperature 293(2)
_diffrn_radiation_wavelength 0.71073

```

```

_diffrn_radiation_type MoK\alpha
_diffrn_radiation_source 'fine-focus sealed tube'
_diffrn_radiation_monochromator graphite
_diffrn_measurement_device_type ?
_diffrn_measurement_method ?
_diffrn_detector_area_resol_mean ?
_diffrn_standards_number ?
_diffrn_standards_interval_count ?
_diffrn_standards_interval_time ?
_diffrn_standards_decay_% ?
_diffrn_reflns_number 2994
_diffrn_reflns_av_R_equivalents 0.0457
_diffrn_reflns_av_sigmaI/netI 0.0325
_diffrn_reflns_limit_h_min -13
_diffrn_reflns_limit_h_max 12
_diffrn_reflns_limit_k_min -6
_diffrn_reflns_limit_k_max 13
_diffrn_reflns_limit_l_min -12
_diffrn_reflns_limit_l_max 13
_diffrn_reflns_theta_min 2.91
_diffrn_reflns_theta_max 28.50
_reflns_number_total 1178
_reflns_number_gt 1025
_reflns_threshold_expression >2sigma(I)

_computing_data_collection ?
_computing_cell_refinement ?
_computing_data_reduction ?
_computing_structure_solution ?
_computing_structure_refinement 'SHELXL-97 (Sheldrick, 1997)'
_computing_molecular_graphics ?
_computing_publication_material ?

_refine_special_details
;
    Refinement of F^2 against ALL reflections. The weighted R-factor wR
and
    goodness of fit S are based on F^2, conventional R-factors R are
based
    on F, with F set to zero for negative F^2. The threshold expression
of
    F^2 > 2sigma(F^2) is used only for calculating R-factors(gt) etc.
and is
    not relevant to the choice of reflections for refinement. R-factors
based
    on F^2 are statistically about twice as large as those based on F,
and R-
    factors based on ALL data will be even larger.
;

_refine_ls_structure_factor_coef Fsqd
_refine_ls_matrix_type full
_refine_ls_weighting_scheme calc
_refine_ls_weighting_details

```

```

'calc w=1/[s^2^(Fo^2^)+(0.0400P)^2^+0.0000P] where
P=(Fo^2^+2Fc^2^)/3'
_atom_sites_solution_primary      direct
_atom_sites_solution_secondary    difmap
_atom_sites_solution_hydrogens   geom
_refine_ls_hydrogen_treatment    mixed
_refine_ls_extinction_method    SHELXL
_refine_ls_extinction_coeff     0.0007(2)
_refine_ls_extinction_expression
'Fc^*^=kFc[1+0.001xFc^2^l^3^/sin(2\q)]^-1/4^'
_refine_ls_number_reflns        1178
_refine_ls_number_parameters    91
_refine_ls_number_restraints    0
_refine_ls_R_factor_all         0.0279
_refine_ls_R_factor_gt          0.0249
_refine_ls_wR_factor_ref        0.0665
_refine_ls_wR_factor_gt         0.0650
_refine_ls_goodness_of_fit_ref  1.072
_refine_ls_restrained_S_all    1.072
_refine_ls_shift/su_max         0.006
_refine_ls_shift/su_mean        0.001

loop_
_atom_site_label
_atom_site_type_symbol
_atom_site_fract_x
_atom_site_fract_y
_atom_site_fract_z
_atom_site_U_iso_or_equiv
_atom_site_adp_type
_atom_site_occupancy
_atom_site_symmetry_multiplicity
_atom_site_calc_flag
_atom_site_refinement_flags
_atom_site_disorder_assembly
_atom_site_disorder_group
Pb1 Pb 0.5000 0.253660(18) 0.2500 0.02164(14) Uani 1 2 d S . .
O1 O 0.3393(3) 0.1367(3) 0.0675(3) 0.0228(6) Uani 1 1 d . .
O2 O 0.2769(3) -0.1199(3) 0.2965(3) 0.0315(7) Uani 1 1 d . .
O3 O 0.3804(3) 0.0799(3) 0.3270(3) 0.0293(7) Uani 1 1 d . .
C1 C 0.2873(4) 0.0079(4) 0.1004(4) 0.0205(8) Uani 1 1 d . .
C2 C 0.3182(4) -0.0113(4) 0.2523(4) 0.0206(8) Uani 1 1 d . .
C3 C 0.1376(4) 0.0025(4) 0.0479(4) 0.0191(8) Uani 1 1 d . .
C4 C 0.0807(4) -0.0977(4) -0.0409(4) 0.0229(8) Uani 1 1 d . .
C5 C 0.0554(4) 0.1015(4) 0.0891(4) 0.0220(8) Uani 1 1 d . .
H1 H 0.088(4) 0.163(5) 0.142(4) 0.015(10) Uiso 1 1 d . .
H2 H 0.139(4) -0.163(5) -0.068(4) 0.016(10) Uiso 1 1 d . .
H3 H 0.324(4) -0.075(4) 0.060(4) 0.011(10) Uiso 1 1 d . .

loop_
_atom_site_aniso_label
_atom_site_aniso_U_11
_atom_site_aniso_U_22
_atom_site_aniso_U_33
_atom_site_aniso_U_23

```

```

_atom_site_aniso_U_13
_atom_site_aniso_U_12
Pb1 0.02410(19) 0.01772(18) 0.02286(18) 0.000 0.00390(10) 0.000
O1 0.0258(15) 0.0214(15) 0.0194(13) 0.0038(11) -0.0002(11) -0.0072(11)
O2 0.044(2) 0.0222(15) 0.0260(16) 0.0066(12) 0.0019(14) -0.0054(13)
O3 0.0379(19) 0.0320(18) 0.0159(14) 0.0002(11) 0.0003(13) -0.0153(13)
C1 0.023(2) 0.0183(19) 0.019(2) 0.0013(14) 0.0026(16) -0.0030(15)
C2 0.020(2) 0.0201(19) 0.020(2) 0.0046(14) 0.0014(15) 0.0016(15)
C3 0.022(2) 0.0172(18) 0.0162(19) 0.0027(13) -0.0003(15) -0.0013(15)
C4 0.025(2) 0.0198(19) 0.023(2) -0.0003(15) 0.0043(17) 0.0001(17)
C5 0.024(2) 0.019(2) 0.021(2) -0.0050(15) 0.0006(16) -0.0039(16)

_geom_special_details
;
All esds (except the esd in the dihedral angle between two l.s.
planes)
are estimated using the full covariance matrix. The cell esds are
taken
into account individually in the estimation of esds in distances,
angles
and torsion angles; correlations between esds in cell parameters are
only
used when they are defined by crystal symmetry. An approximate
(isotropic)
treatment of cell esds is used for estimating esds involving l.s.
planes.
;

loop_
_geom_bond_atom_site_label_1
_geom_bond_atom_site_label_2
_geom_bond_distance
_geom_bond_site_symmetry_2
_geom_bond_publ_flag
Pb1 O3 2.316(3) 2_655 ?
Pb1 O3 2.316(3) . ?
Pb1 O1 2.501(3) . ?
Pb1 O1 2.501(3) 2_655 ?
O1 C1 1.432(5) . ?
O2 C2 1.258(4) . ?
O3 C2 1.261(5) . ?
C1 C3 1.519(6) . ?
C1 C2 1.522(6) . ?
C3 C4 1.382(5) . ?
C3 C5 1.398(6) . ?
C4 C5 1.382(6) 5 ?
C5 C4 1.382(6) 5 ?

loop_
_geom_angle_atom_site_label_1
_geom_angle_atom_site_label_2
_geom_angle_atom_site_label_3
_geom_angle
_geom_angle_site_symmetry_1
_geom_angle_site_symmetry_3

```

```

    _geom_angle_publ_flag
O3 Pb1 O3 85.32(17) 2_655 . ?
O3 Pb1 O1 74.15(10) 2_655 . ?
O3 Pb1 O1 66.35(9) . . ?
O3 Pb1 O1 66.35(9) 2_655 2_655 ?
O3 Pb1 O1 74.15(10) . 2_655 ?
O1 Pb1 O1 125.43(13) . 2_655 ?
C1 O1 Pb1 116.8(2) . . ?
C2 O3 Pb1 123.8(3) . . ?
O1 C1 C3 110.0(3) . . ?
O1 C1 C2 109.3(3) . . ?
C3 C1 C2 110.4(3) . . ?
O2 C2 O3 123.4(4) . . ?
O2 C2 C1 116.5(3) . . ?
O3 C2 C1 120.1(3) . . ?
C4 C3 C5 119.2(4) . . ?
C4 C3 C1 121.4(4) . . ?
C5 C3 C1 119.4(4) . . ?
C5 C4 C3 121.2(4) 5 . ?
C4 C5 C3 119.7(4) 5 . ?

    _diff_rn_measured_fraction_theta_max      0.929
    _diff_rn_reflns_theta_full             28.50
    _diff_rn_measured_fraction_theta_full      0.929
    _refine_diff_density_max        1.716
    _refine_diff_density_min       -1.990
    _refine_diff_density_rms      0.182

```

Table A5.4. Selected interatomic distances and angles for $\text{Pb}(\text{C}_{10}\text{H}_8\text{O}_6)$ (**5-4**).

Atoms 1,2	d 1,2 [Å]	Atoms 1,2	d 1,2 [Å]
Pb1—O3 ⁱ	2.316(3)	C1—C3	1.519(6)
Pb1—O3	2.316(3)	C1—C2	1.522(6)
Pb1—O1	2.501(3)	C3—C4	1.382(5)
Pb1—O1 ⁱ	2.501(3)	C3—C5	1.398(6)
O1—C1	1.432(5)	C4—C5 ⁱⁱ	1.382(6)
O2—C2	1.258(4)	C5—C4 ⁱⁱ	1.382(6)
O3—C2	1.261(5)		

Atoms 1,2,3	Angle 1,2,3 [°]	Atoms 1,2,3	Angle 1,2,3 [°]
O3 ⁱ —Pb1—O3	85.32(17)	C3—C1—C2	110.4(3)
O3 ⁱ —Pb1—O1	74.15(10)	O2—C2—O3	123.4(4)
O3—Pb1—O1	66.35(9)	O2—C2—C1	116.5(3)
O3 ⁱ —Pb1—O1 ⁱ	66.35(9)	O3—C2—C1	120.1(3)
O3—Pb1—O1 ⁱ	74.15(10)	C4—C3—C5	119.2(4)

Table A5.4 continued

O1—Pb1—O1 ⁱ	125.43(13)	C4—C3—C1	121.4(4)
C1—O1—Pb1	116.8(2)	C5—C3—C1	119.4(4)
C2—O3—Pb1	123.8(3)	C5 ⁱⁱ —C4—C3	121.2(4)
O1—C1—C3	110.0(3)	C4 ⁱⁱ —C5—C3	119.7(4)
O1—C1—C2	109.3(3)		

Symmetry codes : (i) 1-x, y, 0.5-z; (ii) -x, -y, -z.
